UNIVERSIDAD AUTÓNOMA DE MADRID

DEPARTAMENTO DE MEDICINA

PAPEL FISIOPATOLÓGICO DEL FACTOR DE RESPUESTA A HIPOXIA HIF2α MEDIANTE EL CONTROL DEL TRANSPORTADOR DE AMINOÁCIDOS SLC7A5 Y EL REGULADOR DE SÍNTESIS PROTEICA mTORC1.

TESIS DOCTORAL

AINARA ELORZA PEREGRINA

MADRID 2013

DEPARTAMENTO DE MEDICINA

FACULTAD DE MEDICINA

UNIVERSIDAD AUTÓNOMA DE MADRID

PAPEL FISIOPATOLÓGICO DEL FACTOR DE RESPUESTA A HIPOXIA HIF2α MEDIANTE EL CONTROL DEL TRANSPORTADOR DE AMINOÁCIDOS SLC7A5 Y EL REGULADOR DE SÍNTESIS PROTEICA mTORC1.

TESIS DOCTORAL presentada por

AINARA ELORZA PEREGRINA

Licenciada en Bioquímica,

para optar al grado de Doctor.

Director: **JULIÁN ARAGONÉS LÓPEZ**

Universidad Autónoma de Madrid

Instituto de Investigación Sanitaria Princesa

El trabajo recogido en la presente memoria ha sido realizado por Ainara Elorza Peregrina, bajo la dirección del Dr. Julián Aragonés López en el Servicio de Inmunología del Hospital Universitario de la Princesa.

Opta al grado de Doctor

Ainara Elorza Peregrina

VºBº del Director de Tesis

Dr. Julián Aragonés López

A aitá

Dejamos de temer aquello que se ha aprendido a entender.

Marie Curie

ÍNDICE

RESUMEN

RESUMEN

La hipoxia activa un programa transcripcional a través de los factores HIF1α y HIF2α, destinado a adaptar a las células a las bajas tensiones de oxígeno. Dentro de estas respuestas adaptativas se encuentra la atenuación de la proliferación autónoma de célula. En este sentido, es bien conocido el efecto represor de la hipoxia, a través de vías dependientes de HIF1α e independientes de HIF, sobre el complejo mTORC1, esencial en el control de la síntesis proteica y por tanto de la proliferación celular. Sin embargo, en los últimos años el factor HIF2α se ha revelado como un elemento promotor de la proliferación en diversos contextos biológicos de los que el carcinoma renal de célula clara deficiente para VHL es el mejor caracterizado. Esta paradójica situación nos ha llevado a profundizar en el estudio del papel específico del factor HIF2α sobre la actividad de mTORC1. El resultado de dicho estudio es el trabajo de tesis aquí presentado, en el que demostramos que HIF2α ejerce un papel activador sobre mTORC1, opuesto al clásicamente descrito para la subunidad HIF1α y otras señales inducidas por hipoxia. El mecanismo molecular a través del cual HIF2α ejecuta esta activación conlleva la inducción del transportador de aminoácidos SLC7A5, que aquí identificamos como una nueva diana transcripcional específica de la isoforma HIF2α. Caracterizamos por tanto un nuevo vínculo entre las rutas de percepción de oxígeno HIF y la regulación de mTORC1 que proporciona además la base molecular a las propiedades pro-tumorales de HIF2α en los carcinomas renales de célula clara deficientes en VHL. Además describimos la operatividad de esta ruta en dos escenarios fisiológicos adicionales, hígado y pulmón, en los que la isoforma HIF2α y la propia hipoxia -en el caso del pulmón- también promueven la actividad de mTORC1 y la expresión de SLC7A5.

ABSTRACT

ABSTRACT

Hypoxia activates a transcriptional programme through the hypoxia-inducible factors HIF1α and HIF2α in order to adapt cells to these low oxygen tensions. One of these adaptive responses involves the attenuation of cell autonomous proliferation. It is also well-known that the mTORC1 complex, which is essential for protein synthesis and cell proliferation, is repressed in certain cell types in hypoxia via HIF1α-dependent and HIF-independent pathways. However, the HIF2α oxygen sensing pathway has emerged in the last years as a proliferation promoting factor in several biological settings, such as renal cell carcinoma upon loss of Von Hippel-Lindau (VHL) tumor suppressor. This paradoxical scenario led us to go in depth in the specific role of HIF2α on mTORC1 regulation. Here we show that HIF2α acts as an mTORC1 activator, which is in sharp contrast with the classically repressive activity described for HIF1α subunit and hypoxia. The molecular mechanism underlying this HIF2α-dependent mTORC1 activation involves the upregulation of the amino acid carrier SLC7A5 expression, which here is described as a new specific transcriptional target of HIF2α isoform. Therefore, we characterize a novel link between the oxygen-sensing HIF pathways and mTORC1 regulation, revealing the molecular basis of the tumor promoting properties of HIF2α in von Hippel-Lindau (VHL)-deficient cells. We also describe relevant physiological scenarios, such as liver and lung, where HIF2α or low oxygen tension also drive mTORC1 activity and SLC7A5 expression.

ABREVIATURAS

ABREVIATURAS

4EBP1: *eIF4E-Binding Protein 1*; Proteína de unión a eIF4E.

ARNm: ARN mensajeros.

ARNT: *Aryl Hydrocarbon Receptor Nuclear Traslocator,* Traslocador nuclear del receptor para aril hidrocarburos.

AMPK: *AMP-activated Protein Kinase*; Quinasa activada por AMP.

bHLH: *Basic-helix-loop-helix*; básico hélice-vuelta-hélice.

bNIP3: *BCL2/adenovirus E1B 19 kDa interacting protein 3.*

C-TAD: *C-terminal Transactivation Domain*; Dominio C-terminal de Transactivación.

ChIP: *Chromatin ImmunoPrecipitation*; Inmunoprecipitación de cromatina.

c-Myc: *Cellular Myelocytomatosis oncogene*.

CAIX: *Carbonic Anhidrase IX*; Anhidrasa carbónica IX.

CBP: *CRE Binding Protein*; Proteína de unión a CRE.

ccRCC: *Clear Cell Renal Cell Carcinoma*; Carcinoma renal de célula clara.

CREB: *cAMP Response Element-Binding*; Elemento de unión y respuesta a cAMP.

EGF-R: *Epidermal Growth Factor-receptor*; Receptor del factor de crecimiento epidérmico.

eIF4E: *eukaryotic translation initiation factor 4E*; Factor 4E de iniciación de la traducción eucariota.

EPAS: *Endothelial PAS protein,* Proteína PAS endotelial.

EPO: *Erythropoietin*; Eritropoyetina.

FGF: *Fibroblast Growth Factor*; Factor de crecimiento epidérmico.

FIH: *Factor Inhibiting HIF*; Factor Inhibidor de HIF.

GAP: *GTPase-Activating Protein;* proteína activadora de GTPasa.

HIF: *Hypoxia-Inducible Factor,* Factor Inducible por Hipoxia.

HRE: *Hypoxia-Response Element,* Elemento de Respuesta a Hipoxia.

IGF: *Insuline-like Growth Factor;* Factor de crecimiento insulínico tipo I.

MAPK: *Mitogen-Activated Protein Kinase*; Proteína quinasa activada por mitógeno.

mTORC: *Mammalian Target Of Rapamycin Complex*; Complejo diana de la rapamicina en mamíferos.

N-TAD: *N-terminal Transactivation Domain*; Dominio N-terminal de transactivación.

OCT4: *Octamer-binding protein* 4.

ODD: *Oxygen-dependent Degradation Domain*; Dominio de degradación dependiente de oxígeno.

PPARγ: P*eroxisome Proliferator-Activated Receptor-γ*.

PDH*:* *Pyruvate Dehydrogenase*; Piruvato deshidrogenasa.

PDK: *Pyruvate dehydrogenase kinase*; Piruvato deshidrogenasa quinasa.

PGK1: *Phosphoglycerate Kinase;* Fosfoglicerato quinasa.

PGC1α: *PPARγ coactivator 1;* Coactivador de PPARγ.

PHD: *Prolyl Hydroxylase Domain containing protein;* Proteína que contiene un dominio prolina hidroxilasa.

PI3K: *Phosphoinositide 3-kinase*; Fosfo-inosítido-3 quinasa.

RAG: *Ras-related GTP-binding protein.*

RCC: *Renal Cell Carcinoma*; Carcinoma de célula renal.

Redd1: *Protein Regulated in Development and DNA Damage Response 1*; Proteína regulada en desarrollo y respuesta a daño de ADN 1.

Rheb: *Ras homolog enriched in brain.*

ROS: *Reactive Oxygen Species*; Especies reactivas de oxígeno.

SDH: *Succinate Dehydrogenase*; Succinato deshidrogenasa.

SLC: *Solute Carrier*; Transportador de solutos.

SREBP: *Sterol Regulatory Element Binding Protein I*; Proteína de unión al elemento de regulador de los esteroles.

siARN: *small interference* ARN; ARN de interferencia pequeño.

shRNA: *short hairpin* ARN.

TSC: *Tuberous Sclerosis Complex*; Complejo de esclerosis tuberoso.

VEGF: *Vascular Endothelial Growth Factor*; Factor de crecimiento del endotelio vascular.

VHL: *Von Hippel-Lindau.*

INTRODUCCIÓN

INTRODUCCIÓN

1. EL OXÍGENO.

La aparición del oxígeno (O_2) en la biosfera hace 2.200 millones de años supuso uno de los momentos claves en la evolución, ya que proporcionó a los organismos la oportunidad de generar energía más eficientemente. De acuerdo con la teoría endosimbiótica, las mitocondrias surgieron a partir de bacterias con capacidad para metabolizar el O_2 que sobrevivieron a la endocitosis por otras especies. La habilidad de estas bacterias simbiontes para realizar la respiración celular en las células hospedadoras, sustituyendo a la fermentación anaerobia, significó una considerable ventaja para estos organismos por su capacidad para generar energía más eficientemente. Este hecho supuso la base de su éxito evolutivo, pero también hizo a estos organismos altamente dependientes del O_2 para su desarrollo y supervivencia, motivo por el que las especies aerobias han desarrollado mecanismos moleculares para detectar fluctuaciones en el aporte de O_2 y regular así numerosas funciones celulares en respuesta a escenarios de hipoxia o hiperoxia.

Es importante destacar, en primer lugar, que las células están expuestas a diferentes tensiones de O_2 ya en condiciones basales, siendo las presiones parciales de O_2 (PO_2) muy diferentes en las distintas localizaciones anatómicas. En la mayoría de los tejidos estas PO_2 varían entre 20 y 70 mmHg (equivalente a ~2.5 a 9.0 KPa), alcanzando valores superiores en la sangre arterial (~100 mmHg ó 13 KPa), e inferiores en ciertos compartimentos tisulares, tales como la médula renal o la médula ósea, que se encuentran de manera natural menos oxigenados y en los que la PO_2 puede llegar a niveles de 10-20 mm Hg (~1,3 a 2,6 KPa) (Aragonés et al., 2009; Ward, 2008). Se desconoce en gran medida cuál es el papel fisiológico de esta hipoxia natural existente en algunas localizaciones anatómicas en situaciones no patológicas. En cualquier caso esta homeostasis basal en el aporte de O_2 puede desbalancearse de manera sistémica (hipoxemia) o local durante el desarrollo de numerosas patologías. Una disminución sistémica en el aporte de O_2 ocurre, por ejemplo, en condiciones de hipoxia crónica en la altura o en la patología pulmonar, escenarios que cursan con disminuciones más o menos notorias en la PO_2 sanguínea que desencadenan un escenario de hipoxemia. En otras patologías tales como la isquemia cardíaca y periférica, la progresión de tumores sólidos, los focos inflamatorios o la expansión del tejido adiposo, el aporte de O_2 se compromete de forma local, únicamente en ciertos grupos de células (por ejemplo, en el miocardio isquémico o en

zonas perinecróticas de los tumores), en las que llegan a alcanzarse incluso situaciones de anoxia (< 0,01 KPa) (Ward, 2008).

2. FACTORES DE TRANSCRIPCIÓN INDUCIBLES POR HIPOXIA (HIF).

Desde que hace casi un cuarto de siglo Carl Wilhelm Scheele descubriera el O_2 y lo denominara "el aire del fuego", ha sido en los últimos años cuando se han producido grandes avances en los conocimientos moleculares sobre cómo las células perciben los niveles de O_2 y cómo estos ejes moleculares son componentes centrales de la fisiopatología. Estos mecanismos están muy conservados evolutivamente e implican, en situaciones de insuficiencia en la disponibilidad de O_2 (hipoxia), un cambio en la expresión génica celular que busca el restablecimiento del aporte de O_2 y al mismo tiempo la adaptación del metabolismo de la célula para procurar su supervivencia. Dicha reprogramación transcripcional la llevan a cabo los factores inducibles por hipoxia HIF (Gu et al., 1998; Tian et al., 1997; Wang et al., 1995).

2.1. Descripción molecular.

Los factores de transcripción HIF son heterodímeros miembros de la familia de los factores de transcripción *basic helix-loop-helix* (bHLH)-PAS. Están formados por una subunidad α (112-120 kDa) y otra β (91-94 kDa) también denominada ARNT (traslocador nuclear del receptor para aril hidrocarburos). Ambas subunidades presentan un dominio bHLH y un dominio PAS implicados en su heterodimerización y en su unión a ADN (Jiang et al., 1996; Wang et al., 1995). La subunidad α posee además dos dominios de transactivación, uno en posición N-terminal (N-TAD) y otro en su extremo C-terminal (C-TAD), mientras que la subunidad β sólo presenta un dominio de transactivación (TAD) C-terminal. Se han descrito tres isoformas de la subunidad α: HIF1α, HIF2α (también denominada EPAS, proteína PAS endotelial) y, la menos caracterizada, HIF3α (Gu et al., 1998). Cada una de estas isoformas está codificada por distintos genes. Con respecto a HIF1α y HIF2α, las más estudiadas, presentan un 48% de homología y comparten similitudes estructurales y bioquímicas. Ambas presentan una expresión preferente en función del tipo de tejido y aunque coinciden en la inducción de algunos genes comunes de respuesta a hipoxia, también presentan ciertas funciones transcripcionales específicas (ver más adelante). Por otro lado existen evidencias que apuntan a que la estabilización de HIF2α requiere de una hipoxia menos severa que la de HIF1α. Aunque los mecanismos responsables son todavía desconocidos, ésto sugiere que HIF2α podría ser una primera línea de

respuesta frente a disminuciones moderadas en el aporte de O_2 (Wiesener et al., 1998).

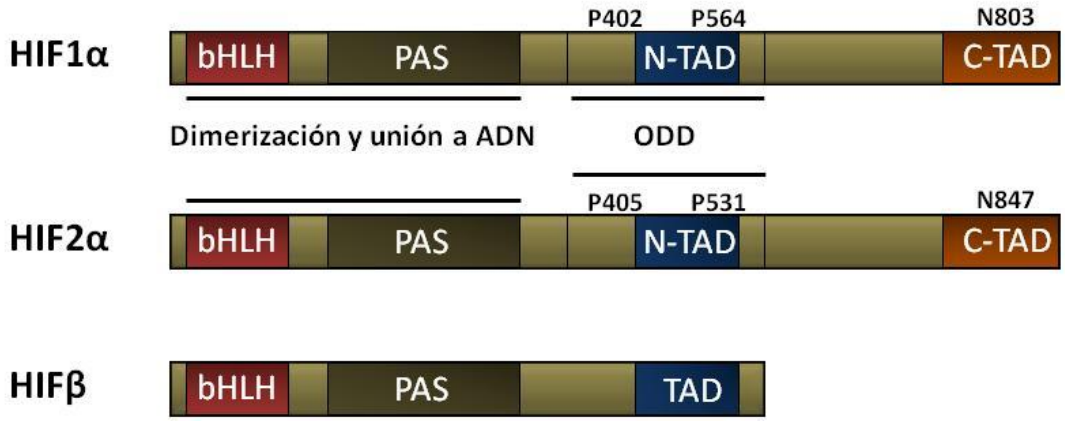

Figura 1. Dominios estructurales de HIF1α, HIF2α y HIFβ. Las tres subunidades presentan los dominios bHLH y PAS responsables de la dimerización y de la unión al ADN. Todas poseen dominios de transactivación TAD. Las subunidades HIF1α y HIF2α presentan dominios de degradación dependiente de oxígeno (ODD) en los que se resaltan las prolinas críticas susceptibles de hidroxilación. También se señala la asparragina hidroxilable del dominio C-TAD en cada una de las subunidades HIF1α y HIF2α que regula su activación transcripcional.

2.2. Regulación de su estabilidad y actividad.

La regulación tanto de la expresión como de la actividad del factor de transcripción HIF ocurre a través de modificaciones postraduccionales en la subunidad α, siendo la expresión de la subunidad β constitutiva. Las subunidades HIFα, en cambio, en presencia de O_2 (normoxia) tienen una vida media de unos 5 minutos, mientras que en hipoxia, cuando la concentración de O_2 se hace limitante, su vida media se incrementa sustancialmente y aumenta su expresión. La base molecular de esta regulación en función de los niveles de O_2 está mediada por la hidroxilación de las subunidades HIFα por una familia de proteínas dioxigenasas dependientes de 2-oxoglutarato, hierro y O_2, denominadas PHDs (proteínas con dominio prolil-hidroxilasa) (Bruick and McKnight, 2001; Epstein et al., 2001). Estas PHDs son consideradas los sensores de O_2 de la célula. Así, en normoxia, las PHDs tiene suficiente O_2 para la hidroxilación de las subunidades HIFα en dos residuos de prolina críticos situados dentro del dominio de degradación dependiente de O_2 (ODD) (Jaakkola et al., 2001) (ver Figura 1). Estos residuos hidroxilados son reconocidos por la proteína Von Hippel

Lindau, VHL, que forma parte de un complejo E3 ubiquitín-ligasa que ubiquitina a las subunidades HIFα hidroxiladas, desencadenando su degradación por el proteasoma (Ivan et al., 2001; Jaakkola et al., 2001). En hipoxia, sin embargo, las PHDs no disponen de suficiente O_2 para hidroxilar las subunidades HIFα, éstas escapan a la degradación vía VHL y por lo tanto su expresión aumenta. Como consecuencia, la subunidad HIFα se transloca al núcleo donde heterodimeriza con la subunidad HIFβ y promueve la transcripción de sus genes diana (Semenza, 2003a) (Figura 2). Un aspecto fundamental de las PHDs es que son las enzimas más sensibles a O_2 conocidas hasta la fecha, de modo que no es necesario que se alcancen situaciones cercanas a la anoxia para que su actividad se inhiba. Su afinidad por el O_2 es muy baja, por lo que en condiciones moderadas de O_2 (< 5% O_2) la actividad de las PHDs ya empieza a comprometerse (Ehrismann et al., 2007; Koivunen et al., 2007). Este es un aspecto clave desde el punto fisiológico ya que la inhibición de las PHDs (y por tanto la activación de los factores HIF) tiene lugar dentro de un rango fisiopatológico que permite, entre otros aspectos, adaptar a las células antes de que puedan encontrarse en situaciones de hipoxia más severa y deletérea para ellas.

Como se ha mencionado anteriormente las subunidades HIFα tiene dos dominios de transactivación, N-TAD y C-TAD. N-TAD es constitutivamente activo y puede funcionar tan pronto como las subunidades HIFα se estabilizan. Sin embargo, el domino C-TAD supone un segundo punto de regulación dependiente de la disponibilidad de O_2, ya que media la interacción con las histonas acetiltransferasas p300 y CBP, que funcionan como co-activadores facilitando la apertura de la estructura de la cromatina a una conformación más permisiva para la transcripción (Arany, 1996; Ema et al., 1999). Esta interacción está controlada por la hidroxilación de un residuo de asparragina situado en el C-TAD (en posición 803 para HIF1α y 847 para HIF2α) que es llevada a cabo por otra dioxigenasa, también dependiente de O_2, denominada Factor Inhibidor de HIF (FIH) (Hewitson et al., 2002; Lando et al., 2002; Mahon et al., 2001). Esta hidroxilación impediría la interacción de C-TAD con p300 y CBP. De manera análoga a lo que ocurre con las PHDs, en condiciones de hipoxia la actividad asparragina-hidroxilasa de FIH se reduce, lo que conlleva una disminución de la hidroxilación de C-TAD que permite la interacción con p300/CBP, promoviéndose la activación transcripcional de HIF1α o HIF2α. Es relevante el hecho de que FIH presenta una mayor afinidad por el O_2 que las PHDs, por lo que para que FIH se inhiba completamente es necesario que la hipoxia sea más severa que la que se necesita para inhibir las PHDs (Dayan et al., 2006; Koivunen et al., 2007). De hecho existen escenarios hipóxicos moderados en los que las enzimas PHDs se encuentran

inhibidas pero en los que FIH retiene todavía su actividad, con lo que los factores HIF sólo funcionan con el dominio N-TAD. Esto permite a las células responder de forma diferencial a los distintos grados de hipoxia y ajustar así su respuesta, activando sólo el N-TAD (en hipoxia moderada) o ambos N-TAD y C-TAD (en hipoxia más severa, cuando FIH también se inhibe). También es necesario mencionar que FIH hidroxila fundamentalmente HIF1α y sólo de forma muy débil HIF2α. Este hecho se encuadra dentro de la descripción anterior de HIF2α como la isoforma que se activa en condiciones hipóxicas más moderadas, ya que desde el punto de vista funcional sólo requeriría para su activación completa la inhibición de la actividad de las PHDs. Por el contrario, la activación completa de la isoforma HIF1α necesita de la inhibición simultánea de las PHDs y de FIH.

Además de la hipoxia, se han descrito alteraciones genéticas en la maquinaria de regulación de HIF que pueden provocar su acumulación y activación constitutiva en normoxia. Un caso de especial relevancia es el del carcinoma renal de célula clara (ccRCC), un tipo de cáncer que supone el 75-80% del total de casos de carcinoma renal y aproximadamente el 2% de la totalidad de los tumores en adultos (Ferlay et al., 2010). Su formación se asocia a la inactivación en ambos alelos de VHL debida a mutaciones, deleciones o hipermetilaciones de su promotor en islas CpG. La deficiencia en la función de VHL lleva al acúmulo de HIFα independientemente de su estado de hidroxilación, dado que no puede ser ubiquitinada y degradada. Otros escenarios de acumulación no hipóxica de HIF son aquellos en los que hay una disfunción en la actividad de las PHDs que impide la hidroxilación de la subunidad α. En concreto se han identificado mutaciones que afectan a subunidades de la enzima succinato deshidrogenasa (SDH) en paragangliomas familiares (Hao et al., 2009) y a la fumarato hidratasa (FH) en cánceres renales y leiomiomas (Tomlinson et al., 2002). Estas mutaciones pueden conducir tanto a la acumulación de succinato y fumarato, que compiten con el 2-oxoglutarato en su unión a las PHDs, como a la producción intracelular de especies reactivas de O_2 (ROS) que pueden inhibir la actividad de las PHDs por oxidación del ión Fe^{2+} en su centro activo (Bell and Chandel, 2007; Guzy et al., 2007). Por último, se han descrito mutaciones de HIF2α asociadas a eritrocitosis, hipertensión pulmonar o paragangliomas que indican que son variaciones de HIF2 que aumentan su actividad (ver más abajo las respuestas comúnmente asociadas a la activación de HIF2α).

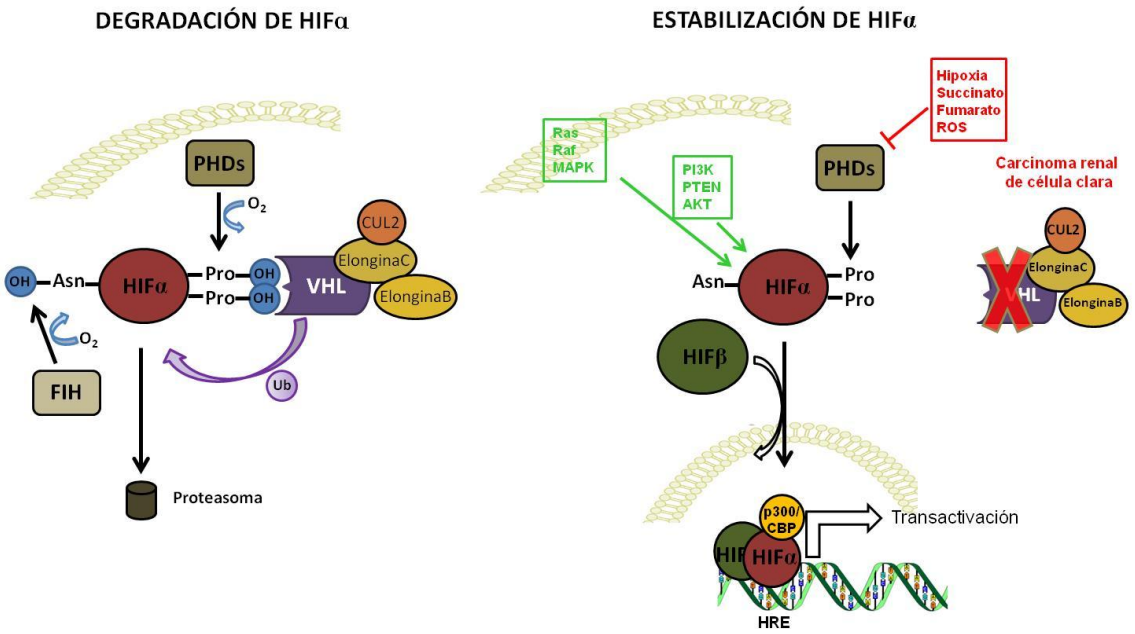

Figura 2. Mecanismo de estabilización y activación de HIF. En presencia de O_2 (parte izquierda de la figura) las enzimas PHDs hidroxilan en la subunidad HIFα los residuos de prolina (Pro), haciendo que el complejo VHL-ubiquitín ligasa la reconozca y ubiquitinice para su degradación por la vía del proteasoma. Además, FIH hidroxila un residuo de asparragina (Asn) impidiendo la unión de los co-activadores p300/CBP. En la parte derecha de la figura, la actividad de las PHDs y de FIH es inhibida por hipoxia. En normoxia esta actividad también puede ser inhibida en ciertos escenarios por determinados metabolitos intracelulares, incluyendo el succinato, el fumarato y las especies reactivas de oxígeno ROS. En todos los casos esta inhibición de las PHDs resulta en la estabilización de HIFα, su dimerización con la subunidad β, translocación al núcleo y activación transcripcional de sus genes dianas por unión a las secuencias HRE. Otros factores como Ras, Raf, MAPK, PI3K, PTEN ó Akt pueden llegar a causar también la acumulación de HIFα.

Además los factores HIFα se pueden inducir alternativamente por otros estímulos no hipóxicos como factores de crecimiento (EGF, FGF2) (Richard et al., 2000; Shi et al., 2007) y hormonas (Insulina, IGF-1, angiotensina II, trombina) (Chen et al., 2005; Gorlach et al., 2001; Page et al., 2008; Pagé et al., 2002; Zelzer et al., 1998). La mayoría de estos estímulos inducen la ruta PI3K (fosfoinosítido-3 quinasa)-AKT-mTOR que favorece la traducción de HIF1α, así como la cascada de las MAPKinasas, promoviendo en última instancia un aumento de la actividad transcripcional de HIF. También ciertos factores pro-inflamatorios como LPS, TNF-α e IL1β estabilizan HIF1α (Blouin et al., 2004; Jung et al., 2003; Zhou et al., 2003), en este caso vía NFKB, que induce la transcripción del ARN mensajero (ARNm) de

HIF1α. Se ha sugerido que esta inducción masiva del mensajero de HIF1α produce demasiada proteína para que pueda ser degradada vía PHDs aun en presencia de O_2. Además algunos de estos estímulos pueden también reducir la expresión de las PHDs y por lo tanto disminuir su actividad independientemente de las limitaciones en el aporte de O_2.

2.3. Actividad transcripcional de HIF

El dímero formado por las subunidades α y β reconoce y se une a secuencias específicas presentes en los promotores de ciertos genes denominadas elementos de respuesta a hipoxia (HREs), que contienen la secuencia conservada G/ACGTG. Ambas isoformas, HIF1 y HIF2, regulan la expresión de genes comunes, tales como VEGF-A (factor de crecimiento del endotelio vascular A) y LDH-A (lactato deshidrogenasa A), así como genes específicos para cada una de ellas, como PGK1 (fosfoglicerato quinasa 1) en el caso de HIF1α y OCT4 (del inglés *Octamer-binding protein 4)* en el de HIF2α. En la actualidad se tiene conocimiento de más de 200 genes cuya transcripción está controlada por los factores HIF. Dos aspectos a destacar entre otros de esta respuesta transcripcional dependiente de HIF son, en primer lugar, que está destinada a restaurar el suministro de O_2 y, por otra parte, que media la adaptación de las células a la escasez de O_2. En este sentido, los factores HIF regulan, entre otros, los siguientes procesos:

Activación de la eritropoiesis: en respuesta a situaciones de hipoxia sistémica el riñón produce eritropoyetina (EPO) vía HIF2, que incrementa el número de glóbulos rojos circulantes en sangre. Los factores HIF también inducen en los hepatocitos la expresión de la transferrina, principal proteína transportadora del hierro en sangre (Rolfs et al., 1997) y de su receptor en diversos tipos celulares. Otro aspecto relevante es que, además de regular la síntesis de EPO, HIF2α controla la captación de hierro de la dieta induciendo la expresión de su transportador DMT-1 (*divalent metal transporter 1*) en los enterocitos (Mastrogiannaki et al., 2009). La importancia de HIF2α en esta respuesta coordinada de inducción de EPO, eritrocitosis y control del metabolismo del hierro viene apoyada por el hecho de que, (i) tanto mutaciones que reducen parcialmente la actividad de VHL (enfermedad de Chuvash) o de PHD2 (Albiero et al., 2011), como (ii) mutaciones que producen ganancia de función en la isoforma HIF2α, desencadenan eritrocitosis patológica.

Activación de la angiogénesis: para restablecer el flujo sanguíneo a un foco hipóxico, HIF promueve la generación de nuevos vasos induciendo la expresión de

VEGF-A y la de su receptor (Flt-1) (Bergers and Benjamin, 2003; Semenza, 2003b). Brevemente, y en relación con la progresión tumoral, células embrionarias ES deficientes en HIF1α o HIF2α generan teratomas con una pobre vascularización (con baja densidad vascular, vasos de menor diámetro, palidez, zonas avascularizadas y bajo flujo sanguíneo) que se asocia a una deficiente perfusión tumoral (Acker et al., 2005; Carmeliet et al., 1998).

Reprogramación metabólica: las células en situación de hipoxia experimentan un cambio en su metabolismo que pasa de ser aerobio a anaerobio. Para ello, HIF1α estimula el flujo glicolítico a través de la inducción de varios genes que incluyen los transportadores de glucosa GLUT1 y GLUT3, las hexoquinasas HK1 y HK2 y la enzima lactato deshidrogenasa LDH-A (Firth et al., 1994; Majmundar et al., 2010)(Firth et al., 1994). Para prevenir la acidificación celular durante la glicolisis HIF también aumenta la expresión del transportador monocarboxílico 4 (MCT4) y del intercambiador de iones Na^+/H^+-1 (NHE-1) promoviendo, respectivamente, la salida de lactato y la de protones (Shimoda et al., 2006; Ullah et al., 2006). Por otro lado, el sistema de HIF disminuye la respiración hasta conseguir una reducción en el consumo de O_2 hasta aproximadamente un 15% de la tasa basal (Sridharan et al., 2008). Esto lo hace restringiendo la conversión de piruvato a acetil-CoA a través de la inducción de las enzimas piruvato deshidrogenasa quinasas 1,3 y 4 (PDK -1,-3,-4), que a su vez inhiben la actividad del complejo piruvato deshidrogenasa (PDH) (Kim et al., 2006a; Papandreou et al., 2006). La inhibición de la actividad PDH por lo tanto enlentece el ciclo de Krebs y por consiguiente la actividad mitocondrial. Además HIF1α induce la expresión de NDUFA4L2, que a su vez inhibe la actividad del complejo I mitocondrial, contribuyendo también a la inhibición del consumo de O_2 (Tello et al., 2011). HIF también disminuye la expresión de la subunidad mitocondrial SDH-B (Dahia et al., 2005) e inhibe la biogénesis mitocondrial reprimiendo c-Myc (Zhang et al., 2007), lo que también contribuye a la disminución en el consumo de O_2 en respuesta a la hipoxia. Finalmente, los factores HIF también median un cambio en los componentes de la citocromo c oxidasa (COX), induciendo COX4-2 y degradando COX4-1 (Fukuda et al., 2007), de forma que se aumenta la eficiencia del transporte electrónico.

Este cambio metabólico se ha sugerido que tiene dos funciones, por un lado ahorrar O_2 en situaciones de hipoxia y por otro atenuar el transporte de electrones en la mitocondria disminuyendo así la generación de ROS que podrían llevar a la muerte de la célula. Este segundo aspecto parece de especial trascendencia en los episodios de isquemia/reperfusión o en isquemias parciales, los cuales son escenarios donde la

formación de ROS procedentes del O_2 que llegan al tejido afectado son en última instancia los responsables de la muerte de la célula. En este sentido, numerosos estudios han demostrado que la activación del sistema HIF *in vivo* atenúa el daño oxidativo tisular en varios escenarios isquémicos como el músculo esquelético, riñón, hígado o corazón (Aragonés et al., 2008; Hill et al., 2008; Schneider et al., 2010). En cuanto a la participación relativa de cada isoforma de HIFα en este ajuste metabólico, es importante destacar que la mayoría de los cambios metabólicos mencionados en esta sección son promovidos fundamentalmente por la isoforma HIF1, al menos en células cultivadas *in vitro*. De hecho algunos cambios metabólicos asociados a represión de la proliferación (inhibición de la actividad mitocondrial y del ciclo de Krebs) están regulados por HIF1α y no por HIF2α en sistemas *in vitro*. Sin embargo hay varias evidencias *in vivo* del papel de HIF2α en la reprogramación del metabolismo celular, aunque regulando sólo alguno de los genes metabólicos que puede llegar a regular HIF1α y controlando también rutas metabólicas que no se habían identificado en los estudios *in vitro.* Es por ejemplo el caso del hígado, donde HIF2 promueve una reprogramación del metabolismo lipídico induciendo la expresión de genes involucrados en el almacenamiento de lípidos (Rankin et al., 2007). También juega un papel relevante en el músculo esquelético, donde HIF2 atenúa el metabolismo oxidativo de la glucosa a través de la activación de PDK4 vía PPARα (del inglés *peroxisome proliferator-activated receptor-α*), lo cual confiere tolerancia al daño oxidativo en situaciones de isquemia (Aragonés et al., 2008). Además HIF2 puede contrarrestar el estrés oxidativo no sólo regulando la actividad mitocondrial sino también manteniendo la homeostasis redox celular a través de la inducción de genes codificantes para enzimas antioxidantes como SOD2, y evitando así la acumulación de ROS dañinos.

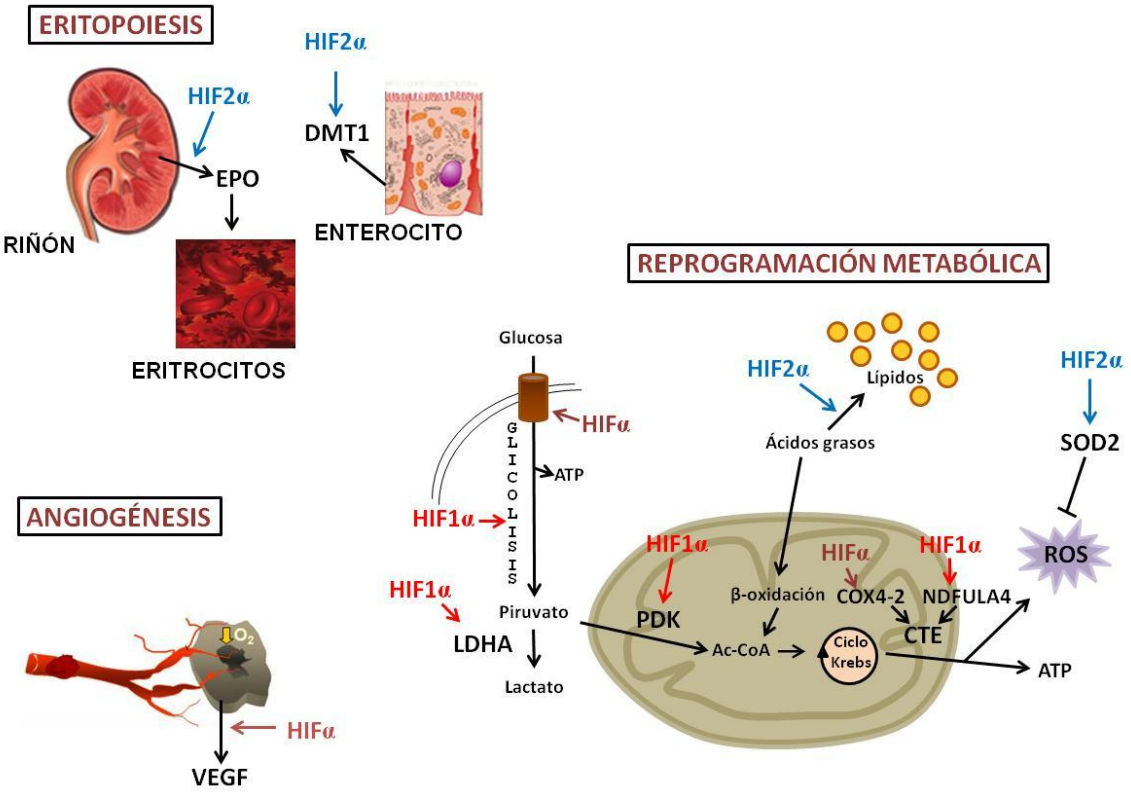

Figura 3. Respuestas centrales adaptativas de la hipoxia. La estabilización de los factores HIF activa una respuesta transcripcional destinada a: (i) restablecer los niveles de O_2 en la sangre, aumentando el número de eritrocitos y su capacidad de transporte de O_2 (mediante la inducción de EPO y de proteínas implicadas en el transporte de hierro, respuesta mediada principalmente por HIF2); (ii) restablecer el flujo sanguíneo en los tejidos hipóxicos, potenciando la angiogénesis mediante la síntesis de VEGF; y por último, (iii) adaptar el metabolismo celular a la ausencia de O_2 mediante la inhibición de la actividad mitocondrial (HIF1 por un lado favoreciendo la glicolisis y reprimiendo el ciclo de Krebs y HIF2 por otro propiciando el almacenamiento de lípidos), el aumento de la eficiencia de transporte electrónico (ambos factores HIF favoreciendo la síntesis de COX4-2 y HIF1 induciendo NDFULA4) y, como consecuencia, disminuyendo la producción de ROS (que HIF2 también mitiga mediante la inducción de enzimas antioxidantes).

3. FACTORES HIF Y PROLIFERACIÓN AUTÓNOMA DE CÉLULA.

Debido a su relevancia en esta tesis, merece una mención especial el papel de la vía de señalización de HIF en el control de la proliferación autónoma celular. Uno de los procesos biológicos fundamentales regulados por la disponibilidad de O_2 es la división celular. Los estudios en este aspecto han revelado que la hipoxia y la activación del sistema de HIF pueden desencadenar efectos opuestos, bien inhibiendo

o bien activando la proliferación. La repuesta inhibidora parece lógica en una situación hipóxica en la que la célula disminuye su actividad mitocondrial, que es esencial para generar metabolitos pro-proliferativos (como el citrato). Sin embargo, los escenarios hipóxicos no siempre se asocian a una inhibición de la proliferación, y en cierto tipo de células especializadas ésta puede ser inducida. La existencia de estas respuestas dispares pro- y anti-proliferativas sugiere la presencia de mecanismos dependientes de O_2 opuestos, capaces tanto de promover la mitosis como de inhibirla. En este sentido diferentes estudios indican que la isoforma HIF1α funciona como un atenuador de la proliferación autónoma de célula mientras que HIF2α presenta el efecto contrario. A modo de valoración, es posible que en condiciones de hipoxia moderada (en las que la actividad HIF2α puede inducirse más fácilmente, como ya se ha comentado) la cantidad de O_2 sea todavía compatible con efectos pro-proliferativos. Por el contrario, en condiciones de hipoxia más severa donde también se induce HIF1α, niveles más bajos de O_2 pueden apremiar a la célula a atenuar su proliferación.

3.1. HIF1α

Numerosos trabajos han descrito una inhibición de la progresión del ciclo celular en células sometidas a hipoxia (0,5-1% O_2), tanto en células primarias (células madre embrionarias y fibroblastos embrionarios murinos) (Carmeliet et al., 1998; Gardner et al., 2001; Mack et al., 2005), como en células transformadas (Gordan et al., 2007; Koshiji et al., 2004). Esta respuesta a hipoxia se asocia a la hipofosforilación de la proteína de retinoblastoma Rb y al consiguiente arresto del ciclo celular en la fase G1. Haciendo uso de células deficientes en HIF1α se ha podido demostrar que HIF1α antagoniza la actividad del proto-oncogén c-Myc (del inglés *Cellular Myelocytomatosis oncogene)*, lo que conlleva la inducción génica de ciertos inhibidores de quinasas dependientes de ciclina (CDKIs) claves para la transición de fase G1/S, tales como p21 y p27. A nivel molecular, HIF1α desplaza a c-Myc de los promotores de los genes a los que éste reprime - p21 y p27- (Koshiji et al., 2004, 2005). Existen estudios adicionales que indican que la inducción de p27 y el arresto de ciclo de las células en hipoxia también puede tener lugar de manera independiente de HIF1α, pero los mecanismos de esta respuesta permanecen desconocidos (Green et al., 2001). Independientemente de los efectos mediados por c-Myc y en línea con lo mencionado en el apartado anterior, los cambios metabólicos asociados a HIF1α también tienen un efecto anti-proliferativo, ya que enlentecen el ciclo de Krebs y disminuyen las reservas de citrato, que es necesario para la biosíntesis de lípidos requerida para la división celular (Wise et al., 2011).

Los primeros estudios de HIF1α en tumores demostraron que es un elemento esencial para la progresión tumoral ya que adapta a la célula a la hipoxia y promueve la angiogénesis tumoral. Sin embargo numerosos trabajos posteriores han revelado que los efectos anti-proliferativos de HIF1α pueden, en algunos tumores, llegar a ser más potentes que esos efectos pro-tumorales y que por lo tanto HIF1α puede funcionar como un elemento supresor de tumorogénesis. Este efecto anti-proliferativo de HIF1α se pone especialmente de manifiesto en el carcinoma renal de célula clara (ccRCC) anteriormente mencionado. En estas células deficientes para VHL, HIF1α y HIF2α se acumulan independientemente de su estado de hidroxilación, por lo que esta vía de señalización se encuentra constitutivamente activada. Estudios realizados en lesiones pre-neoplásicas de riñones de pacientes con deficiencia en VHL han demostrado que la activación de HIF1α ocurre en un estadío muy temprano de la evolución del tumor (Mandriota et al., 2002; Raval et al., 2005) pero que, curiosamente, su expresión disminuye y llega a perderse hasta en un 30% de los carcinomas en estadios avanzados, quedando exclusivamente presente la isoforma HIF2α (Biswas et al., 2010; Gordan et al., 2008; Maxwell et al., 1999). Estos tumores carentes de la isoforma HIF1α presentan mayor tamaño y agresividad, lo que claramente sugiere que su pérdida constituye una ventaja para la progresión de estos tumores en humanos. Estas evidencias se han visto recientemente reforzadas por la constatación de que la pérdida del cromosoma 14q (donde se encuentra el *locus* de HIF1α), es una anomalía genética muy frecuente en los carcinomas renales deficientes para VHL y está asociada a la transformación maligna de lesiones preneoplásicas (Mandriota et al., 2002) y a un peor pronóstico de estos carcinomas (Alimov et al., 2004; Kaku et al., 2004; Klatte et al., 2009; Mitsumori et al., 2002). En algunos casos, estas deleciones son focales e implican sólo la pérdida de algunos exones del gen, lo que da lugar a la expresión de formas aberrantes de la proteína que pierden por completo su capacidad para suprimir proliferación y tumorogénesis en los carcinomas deficientes para VHL (Shen et al., 2011). Además estudios genéticos han demostrado que la restauración de HIF1α en células deficientes en VHL que sólo expresan HIF2α disminuye su capacidad proliferativa y tumorogénica (Kondo et al., 2002; Raval et al., 2005; Shen et al., 2011). Por último, la inhibición de HIF1α en células de carcinoma renal deficientes para VHL que expresan las dos isoformas promueve su proliferación y favorece la tumorogénesis (Gordan et al., 2008; Shen et al., 2011).

El papel de HIF1α como supresor tumoral ha sido también documentado en otros modelos. En primer lugar destacar que el *locus* de HIF1α se ha encontrado inactivado no sólo en ccRCC sino también en otros tipos tumorales, indicando que

HIF1α podría actuar como un supresor de tumores en diferentes contextos cancerígenos (Shen et al., 2011). También mencionar que la formación de fibrosarcomas utilizando MEFs transformados se reprime tras la inactivación de VHL debido a la estabilización de HIF1α (Mack et al., 2005). Por otro lado, la inactivación de HIF1α aumenta el crecimiento de astrocitomas murinos en el parénquima cerebral (Blouw et al., 2003) y de teratocarcinomas subcutáneos procedentes de células ES (Carmeliet et al., 1998), aunque en el caso de los teratocarcinomas existen estudios contradictorios a este respecto (Hopfl et al., 2002; Ryan et al., 1998). Todos estos estudios indican que los tumores pueden llegar a prescindir de HIF1α y que el papel de HIF1α como inhibidor de la proliferación tiene un impacto en la progresión de los modelos tumorales descritos anteriormente. Es importante destacar de nuevo que la inactivación de HIF1α sólo ocurre en algunos tumores, ya que este factor transcripcional también presenta aspectos que favorecen la progresión del tumor, tales como la angiogénesis, que, según el tipo de tumor o de su localización pueden ser necesarios para su desarrollo (Blouw et al., 2003). Por lo tanto aunque inicialmente se presentó a HIF1α como un elemento esencial para la progresión tumoral, en ciertos contextos tumorales HIF1α es un freno para el crecimiento del tumor, por lo que, tras su inactivación, los tumores progresan más agresivamente.

3.2. HIF2α

Numerosas evidencias sugieren que HIF2α, al contrario que HIF1α, promueve el crecimiento tumoral en los carcinomas renales deficientes para VHL (Kondo et al., 2003; Maranchie et al., 2002; Raval et al., 2005). De hecho, estos carcinomas siempre conservan la isoforma HIF2α, y su expresión es obligada para la progresión de estos tumores, al contrario de lo que ocurre con HIF1α, que puede llegar a inactivarse (Gordan et al., 2008; Maxwell et al., 1999). En este sentido, las lesiones preneoplásicas incipientes en riñones de pacientes con carcinoma renal deficiente en VHL, ganan necesariamente la expresión de HIF2α y ésta correlaciona con mayores evidencias histológicas de malignidad (Mandriota et al., 2002). Numerosos trabajos han confirmado además que la sola sobreexpresión de una forma estable y transcripcionalmente activa de HIF2α (pero no de HIF1α) en líneas celulares de carcinoma renal con la expresión de VHL restaurada, es capaz de recuperar su capacidad para formar tumores en modelos animales (Kondo et al., 2002, 2003; Maranchie et al., 2002). En este mismo sentido, la inhibición de HIF2α es suficiente para suprimir la generación de tumores por células de carcinoma defectivas para VHL en modelos preclínicos (Kondo et al., 2003; Zimmer et al., 2004). Es importante

además destacar que un estudio reciente ha relacionado el riesgo de carcinoma renal con ciertos polimorfismos de HIF2α (Purdue et al., 2011). Este efecto pro-tumoral de HIF2α es principalmente producto de una inducción de la proliferación autónoma de célula (Franovic et al., 2009). Es además importante reseñar que dicho efecto promotor de la proliferación en células deficientes en VHL no siempre se pone de manifiesto en condiciones *in vitro*, cuando las células son cultivadas en las condiciones estándar de nutrientes y factores de crecimiento, sino que se observa cuando las células se inyectan *in vivo* para formar tumores y por tanto quedan expuestas al microambiente tumoral con deficiencia parcial en elementos nutricionales claves para la célula (ver más adelante el apartado de Discusión). El efecto pro-proliferativo y pro-tumoral de HIF2α se ha puesto de manifiesto también en otros contextos cancerígenos. Así, teratomas subcutáneos generados en ratón a partir de células ES con dos veces mayor expresión de HIF2α (células *"knock in"* del cDNA de HIF2α en el *locus* de HIF1α), mostraron un tamaño 4 veces superior al de los teratomas *wild type*, efecto principalmente debido a una proliferación exacerbada (Covello et al., 2005). También se ha demostrado que la inhibición de HIF2α reduce el crecimiento de neuroblastomas en ratones atímicos, y que la expresión de HIF2α correlaciona con estadios clínicos avanzados de estos tumores y de peor pronóstico (Holmquist-Mengelbier et al., 2006). Y la misma implicación parece que tiene lugar en la patogénesis y prognosis del cáncer de pulmón de células no pequeñas, donde algunos estudios han demostrado que la frecuente sobreexpresión de los niveles proteicos de HIF2α, al contrario que la de HIF1α, también correlaciona con una menor supervivencia (Kim et al., 2009).

En relación a este papel pro-proliferativo de HIF2α debe mencionarse que su papel no se centra exclusivamente en escenarios tumorales. Este efecto pro-proliferativo parece también relevante en la fisiología del pulmón, y en concreto en el desarrollo de la hipertensión arterial pulmonar asociada a exposiciones crónicas a hipoxia. La hipertensión arterial pulmonar se produce por un incremento en la resistencia al paso de la sangre debida a una remodelación vascular en el pulmón: la proliferación de las células SMC pulmonares (del inglés *Smooth Muscle Cells,* células de músculo liso) conduce a la muscularización de los vasos pulmonares, lo que provoca vasoconstricción. Este fenómeno ocurre tras exposiciones prolongadas a hipoxia (Stenmark et al., 2006) pero también en ciertas patologías como la policitemia de Chuvash, que también activa HIF2α en el tejido pulmonar (Bushuev et al., 2006; Smith et al., 2008). En un modelo murino que mimetiza esta patología se ha demostrado que la deficiencia en heterocigosis de HIF2α protege a estos ratones de

dicha hipertensión así como del incremento en el número de vasos pulmonares muscularizados por hiperproliferación de las células SMC (Hickey et al., 2010).

4. mTORC1.

Las células eucariotas y procariotas han desarrollado mecanismos sensores para detectar la disponibilidad de nutrientes en el ambiente intra y extracelular, y en función de ésta coordinar de forma adecuada procesos celulares clave tales como el crecimiento y división celular, la expresión génica y la mayoría de los programas de biosíntesis de macromoléculas. En eucariotas, desde levadura hasta mamíferos, dicho punto de control central es la serina/treonina quinasa TOR (del inglés *Target of Rapamycin*) (Zoncu et al., 2011). En mamíferos, en concreto, esta quinasa (denominada mTOR, del inglés *mammalian TOR*) integra múltiples vías de señalización reguladas por el estatus energético celular, los factores de crecimiento, el nivel de aminoácidos o la tensión de O_2. De esta forma promueve el crecimiento celular cuando las condiciones ambientales son favorables o bien suprime rápidamente la biosíntesis y potencia el reciclaje de proteínas y orgánulos cuando hay escasez de nutrientes, energía o una situación de estrés, proveyendo de este modo a la célula de una fuente interna de metabolitos y reduciendo o parando la tasa de proliferación para evitar un desbalance energético y la muerte celular.

4.1. Descripción molecular.

mTOR pertenece a la familia de las quinasas relacionadas con la fosfoinosítido-3-quinasa (PIKKs), con un dominio quinasa C-terminal similar a la PI3K. También posee dos dominios FRAP-ATMTTRAP (FAT) de función poco conocida y un dominio FRB (*FKBP12-rapamycin-binding*). Este último dominio media la inhibición por rapamicina, uno de los represores de mTORC1. Además posee numerosos dominios de repetición HEAT en la mitad N terminal que median sus interacciones con el resto de componentes del complejo.

mTOR es la subunidad catalítica de dos complejos diferentes denominados complejo 1 (mTORC1) y 2 (mTORC2). mTORC1 es un homodímero formado por cuatro proteínas accesorias que se unen a mTOR: Raptor (*Regulatory-Associated Protein of mTOR*), mLST8 (*mammalian Lethal with Sec13 protein 8*), PRAS40 (*Proline-Rich AKT Substrate 40 kDa*) y Deptor (*DEP-domain-containing mTOR-interacting protein*). Raptor cumple numerosas funciones: regula el ensamblaje de mTORC1,

recluta ciertos sustratos y parece que juega un papel esencial en su localización subcelular y en su capacidad para responder a las fluctuaciones en el aporte de aminoácidos (Sancak et al., 2008). El papel de mLST8 es desconocido, ya que su deleción no tiene efecto sobre la actividad de mTORC1 (Guertin et al., 2006). PRAS40 y Deptor son tanto componentes como sustratos de mTORC1 y en el estado defosfoforilado parece que reprimen la actividad de mTORC1. Cuando mTORC1 está activado, la subunidad mTOR fosforila a ambos, lo cual debilita su asociación con mTORC1 y promueve la actividad quinasa del complejo. Una característica a resaltar del complejo mTORC1 es su sensibilidad a la inhibición por el antibiótico natural e inmunosupresor rapamicina. Tras entrar en la célula, la rapamicina interacciona con alta afinidad con la proteína de unión a la inmunofilina FKBP12. El complejo droga-receptor resultante se une entonces al dominio FRB presente en la subunidad mTOR, impidiendo su unión a Raptor y limitando su acceso únicamente a ciertos sustratos.

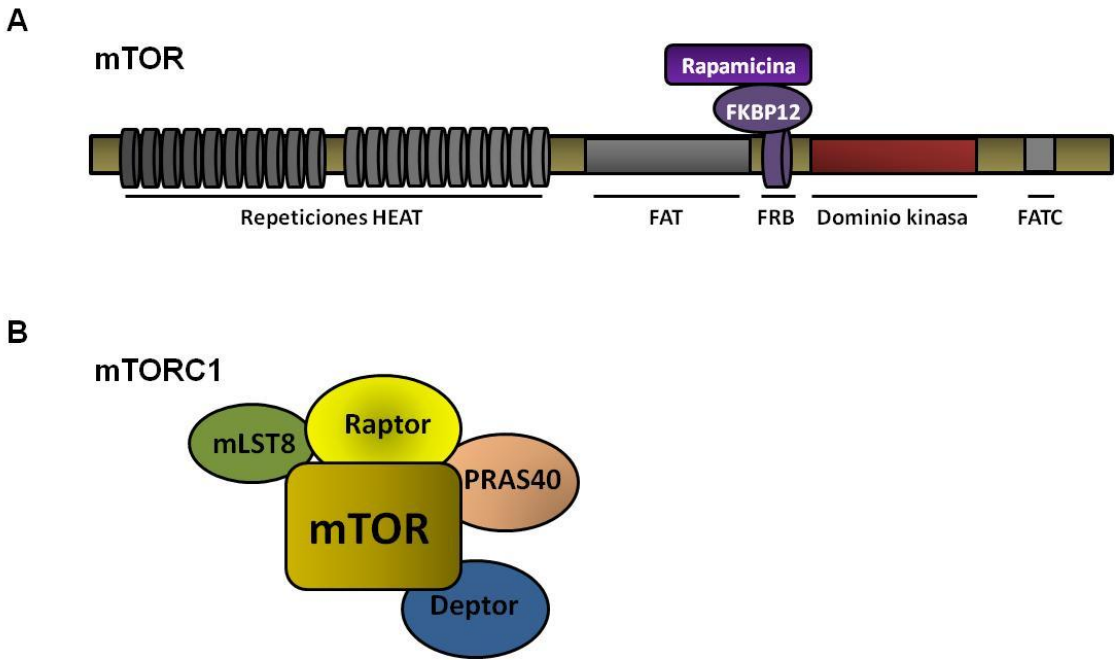

Figura 5. A) Dominios estructurales de mTOR. El extremo amino-terminal de mTOR contiene repeticiones HEAT en tandem que son dominios de interacción proteica, mientras que en en la mitad carboxi-terminal contiene un dominio FAT, seguido del dominio FRB, el dominio quinasa y por último otro dominio FAT C-terminal (FATC). La rapamicina se une a la inmunofilina FKBP12 para generar un potente y específico inhibidor de mTORC1 a través de la unión directa al dominio FRB de la subunidad mTOR. **B) Estructura del complejo mTORC1**. El complejo mTORC1 está compuesto por mTOR, Raptor, mLST8, PRAS40 y Deptor.

El complejo mTORC2 es también un multímero y, entre todos sus componentes, se define por la interacción de mTOR con la subunidad Rictor, esencial para su actividad catalítica y mutuamente excluyente con Raptor en su unión a mTOR. Tanto los estímulos que regulan su actividad como sus dianas de actuación son mucho menos conocidos que los de mTORC1, aunque se sabe que regula la fosforilación de AKT/PKB, PKCα y Rho/Rac para controlar la polaridad celular y el citoesqueleto de actina.

4.2. Regulación de mTORC1.

La regulación de mTORC1 está sometida a un estrecho control. Integra fundamentalmente cuatro grandes señales (factores de crecimiento, estatus energético, O_2 y aminoácidos) para regular numerosos procesos implicados en la promoción del crecimiento y la proliferación celular. Uno de los sensores más importantes que controlan la actividad de mTORC1 es el complejo TSC1/2 (*Tuberous Sclerosis Complex*) el cual es un represor de la actividad de mTORC1. TSC1/2 actúa como una proteína activadora de GTPasa (GAP) de una proteína G pequeña, Rheb (*Ras homolog enriched in brain*) (Avruch et al., 2009). La forma activa de Rheb, con GTP unido, interacciona directamente con mTORC1 para estimular su actividad. Con su actividad GAP, TSC1/2 regula negativamente mTORC1 convirtiendo Rheb a su forma inactiva con GDP. Consistente con este papel, mutaciones inactivantes o la inactivación del complejo TSC1/2 dan lugar al síndrome denominado esclerosis tuberosa, caracterizado por la aparición de hamartomas en múltiples órganos (Crino et al., 2006). Estos pacientes además exhiben una alta predisposición al desarrollo de RCC, aunque no se han encontrado mutaciones en TSC1 ó TSC2 en ccRCC esporádicos (Parry et al., 2001).

Factores de crecimiento

Los factores de crecimiento y hormonas relacionadas estimulan mTORC1 a través de la activación de las vías clásicas PI3K-AKT y Ras-ERK (quinasa reguladora de señales extracelulares) (Shaw and Cantley, 2006), que inducen la fosforilación de TSC2 por Akt, ERK1/2 y RSK1 (quinasa ribosomal S6-1) en varios residuos. Dichas fosforilaciones inactivan al complejo TSC1/2 y consecuentemente promueven la activación de mTORC1. Además la activación de Akt puede activar mTORC1 de forma independiente de TSC1/2 promoviendo la fosforilación y disociación de PRAS40 de mTORC1.

Estatus energético celular

Los niveles de ATP intracelulares son señalizados a mTORC1 a través de la AMPK (del inglés *AMP-activated protein kinase*), que es el principal sensor del estatus energético de la célula. En respuesta a una depleción energética (ratio ATP:ADP bajo), AMPK se activa y fosforila TSC2 en el residuo Ser1345, potenciando la actividad TSC1/2 y reduciendo por tanto la actividad de mTORC1 (Inoki et al., 2003). AMPK también puede inhibir directamente a mTORC1 en respuesta a la depleción de energía a través de la fosforilación de Raptor en dos residuos de serina bien conservados (Gwinn et al., 2008).

Niveles de O_2

Destacar que la hipoxia puede inhibir mTORC1 utilizando vías de señalización dependientes de HIF1α o totalmente independientes de HIF. En condiciones de hipoxia, de manera independiente de HIF, tiene lugar una activación de AMPK que desencadena una inhibición de la actividad de mTORC1. La hipoxia además puede activar al complejo TSC1/2 a través de la inducción transcripcional de la proteína Redd1 (*Protein Regulated in Development and DNA Damage Response 1*, también conocida como DDIT4) vía HIF1α. Redd1 regula negativamente mTORC1 mediante la liberación de TSC2 de su interacción inhibitoria con las proteínas 14-3-3, unión activada en respuesta a factores de crecimiento. Además se ha descrito que tanto el supresor tumoral promielocítico PML como la proteína inducible por HIF1α bNIP3 (*BCL2/adenovirus E1B 19 kDa interacting protein 3*), reducen la actividad de mTORC1 en situaciones de hipoxia mediante la disrupción de la interacción entre mTORC1 y Rheb. Paradójicamente, mTORC1 parece estar ampliamente activado en ccRCC deficientes en VHL, que presentan una activación constitutiva del sistema HIF. De hecho los inhibidores de mTORC1 son efectivos en el tratamiento de pacientes con carcinoma renal deficiente en VHL. Encontrar una explicación a la paradoja que supone la coexistencia de estos dos hechos aparentemente incompatibles, la inducción de HIF en tumores VHL deficientes y la activación de la ruta de mTORC1, es en sí mismo el origen de los estudios de esta tesis doctoral.

Aminoácidos

Por último, los aminoácidos representan una potente señal reguladora de la actividad de mTORC1. Una disminución en la entrada de aminoácidos depriva a la célula no sólo de sustratos para la síntesis de proteínas, sino también de intermediarios para alimentar el ciclo de los ácidos tricarboxílicos y otros procesos

metabólicos. Además una reducción en el aporte de aminoácidos inhibe la actividad de mTORC1 en proporciones variables, habiéndose encontrado que la retirada de leucina, arginina o glutamina mimetiza casi por completo la deprivación total de aminoácidos (Hara et al., 1998; Nicklin et al., 2009). La activación de mTORC1 por aminoácidos es independiente del complejo TSC1/2, ya que en células que carecen de TSC1/2 y presentan por tanto una activación constitutiva de mTORC1, su actividad sigue siendo completamente inhibible cuando el aporte de aminoácidos se reduce. La regulación de mTORC1 por aminoácidos se lleva a cabo a través de las proteínas Rag GTPasas (*Ras-related GTP-binding protein*), que se encuentran formando heterodímeros de RagA ó B con RagC ó D, en los que cada miembro del dímero tiene una carga de nucleótido opuesta. En ausencia de aminoácidos, RagA (ó RagB) se encuentran cargadas con GDP, mientras RagC (ó RagD) contienen GTP, siendo ésta la conformación inactiva del dímero. La presencia de aminoácidos causa el cambio de carga y pasa a un estado activo que le permite al dímero interaccionar de forma directa con Raptor, promoviendo la relocalización del complejo mTORC1 desde el citoplasma a la región perinuclear de endosomas tardíos y lisosomas que es donde se encuentra el activador Rheb. La disociación física entre mTORC1 y Rheb explica por qué en ausencia de aminoácidos, activadores de Rheb como los factores de crecimiento no pueden estimular mTORC1. Las proteínas Rag se anclan a las membranas lisosomales a través de una serie de proteínas adaptadoras (p14, MP1 y p18) que forman el denominado Ragulator.

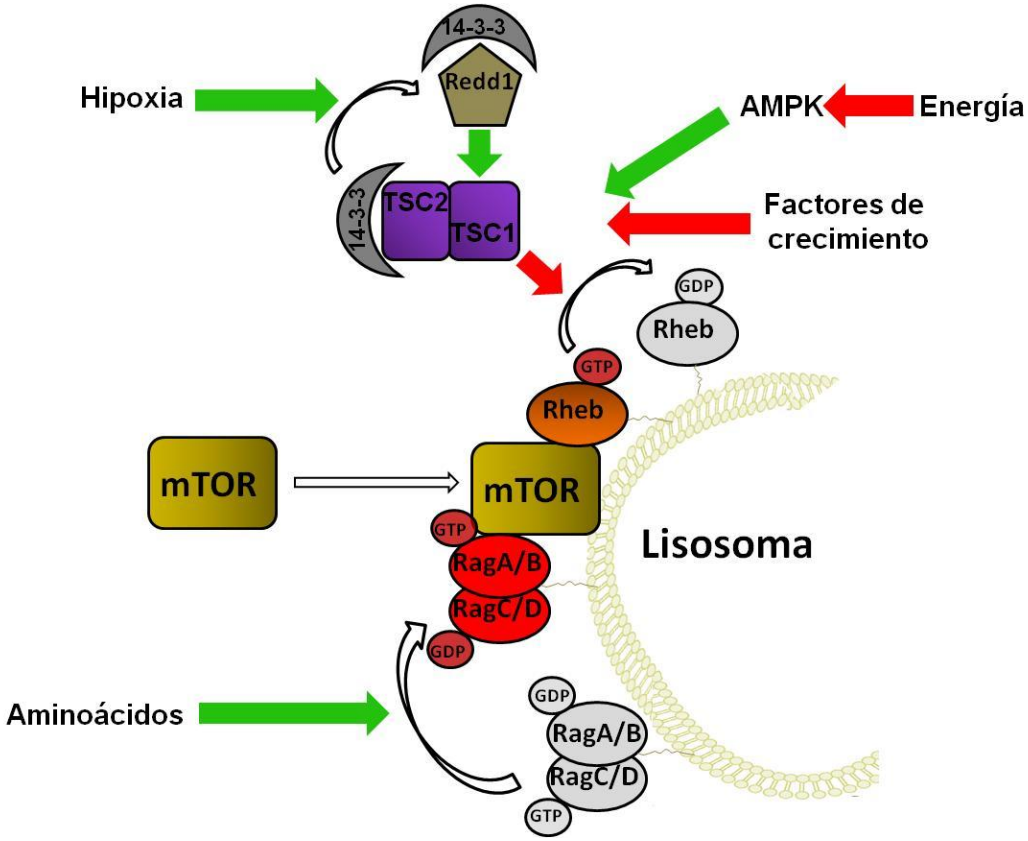

Figura 6. Regulación de mTORC1. mTORC1 integra las señales generadas por la disponibilidad de aminoácidos, la presencia de factores de crecimiento, el estatus energético celular (a través de la enzima AMPK) y la hipoxia. El primer punto de integración ocurre a nivel del complejo TSC1/2, que resulta inhibido por la fosforilación desencadenada por la señalización de los factores de crecimiento. Su fosforilación por AMPK y el secuestro de las proteínas 14-3-3 promovido por Redd1, proteína a su vez inducida por el factor HIF, conducen a la activación de TSC1/2. Este complejo inactiva a la proteína Rheb, necesaria a su vez para la activación de mTORC1. El segundo nivel de integración ocurre en respuesta a la disponibilidad de aminoácidos. En su presencia, las proteínas Rag GTPasas activas reclutan a mTORC1 a la superficie de los lisosomas, permitiendo que interaccione con su activador Rheb. Las flechas verdes indican activación y las rojas inhibición, en cada caso, de la proteína a la que apuntan.

4.3. Acciones de mTORC1.

Una de las principales funciones de mTORC1 es el control de la síntesis de proteínas en la célula. Este es un proceso energéticamente muy costoso que requiere grandes cantidades de ATP y GTP y la producción de un alto número de ribosomas. mTORC1 regula la actividad de la maquinaria celular de traducción de forma global y además controla específicamente la traducción de un grupo de ARN mensajeros (ARNm) que promueven crecimiento y proliferación celular. Estas funciones las lleva a

cabo principalmente a través de la fosforilación de sus dos sustratos mejor caracterizados: la quinasa S6K1 y la proteína de unión al factor 4E de iniciación de la traducción eucariota eIF4E (4EBP1). En respuesta a su fosforilación mediada por mTORC1, la proteína S6K1 actúa como un regulador positivo de la iniciación y elongación de la traducción a través de la fosforilación de múltiples sustratos, incluyendo a un componente de la subunidad ribosómica 40S, la proteína rpS6, además de otras tales como eEF2K, SKAR, CBP80 and eIF4B. Por otra parte, 4EBP1, en su estado defosforilado, impide con su unión a eIF4E la formación del complejo de iniciación de la traducción dependiente de cap, eIF4F. En cambio la fosforilación de 4EBP1 por el complejo mTORC1 activo permite su disociación de eIF4E y el ensamblaje del complejo eIF4F, que permite la traducción de la mayoría de ARNm, como los m^7G cap-ARNm (con un grupo metilo marcando la guanosina del extremo 5´) o los denominados 5´ TOP ARNm (con un tramo de pirimidinas en sus extremos 5´ UTR), que suelen codificar para componentes de la maquinaria de traducción.

Cuando mTORC1 está activo se induce la traducción proteica y la síntesis ribosómica, pero al inhibirse desencadena procesos de autofagia. La autofagia es la auto-degradación de los componentes celulares, desde proteínas individuales hasta orgánulos completos, con el objetivo de reciclar componentes celulares dañados, redundantes o incluso peligrosos. Supone además una importante fuente de sustratos para proveer a la célula de energía en periodos de escasez de nutrientes extracelulares. En dichas situaciones de escasez, así como en presencia de algún estrés, mTORC1 se encuentra en conformación inactiva, lo cual promueve fuertemente la autofagia. Por el contrario, en presencia de nutrientes o factores de crecimiento, mTORC1 reprime activamente la autofagia (Noda and Ohsumi, 1998) a través de la fosforilación e inhibición de las proteínas Atg13, ULK1 y ULK2, críticas en la formación del autofagosoma.

Por último, como sensor de nutrientes y factores de crecimiento que es mTORC1, dentro de sus funciones se incluye también el control de numerosas rutas metabólicas. Se ha descrito que mTORC1 se activa cuando el aporte de nutrientes es adecuado y se inhibe en periodos de ayuno. En este contexto, fundamentalmente estudiado en el hígado, se ha descrito su papel activador sobre el factor de transcripción SREBP-1 (del inglés *sterol regulatory element binding protein 1*) (Porstmann et al., 2008) y de PPARγ (Kim and Chen, 2004), dos factores de transcripción que controlan la expresión de genes codificantes para proteínas implicadas en la síntesis de lípidos y colesterol. Además, mTORC1 también regula el

metabolismo y la biogénesis mitocondrial a través del control de la actividad transcripcional de PGC1α (*PPARγ coactivator 1*) (Cunningham et al., 2007).

5. TRANSPORTADORES DE AMINOÁCIDOS.

Los aminoácidos son fundamentales no sólo por su papel en la síntesis de proteínas, sino que también funcionan como precursores de numerosos metabolitos y moléculas de señalización. En función de su modo de obtención por parte de la célula se clasifican en aminoácidos esenciales (aquellos que han de ser ingeridos en la dieta debido a que la célula no puede sintetizarlos; en humanos Valina (V), Leucina (L), Treonina (T), Lisina (K), Triptófano (W), Histidina (H), Fenilalanina (F), Isoleucina (I), Arginina (R), Metionina (M)); y los no esenciales (que pueden ser sintetizados por la célula; en humanos Alanina (A), Prolina (P), Glicina (G), Serina (S), Cisteína (C), Asparagina (N), Glutamina (Q), Tirosina (Y), Ácido aspártico (D) y Ácido glutámico (E)). Los aminoácidos atraviesan las membranas celulares mediante proteínas transportadoras que resultan esenciales no sólo para su absorción en la dieta sino también para mediar su transporte inter e intracelular. En mamíferos, estos transportadores están agrupados en 11 familias denominadas genéricamente SLC (del inglés, *solute carrier*), que a su vez están subclasificadas atendiendo a criterios funcionales tales como la preferencia de sustrato y la dependencia del ión Na^+ (Bröer and Palacín, 2011; McCracken and Edinger, 2013). Por su relevancia para este trabajo nos centraremos en describir el sistema principal de transportadores que controla la activación de mTORC1 por aminoácidos esenciales. Este transportador es un heterodímero formado por una subunidad pesada, SLC3A2, crítica para que el transportador se exprese en la superficie celular (Torrents et al., 1998) y una cadena ligera, SLC7A5, que cataliza la función de transporte (Reig et al., 2002). Las dos subunidades están unidas por un puente disulfuro conservado (Verrey et al., 2004). La proteína SLC7A5 presenta 12 dominios transmembrana (Gasol et al., 2004) y un elemento estructural característico consistente en 5 hélices transmembrana en la mitad N-terminal de la proteína que se repiten con simetría pseudo-duplicada en la mitad C-terminal (Figura 7).

Este transportador se clasifica dentro del sistema L, que agrupa a aquellos que transportan, de forma independiente de Na^+, aminoácidos grandes neutros tales como la leucina, y en concreto SLC7A5 intercambia aminoácidos neutros aromáticos o ramificados. Dentro de esta categoría están incluidos la mayor parte de los aminoácidos esenciales en humanos, tales como la fenilalanina (F), leucina (L),

isoleucina (I), valina (V), triptófano (W), histidina (H), tirosina (Y) y metionina (M), por los cuales tiene alta afinidad (Km= 50 µM) y otros no esenciales como la glutamina (Q) y la asparragina (N) por los que presenta baja afinidad (Km= 2mM) (Yanagida et al., 2001). El dímero SLC7A5/SLC3A2 funciona como un intercambiador de estequiometria 1:1, con un rango de especificidad similar para los aminoácidos importados y exportados pero una gran asimetría en la afinidad por éstos a ambos lados de la membrana plasmática (ver más adelante) (Meier et al., 2002). A pesar de la incapacidad de SLC7A5 para el importe neto de aminoácidos su sobreexpresión en células proliferantes provoca un incremento neto en la entrada de aminoácidos esenciales, que, como se ha mencionado anteriormente, son potentes activadores de mTORC1, por lo que colabora en el sostén del acelerado metabolismo tumoral y potencia su crecimiento y supervivencia. Dicha sobreexpresión de SLC7A5 se ha descrito en un amplio espectro de cánceres humanos primarios, tales como cáncer de colon, pulmón, cerebro, hígado, piel, próstata, estómago y laringe, así como en metástasis (Fuchs and Bode, 2005; Kaira et al., 2008). La inhibición de este transportador, bien mediante el uso del inhibidor competitivo BCH (ácido 2-aminobiciclo-(2, 2,1)-heptanocarboxílico) (Fan et al., 2010; Kaji et al., 2010), o bien mediante el silenciamiento de su expresión con el uso de ARN de interferencia o anticuerpos bloqueantes (Fan et al., 2010; Ohkawa et al., 2011) o a través de la sobreexpresión del miR-145 (Lee et al., 2012), disminuyen la proliferación celular, la formación de colonias y tumores e incluso la migración de las células tumorales. También se ha descrito un papel importante de SLC7A5 en la activación antigénica de linfocitos T, en los que media la entrada de los aminoácidos necesarios para su expansión clonal y su diferenciación a células efectoras (Sinclair et al., 2013).

Además de la cadena ligera SLC3A2, SLC7A5 requiere para su funcionamiento trabajar en coordinación con otro transportador de aminoácidos denominado SLC1A5, cuya expresión también se encuentra elevada en numerosos tumores humanos (Fuchs and Bode, 2005). SLC1A5, también denominado ASCT2, pertenece al sistema de transportadores neutros ASC, y transporta preferencialmente alanina (A), serina (S), cisteína (C), treonina (T) y glutamina (Q), este último con alta afinidad (Km~20 µM) (Bröer et al., 1999). ASCT2 en humanos media el intercambio electroneutro de aminoácidos neutros e iones Na^+ (Bröer et al., 2000). Debido a las diferencias de afinidad intra y extracelular que el transportador SLC3A2/SLC7A5 muestra hacia sus sustratos, la velocidad de intercambio está controlada por la concentración aminoacídica intracelular, por lo que su actividad se regula en función del flujo de entrada de aminoácidos, el metabolismo celular o la síntesis y degradación proteica

(Meier et al., 2002). ASCT2 media la entrada neta de glutamina, de forma que SLC7A5 la emplea como sustrato de intercambio para la entrada de los aminoácidos esenciales (Nicklin et al., 2009; Yanagida et al., 2001). Parece que la entrada de glutamina es el paso limitante para la regulación de mTORC1 dependiente de los aminoácidos y factores de crecimiento. Tras su entrada en la célula, el flujo de L-glutamina ocurre a los 1-2 minutos de la adición de los aminoácidos esenciales, llevando a la entrada simultánea de leucina y a la rápida activación de mTORC1 (Nicklin et al., 2009). De este modo, parece que SLC7A5 emplea el sustrato de ASCT2 para ajustar la concentración de los aminoácidos esenciales de acuerdo a las demandas metabólicas y para la señalización correspondiente a mTORC1.

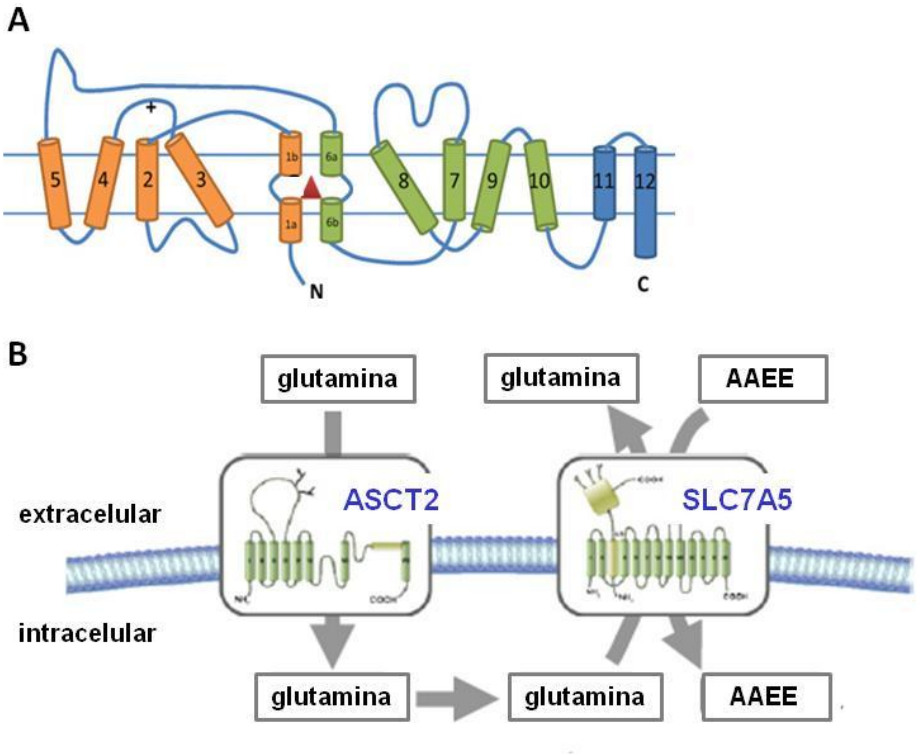

Figura 7. A) Estructura del transportador de aminoácidos SLC7A5. Presenta 12 dominios transmembrana con un motivo característico pseudo-simétrico que se repite invertido, indicado en naranja y en verde. El sitio de unión de sustrato, indicado con el triángulo rojo, se encuentra delimitado entre las hélices 1 y 6, cuya parte central se encuentra desenrollada. El símbolo + indica la posición del puente disulfuro entre SLC7A5 y la subunidad pesada SLC3A2. Figura adaptada de Bröer and Palacín, 2011. **B)** Esquema del funcionamiento coordinado de SLC7A5 y ASCT2. La entrada al interior celular de glutamina a través del transportador ASCT2 lleva a su rápido intercambio con aminoácidos esenciales mediado por el transportador SLC7A5, que se encuentra en la membrana formando un dímero con la proteína SLC3A2 (representada en amarillo). Figura adaptada de Nicklin et al., 2009.

OBJETIVOS

OBJETIVOS

El objetivo principal de este trabajo de tesis es dar respuesta a la paradoja planteada hasta el momento en la literatura científica a cerca de la coexistencia de dos procesos aparentemente incompatibles: por un lado el papel atribuido a la hipoxia como estímulo inhibidor del principal complejo regulador de la síntesis proteica, mTORC1, y por otro el papel demostrado del factor HIF2α, mediador de numerosas acciones de la hipoxia, como promotor de la proliferación en ciertos escenarios tumorales.

Con esta finalidad se plantearon los siguientes objetivos específicos:

1. Evaluación del papel de la isoforma HIF2α sobre la actividad del complejo mTORC1 en carcinoma renal.

2. Caracterización del mecanismo molecular implicado en la regulación de mTORC1 vía HIF2α. Identificación de los genes dependientes de HIF2α involucrados y caracterización de los mecanismos transcripcionales implicados.

3. Evaluación de la relevancia biológica de la ruta descrita en distintos contextos fisiopatológicos: proliferación de células de carcinoma renal de célula clara *in vitro* y formación de tumores en modelos animales preclínicos. Evaluación de la existencia de estos mecanismos dependientes de HIF2α en muestras humanas de carcinoma renal.

4. Evaluación de la regulación de mTORC1 vía HIF2α en escenarios *in vivo* no tumorales en los que HIF2α es relevante para sus funciones biológicas, tales como el pulmón o el hígado.

5. Identificación de escenarios hipóxicos *in vivo* que desencadenen la activación de mTORC1.

MATERIALES Y MÉTODOS

MATERIALES Y MÉTODOS

1. Líneas celulares y reactivos.

Se utilizó la línea celular derivada de adenocarcinoma renal humano de célula clara 786-O, deficiente en la expresión de VHL, así como esta misma línea transfectada de forma estable con los vectores retrovirales pRV-VHL y pRV vacío, para generar, respectivamente, las líneas 786-O-VHL (que expresa de forma estable el gen VHL codificante para una proteína funcional) y 786-O-pRV (células 786-O control) (Kondo et al., 2003).

También se utilizó la línea celular WT8, generada a partir de células 786-O en las que se ha restablecido la expresión de VHL de forma estable (vector pRc/CMV-HA-VHL). Estas células WT8 fueron amablemente cedidas por el Dr.Willian Kaelin (Instituto Dana-Farber, Boston, MA). A partir de este tipo celular se generaron en nuestro laboratorio mediante transducción retroviral una serie de transfectantes estables: las células WT8 HIF2α $(P\text{-}A)^2$, que expresan la construcción HIF2α P405A;P531A, una forma estable de HIF2α, carente de los residuos de prolina susceptibles de hidroxilación por las PHDs y (P405 y P531) que por tanto no puede ser degradada, siendo constitutivamente activa con independencia de la concentración de oxígeno (Kondo et al., 2003); las células WT8 HIF2α $(P\text{-}A)^2$bHLH*, infectadas con un vector que codifica para el gen HIF2α 405A;P531A;bHLH*, una versión de la forma estable HIF2α $(P\text{-}A)^2$ que contiene además la sustitución de cinco aminoácidos en el dominio *basic helix-loop-helix* (bHLH) que resulta en la pérdida de su actividad transcripcional (Kondo et al., 2003; Kondo et al., 2002); las células WT8 HIF1α $(P\text{-}A)^2$, que expresan la construcción HIF1α P402A;P564A, una forma constitutivamente activa de HIF1α, por carecer igualmente de sus residuos críticos de prolina (Yan et al., 2007); y como control de todas ellas, las células WT8 control infectadas con el vector retroviral vacío pBabe.

A partir de la línea 786-O se generaron también, mediante infección lentiviral, los transfectantes estables 786-O-shSLC7A5 y su correspondiente control 786-O-shSCR.

Todas estos tipos celulares se cultivaron en medio RPMI 1640 con GLUTAMAX-I (GIBCO) suplementado con 100 unidades/ml de penicilina, 100 µg/ml de estreptomicina y un 10% de suero fetal bovino (FBS, Cultek). Las células empaquetadoras utilizadas para la transducción (HEK293-T) se cultivaron en medio

DMEM complementado igualmente con 100 unidades/ml de penicilina, 100 µg/ml de estreptomicina y un 10% de FBS. Para preparar los medios con bajo contenido en aminoácidos se diluyó en las proporciones adecuadas medio RMPI comercial con el correspondiente volumen de RPMI libre de aminoácidos. Los medios con contenido reducido de aminoácidos esenciales y glutamina se prepararon añadiendo los correspondientes volúmenes de aminoácidos esenciales y no esenciales al medio RPMI libre de aminoácidos. Todos los medios deprivados de aminoácidos se suplementaron con un 10% de FBS dializado (Sigma-Aldrich).

Las condiciones de mantenimiento de los cultivos celulares fueron en una atmósfera al 5% de CO_2 saturada de vapor de agua y a una temperatura de 37ºC.

Los anticuerpos usados en este trabajo incluyen anticuerpos policlonales generados en conejo frente a fosfo-4EBP1 (residuos Thr37/46), fosfo-4EBP1 (residuo Ser 65), 4EBP1, fosfo-rpS6 (residuos Ser235/236), rpS6, fosfo-p70-S6K (residuos Thr389) y p70-S6K , todos ellos suministrados por Cell Signaling y usados en concentración 1:1000; anti- HIF2α (1:2000) (Abcam, ab199), anti- HIF1α murino (1:1000) (Cayman, 10006421) y anti-SLC7A5 (Abcam, ab85226). También se emplearon anticuerpos monoclonales anti- HIF1α humano (1:1000) (BD Transduction Laboratories, 610959), anti-tubulina (1:2000) (Sigma, T6199) y el anticuerpo policlonal generado en cabra frente a actina (1:1000) (Santa Cruz, I-19, sc-1616). Para la detección de los anticuerpos primarios se utilizó, según el caso, un anticuerpo anti-conejo (1:3000) (GE Healthcare, NA934V), anti-ratón (1:5000) (Pierce, 32430) o anti-cabra (1:15.000) (Novus Biologicals, NB710-H), todos ellos acoplados a HRP (*Horseradish peroxidase*).

Los anticuerpos empleados para analizar las muestras clínicas biopsiadas de pacientes fueron anticuerpos policlonales generados en conejo frente a SLC7A5 (1:1000) (Cell Signaling, 5347), CAIX (Abcam, ab15086) y Erk2 (1:1000) (c-14, Santa Cruz, sc-154).

Los anticuerpos utilizados para las tinciones inmunohistoquímicas fueron anticuerpos policlonales generados en conejo frente a SLC7A5 (1.400) (Sigma-Aldrich, SAB1500586) y frente a fosfo-rpS6 (residuos Ser235/236) (1:300) (Cell Signaling). La Rapamicina se adquirió de Sigma-Aldrich.

2. Transducción celular mediante infección viral.

La expresión estable de VHL y las formas mutadas de HIF2α y HIF1α se realizó mediante transducción retroviral. Para ello se transfectaron en placas p60 células HEK293-T con 4 ug de cada vector retroviral y 4 ug del pCL-Ampho Retrovirus Packaging Vector (Imgenex), usando Lipofectamine 2000 (Invitrogen) de acuerdo a las instrucciones del fabricante. Pasadas 48 horas de la transfección se recogió el sobrenadante celular conteniendo el virus, se filtró con filtros de 0,22 µm, se diluyó 1:2 con medio fresco y se le añadió polibreno a una concentración final de 6 µg/ml. Este medio con retrovirus se añadió a las células 786-O y WT8 plaqueadas inicialmente a una confluencia del 20%. El proceso se repitió nuevamente los dos siguientes días, transcurridos los cuales se seleccionaron las células infectadas añadiendo en el medio de cultivo neomicina (para los vectores pRV) o puromicina (para los vectores pBabe) a una concentración final en ambos casos de 1 µg/ml.

Para inhibir de forma estable la expresión de SLC7A5 se cultivaron durante 24 horas las células 786-O con las partículas lentivirales comerciales (Santa Cruz Biotechnology) de *small hairpin* (shARN) frente a SLC7A5 (sc-62555-V) y su correspondiente control shSCR (sc-108080), de acuerdo a las instrucciones del fabricante. Posteriormente se seleccionaron las células infectadas con puromicina a una concentración final de 1 µg/ml.

3. Modelos animales.

Los ratones Vhl^{floxed}-UBC-Cre-ER^{T2} se generaron cruzando los ratones C;129S-*Vhlh*^{tm1Jae}/J (Jackson Laboratories, stock no. 4081), que contienen dos sitios loxP flanqueando el promotor y el exón 1 del locus murino Vhl (Haase et al., 2001), con los ratones B6.Cg-Tg(UBC-Cre/ER^{T2})1Ejb/J (Jackson Laboratories, stock no. 008085), que expresan de forma ubicua la recombinasa Cre (Cre-ER^{T2}) (Ruzankina et al., 2007).

Los ratones Vhl^{floxed} HIF2α^{floxed}-UBC-Cre-ER^{T2} se generaron a través de los cruces apropiados usando los ratones Epas1tm1Mcs/J (Jackson Laboratories, stock no. 008407), que contienen dos sitios loxP flanqueando el exón 2 del locus de HIF2α.

Los ratones fueron criados en el área específica libre de patógenos del animalario de la Universidad Autónoma de Madrid (UAM). Todos los procedimientos experimentales fueron aprobados por el Comité Ético de Investigación de la UAM y se llevaron a cabo bajo la supervisión del Responsable del Animalario de la UAM de

acuerdo con la normativa española y europea (B.O.E, 18 March 1988, and 86/609/EEC *European Council Directives*).

El genotipaje de los ratones se llevó a cabo a partir de una biopsia de la cola, que fue incubada durante 16 horas a 56ºC con 200µl de tampón de lisis (100mM Tris/HCl pH8, 5mM EDTA, 0,2% SDS, 200mM NaCl) y proteinasa K a una concentración final de 100µg/ml. Tras eliminar por centrifugación los restos celulares, se precipitó del sobrenadante obtenido el ADN por adición de isopropanol en volumen 1:1. Este ADN genómico se caracterizó mediante PCR usando los oligonucleótidos descritos en la **Tabla I**.

Diana	Especie	Dirección (5´->3´)	Secuencia
VHL	Ratón	F	CTCAGGTCATCTTCTGCAACC
		R	TCTGTCTTGGCCTCCTGAGT
HIF2α	Ratón	F	GAGAGCAGCTTCTCCTGGAA
		R	TGTAGGCAAGGAAACCAAGG
Cre	Ratón	F	GCGGTCTGGCAGTAAAAACTATC
		R	GTGAAACAGCATTGCTGTCACTT

Tabla I: Secuencias de oligonucleótidos. Parejas de oligonucleótidos empleados para la amplificación por PCR.

Para la inactivación génica, los ratones Vhl^{floxed}-UBC-Cre-ER^{T2} y Vhl^{floxed} $HIF2\alpha^{floxed}$-UBC-Cre-ER^{T2} fueron alimentados a voluntad durante 10 días con una dieta que contienen 400mg de citrato de 4-hidroxi-tamoxifeno/Kg dieta Teckland CRD TAM^{400}/CreER (Harlan Teklad). Tras este periodo de tiempo con esta dieta se les volvió a alimentar con una dieta estándar para ratón (Safe®, Augy, France) durante 10 días más. Para someter a los ratones *in vivo* a hipoxia se les emplazó en una cámara hermética con válvulas de entrada y salida de aire insuflada con una mezcla de 10% de O_2 y 90% de N_2 (Carburos Metálicos).

4. Inmunodetección de proteínas mediante Western Blot.

Las células, tras lavarse con PBS frío, se lisaron en Laemmli (2% SDS, 10% glicerol, 10mM DTT, 62mM Tris pH 6,8 y 0,004% de azul de bromofenol). Los pulverizados de los hígados y pulmones murinos se homogeneizaron en tampón de lisis (50mM Tris HCl, pH 7,4, 1% Triton X-100, 0,2% SDS, 1 mM EDTA) suplementado con inhibidor de proteasas libre de EDTA e inhibidor de fosfatasas (ambos de Roche) y se cuantificaron mediante BCA (Bicin-Choninic Acid Protein Assay Kit, Pierce). Las proteínas contenidas en estos lisados se resolvieron en geles de poliacrilamida-SDS al 8 o al 10% y posteriormente se transfirieron a membranas de nitrocelulosa (Bio-Rad). Las membranas se bloquearon con TBS-T (50mM Tris HCl, pH 7,6, 150mM NaCl pH, 0,1% Tween-20) y 5% de leche en polvo desnatada y se incubaron al menos 16 horas a 4ºC en cámara húmeda con los anticuerpos primarios correspondientes. Tras la incubación, se lavaron las membranas con TBS-T para eliminar el exceso de anticuerpo primario y se incubaron con los respectivos anticuerpos secundarios. La unión del anticuerpo se detectó mediante quimioluminiscencia potenciada (SuperSignal West Femto Maximum Sensivity Substrate, Thermo Scientific) y se visualizó con un analizador de imagen (Image Quant LAS400 mini).

5. Silenciamiento génico mediante siARN.

Los silenciamientos se realizaron mediante ARN de interferencia utilizando oligonucleótidos siARN humanos dirigidos frente a SLC7A5, RagA, RagB y *non-targeting pool* como control (siSCR), todos ellos SMARTpool de Dharmacon; así como frente a HIF2α (MISSION HIF2α siARN, SASI_Hs_00019152) y su correspondiente control MISSION siARN *Universal Negative Control #1* (siSCR) de Sigma. Las células se transfectaron con dichos siARNs a una concentración final de 100nM usando Lipofectamine 2000 (Invitrogen) según las instrucciones del fabricante. Tres días después de la transfección se analizó el grado de interferencia y el efecto de la misma en los distintos procesos analizados.

6. Extracción de ARN y PCR cuantitativa a tiempo real.

El ARN total procedente de células se aisló mediante el uso de Ultraspec (Biotecx) según las especificaciones del fabricante. Los hígados y pulmones murinos fueron homogeneizados en Trizol (Invitrogen) con dos ciclos de congelación/descongelación. El ARN total fue aislado usando el RNeasy ARN

extraction kit (Quiagen). El ARN extraído se cuantificó usando el Nanodrop (ThermoFisher Scientific; Waltham). Se usó 1µg de ARN para retrotranscribir a ADNc (Improm-II reverse transcritase, Promega), y se utilizó 1µl del ADNc resultante como molde para las reacciones de amplificación llevadas a cabo con Power SYBR Green PCR Master Mix kit (Applied Biosystems). Los datos se analizaron con StepOne Software versión 2.0 (Applied Biosystems). Para cada muestra se realizaron medidas por duplicado y todos los valores se normalizaron en base a los niveles de expresión del gen *Hprt*. Las parejas de oligonucleótidos usados para las amplificaciones se diseñaron de forma que hibridaran en distintos exones para evitar de este modo amplificaciones de ADN genómico. Dicho diseño se realizó con ayuda del programa Primer Express. Las parejas de oligonucleótidos usados se especifican en la **Tabla II**.

Diana	Especie	Dirección (5´->3´)	Secuencia
OCT4	Humano	F R	GCTTAGCTTCAAGAACATGTGTA CTCTCACTCGGTTCTCGAT
SLC7A5	Humano	F R	GGAACATTGTGCTGGCATTATACA CCTCTGTGACGAAATTCAAGTAATTC
bNIP3	Humano	F R	GTCTGGACGGAGTAGC GGCCGACTTGACCAAT
SLC7A5	Ratón	F R	GTGGAAGAACAAGCCCAAGTG GGCAGAGCACCGTCACAGA
VHL	Ratón	F R	TCAGCCCTACCCGATCTTACC ATCCCTGAAGAGCCAAAGATGA
HIF2α	Ratón	F R	CCTGGCCATCAGCTTCCTT GGTCGGCCTCAGCTTCAG
PGK-1	Ratón	F R	GGTGCTCAACAACATGG CAATCTGCTTAGCCCGA
HPRT1	Humano	F R	ATTGTAATGACCAGTCAACAGGG GCATTGTTTTGCCAGTGTCAA
HPRT1	Ratón	F R	GTTAAGCAGTACAGCCCCAAA AGGGCATATCCAACAACAAACTT

Tabla II: **Secuencias de oligonucleótidos**. Parejas de oligonucleótidos usados para la amplificación por PCR a tiempo real.

7. Ensayos de inmunoprecipitación de cromatina (ChIP).

Los distintos transfectantes estables de las líneas WT8 y 786-O se cultivaron en placas de 10cm hasta una confluencia de 85% y se fijaron con 1% (v/v) de formaldehido (concentración final) durante 12 minutos a 37ºC. A continuación se lavaron con PBS frío y posteriormente se lisaron en 1ml de tampón de lisis (1% SDS, 10 mM EDTA, 50 mM Tris/HCl, pH 8.1, y el inhibidor de proteasas Complete (Roche Diagnostics)). Los lisados celulares se incubaron en hielo durante 10 minutos y después se sonicaron bajo las condiciones establecidas para cortar el ADN en fragmentos que se encuentren entre 200 y 1500 pb. Seguidamente se retiró el material insoluble por centrifugación y fueron recogidos y guardados 30µl de cada muestra (*Input*). El resto se diluyó en tampón de inmunoprecipitación (1% Tritón X-100, 2 mM EDTA, 150 mM NaCl y 20 mM Tris/HCl, pH 8.1). Los lisados fueron preclareados con suero preinmune y 200µg de ADN de esperma de salmón/Proteína A agarosa (Upstate Biotechnology) durante 1h a 4ºC. Las muestras se inmunoprecipitaron dos veces, inicialmente con suero de conejo durante 6h (IgG control) y después durante la noche a 4ºC con los anticuerpos policlonales anti-HIF2α (Novus Biologicals, NB100-132) o anti-HA (Abcam, ab9110). Los inmunocomplejos se recuperaron por la adición 400µg Proteína A agarosa a las muestras y posteriormente se lavaron repetidamente durante 15 minutos en TSE I (0.1% SDS, 1% Tritón X-100, 2 mM EDTA, 20 mM Tris/HCl, pH 8.1 y 150 mM NaCl), TSE II (0.1% SDS, 1% Tritón X-100, 2 mM EDTA, 20 mM Tris/HCl, pH 8.1 y 500 mM NaCl) y tampón III (0.25 M LiCl, 1% Nonidet P40, 1% deoxicolato, 1 mM EDTA y 10 mM Tris/HCl, pH 8.1). Finalmente, los complejos, se lavaron dos veces con tampón TE (10 mM Tris, pH 8.0, y 1 mM EDTA) y fueron extraídos dos veces con un tampón que contiene 1% SDS y 0.1 M $NaHCO_3$. Las proteínas fueron extraídas por adición de proteinasa K (30 µg/muestra) durante 2h a 42ºC, y el ADN fue purificado usando un kit de extracción PCR de Qiagen, eluyendo en 50 µl de agua. El ADN inmunoprecipitado fue amplificado por RT- PCR para evaluar la unión de HIFα al promotor proximal de *Slc7a5*, usando los siguientes oligonucleótidos: en el promotor proximal del gen (forward, 5´-TCGGTTCTTCCCTCGTC-3´; reverse, 5´-GGAACCTAGGCTCCTGT-3´); en el intrón 1 del gen (forward, 5´-TTTACGTTCCTGGACCATCC-3´; reverse, 5´-CAAGAGGCTGGGAGTATTGC-3´). Para la evaluación de la unión de la isoforma HIF1α a las secuencias reguladoras del gen Pdk1 se realizaron RT-PCR usando los oligonucleótidos previamente descritos (Kim et al., 2006a; Papandreou et al., 2006): región #1 de Pdk1 positiva para la unión (forward, 5´- CGCGTTTGGATTCCGTG-3´; reverse, 5´-CCAGTTATAATCTGCCTTCCC TATTATC-3´); región #2 de Pdk1 negativa

para la unión (forward, 5´- AAAGGACATTCTACAACGATTCTGC-3´; reverse, 5´-CAATTGTCTGGTTACTGAAAGTCTCC-3´).

8. Generación de tumores en ratones inmunodeficientes.

Un total de 18 ratones inmunodeprimidos SCID (Charles Rivers) fueron inoculados subcutáneamente con células 786-O infectadas establemente con el shARN control (786-O-shSCR) o con shARN frente a SLC7A5 (786-shSLC7A5). Estando las células 786-O en su fase exponencial de crecimiento se tripsinizaron y resuspendieron en medio RPMI sin suero. Cada ratón fue inyectado en cada flanco dorsal con 4,4 x 10^6 células en 0,2ml de medio. En el flanco izquierdo se inocularon las células control y en el flanco derecho las células con la expresión de SLC7A5 silenciada. A partir del día 15 tras la inyección se monitorizó semanalmente la presencia y tamaño de la masa tumoral con calibres digitales en diámetros perpendiculares. El volumen de los tumores se calculó usando la fórmula [D*d*d]/2, donde “D” es el diámetro más largo del tumor y “d” el más corto. Los animales fueron humanamente sacrificados de acuerdo con las recomendaciones y procedimientos del comité de bioética para este experimento concreto (CBA PA 77_2011-v2).

9. Inmunodetección proteica en el material clínico tumoral.

Las muestras renales humanas procedentes de biopsias se obtuvieron de pacientes diagnosticados y tratados quirúrgicamente en el Servicio de Urología del Complejo Universitario de Albacete bajo la supervisión del comité ético local y fueron analizadas histológicamente por el Servicio de Patología. Todos los casos fueron revisados y diagnosticados de acuerdo a la clasificación de la Organización Mundial de la Salud. Los tejidos fueron disgregados usando el *Polyton dispersing system PT-2100* (Kinematica AG) en tampón de lisis (100mM HEPES, pH 7.5, 50mM NaCl, 0,1% Triton X-100, 5mM EDTA, 0,125M EGTA) con inhibidores de proteasas y fosfatasas (0.2 mg/ml Leupeptina, 2mg/ml, Aprotinina, 1mM PMSF and 0.1mM Na_3VO_4). Tras cuantificar las muestras por BCA (Pierce) se cargaron en geles de poliacrilamida-SDS del 6 ó 12% 100 µg de proteína procedente del tejido neoplásico y del tejido sano renal adyacente y una vez separadas las proteínas se transfirieron a una membrana de PVDF, donde se analizaron empleando los anticuerpos anteriormente descritos.

10. Inmunodetección de proteínas mediante inmunohistoquímica.

Para realizar el análisis inmunohistoquímico se procedió a la inclusión en parafina de los hígados y pulmones murinos tras haberlos fijado con paraformaldehido al 4% durante 16 horas. A continuación las secciones de los tejidos se colocaron en portaobjetos y se sometieron a eliminación de antígenos inducida por microondas (15 minutos a 240W) en citrato de sodio 0,01M a pH 6. La peroxidasa y biotina endógena fueron bloqueadas usando H_2O_2 al 0,3% en metanol y un kit de bloqueo de avidina/biotina (Vector Laboratories), respectivamente. Las secciones se incubaron durante 16 horas con los anticuerpos anteriormente descritos. La unión de los anticuerpos se detectó usando un kit LSAB+Peroxidasa con 3, 3´-diaminobencidina como cromógeno (Dako), de acuerdo a las recomendaciones del fabricante. Finalmente las seccciones fueron deshidratadas y montadas con medio de montaje Eukitt (Sigma-Aldrich).

11. Análisis estadístico de los datos.

Los datos experimentales se analizaron con PrismTM GraphPad (versión 5.00) software, de los cuales se muestra el valor medio ± el error estándar de la media (SEM). Las diferencias estadísticas entre los grupos se analizaron usando el test de Student.

RESULTADOS

RESULTADOS

1. La activación de mTORC1 es inducida específicamente por la isoforma HIF2α.

Con el fin ya comentado de evaluar el papel de HIF2α en la regulación de la actividad de mTORC1 empleamos como primera aproximación el modelo celular WT8, de uso muy extendido en el estudio de las funciones biológicas de HIF2α (Kondo et al., 2002, 2003; Raval et al., 2005). Estas células derivan de la línea de carcinoma renal de célula clara 786-O que únicamente expresa la isoforma HIF2α, en la que se ha restaurado la expresión de una proteína VHL funcional, por lo que la ruta de HIF (en este caso sólo HIF2α) se regula normalmente en hipoxia. Estas células WT8 "normalizadas" se han utilizado ampliamente para estudiar las funciones de HIF2α expresando exógenamente en ellas formas constitutivamente estables de HIF2α (Kondo et al., 2002, 2003). Así, utilizando como base las células WT8, generamos un nuevo transfectante estable que expresaba una variante de HIF2α constitutivamente activa con los dos residuos de prolina hidroxilables mutados por alaninas, denominada HIF2α(P-A)^2. Esta forma no puede por tanto ser degradada por VHL y es constitutivamente activa en normoxia. Además se generó otra línea estable que expresaba esa misma forma de HIF2α pero con el dominio de unión a ADN mutado y por lo tanto transcripcionalmente inactiva (denominada HIF2α(P-A)^{2}bHLH*) (Figura 8).

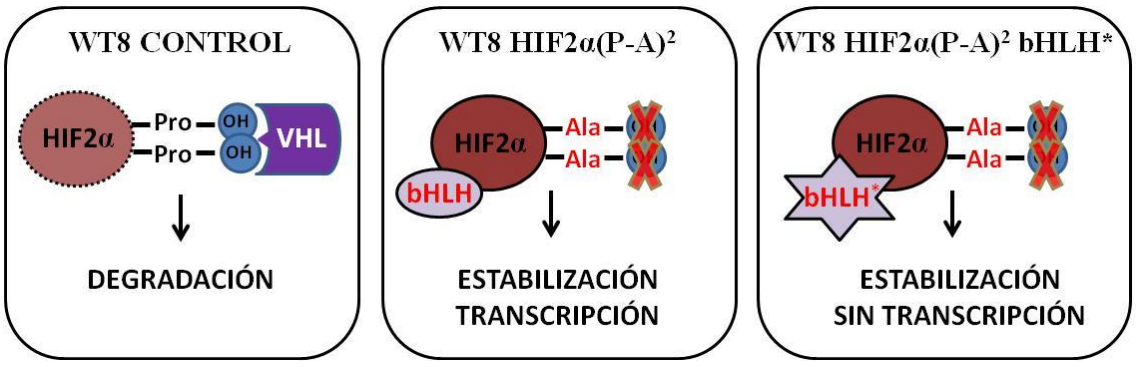

Figura 8. Modelo celular empleado y su regulación por VHL. Para el estudio del efecto de HIF2α sobre la activación de mTORC1 se emplearon las células WT8 procedentes de la línea de carcinoma renal de célula clara 786-O transfectada establemente con un gen *Vhl* funcional. Estas células WT8 se infectaron a su vez para expresar de forma estable un plásmido codificante para la forma constitutivamente estable y transcripcionalmente activa HIF2α(P-A)^2, para la forma constitutivamente estable pero transcripcionalmente inactiva HIF2α(P-A)^{2}bHLH* o con el plásmido vacío (células WT8 control).

En la Figura 9 se puede observar que ambas formas de HIF2α se expresaron de forma eficiente en las células WT8 HIF2α(P-A)^2 y WT8 HIF2α(P-A)^{2}bHLH*, comparada su expresión con las células WT8 control infectadas con el vector vacío. Como control interno de la actividad de estas versiones de HIF2α, evaluamos la expresión del gen *Oct4*, un gen diana bien conocido específico de la subnidad HIF2α (Covello et al., 2005). Como esperábamos, los niveles de ARN mensajero (ARNm) de dicho gen aumentaban en las células WT8 HIF2α(P-A)^2 respecto a las WT8 control pero esto no ocurría en las células WT8 HIF2α(P-A)^2 bHLH* (Figura 9).

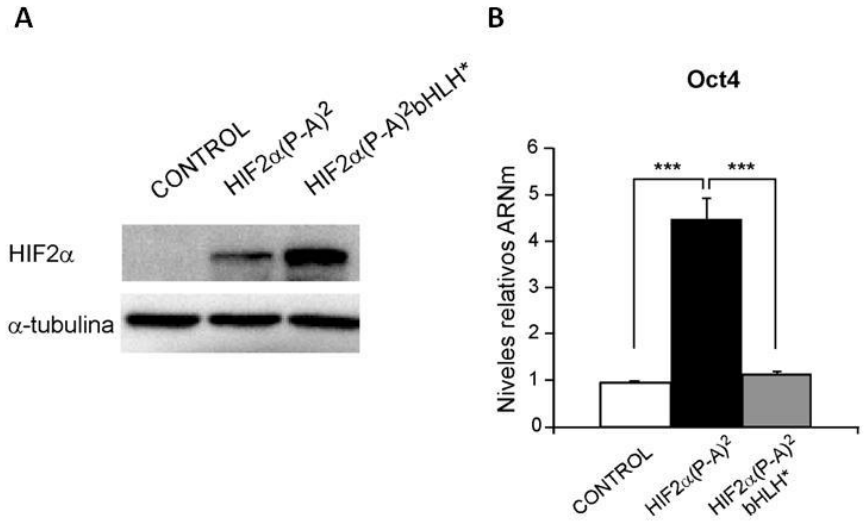

Figura 9. Análisis de la expresión proteica y de la actividad transcripcional de HIF2α(P-A)^2 y HIF2α(P-A)^{2}bHLH*. (A) Se analizaron mediante Western blot los niveles proteicos de HIF2α y α-tubulina en lisados totales de células WT8 infectadas con el vector lentiviral vacío (WT8 control) o con las construcciones retrovirales HIF2α(P-A)^2 y HIF2α(P-A)^{2}bHLH*. **(B)** Se analizaron mediante RT-PCR cuantitativa los niveles relativos de ARNm del gen *Oct4* en estos mismos tipos celulares normalizados con respecto a la expresión de *Hprt*. Se muestra la media; las barras de error representan el SEM; n= 6; ***p<0,001.

A continuación quisimos evaluar la actividad de mTORC1 en cada uno de estos tipos celulares y lo hicimos determinando el estado de fosforilación de sus dos dianas más comúnmente usadas para este fin (Cam et al., 2010; Sonenberg and Hinnebusch, 2009), las proteínas 4EBP1 y rpS6. Los niveles de fosforilación de ambas proteínas

fueron ensayados con los anticuerpos frente los residuos fosforilados Ser^{65} y $Thr^{37/46}$ de 4EBP1 y $Ser^{235/236}$ de rpS6 (ver Introducción). Nuestros primeros datos revelaron que (i) los niveles basales de fosforilación de 4EBP1 y rpS6 estaban ya elevados en las células control WT8 y (ii) que estos niveles eran similares en las células WT8 HIF2α(P-A)^2 y WT8 HIF2α(P-A)^{2}bHLH* (Figura 10). En este sentido, se observa que la mayor parte de la proteína 4EBP1 estaba presente en la banda superior en los tres tipos celulares, indicativo de un estado de hiperfosforilación y por tanto de activación de mTORC1.

En base a estos datos razonamos que quizá las condiciones de cultivo comúnmente usadas para cultivar estas células (RPMI 1640) eran responsables del elevado nivel de activación de mTORC1 en todas ellas, y que esto podría estar por tanto enmascarando un posible papel de HIF2α sobre la actividad de mTORC1. Quisimos entonces investigar si la forma HIF2α(P-A)^2 podría inducir la actividad basal de mTORC1 en células WT8 control cuando su actividad basal estuviera disminuida. Dado que la actividad de mTORC1 es dependiente de la concentración extracelular de aminoácidos (Hara et al., 1998; Nicklin et al., 2009; Wang et al., 1998), decidimos cultivar las células en un medio de cultivo con el 50% de la concentración normal de aminoácidos. Se ha considerado que unas condiciones más limitantes de aminoácidos son más similares a las que las células tanto tumorales como no tumorales experimentan *in vivo* con lo cual podrían considerarse más adecuadas para investigar la función de HIF2α sobre mTORC1. En estas condiciones limitantes comprobamos en las células WT8 control, mediante Western blot, que la proteína 4EBP1 total se encontraba mayoritariamente presente en la banda inferior, lo cual es indicativo de un estado de hipofosforilación y por tanto de inactivación de mTORC1. Sin embargo en las células WT8 HIF2α(P-A)^2 la mayor parte de la proteína 4EBP1 estaba presente en la banda superior, indicativo de un estado de hiperfosforilación y por tanto de activación de mTORC1. Al incubar las membranas con los anticuerpos dirigidos frente a los residuos fosforilados Ser^{65} y $Thr^{37/46}$ de 4EBP1 también se detectó mayor presencia de estas bandas superiores. Este efecto era totalmente dependiente de la capacidad de unión a ADN de HIF2α, ya que los niveles de fosforilación de 4EBP1 en las células WT8 HIF2α(P-A)^{2}bHLH*, que expresan la forma de HIF2α transcripcionalmente inactiva, eran muy similares a los de las células WT8 control. El mismo efecto observamos en los niveles de fosforilación de los residuos $Ser^{235/236}$ de la otra diana de mTORC1 evaluada, la proteína rpS6.

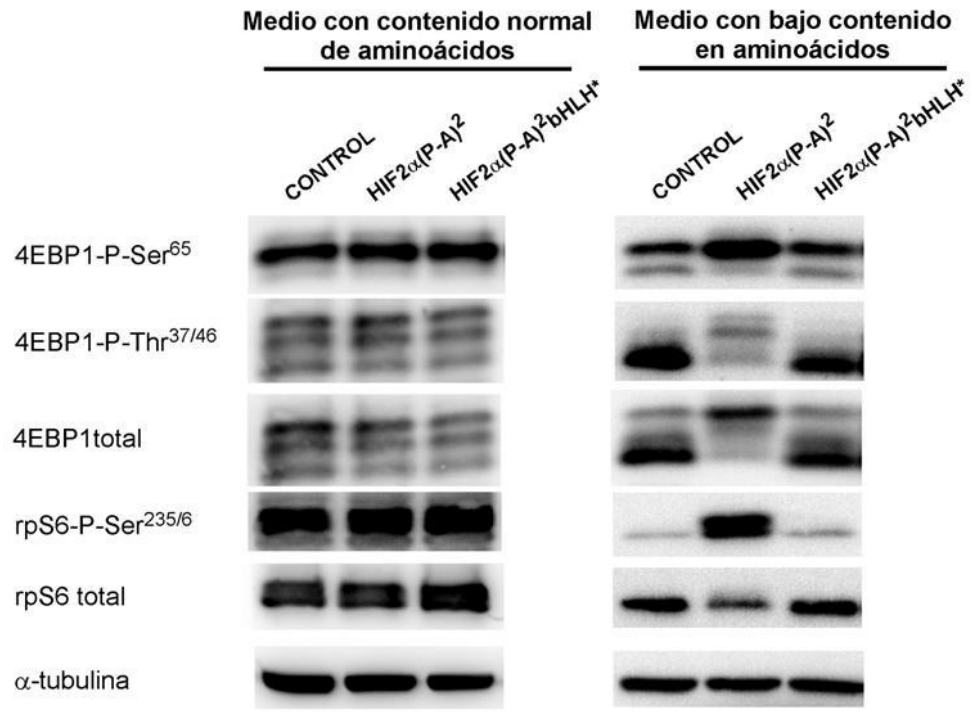

Figura 10. Efectos de la actividad de HIF2α sobre el estado de activación de mTORC1 en las células WT8. Análisis por Western blot del estado de fosforilación de las dianas de mTORC1 4EBP1 y rpS6 en lisados totales de células WT8 control, HIF2α(P-A)^2 y HIF2α(P-A)^{2}bHLH* cultivadas durante 72 horas en un medio de cultivo estándar (panel izquierdo) o en un medio con un 50% del contenido normal de aminoácidos (panel derecho).

Para evaluar si el efecto activador sobre mTORC1 era específico de la isoforma HIF2α llevamos a cabo el mismo experimento con células WT8 infectadas con una forma constitutivamente activa de HIF1α en la que también los dos residuos de prolina críticos para su hidroxilación y degradación han sido mutados, generando las células WT8 HIF1α (P-A)^2. En la Figura 11 se observa que las células WT8 HIF1α (P-A)^2, cuando se comparan con las células control WT8, expresan eficientemente HIF1α a nivel proteico (panel A) y presentan niveles elevados del ARNm del gen bNIP3 (panel B), un gen diana específico de HIF1α (Raval et al., 2005). Sin embargo estas células, aún cultivadas en un medio con bajo contenido en aminoácidos (50%), no presentaban diferencias en el estado de fosforilación de las dianas de mTORC1 4EBP1 y rpS6 (Figura 11).

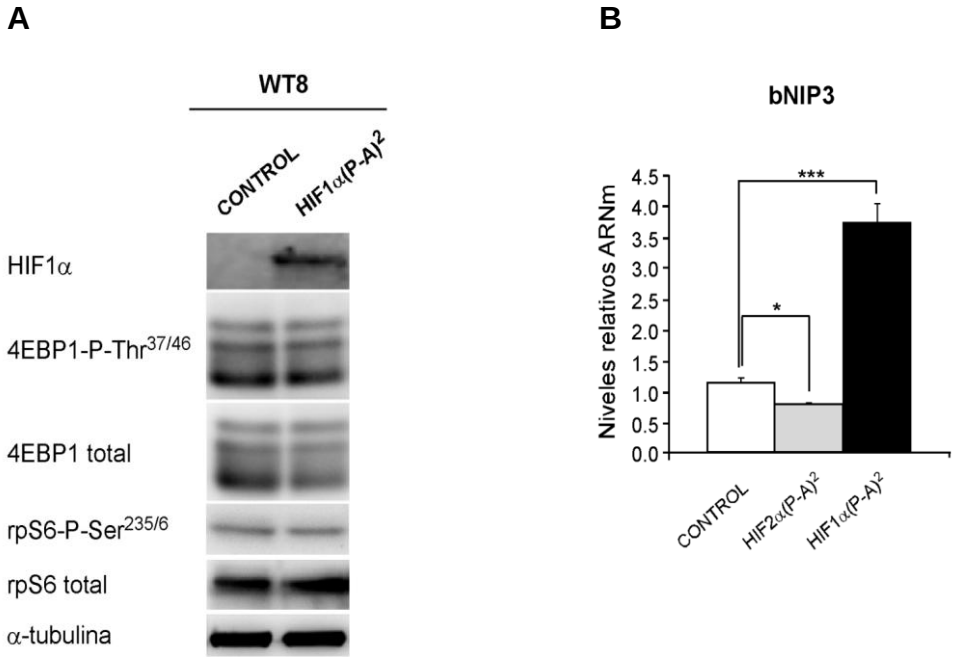

Figura 11. **Expresión y actividad transcripcional de HIF1α y sus efectos sobre el estado de activación de mTORC1 en las células WT8**. **(A)** Se analizó por Western blot el estado de fosforilación de las dianas de mTORC1 4EBP1 y rpS6 en lisados totales de las células WT8 control y WT8 HIF1α(P-A)^2 cultivadas durante 72 horas en un medio de cultivo con un 50% del contenido normal de aminoácidos. **(B)** Análisis mediante RT-PCR cuantitativa de los niveles relativos de ARNm del gen *bNIP3* en estos mismos tipos celulares, normalizados con respecto a la expresión de *Hprt*. Se muestra la media; las barras de error representan el SEM; n= 4, *p<0,05;***p<0,001.

En conjunto estos datos indican que HIF2α es capaz de sostener la actividad de mTORC1 cuando el suministro de aminoácidos se encuentra limitado y que dicha capacidad es exclusiva de esta isoforma y totalmente dependiente de su actividad transcripcional.

2. El transportador de aminoácidos SLC7A5, activador de mTORC1, es específicamente inducido por HIF2α.

En base a los resultados anteriores quisimos profundizar en los mecanismos moleculares que podrían subyacer a la activación de mTORC1 por HIF2α. Es conocido

que los transportadores de aminoácidos SLC1A5 (ASCT2) y SLC7A5 (LAT1) son elementos críticos en el mantenimiento de la actividad de mTORC1 (Fuchs and Bode, 2005; Nicklin et al., 2009), debido a que le proporcionan aminoácidos esenciales, claves para su activación. Decidimos por tanto investigar si HIF2α podría estar alterando la expresión de estos transportadores. Al evaluar los niveles de ARNm de estos genes observamos que efectivamente la expresión del gen *Slc7a5* se encontraba claramente inducida en las células WT8 HIF2α $(P\text{-}A)^2$ comparada con las células WT8 HIF2α$(P\text{-}A)^2$bHLH* y las células WT8 control (Figura 12A). Sin embargo los niveles de ARNm del transportador ASCT2 estaban mínimamente afectados (Figura 12B). De nuevo este efecto resultó ser específicamente causado por HIF2α, dado que las células WT8 HIF1α$(P\text{-}A)^2$ mostraban, por el contrario, una leve inhibición de la expresión del gen *Slc7a5*. Adicionalmente, un análisis por Western blot de lisados totales de estos tipos celulares también reveló un incremento de los niveles de proteína SLC7A5 en las células WT8 HIF2α$(P\text{-}A)^2$ (Figura 13).

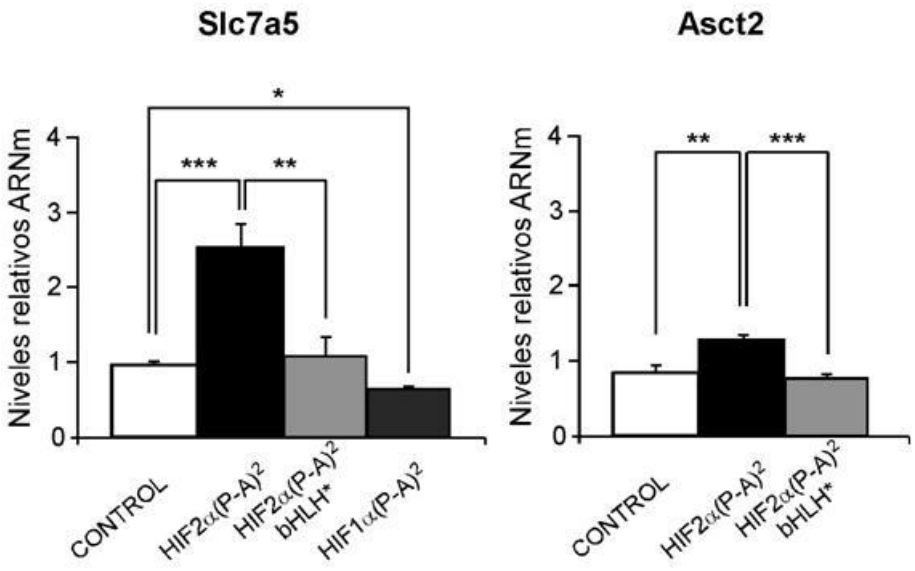

Figura 12. Análisis del efecto transcripcional de HIF1α y HIF2α sobre la expresión génica de transportadores de aminoácidos. Análisis mediante RT-PCR cuantitativa de los niveles relativos de ARNm de los genes *Slc7a5* **(A)** y *Asct2* **(B)** en las células WT8 control, HIF2α$(P\text{-}A)^2$ y HIF2α$(P\text{-}A)^2$bHLH*. Para *Slc7a5* también se muestran en las células WT8 HIF1α$(P\text{-}A)^2$ **(A)**. Los datos se han normalizado con respecto a la expresión de *Hprt*. Se muestra la media; las barras de error representan el SEM; n= 4, *p<0,05;**p<0.01; ***p<0,001.

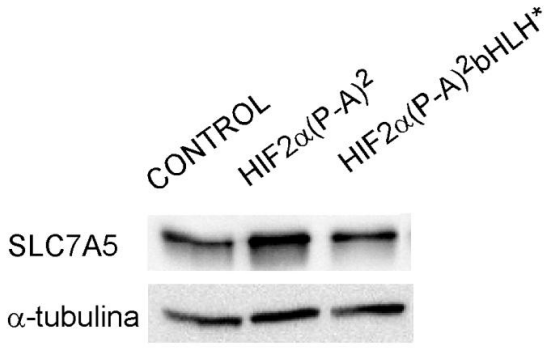

Figura 13. Análisis de la función transcripcional de HIF2α sobre la expresión proteica de SLC7A5. Análisis por Western blot de la expresión de la proteína SLC7A5 en las células WT8 control, HIF2α(P-A)^2 y HIF2α(P-A)^{2}bHLH* y su correspondiente control de carga α-tubulina.

3. El transportador SLC7A5 media la activación de mTORC1 por HIF2α.

Para evaluar si el aumento en la expresión de SLC7A5 era el responsable de la activación de mTORC1 dependiente de HIF2α observada, decidimos a continuación silenciar el gen *Slc7a5* en las células WT8 HIF2α(P-A)^2 (Figura 14). Al interferir moderadamente la expresión del transportador -aproximadamente hasta el nivel que presenta en normoxia - observamos una clara represión de la actividad de mTORC1 en estas células, hasta niveles similares a los observados en las células WT8 control. Esto se observa en el análisis por Western blot de la proteína 4EBP1 total, cuya proporción de la banda inferior aumenta claramente, y de su residuo fosforilado Thr$^{37/46}$, que disminuye igualmente tras el silenciamiento de *Slc7a5* (Figura 14A). Igualmente se observa que la hiperfosforilación de rpS6 en las células WT8 HIF2α(P-A)^2 es mucho menos eficiente tras la interferencia del gen de *Slc7a5* (Figura 14). Es interesante recalcar que las diferencias en la expresión del transportador SLC7A5 sólo son capaces de alterar el estado de activación de mTORC1 cuando las células son cultivadas en un medio con un contenido reducido de aminoácidos (Figura 14, panel izquierdo), pero que este efecto se pierde cuando el experimento se realiza en las condiciones de cultivo celular estándar (Figura 14, panel derecho).

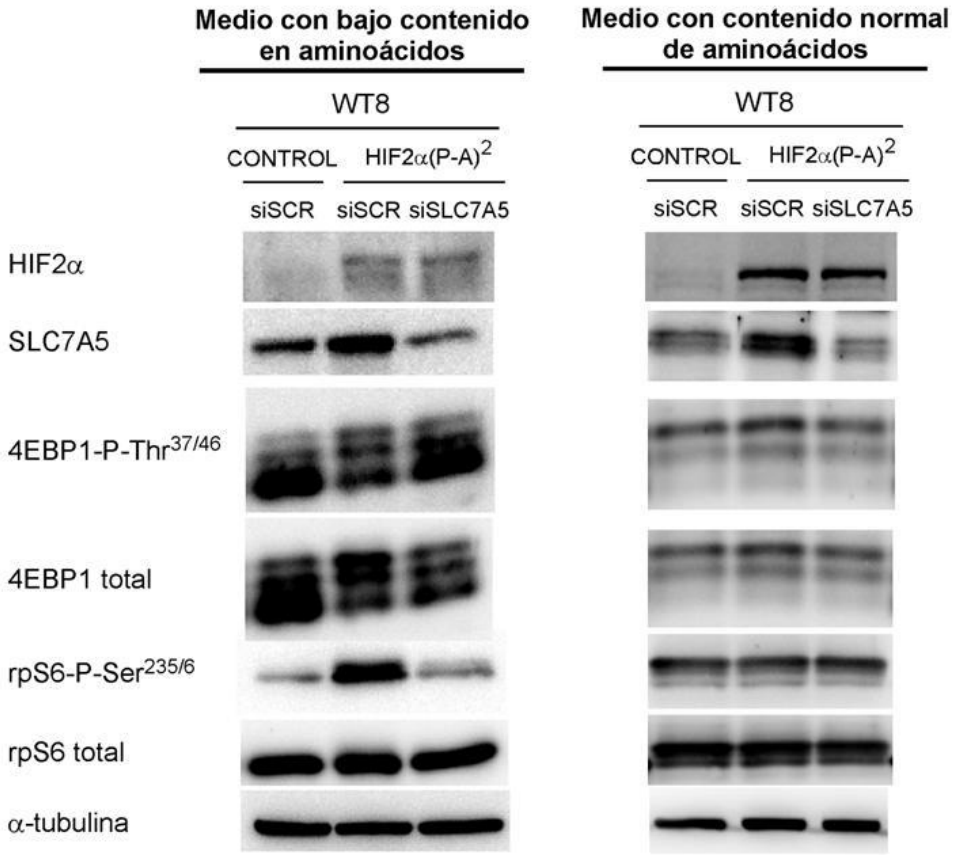

Figura 14. C**ontribución de la expresión de SLC7A5 a la activación de mTORC1 dependiente de HIF2α en un medio con concentración reducida o normal de aminoácidos.** Las células WT8 control fueron transfectadas con un siARN control (siSCR), al igual que las células WT8 HIF2α(P-A)^2, que además se interfirieron con un siARN dirigido frente a *Slc7a5* (siSLC7A5). A continuación se cultivaron durante 72 horas en un medio de cultivo con un 50% del contenido normal de aminoácidos (panel izquierdo) o con la concentración normal de aminoácidos (panel derecho). Los lisados totales de dichas células se analizaron por Western blot para comprobar la expresión de HIF2α, SLC7A5 y el estado de fosforilación de las dianas de mTORC1 4EBP1 y rpS6.

Como se comentó previamente, es conocido el papel clave de SLC7A5, junto con ASCT2, en la activación de mTORC1 por su capacidad para introducir aminoácidos esenciales en la célula a cambio de glutamina (Fuchs and Bode, 2005; Nicklin et al., 2009). Decidimos por tanto confirmar si las células WT8 HIF2α(P-A)^2 eran también capaces de preservar el incremento en la actividad de mTORC1 cuando eran cultivadas en un medio con una reducción específica de su contenido en aminoácidos esenciales (AAEE) y glutamina (Gln). Como se muestra en la Figura 15, HIF2α

también promueve la actividad de mTORC1en estas condiciones más específicas de deprivación de aminoácidos. Además, el silenciamiento de las proteínas RagA/B, previamente identificadas como mediadores centrales de la actividad de mTORC1 dependiente de aminoácidos esenciales (Kim et al., 2008; Sancak et al., 2008), también comprometía la actividad de mTORC1 en las células WT8 HIF2α(P-A)^2 (Figura 16). Todos estos datos sugieren que, por debajo de cierto umbral de contenido extracelular de aminoácidos, la expresión de SLC7A5 dependiente de HIF2α se convierte en un factor limitante para la actividad de mTORC1. Esto podría estar reflejando el hecho de que los niveles de aminoácidos en el medio de cultivo normal exceden aquellos encontrados normalmente por las células en contextos *in vivo* tales como los escenarios intra-tumorales (Reid et al., 2013).

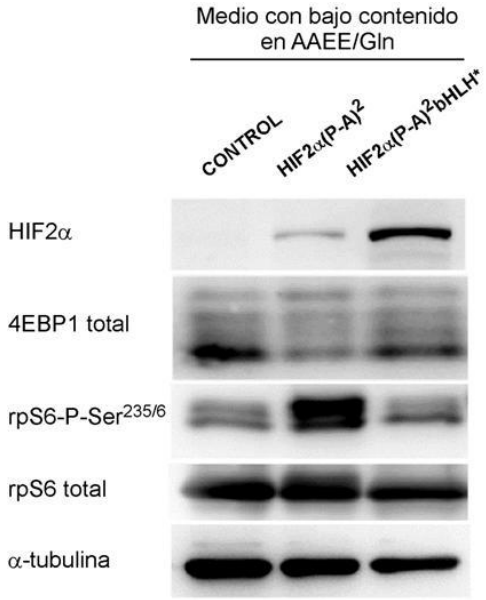

Figura 15. Efectos de la actividad de HIF2α sobre el estado de activación de mTORC1 en células WT8 en medio deprivado específicamente de aminoácidos esenciales (AAEE) y glutamina (Gln). Análisis por Western blot del estado de fosforilación de las dianas de mTORC1 4EBP1 y rpS6 en lisados totales de células WT8 control, HIF2α(P-A)^2 y HIF2α(P-A)^{2}bHLH* cultivadas durante 72 horas en un medio con bajo contenido en AAEE y Gln.

Figura 16. Contribución de las proteínas RagA y B a la actividad de mTORC1 dependiente de HIF2α. Las células WT8 HIF2α(P-A)^2 fueron transfectadas con un siARN control (siSCR) o con siARNs frente a *RagA* y *RagB* (siRagA/B), alcanzando un silenciamiento del 86% y 71% respectivamente. Seguidamente se cultivaron durante 72 horas en un medio con un 50% del contenido normal de aminoácidos. Los lisados totales de dichas células se analizaron por Western blot para comprobar el estado de fosforilación de las dianas de mTORC1 4EBP1 y rpS6.

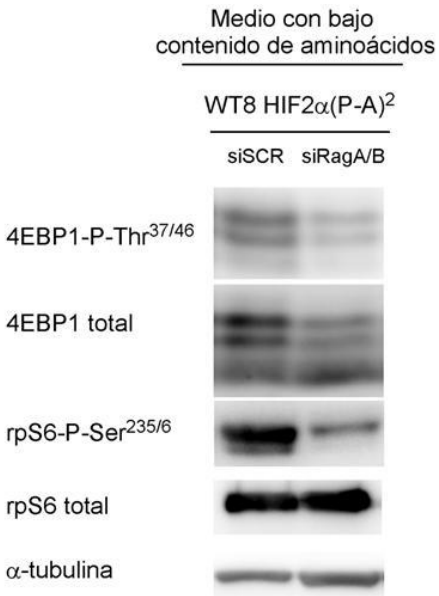

4. La proteína HIF2α endógena también activa mTORC1 a través de SLC7A5 en condiciones de escasez de aminoácidos.

Habiendo confirmado el papel de una forma exógena de HIF2α en el modelo célular WT8, quisimos comprobar si también la proteína HIF2α endógena es capaz de activar la vía de señalización de mTORC1 así como la expresión de SLC7A5. Para ello usamos la línea celular original de carcinoma renal deficiente para VHL, 786-O, que expresa de forma constitutiva HIF2α en normoxia (Kondo et al., 2002). El silenciamiento de HIF2α resultó en una clara represión de la expresión de SLC7A5 y de la actividad de mTORC1 en células 786-O cuando eran cultivadas en medio con un contenido reducido en aminoácidos esenciales (AAEE) y glutamina (Gln) (Figura 17A), pero no así en medio con un contenido normal de aminoácidos (datos no mostrados). Así observamos que al silenciar HIF2α se producía un aumento en la proporción de la banda inferior de 4EBP1 y disminuía el nivel de fosforilación de la proteína rpS6. Los mismos resultados se observaron cuando se eliminó la proteína HIF2α restaurando la expresión de VHL en las células 786-0 (Figura 17B).

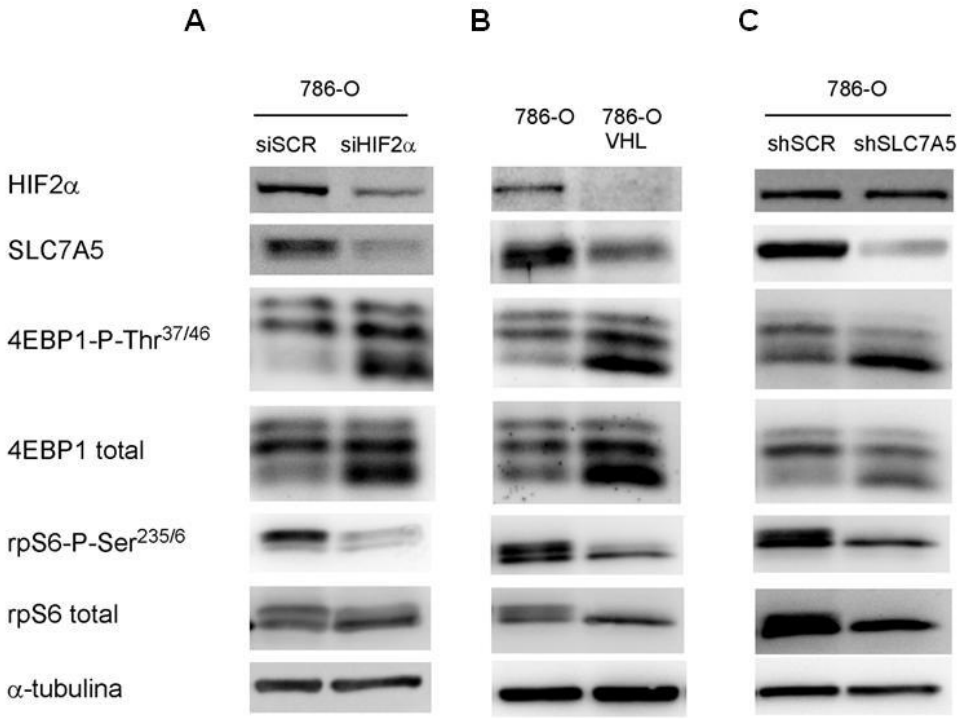

Figura 17. Efecto de la proteína HIF2α endógena sobre la actividad de mTORC1 y la expresión de SLC7A5 en células 786-O deficientes para VHL en un medio de cultivo con un contenido disminuido de aminoácidos. Análisis por Western blot de la expresión de HIF2α y SLC7A5 y del estado de fosforilación de las dianas de mTORC1 4EBP1 y rpS6 en lisados totales de células **(A)** 786-0 con la expresión de HIF2α silenciada (siHIF2α) y su correspondiente control de células 786-O transfectadas con el siARN control (siSCR) transcurridas 72 horas de la transfección; **(B)** células 786-O y sus homólogas 786-O-VHL en las que la expresión de VHL ha sido restituida y **(C)** células 786-O con la expresión de SLC7A5 silenciada (shSLC7A5) y su correspondiente control de células 786-O infectadas con el shARN control (shSCR). Todos estos experimentos se realizaron cultivando las distintas células 786-O durante 48 horas en un medio con un 5% del contenido normal de aminoácidos esenciales (AAEE) y glutamina (Gln).

Finalmente evaluamos la contribución relativa de la inducción de SLC7A5 por HIF2α en la actividad de mTORC1 en las células 786-O. Para ello generamos la línea celular 786-O-shSLC7A5 (ver Materiales y métodos) en la que la expresión de SLC7A5 se encuentra disminuida hasta niveles similares a los obtenidos tras el silenciamiento del HIF2α endógeno (comparar paneles A y C de la Figura 17). De nuevo los niveles de fosfo-rpS6 disminuyeron tras el silenciamiento de SLC7A5 respecto a su correspondiente control 786-O-shSCR. Además, las células 786-O-shSLC7A5 también mostraban una predominancia en la forma inferior hipofosforilada de 4EBP1 (Figura 17C). En conjunto estos datos indican que la expresión endógena de HIF2α en células 786-O también regula la actividad de mTORC1 debido a su capacidad para inducir la expresión de SLC7A5 cuando el suministro de aminoácidos está limitado.

5. HIF2α se une al promotor proximal de *Slc7a5.*

Los resultados anteriores nos llevaron a preguntarnos si SLC7A5 podría ser una diana transcripcional directa de HIF2α. Para ello investigamos si HIF2α era capaz de unirse a las secuencias reguladoras de ADN en el *locus* de *Slc7a5*. Un análisis de

la secuencia de este gen reveló que el promotor proximal *de Slc7a5* humano contiene dos sitios potenciales de unión de HIF en las posiciones -112 y -458 (Figura 18).

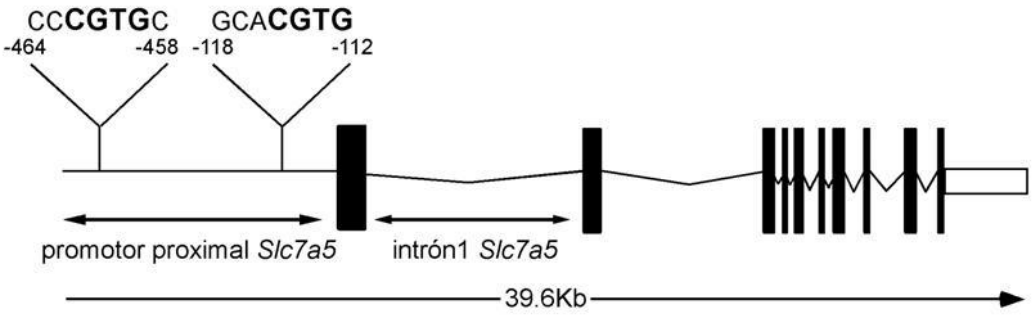

Figura 18. Representación esquemática del gen humano de *Slc7a5*. Se indican las posiciones del promotor proximal y del intrón 1 así como, resaltadas en negrita, las secuencias de nucleótidos correspondientes a dos potenciales elementos de respuesta a hipoxia.

Al realizar un ensayo de inmunoprecipitación de cromatina (ChIP) en las células WT8 HIF2α(P-A)^2, HIF2α(P-A)^2 bHLH* y las células WT8 control observamos que la unión de HIF2α al promotor proximal de *Slc7a5* estaba aumentada en las células WT8 HIF2α(P-A)^2 comparadas con las células WT8 HIF2α(P-A)^2 bHLH* y las WT8 control (Figura 19A). Esta unión era específica al promotor proximal ya que no se detectaba cuando se utilizaban oligonucleótidos correspondientes al intrón 1 (Figura 19A). Además, también se observó la unión constitutiva de la proteína HIF2α endógena al promotor proximal de *Slc7a5*, pero de nuevo no al intrón 1, en células 786-O control comparadas con células 786-O-VHL (Figura 19B).

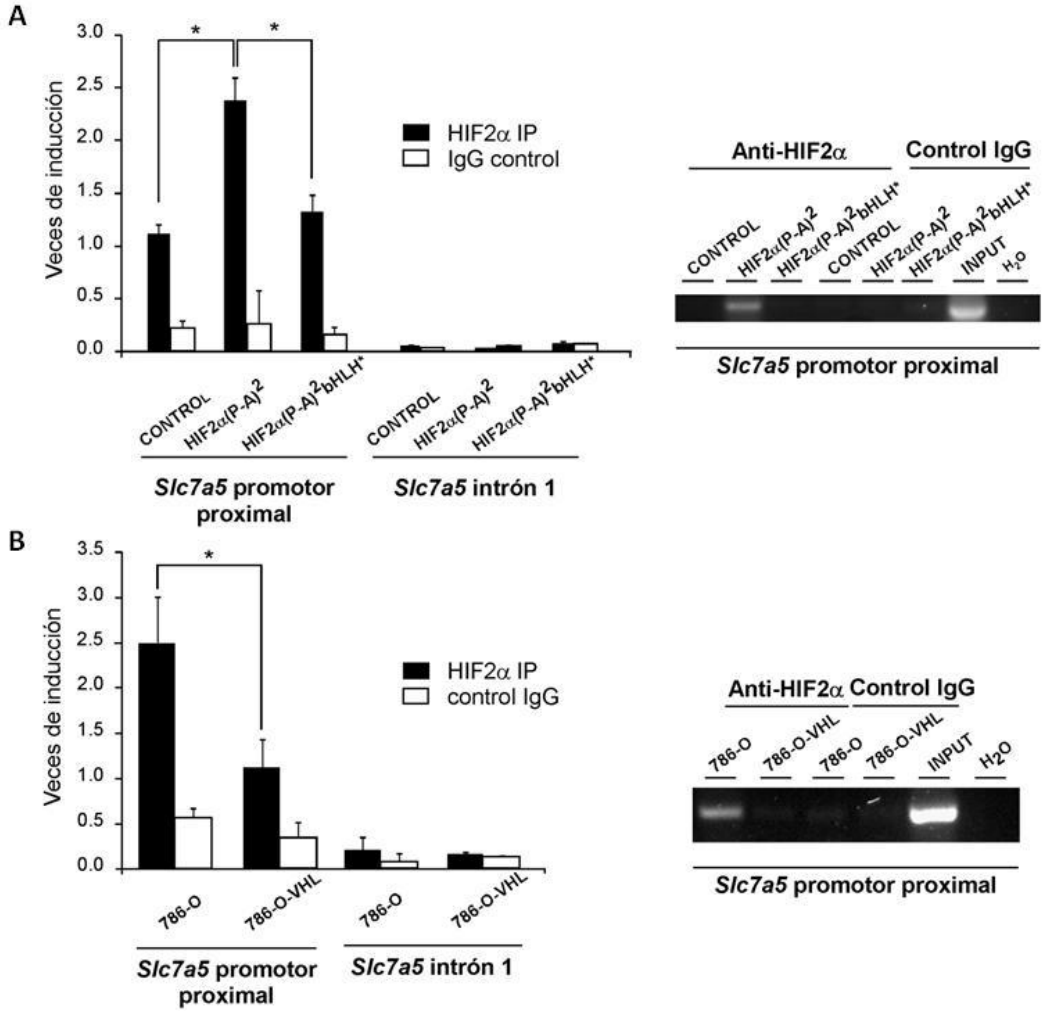

Figura 19. HIF2α se une al promotor proximal de *Slc7a5*. Ensayo de inmunoprecipitación de cromatina (ChIP) para comprobar la actividad relativa de unión de HIF2α al promotor proximal del gen humano de *Slc7a5* o al intrón 1 en **(A)** células WT8 control, HIF2α(P-A)^2 y HIF2α(P-A)^{2}bHLH* o **(B)** células 786-O y sus homólogas 786-O con la expresión de VHL restituida. Los datos se representan como el cambio relativo a las células WT8 control. Se muestra la media; las barras de error representan el SEM; n=5; *p<0,05. En los paneles de la derecha se muestran geles representativos del ADN amplificado en los ensayos de ChIP.

Pudimos confirmar que la unión de la isoforma HIF2α era específica ya que un análisis en paralelo en idénticas condiciones experimentales en células WT8 HIF1α(P-A)^2 no reveló unión del factor HIF1α al promotor proximal de *Slc7a5*, mientras que sí se

observaba su unión al promotor de la piruvato deshidrogenasa quinasa 1 (*Pdk1*), un conocido gen dependiente de HIF1α (Figura 20). En conjunto estos resultados indican que HIF2α -pero no HIF1α - se une específicamente al promotor proximal de *Slc7a5* a través de su dominio de unión a ADN y está por tanto potencialmente implicado en el aumento de expresión de SLC7A5.

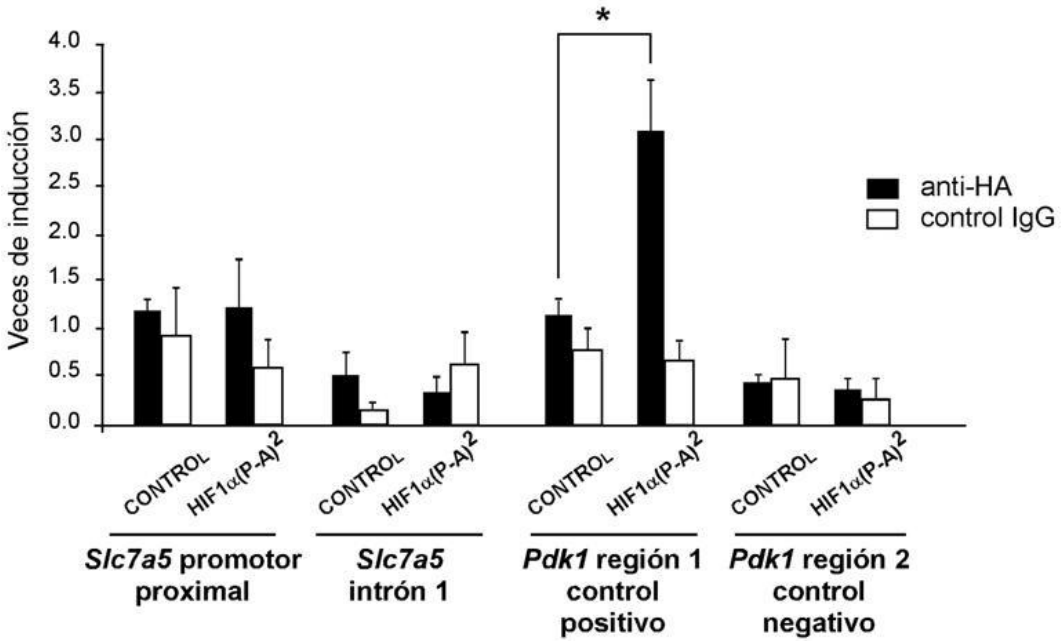

Figura 20. HIF1a no se une al promotor proximal de *Slc7a5*. Ensayo ChIP para comprobar la actividad relativa de unión de HIF1α al promotor proximal del gen humano de *Slc7a5* o al intrón 1 en células WT8 control y WT8 HIF1α(P-A)^2, así como al promotor proximal y a una región de unión negativa del gen humano *Pdk1.* Para realizar este ensayo se emplearon anticuerpos anti-HA, dado que la forma HIF1α(P-A)^2 es una versión marcada con el epítopo HA. Los datos se representan como el cambio relativo a las células WT8 control. Se muestra la media; las barras de error representan el SEM; n=3; *p<0,05.

6. HIF2α induce la proliferación de células de carcinoma renal y el crecimiento tumoral a través de SLC7A5

Es bien conocido que la expresión de HIF2α en carcinomas renales de célula clara deficientes para VHL favorece el crecimiento tumoral (Kondo et al., 2002, 2003; Raval et al., 2005). Dada la relevancia que la activación de mTORC1, como máximo responsable de la síntesis de proteínas, puede tener en este proceso, quisimos investigar la contribución de la vía HIF2α-SLC7A5 a la proliferación de las células WT8 HIF2α(P-A)^2. Estas células no proliferan más rápidamente que las WT8 control o las

WT8 HIF2α(P-A)^2 bHLH* cuando se cultivan en un medio con un contenido normal de aminoácidos. De hecho, se observa incluso cierta tendencia hacia una menor tasa de proliferación al compararlas con las WT8 HIF2α (P-A)^2 bHLH* (Figura 21A). Dado el papel de SLC7A5 como transportador de aminoácidos y la regulación de mTORC1 por HIF2α cuando los aminoácidos son limitantes, quisimos investigar si la presencia de HIF2α puede suponer una ventaja proliferativa cuando las células son cultivadas en condiciones de baja disponibilidad de aminoácidos. Efectivamente, al cultivar las células en medio con un 5% del contenido estándar de aminoácidos, las células WT8 HIF2α(P-A)^2 mostraron una proliferación mayor que las células WT8 control o las WT8 HIF2α(P-A)^2 bHLH* (Figura 21B). En estas condiciones de deprivación de aminoácidos las células simplemente continuaron proliferando, aunque con una menor tasa de lo que lo hacen en medio con contenido normal de aminoácidos, pero sin mostrar señales de apoptosis. A continuación quisimos evaluar el papel tanto del transportador SLC7A5 como de mTORC1 en esta ventaja proliferativa de las células WT8 HIF2α(P-A)^2. Para ello realizamos el mismo tipo de experimento interfiriendo por un lado dichas células con el siARN de *Slc7a5* o un siSCR control, y por otro lado, inhibiendo farmacológicamente mTORC1 mediante el uso de rapamicina. Tanto el silenciamiento del gen *Slc7a5* (Figura 21C) como la inhibición de mTORC1 (Figura 21D) eliminaron la ventaja proliferativa de las células WT8 HIF2α(P-A)^2 en el medio con bajo contenido de aminoácidos, dejándola al nivel de las células WT8 control. Estos resultados apoyan el papel del eje molecular HIF2α-SLC7A5-mTORC1 en el aumento de la capacidad proliferativa autónoma de la célula cuando el suministro de aminoácidos se encuentra limitado, circunstancias que se han demostrado ocurren en el microambiente intratumoral durante el crecimiento del tumor (Reid et al., 2013).

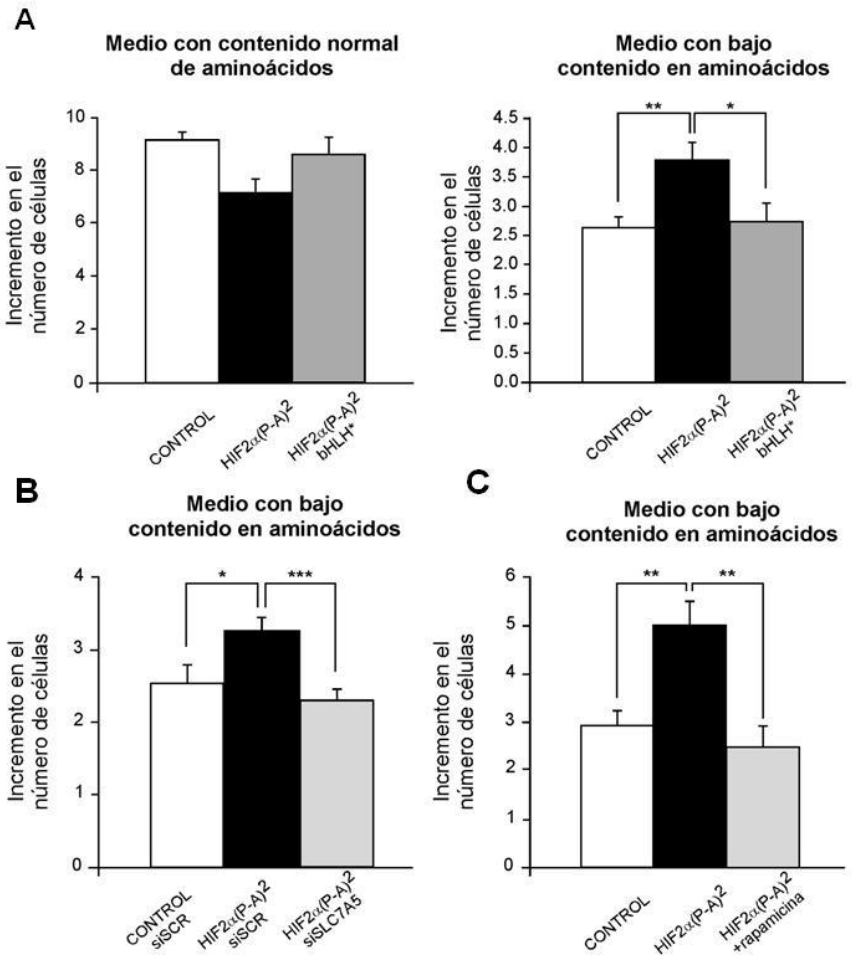

Figura 21. Papel del eje molecular HIF2α-SLC7A5-mTORC1 en la proliferación celular. (A) Inducción relativa del número de células WT8 control, WT8 HIF2α(P-A)^2 y WT8 HIF2α(P-A)^2 bHLH* cultivadas durante 72 horas en medio normal (panel izquierdo) o en medio con un 5% de la concentración normal de aminoácidos (panel derecho). Los valores están normalizados respecto al número inicial de células. Se muestra la media de 4 experimentos; las barras de error representan el SEM; la significancia estadística se indica sólo cuando el ratio de proliferación de las células WT8 HIF2α (P-A)^2 varía significativamente con respecto al de los otros dos tipos celulares. **(B)** Las células WT8 control fueron transfectadas con siARN control (siSCR), y las células WT8 HIF2α(P-A)^2 se transfectaron con siSCR y con un siARN frente a *Slc7a5* (siSLC7A5). 24 horas después de la transfección, las células se plaquearon a la misma confluencia en un medio con un 5% del contenido normal de aminoácidos, y el incremento en el número de células se analizó tras 72 horas. Se muestra la media de 4 experimentos. Las barras de error representan el SEM. **(C)** Células WT8 control y células WT8 HIF2α(P-A)^2 fueron tratadas con rapamicina (20nM) y cultivadas en medio con un 5% de la

concentración de aminoácidos usual. El incremento en el número de células se analizó tras 72 horas. Se muestra la media de 8 experimentos. En todos los paneles, * p<0,05; **p<0,01;***p<0,01.

A continuación consideramos esencial evaluar el papel de la vía HIF2α-SLC7A5 *in vivo*, para lo cual empleamos el modelo celular de las 786-O, que ha sido ampliamente utilizado para valorar las propiedades protumorales de HIF2α en el carcinoma renal. Para ello usamos las células 786-O-shSLC7A5, en las cuales la expresión de SLC7A5 se encuentra reducida a niveles similares a los encontrados en células 786-O con HIF2α silenciado (comparar paneles A y C de Figura 17). Cuando inyectamos subcutáneamente estas células (y su correspondiente control 786-O-shSCR) en ratones inmunodeprimidos, encontramos que la capacidad de crecimiento de los xenoinjertos de las células 786-O-shSLC7A5 se encontraba claramente disminuida al compararla con el de las células 786-O-shSCR (Figura 22). De hecho, 45 días después de la inyección subcutánea de las células, el tamaño de los tumores 786-O-shSLC7A5 era muy inferior (345.6 ± 89 mm3 en los xenoinjertos 786-O-shSCR frente a 56.62 ± 16 mm3 en los xenoinjertos 786-O-shSLC7A5, donde n = 18 y p = 0.0039).

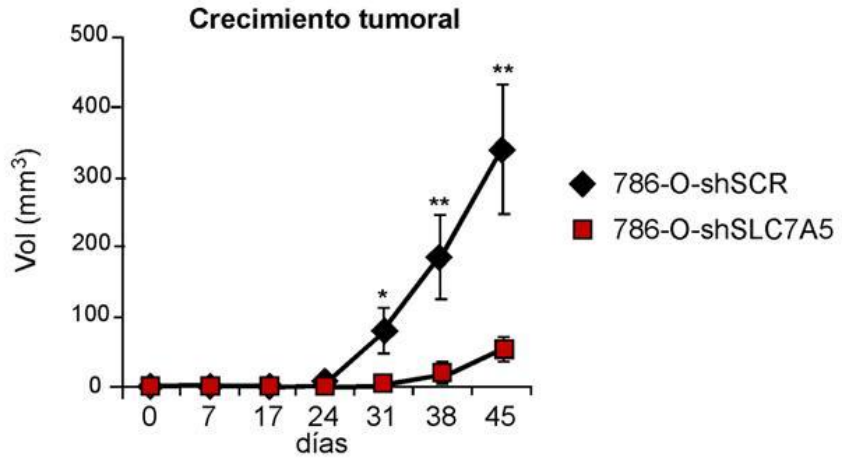

Figura 22. Papel de la inducción de SLC7A5 dependiente de HIF2α en el crecimiento de xenoinjertos. Evolución a lo largo de 45 días del volumen (Vol) de tumores de células 786-O con SLC7A5 silenciado (cuadrados rojos) y sus correspondientes controles 786-O-shSCR (cuadrados negros) inyectados subcutáneamente en los flancos dorsales de ratones inmunodeprimidos. Se muestra la media de 18 muestras; las barras de error representan el SEM. * p<0,05; **p<0,01.

Estos resultados indican que la inducción de SLC7A5 dependiente de HIF2α es crítica para explicar sus propiedades pro-tumorales y proporcionan una base molecular para explicar este fenómeno crítico en carcinoma renal.

Para intentar encontrar un posible valor clínico a nuestros datos, decidimos también evaluar la expresión de SLC7A5 en nefrectomías procedentes de pacientes con carcinomas renales de célula clara deficientes para VHL (ccRCCs) o de pacientes con carcinomas renales de célula no clara (ncRCCs), con expresión normal de VHL. En línea con lo previamente descrito (Mandriota et al., 2002) y a modo de control positivo, evaluamos en las muestras la expresión de la proteína anhidrasa carbónica IX (CAIX). Todos las muestras de ccRCC (n = 5) mostraban una expresión elevada de CAIX, ya identificada como un gen dependiente de HIF cuando se compara con tejido renal sano. Al analizar en paralelo por Western blot la expresión de SLC7A5, presente en este tipo de muestras como dos bandas, comprobamos que estaba elevada en las muestras de ccRCC al compararla con el tejido sano, y correlacionaba con la expresión de CAIX (Figura 24). Las dos bandas de señal detectadas fueron identificadas como SLC7A5 mediante el empleo de 4 anticuerpos distintos dirigidos contra diferentes epítopos de esta proteína. La muestra ccRCC #4 no mostraba inducción de SLC7A5, lo cual está acorde con una más leve elevación de la expresión de CAIX en esta muestra particular. Se observa además que, al contrario que en las muestras ccRCCs, ni la expresión de SLC7A5 ni la de CAIX está alterada en las muestras ncRCCs analizadas (n = 3). En conjunto estos resultados, junto con los mostrados en el ensayo de crecimiento de xenoinjertos (Figura 22), muestran la relevancia de la vía HIF2α-SLC7A5 en la progresión de los carcinomas renales de célula clara, desentrañando nuevos aspectos de las propiedades tumorales y proliferativas de HIF2α.

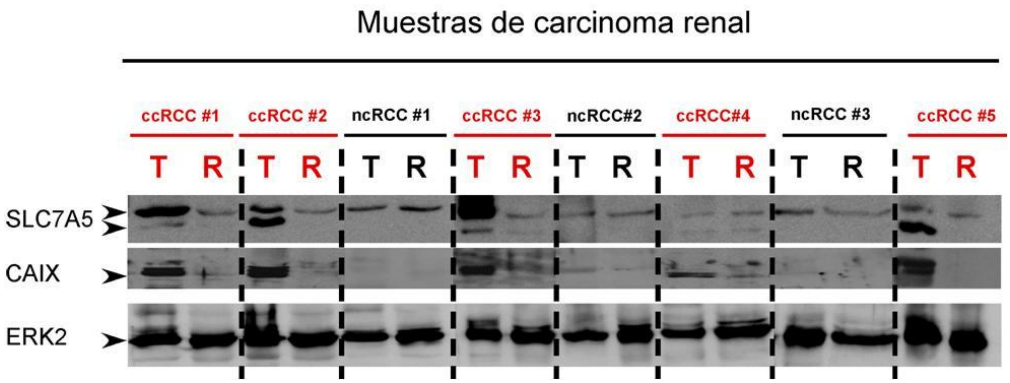

Figura 24. Expresión proteica de SLC7A5 en carcinomas renales y en el tejido renal sano adyacente. Análisis por Western blot de la expresión de SLC7A5 en 5 muestras de ccRCC deficientes para VHL y 3 carcinomas renales de célula no clara (ncRCC), incluyendo su correspondiente control de tejido renal no afectado. Las muestras ncRCC #1 y #2 fueron diagnosticadas como carcinomas oncocitomas de célula renal y la muestra #3 corresponde a un carcinoma cromófobo de célula renal. T= tumor y R= tejido renal sano. Las dos bandas indicadas por flechas fueron identificadas como SLC7A5. Todos los ccRCC empleados en este análisis (n=5) eran positivos para la expresión de anhidrasa carbónica IX (CAIX). La expresión de ERK2 se empleó como control de carga.

7. HIF2α regula la expresión génica de *Slc7a5* y la actividad de mTORC1 en ratones tras la inactivación génica de *Vhl* o su exposición a hipoxia *in vivo*.

A continuación exploramos si el eje activador HIF2α-mTORC1 podría ser activo en otros escenarios biológicos. Decidimos en concreto investigar esta vía en la respuesta pulmonar a hipoxia, donde razonamos que podría ser de especial relevancia debido a dos motivos: en primer lugar, porque el pulmón exhibe los mayores niveles de expresión de HIF2α en roedores (Wiesener et al., 2003) y, en segundo lugar, porque la hipoxia promueve respuestas proliferativas en el pulmón (Brusselmans et al., 2003; Niedenzu et al., 1981). Los ratones fueron expuestos durante 4 días a condiciones de hipoxia (10% de concentración de O_2), el cual es un protocolo experimental ampliamente utilizado para estudiar respuestas biológicas pulmonares dependientes de HIF2α en hipoxia *in vivo* que llevan a la estabilización de HIF2α en el pulmón (Brusselmans et al., 2003). Ensayos de Western blot revelaron un marcado

incremento en los niveles de rpS6 fosforilada en los pulmones de los ratones hipóxicos. Así mismo, también la hipoxia provocó un aumento en los niveles de fosforilación de la proteína 4EBP1, (Figura 25A), en base a los datos obtenidos con los anticuerpos generados contra la Ser^{65} y las $Thr^{37/46}$ fosforiladas, que se sitúan preferencialmente en la banda superior hiperfosforilada. Así mismo quisimos conocer la localización celular dentro del tejido en la que estaba ocurriendo la activación de mTORC1. Para ello realizamos una inmunohistoquímica de la proteína rpS6 en los pulmones que reveló que la activación de mTORC1 inducida por la hipoxia ocurría fundamentalmente en el epitelio bronquial, donde se detectaba un claro incremento en el número de células positivas para $rpS6^{235/236}$ (Figura 25B).

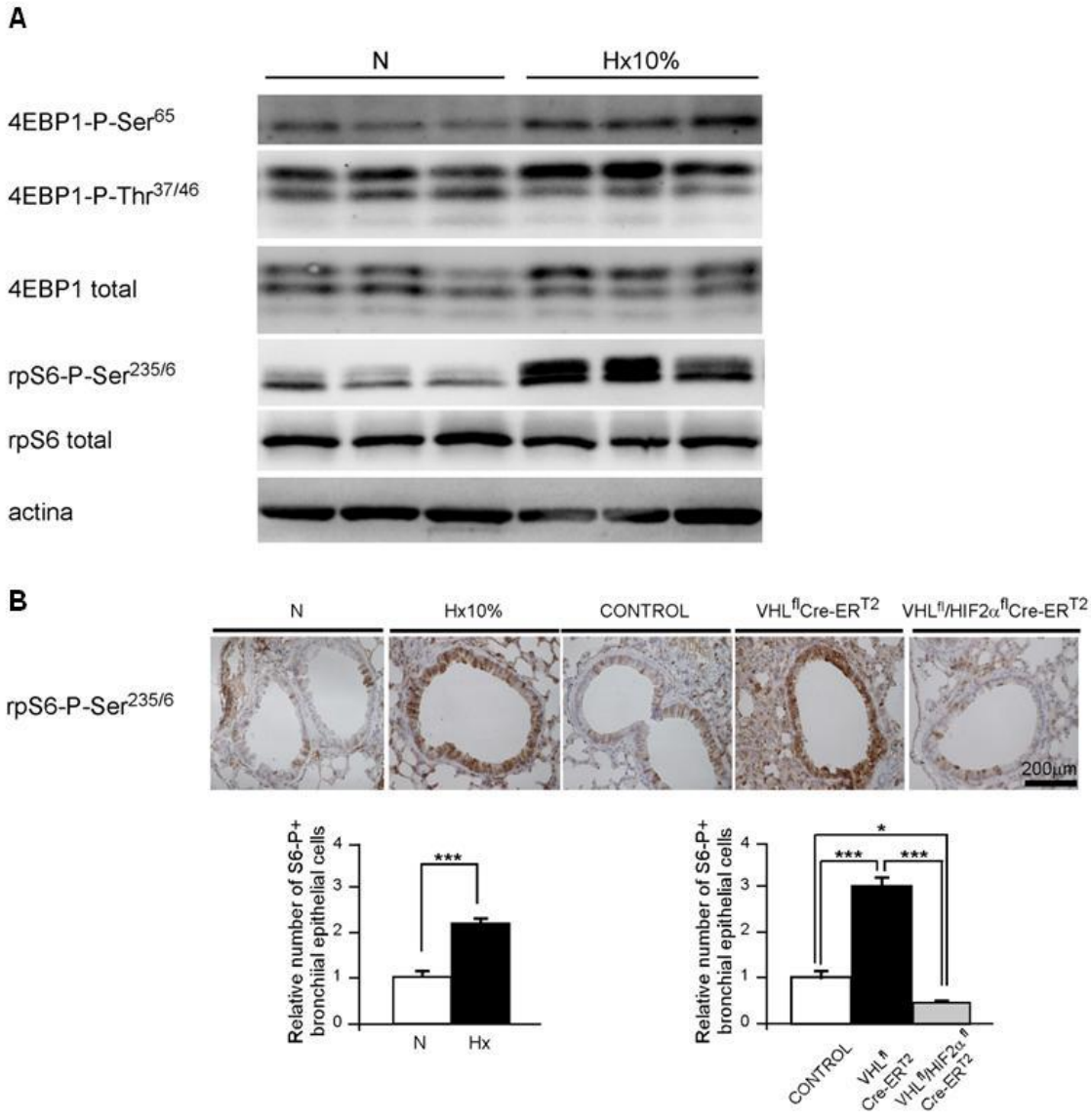

Figura 25. Actividad de mTORC1 dependiente de hipoxia y de HIF2α en el pulmón. (A) Se expusieron ratones salvajes a hipoxia 10% O_2 (Hx10%) o a normoxia (N) durante 4 días. Se analizaron los extractos proteicos pulmonares de dichos ratones por Western blot para comprobar el estado de fosforilación de las dianas de mTORC1, 4EBP1 y rpS6. **(B)** Se analizaron mediante inmunohistoquímica los niveles de fosfo-rpS6$^{Ser235/6}$ de pulmones de ratones salvajes expuestos a hipoxia 10% O_2 (Hx10%) durante 4 días o a normoxia (N), y de ratones Vhl^{floxed}-UBC-Cre-ER^{T2}, Vhl^{floxed}HIF2α^{floxed}-UBC-Cre-ER^{T2} y sus correspondientes controles. Cuantificación del número de células del epitelio bronquial positivas para la tinción con fosfo-rpS6$^{Ser235/6}$ de ratones salvajes expuestos a hipoxia 10% O_2 (n=4) durante 4 días o a normoxia (n=4), y de ratones Vhl^{floxed}-UBC-Cre-ER^{T2} (n=4), Vhl^{floxed}HIF2α^{floxed}-UBC-Cre-ER^{T2} (n=4) y sus correspondientes controles (n=3). Se analizaron 5 bronquios de cada animal y más de 1500 células de cada grupo. Se muestra la media; las barras de error representan el SEM. *p<0,05; **p<0,01;***p<0,001.

A continuación nos preguntamos si la estabilización de HIF2α era suficiente para mimetizar esta activación localizada de mTORC1 en los pulmones causada por la hipoxia. Para contestar a esta pregunta hicimos uso de ratones adultos Vhl^{floxed}-UBC-Cre-ER^{T2} en los cuales el gen *Vhl*, un represor central de la actividad de HIF, puede ser delecionado de forma aguda (Elorza et al., 2012; Miró-Murillo et al., 2011), así como ratones Vhl^{floxed}HIF2α^{floxed}-UBC-Cre-ER^{T2}, en los cuales tanto *Vhl* como *HIF2α* son inactivados simultáneamente. Para ello estos ratones fueron tratados durante 10 días con 4-hidroxi-tamoxifeno, que permite la translocación global de la recombinasa UBC-Cre-ER^{T2} al núcleo de las células. Una vez allí actúa sobre los sitios loxP promoviendo la recombinación de las secuencias flanqueadas, el promotor y exón 1 en el caso de *Vhl*, y el exón 2 en HIF2α, lo que conduce a la inactivación génica de estos *loci* (Figuras 26 y 27A).

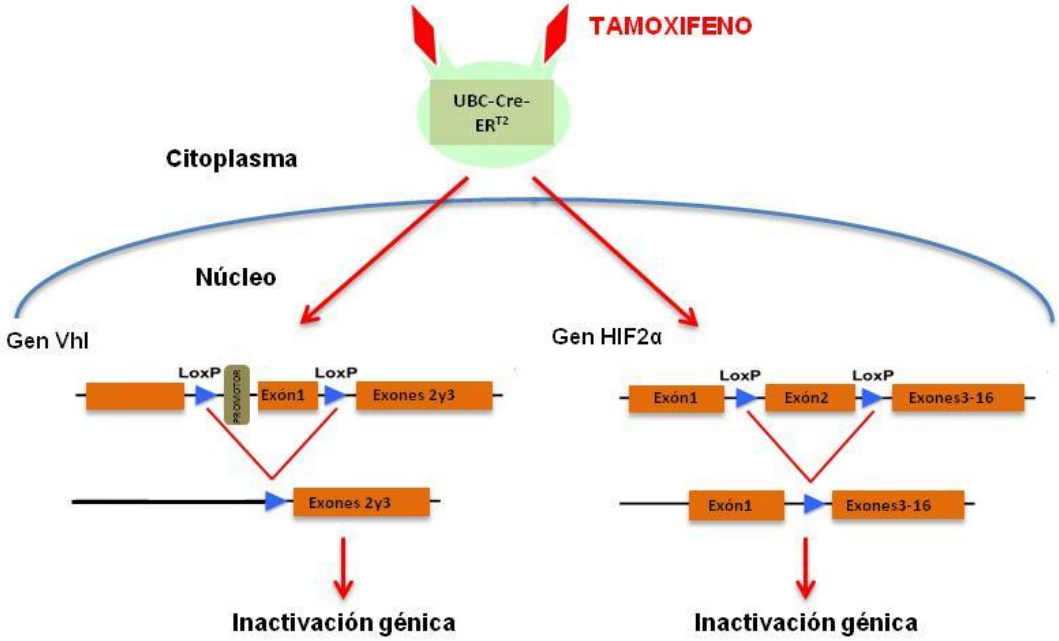

Figura 26. Generación de ratones deficientes para VHL y HIF2α. Modelo de actuación del 4-hidroxi-tamoxifeno. La translocación de la Cre recombinasa al núcleo provoca la recombinación y deleción del ADN flanqueado por los sitios loxP en los ratones Vhl^{floxed}-UBC-Cre-ER^{T2} y Vhl^{floxed}HIF2α^{floxed}-UBC-Cre-ER^{T2}, causando la inactivación génica.

Así se puede observar que los niveles de proteína de HIF2α están claramente elevados en los pulmones de los ratones Vhl^{floxed}-UBC-Cre-ER^{T2} pero no en los Vhl^{floxed}HIF2α^{floxed}-UBC-Cre-ER^{T2}. En cambio, los niveles proteicos de HIF1α se encuentran inducidos en ambas líneas de ratones (Figura 27B). Como se puede observar en la Figura 25B, la activación de mTORC1 inducida por hipoxia es mimetizada cuando HIF2α se encuentra activado de manera constitutiva en el pulmón de los ratones Vhl^{floxed}-UBC-Cre-ER^{T2}. De hecho, el número de células epiteliales bronquiales rpS6-Ser$^{235/236}$ se encontraba aumentado en los pulmones de los ratones Vhl^{floxed}-UBC-Cre-ER^{T2}. Sin embargo este efecto no se observa en los ratones Vhl^{floxed}HIF2α^{floxed}-UBC-Cre-ER^{T2}, lo cual indica que HIF2α media esta activación de mTORC1 en el epitelio pulmonar. A continuación quisimos analizar la expresión del gen codificante para *Slc7a5* en estos pulmones. Como se observa en la Figura 28A y B, los niveles de ARNm de este transportador se inducen notablemente tanto en los pulmones expuestos a bajas concentraciones de O_2 como en los ratones Vhl^{floxed}-UBC-Cre-ER^{T2} con el gen *Vhl* delecionado, pero no así en los ratones Vhl^{floxed}HIF2α^{floxed}-UBC-Cre-ER^{T2}. La especificidad del papel de HIF2α en este efecto queda demostrada al comprobar que la expresión de la fosfoglicerato quinasa 1 (*Pgk1*), un gen

ampliamente reconocido como dependiente de HIF1α *in vivo* (Rankin et al., 2007), no se encuentra disminuida en los ratones Vhl^{floxed}HIF2α^{floxed}-UBC-Cre-ER^{T2} (Figura 28C). Estos datos indican que tanto las bajas tensiones de O_2 como la inducción de HIF2α provocan la activación de mTORC1 y aumentan la expresión de SLC7A5 en el pulmón simultáneamente y, lo que es más importante, definen un escenario hipóxico en el que se potencia la activación de mTORC1 en lugar de la represión observada en otros escenarios hipóxicos.

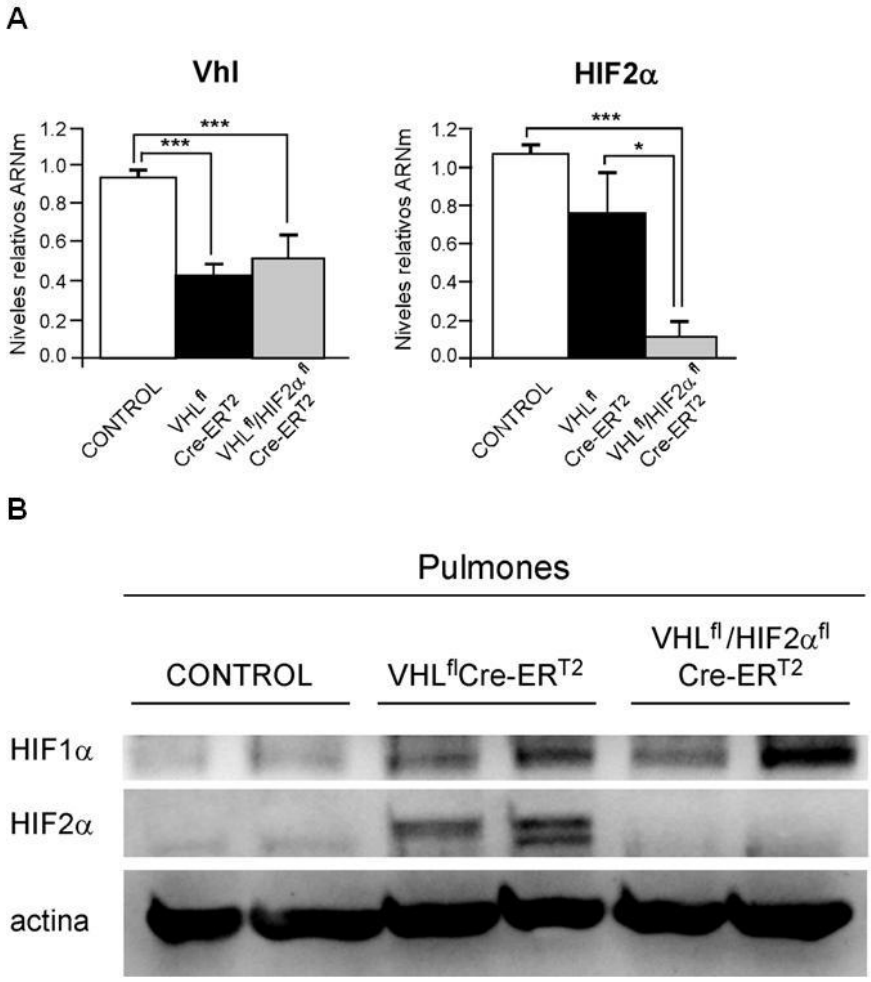

Figura 27. Expresión génica de *Vhl* y *HIF2α* y de los niveles proteicos de HIF1α y HIF2α en pulmón tras la inactivación génica de *Vhl*. (A) Expresión relativa de los ARNm de los genes *Vhl* y *HIF2α* en los pulmones de ratones Vhl^{floxed}-UBC-Cre-ER^{T2} (n=5), Vhl^{floxed}HIF2α^{floxed}-UBC-Cre-ER^{T2} (n=5) y sus correspondientes controles (n=6), normalizada a la expresión de *Hprt*. Se muestra la media; las barras de error representan el SEM. *p<0,05; ***p<0,01. **(B)** Se analizaron extractos proteicos de los pulmones mediante Western blot para la detección de HIF1α, HIF2α y actina como control de carga.

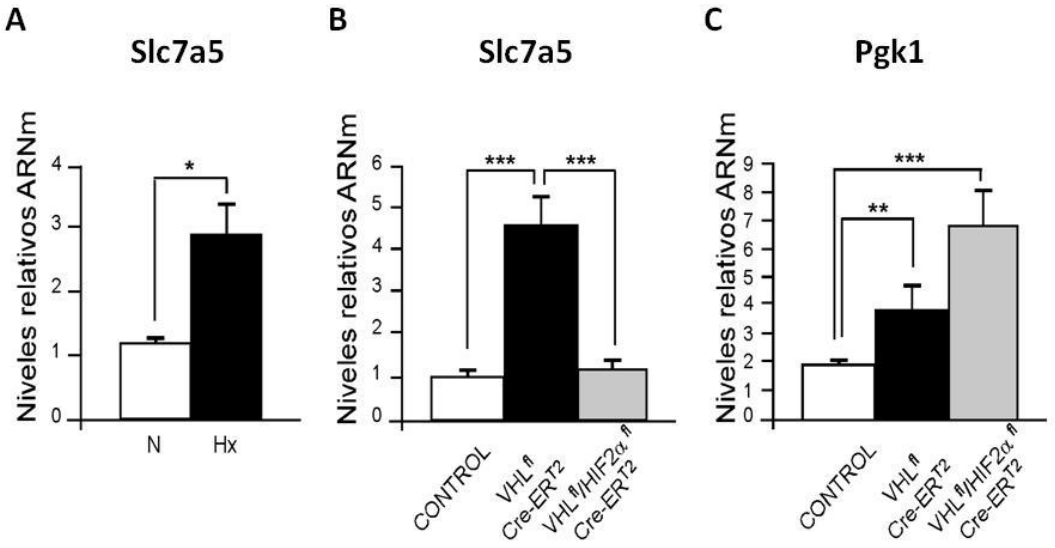

Figura 28. Expresión de *Slc7a5* dependiente de hipoxia y de HIF2α en el pulmón. Análisis mediante RT-PCR cuantitativa de los niveles relativos de ARNm del gen *Slc7a5* en los pulmones de ratones sometidos a normoxia (N; n=7) o hipoxia (Hx; n=6) **(A)** y *Slc7a5* **(B)** y *Pgk1* **(C)** en ratones Vhl^{floxed}-UBC-Cre-ER^{T2} (n=5), Vhl^{floxed}HIF2α^{floxed}-UBC-Cre-ER^{T2} (n=5) y sus correspondientes controles (n=6), normalizada a la expresión de *Hprt*. Se muestra la media; las barras de error representan el SEM. *p<0,05; **p <0,01; ***p<0,001.

La activación constitutiva de HIF2α también ha sido asociada a signos de proliferación celular en el tejido hepático *in vivo* (Kim et al., 2006b). Quisimos por tanto finalmente investigar si HIF2α también era capaz de producir la activación de mTORC1 en este tejido. Utilizando el mismo sistema *in vivo* descrito anteriormente para los estudios en pulmón, encontramos que tras la deleción de *Vhl* en los ratones Vhl^{floxed}-UBC-Cre-ER^{T2} se detectaba una elevación de los niveles proteicos de HIF2α, mientras la expresión de HIF1α se inducía más modestamente (Figura 29). Como era previsible, al inactivar simultáneamente *Vhl* y *HIF2α* en los ratones Vhl^{floxed}HIF2α^{floxed}-UBC-Cre-ER^{T2} (Figura 30), los niveles de HIF2α se hacían prácticamente indetectables, mientras que la débil expresión de HIF1α se mantenía (Figura 29).

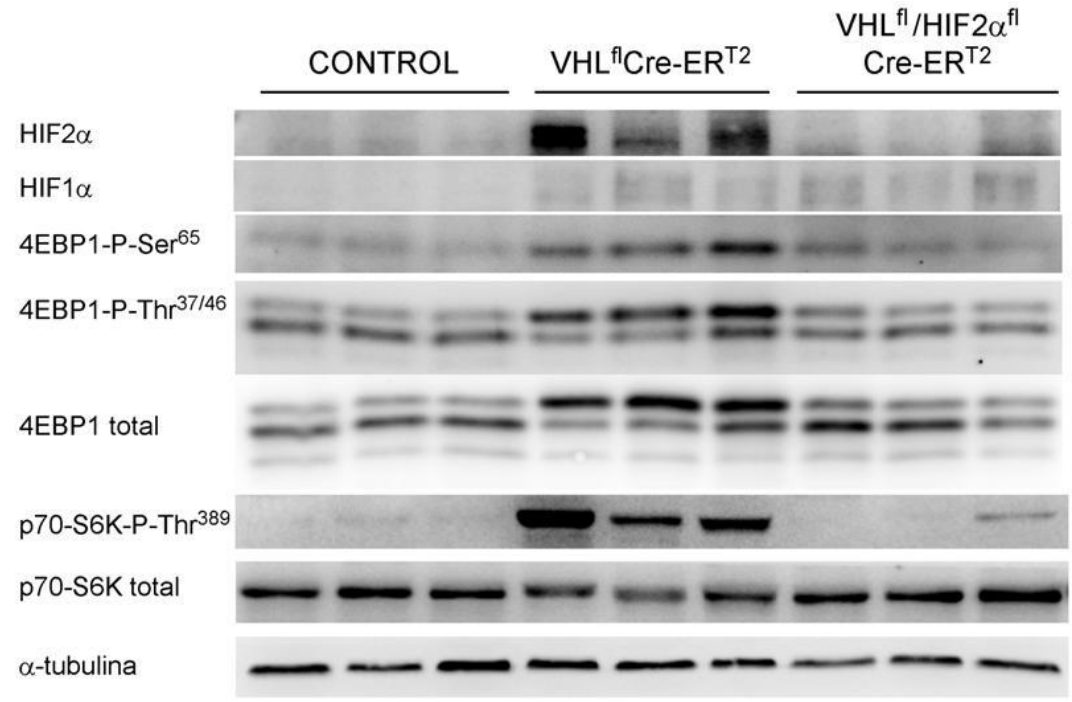

Figura 29. Dependencia de la actividad de mTORC1 de la expresión de HIF2α en hígado. Se analizaron por Western blot extractos proteicos de los hígados de ratones Vhl^{floxed}-UBC-Cre-ER^{T2}, Vhl^{floxed}HIF2α^{floxed}-UBC-Cre-ER^{T2} y sus respectivos controles y se evaluó la expresión de HIF2α, HIF1α y el estado de fosforilación y proteína total de las dianas de mTORC1 4EBP1 y p70-S6K.

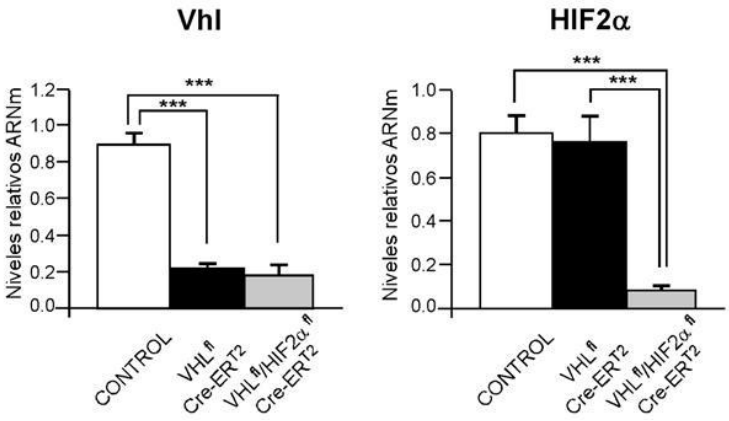

Figura 30. Expresión génica de *Vhl* y *HIF2α* en hígado tras la inactivación génica de *Vhl.* Inducción relativa de los ARNm de los genes *Vhl* y *HIF2α* en los hígados de ratones Vhl^{floxed}-UBC-Cre-ER^{T2} (n=7), Vhl^{floxed}HIF2α^{floxed}-UBC-Cre-ER^{T2} (n=6) y sus correspondientes controles (n=6), normalizada a la expresión de *Hprt*. Se muestra la media; las barras de error representan la SEM. ***p<0,01.

El análisis por Western blot mostró que los niveles de fosforilación tanto de 4EBP1 como de p70-S6K, otra diana de mTORC1, se inducían en ratones Vhl^{floxed}-UBC-Cre-ER^{T2} pero no en Vhl^{floxed}HIF2α^{floxed}-UBC-Cre-ER^{T2}, demostrando el papel de HIF2α en la activación de la vía de mTORC1 también en tejido hepático (Figura 29). Quisimos además realizar un análisis más detallado de los hepatocitos mediante inmunohistoquímica, el cual mostró que las señales basales de rpS6-Ser$^{235/236}$ (Figura 31) y de SLC7A5 (Figura 32) se incrementaban tras la inactivación del gen *Vhl* y que este incremento se perdía cuando se inactivaban simultáneamente *Vhl* y *HIF2α*. En un análisis paralelo observamos que la expresión del ARNm del gen *Slc7a5* así como la del gen dependiente de HIF1α, *Pgk1* (ver más arriba) se encontraba elevada tras la inactivación de *Vhl*. Además, en línea con el papel central de HIF2α en la activación de SLC7A5, los ratones Vhl^{floxed}HIF2α^{floxed}-UBC-Cre-ER^{T2} no mostraban aumento en la expresión de *Slc7a5*, mientras la expresión del gen *Pgk1* se mantenía (Figura 32B).

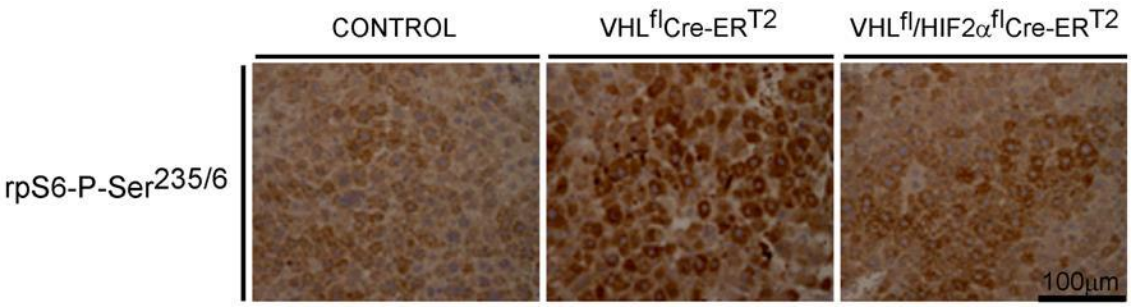

Figura 31. Dependencia de HIF2α de la activación de mTORC1 en hígado tras la deleción génica de *Vhl*. Se analizaron mediante inmunohistoquímica los niveles de fosfo-rpS6$^{Ser235/6}$ en hígados de ratones Vhl^{floxed}-UBC-Cre-ER^{T2}, Vhl^{floxed}HIF2α^{floxed}-UBC-Cre-ER^{T2} y los correspondientes ratones control (n=6).

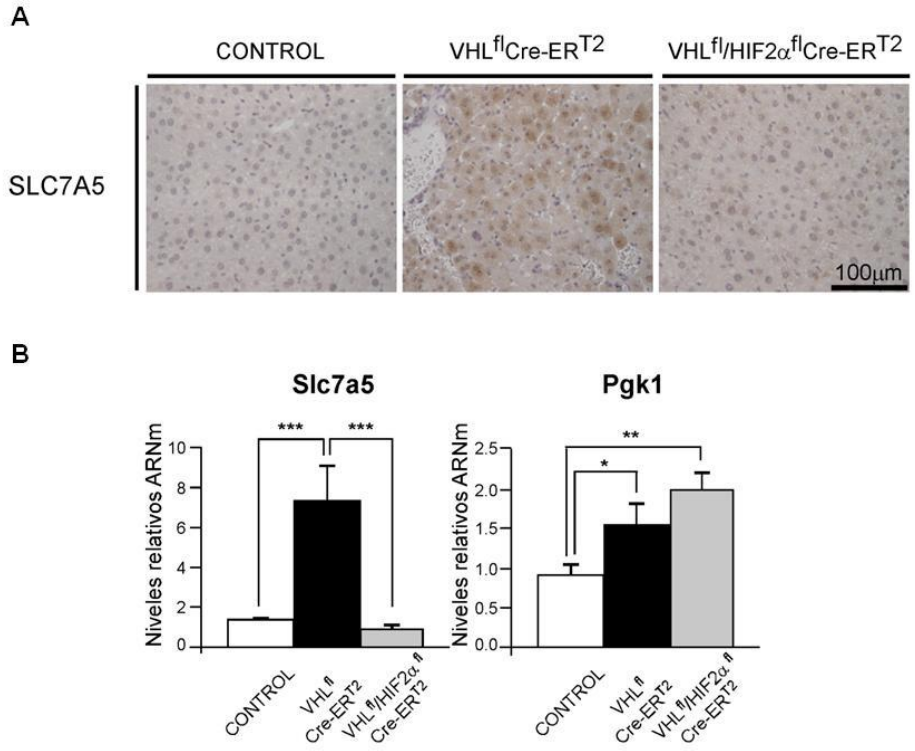

Figura 32. Expresión de SLC7A5 y *Pgk1* en hígado tras la inactivación génica de *Vhl*. (A) Se analizaron mediante inmunohistoquímica los niveles de SLC7A5 en hígados de ratones Vhl^{floxed}-UBC-Cre-ER^{T2}, Vhl^{floxed}HIF2α^{floxed}-UBC-Cre-ER^{T2} y los correspondientes ratones control. **(B)** Expresión relativa de los ARNm de los genes *Slc7a5* y *Pgk1* en los hígados de ratones Vhl^{floxed}-UBC-Cre-ER^{T2} (n=7), Vhl^{floxed}HIF2α^{floxed}-UBC-Cre-ER^{T2} (n=6) y sus correspondientes controles (n=7), normalizada a la expresión de *Hprt*. Se muestra la media; las barras de error representan la SEM. *p<0,05; **p<0,01;***p<0,01.

En conjunto estos resultados indican que la activación de HIF2α también aumenta la actividad de mTORC1 y la expresión de SLC7A5 en el hígado, demostrando por tanto que el eje molecular HIF2α-SLC7A5-mTORC1 está presente en distintos escenarios biológicos.

Por lo tanto, nuestros datos indican que HIF2α promueve la activación de mTORC1 y la expresión de SLC7A5 en diferentes escenarios tumorales y no tumorales y, además, define el pulmón hipóxico como un importante contexto fisiológico en el que la hipoxia causa la activación de mTORC1 en lugar de su inhibición, como se ha descrito al menos *in vitro* en otros contextos hipóxicos (ver Discusión).

DISCUSIÓN

DISCUSIÓN

La respuesta biológica a las fluctuaciones de O_2 ha alcanzado un gran interés biomédico ya que es un elemento central en numerosos escenarios patológicos tales como la progresión tumoral, la isquemia cardiaca o la patología pulmonar. Una de las funciones celulares que es regulada en función del aporte de O_2, y que ha sido fundamentalmente estudiada en el contexto de la progresión tumoral, es la proliferación autónoma de célula. La hipoxia, tradicionalmente estudiada en cultivos celulares *in vitro* y en condiciones relativamente severas de hipoxia, ha sido descrita clásicamente como un estímulo inhibidor tanto de la proliferación celular como del sensor de aminoácidos mTORC1, lo cual responde al razonamiento lógico de que, en ausencia de O_2, procesos muy costosos energéticamente como son la síntesis proteica (controlada por mTORC1) y la división celular deben ser reprimidos. Estos efectos anti-proliferativos son ejecutados fundamentalmente por el factor HIF1α así como por mecanismos independientes de la ruta de HIF (Liu et al., 2006). Sin embargo varios estudios recientes en sistemas *in vivo* han revelado que el papel de la hipoxia en proliferación celular es más complicado de lo que inicialmente podía anticiparse, dado que, sorprendentemente, algunos escenarios hipóxicos desencadenan proliferación autónoma celular.

HIF2α como factor promotor de la proliferación

Los estudios que han cuestionado el papel de la señalización de la hipoxia como represora de la proliferación han surgido de las investigaciones de la isoforma HIF2α. De hecho, esta isoforma HIF2α se ha revelado en los últimos años como un factor promotor de la proliferación, aunque los mecanismos moleculares involucrados (tema principal de este trabajo de tesis) siguen siendo poco conocidos. Las primeras evidencias del papel pro-proliferativo de HIF2α surgieron de los estudios en carcinomas renales de célula clara (ccRCC) deficientes para VHL, en los que la expresión de la isoforma HIF2α favorece un mayor y más rápido crecimiento de las lesiones tumorales (Gordan et al., 2007; Mandriota et al., 2002; Raval et al., 2005). En el trabajo que presentamos en esta tesis demostramos que la activación de la vía de HIF2α en estas células tumorales deficientes para VHL incrementa la actividad de mTORC1 mediante la inducción de la expresión del transportador de aminoácidos SLC7A5, crítico para su actividad. La caracterización de este mecanismo molecular, que interrelaciona HIF2α con el metabolismo intracelular de aminoácidos, proporciona

una base molecular para explicar el papel pro-tumoral de HIF2α. Además este nuevo eje de acción proliferativa HIF2α-SLC7A5-mTORC1, aunque contrasta con el históricamente supuesto dogma de la hipoxia como represor de la proliferación celular, se contextualiza muy adecuadamente con una serie de estudios, enumerados a continuación, que señalan que la activación del sistema HIF (en concreto la isoforma HIF2α) también funciona como una señal pro-proliferativa:

1) Se estima que entre un 60 y un 85% de los mencionados ccRCC deficientes para VHL y por tanto HIF2α positivos, presentan mTORC1 en estado activado (Pantuck et al., 2007; Robb et al., 2007) y éste además participa en la patogénesis, habiéndose de hecho mostrado efectivos para su tratamiento el uso de inhibidores de mTORC1 en ensayos clínicos actualmente en fase III (Hudes et al., 2007; Motzer et al., 2008).

2) Se ha descrito que HIF2α promueve la carcinogénesis en estos tumores deficientes para VHL en parte a través de su interacción con el oncogen c-Myc, que de este modo estabilizaría su dimerización con cofactores adicionales (Max, Sp1 o Miz1) incrementando así su actividad transcripcional. Este papel es exclusivo de la isoforma HIF2α y es independiente de su unión a ADN (Gordan et al., 2007). Es importante destacar que aunque existen evidencias que apuntan a SLC7A5 como un gen c-Myc dependiente (Gao et al., 2009; Hayashi et al., 2012), nuestros datos indican que HIF2α se une al promotor proximal de SLC7A5 y que esta unión parece fundamental para la inducción de su transcripción, por lo que su expresión dependiente de HIF2α no puede explicarse mediante el modelo previamente descrito de transactivación de c-Myc. Independiente de estas diferencias en el mecanismo molecular subyacente, el eje molecular descrito en este estudio está en la línea que implica a HIF2α como desencadenante de proliferación celular.

3) El complejo mTORC2, que se forma por la interacción de mTOR con la proteína Rictor y es también un elemento importante, aunque menos conocido que mTORC1, en el control de la proliferación celular, regula la traducción de HIF2α (Toschi et al., 2008). Este hecho sugiere que parte de los efectos proliferativos ejecutados por mTORC2 podrían ser efectuados por HIF2α, entre los que podría situarse el eje molecular descubierto en nuestros estudios de captación de aminoácidos esenciales a través de la inducción de la expresión de SLC7A5.

4) HIF2α también induce transcripcionalmente otros genes involucrados en progresión de ciclo celular, tales como la ciclina D1 (Raval et al., 2005; Wykoff et al., 2004). Se ha descrito además la activación por parte de HIF2α del eje TGFα-EGF-R, que se encuentra sobreexpresado en los ccRCC y que es en parte responsable del crecimiento autónomo en cultivo de estas células y de la formación de tumores *in vivo* (Gunaratnam et al., 2003; De Paulsen et al., 2001; Raval et al., 2005). Sin embargo esta activación podría ser secundaria a la de HIF2α, ya que no se ha demostrado que estas proteínas sean dianas transcripcionales primarias de HIF2α como es el caso de SLC7A5. Además los efectos de HIF2α sobre estos genes sólo se han descrito en células de carcinoma renal y no en otros contextos, por lo que no parecen tan generales como lo es el caso de SLC7A5, que responde a la activación de HIF2α en diferentes tipos celulares.

5) HIF2α puede aumentar la actividad de mTORC1 a través del incremento en la señalización de factores de crecimiento, ya que puede inducir transcripcionalmente la expresión de PDGFβ, IGF1 o el propio TGFα, promoviendo la activación de AKT y por tanto de mTORC1. En concreto en el caso de TGFα ha sido descrito un mecanismo de actuación autocrino (De Paulsen et al., 2001) que podría ser también operativo para el resto de factores de crecimiento mencionados.

En conjunto estos estudios apoyan el hecho de que HIF2α puede actuar como un factor favorecedor de la proliferación y proporcionan un buen contexto biológico para explicar nuestros hallazgos a cerca de HIF2α como activador de mTORC1.

Hipoxia y mTORC1

Como ya se ha comentado, nuestros datos suponen un contraste a los efectos previamente descritos de la hipoxia como estímulo represor de la actividad de mTORC1, vía mecanismos tanto dependientes de HIF1α (a través de la inducción transcripcional de genes tales como Redd1 y bNIP3) como independientes de la ruta de HIF (a través de la activación de la ruta de la AMPK). Sin embargo consideramos que todos estos estudios emplean unos escenarios hipóxicos muy concretos que entendemos pueden no reflejar la totalidad de la respuesta a hipoxia. En este sentido, es importante considerar que los trabajos que describen la represión de mTORC1 en

hipoxia han sido desarrollados a partir de estudios realizados en sistemas celulares *in vitro* y en condiciones de hipoxia muy concretas y relativamente severas (0,5-1% O_2). Por el contrario, en nuestro trabajo se evalúa por vez primera el papel de HIF sobre mTORC1 en un contexto *in vivo*. Y, sorprendentemente, nuestros datos demuestran que HIF2α actúa como un factor activador de mTORC1 a través de la inducción del transportador de aminoácidos SLC7A5. Es posible que los efectos represores de la hipoxia sobre mTORC1, tanto los dependientes de la isoforma HIF1α como los independientes de HIF, (i) sean tejido-específicos y por lo tanto no sean operativos en ciertos tipos celulares como es el caso del epitelio bronquial; (ii) sean operativos sólo en condiciones de hipoxia *in vitro* o bien (iii) sean contrarrestados por la activación de HIF2α en el pulmón ya que esta isoforma es especialmente abundante en el tejido pulmonar. En concreto, respecto a los aspectos específicos de célula, es sabido que la anoxia o la hipoxia relativamente severa pueden llevar a la activación de la enzima AMPK (Liu et al., 2006), aunque no en todos los tipos celulares (Arsham et al., 2003), puesto que algunos son capaces de adaptarse a la escasez de O_2 y mantener los niveles normales de ATP (Wolff et al., 2011). Esta incapacidad para activar AMPK en respuesta a hipoxia se ha descrito por ejemplo para el caso de los fibroblastos embrionarios (Wolff et al., 2011) y, a la vista de nuestros datos, quizá tampoco sea operativo en células epiteliales del bronquio expuestas a hipoxia. En cualquier caso esta variabilidad en función del tipo celular en cuanto a la represión de mTORC1 en hipoxia, a través de rutas independientes de HIF, se ha descrito en estudios *in vitro* exponiendo diferentes cultivos celulares a hipoxia. Por lo tanto es necesario investigar todavía si las rutas represoras de mTORC1 en hipoxia son operativas *in vivo*. Otro aspecto a tener en cuenta para reconciliar nuestro estudio con el dogma de la hipoxia como represora de mTORC1 es la diferencia en la severidad de la hipoxia aplicada que, en nuestro trabajo, *in vivo*, es del 10% O_2 en lugar del 1% O_2 normalmente empleado en los estudios *in vitro*. Es razonable considerar que estas condiciones de hipoxia más suaves no sean interpretadas por la célula como un escenario que requiera reprimir mTORC1 ni la proliferación celular, sino que sea un aporte de O_2 aún suficiente para promover proliferación celular en escenarios tales como el epitelio bronquial. En este contexto, se sabe que la isoforma HIF2α es más sensible a la respuesta a hipoxias moderadas que HIF1α, dado que la enzima FIH hidroxila sólo débilmente a HIF2α. Se sabe además que la isoforma HIF2α, nuevamente al contrario que HIF1α, se expresa abundantemente y es transcripcionalmente activa en lesiones neoplásicas de neuroblastoma bien vascularizadas y aparentemente no hipóxicas, así como en cultivos celulares mantenidos a concentraciones de O_2 fisiológicas del 5%.

Podría ser por tanto que las hipoxias moderadas que previsiblemente se producen en contextos fisiológicos favorezcan la estabilización de la isoforma HIF2α, que a través del mecanismo que proponemos en este trabajo, llevaría a cabo la activación de mTORC1. Por el contrario, se podría anticipar (aunque no ha sido demostrado) que *in vivo* una hipoxia más severa tal como la que puede tener lugar en los focos tumorales, indujera HIF1α así como señales independientes de HIF, que promovieran la represión de la actividad de mTORC1 y de la proliferación celular. En función de nuestros datos, proponemos que la activación en hipoxia de mTORC1 en el pulmón vía HIF2α sea debida a un aumento en la expresión de SLC7A5 en las células del epitelio bronquial. De hecho, datos preliminares de inmunohistoquímica (no publicados) indican un aumento de SLC7A5 específicamente en el epitelio bronquial. Esta inducción de la expresión de SLC7A5 facilitaría la entrada de los aminoácidos esenciales en las células epiteliales del bronquio para promover en ellas la activación de mTORC1. En definitiva este eje de acción domina en el pulmón hipóxico frente a otras rutas represoras de mTORC1 vía HIF1α o vías independientes de HIF.

Por otra parte, en un trabajo reciente que muestra tinciones inmunohistoquímicas de 160 muestras de cáncer pulmonar de célula no pequeña encuentran una correlación significativa en la tinción de SLC7A5, activación de mTORC1 y activación de genes dependientes de HIF como es el caso de GLUT1 y VEGF (Kaira et al., 2011), lo que plantea un nuevo escenario en el que la hipoxia y la activación de mTORC1 ocurren simultáneamente. En estos tumores además es común la sobreexpresión de SLC7A5 y es un mal factor pronóstico (Kaira et al., 2009). Por lo tanto, estos datos sugieren que el eje molecular HIF2α-SLC7A5-mTORC1 descrito en el pulmón hipóxico podría ser también operativo en ciertas áreas hipóxicas (quizá de hipoxia moderada) en cáncer pulmonar de célula no pequeña.

Deficiencia de VHL y mTORC1

Al margen de la situación de hipoxia, otro escenario en el que observamos el papel activador de HIF2α sobre mTORC1 a pesar de la activación simultánea de HIF1α es en los tejidos deficientes para VHL, que expresan de forma concomitante ambas isoformas. En este caso la activación de ambas subunidades HIFα ocurre en normoxia, por lo que la posible acción represora *in vivo* (nunca demostrada) sobre mTORC1 de las rutas hipóxicas independientes de HIF no sería operativa en estos escenarios (aunque sí potencialmente la de las vías dependientes de HIF1α). Sin embargo este supuesto efecto represivo vía HIF1α no se observa ni en los pulmones

ni en el hígado de los animales modificados genéticamente para delecionar VHL, lo cual nos hace plantearnos de nuevo que, como en el caso del pulmón hipóxico comentado previamente, o bien HIF1α no es capaz de reprimir mTORC1 en estos tejidos o bien que el posible efecto inhibidor es fuertemente contrarrestado por la activación de HIF2α. Con respecto a los aspectos específicos de célula en cuanto a su capacidad para reprimir mTORC1 (ver más arriba), es también necesario comentar aquí que el papel de HIF1α como represor de mTORC1 resulta actualmente controvertido. Trabajos anteriores han descrito que la inducción por HIF de Redd1 (activador del complejo TSC1/2 y por tanto inhibidor de mTORC1) no promueve la inactivación de mTORC1 en todos los tipos celulares, y en particular se ha demostrado que no es capaz de hacerlo en hepatocitos primarios (Wolff et al., 2011), lo cual explicaría el hecho de que HIF1α no contrarreste la activación de mTORC1 vía HIF2α en el hígado de los animales deficientes para VHL. Un escenario similar podría explicar nuestros datos en los pulmones de estos mismos ratones deficientes para VHL, donde HIF2α también promueve la activación de mTORC1 a pesar de la presencia de HIF1α. Sorprendentemente el mismo efecto hemos observado en nuestro laboratorio en experimentos con fibroblastos murinos embrionarios deficientes para VHL, que estabilizan exclusivamente la isoforma HIF1α, en los que tampoco ocurre inactivación de mTORC1 (datos no publicados). Por lo tanto, se hace necesario reconsiderar en qué contextos *in vivo* e *in vitro* HIF1α funciona realmente como un represor de mTORC1.

El caso del carcinoma renal deficiente para VHL es el otro escenario en el que se describe en este trabajo la capacidad de la vía HIF2α-SLC7A5 para promover la activación de mTORC1, proporcionando la base molecular que explica la importancia de la expresión de HIF2α para la progresión de estos tumores. Destacar aquí que un 30% de los tumores deficientes en VHL carecen de la isoforma HIF1α, con lo cual estas células no presentarían ninguna de las rutas represoras de mTORC1 por mecanismos dependientes e independientes de HIF1α que venimos comentando en esta discusión y que en cualquier caso están aún en debate (ver discusión más arriba). Además en algunos de estos tumores que conservan la isoforma HIF1α se ha descrito la evolución de mecanismos que impedirían la inhibición de mTORC1 a pesar de la expresión de Redd1, como mutaciones inactivantes en TSC1 (Kucejova et al., 2011). Este estudio permite también explicar nuestros datos sobre la no inhibición de la isoforma HIF1α de la actividad de mTORC1 en las células WT8 HIF1α(P-A)^2.

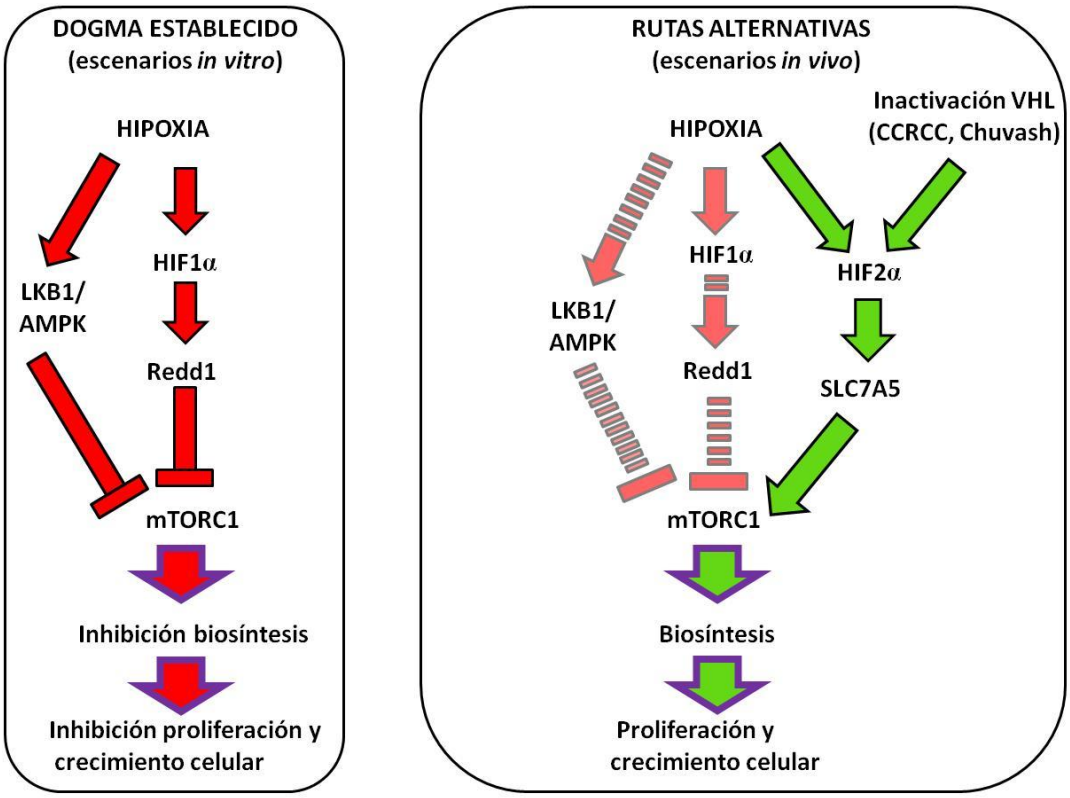

Figura 33. Descripción de las rutas de señalización que promueven la represión (panel izquierdo) o la activación (panel derecho) de mTORC1 en escenarios hipóxicos o pseudohipóxicos. Tradicionalmente, a partir de estudios *in vitro* y en hipoxias severas, se ha descrito la hipoxia como un estímulo inhibitorio de la actividad de mTORC1 (a través de mecanismos dependientes de HIF1α -vía Redd1- y no dependientes de HIF -a través de la enzima AMPK-) y consecuentemente de la proliferación. Publicaciones recientes plantean excepciones a estas vías de inactivación en determinados tipos celulares o tejidos así como dependientes de la severidad de la hipoxia (ver Discusión), explicando situaciones fisiológicas en las que ocurre de forma concomitante la activación de la ruta de señalización de hipoxia y la de mTORC1, con la consiguiente proliferación celular.

Otras posibles funciones biológicas del eje molecular HIF2α-SLC7A5-mTORC1.

Como acabamos de comentar, en este trabajo demostramos cómo la activación de mTORC1 vía HIF2α media proliferación en las células de carcinoma renal deficientes en VHL. Inicialmente razonamos que esta ruta de señalización podría también mediar la proliferación descrita en hepatocitos de animales deficientes en VHL

detectada mediante tinción con el marcador de proliferación celular Ki67 (Kim et al., 2006b). En este mismo sentido, también es conocido el efecto regenerador que tiene la inhibición del sensor de O_2 PHD1 -vía activación de HIF2α- sobre hígados parcialmente hepatectomizados, promoviendo la proliferación de los hepatocitos (Mollenhauer et al., 2012). Nuestros propios estudios en hígados deficientes para VHL -no sometidos a hepatectomía- indican que el aumento en el número de células positivas para el marcador de proliferación celular Ki67 parece corresponderse con la presencia de un mayor número de células inflamatorias, que son las que resultan marcadas. Por lo tanto podría ser que la proliferación de hepatocitos ocurriera a través del eje HIF2α-SLC7A5-mTORC1 de forma exclusiva en el contexto de la regeneración tisular. En este sentido, puesto que mTORC1, además de proliferación también media crecimiento celular, es razonable pensar que este efecto sea el responsable de la hepatomegalia que sí se observa en los ratones deficientes para VHL. También ha sido descrita hepatomegalia asociada a la policitemia de Chuvash, una enfermedad hereditaria causada por una mutación que reduce parcialmente la actividad de VHL, lo que promueve una continua elevación de los niveles de expresión de HIF. Esta patología cursa además con un aumento en el tamaño de otros órganos como bazo y riñones, habiéndose demostrado con modelos murinos transgénicos que el aumento en la hepatomegalia es dependiente de la expresión de HIF2α (Yoon et al., 2010).

Por otro lado, la activación de mTORC1 en el hígado dirigida por HIF2α podría también tener un papel orientado al control del metabolismo hepático, dado que es conocida la capacidad de mTORC1 para regular rutas metabólicas en diversos tejidos a nivel transcripcional, traduccional y postraduccional. Este es el caso del factor de transcripción SREBP-1, cuyo procesamiento postraduccional y consiguiente activación es favorecida por mTORC1 a través de p70-S6K1, lo que promueve que active la transcripción de genes implicados en la biosíntesis de esteroles y lípidos y la vía oxidativa de la ruta de las pentosas fosfato. También es conocido el efecto potenciador de mTORC1 sobre la actividad transcripcional del coactivador de PPARγ, PGC1α, un factor nuclear que juega un importante papel en la biogénesis mitocondrial y el metabolismo oxidativo (Cunningham et al., 2007). Este control sobre el metabolismo que ejerce mTORC1 se refleja en el fenotipo de los ratones transgénicos con mutaciones en sus dianas principales p70-S6K1 y 4EBP1. Ambos exhiben profundas alteraciones en su metabolismo, que los hacen resistentes a la obesidad en el caso de los animales deficientes para p70-S6K1 y propensos a ella en el de los deficientes para 4EBP1. En línea con el papel metabólico de esta activación de mTOCR1 dependiente de HIF2α, es necesario mencionar que HIF2α se ha identificado como un

factor controlador de la ingesta alimenticia cuando se estabiliza en las células POMC del hipotálamo. Esta estabilización se debe a la inhibición química de los sensores PHDs por el acúmulo de metabolitos derivados de la glucosa durante la ingesta: piruvato, oxalacetato (Lu et al., 2005), fumarato y succinato (Zhang et al., 2011). Su activación promueve en estas células la transcripción del gen *Pomc*, una molécula clave en el control de la ingesta y el balance del peso corporal. Estas células POMC también responden a la cantidad de aminoácidos extracelulares tras la ingesta y por lo tanto podría especularse con el hecho de que esta activación de HIF2α pudiera controlar su respuesta al aporte aminoacídico vía SLC7A5.

Por otro lado, a pesar de que la proliferación de la mayoría de las células cancerosas depende de la señalización por mTORC1, se sabe que su activación mantenida bajo condiciones de estrés, como la deprivación de glucosa en MEFs deficientes para TSC1/2 (Lee et al., 2007) o la hipoxia en una línea celular de fibroblastos deficientes para el gen ATM (Cam et al., 2010) conduce a muerte por apoptosis mediada por p53. Igualmente se ha descrito en un trabajo reciente que MEFs deficientes para TSC2 sometidos a la compleja mezcla de los estreses propios de un tumor (deprivación simultánea de suero, O_2 y glucosa) producen una respuesta a proteínas mal plegadas (UPR, *Unfolded Protein Response*) exacerbada que les lleva a la muerte celular. HIF2 se ha descrito como un factor que favorece el crecimiento tumoral en numerosos escenarios como es el caso del carcinoma renal (Kondo et al., 2003; Maranchie et al., 2002; Raval et al., 2005), pero también se han descrito en ciertos tipos tumorales como las células de glioma un papel inhibidor del crecimiento tumoral debido a un aumento de apoptosis (Acker et al., 2005). Por lo tanto la activación de mTORC1 por HIF2 no tiene por qué desembocar exclusivamente en crecimiento tumoral (como en el caso del ccRCC), sino que podría resultar también en una maladaptación celular y apoptosis vía HIF2α en determinados contextos tumorales (como el glioma) pero este aspecto necesitaría ser evaluado utilizando, entre otros abordajes, el silenciando específico de SLC7A5 en estos tipos tumorales.

SLC7A5 y cáncer

Existen numerosos transportadores de aminoácidos cuya sobreexpresión ha sido descrita en diversos tipos de cáncer y que se ha demostrado además importante para el crecimiento tumoral. Este aumento en su expresión ocurre en respuesta a la enorme demanda de nutrientes que tienen las células proliferantes para la generación de la biomasa necesaria para su división. Tiene sentido por tanto, dado el papel pro-

tumoral de HIF2α en varios contextos tumorales, que este factor de transcripción incluya dentro de su acción génica la inducción de alguno de estos transportadores. El presente trabajo es el primero en describir la regulación transcripcional por parte de HIF2α del intercambiador de aminoácidos SLC7A5, cuya función es clave para la actividad de mTORC1, y cuya inducción media la progresión tumoral, dado que el silenciamiento de su expresión en las células 786-O deficientes en VHL conduce a una pronunciada supresión de su capacidad para formar tumores. Es interesante mencionar que el silenciamiento de la expresión de SLC7A5 no altera la proliferación *in vitro* de estas mismas células cuando se cultivan en condiciones normales de nutrientes (datos no mostrados). Estos mismos resultados han sido descritos en un trabajo anterior desarrollado en líneas de cáncer de ovario humano - SKOV3 e IGROV1- en las que el silenciamiento de este transportador tampoco afectaba a su proliferación *in vitro* pero sin embargo reducía fuertemente la capacidad para la formación de colonias. Igualmente, células 786-O en las que se apaga la expresión de HIF2α sólo ven afectada su capacidad de formación de tumores pero no su proliferación *in vitro*, lo cual indica que el papel promotor de la proliferación de HIF2α sólo se manifiesta en microambientes tumorales en los que el aporte de aminoácidos está fuertemente disminuido (Reid et al., 2013). Nuestros datos refuerzan esta idea ya que demuestran que la expresión de SLC7A5, dependiente de HIF2α, es crítica para la proliferación de las células 786-O en el contexto intratumoral, y que la ventaja proliferativa que supone su inducción sólo se pone de manifiesto en condiciones en las que la disponibilidad de aminoácidos se encuentra limitada, como ocurre en el microambiente tumoral. Por lo tanto, nuestros resultados muestran que la vía de activación de mTORC1 aquí descrita (a través del eje HIF2α-SLC7A5) no es un factor limitante en situaciones en las que el suministro de aminoácidos es abundante, pero sí resulta esencial para mantener la actividad de mTORC1 en escenarios de baja disponibilidad de estos nutrientes, en los que las células que induzcan SLC7A5 podrán captarlos mejor. Es importante considerar además que la cantidad de aminoácidos presente en los medios de cultivo no sólo es superior a la del ambiente intratumoral sino que también es mayor que las concentraciones encontradas habitualmente en plasma. Por tanto el aporte de aminoácidos a cualquier tejido bien perfundido podría también estar en cierta medida limitado cuando se compara con los medios normales de cultivo (Bertout et al., 2008). Por lo tanto la activación de SLC7A5 *in vivo* en hígado y pulmón favorecería la activación de mTORC1 como hace en el caso de las células de carcinoma renal. Además de los datos preclínicos mencionados, es relevante destacar que el análisis de muestras humanas de pacientes con carcinomas renales

de célula clara deficientes para VHL muestra una clara sobreexpresión del transportador SLC7A5, poniendo de relevancia el valor clínico del eje HIF2α-SLC7A5-mTORC1.

Nuestro estudio es uno de los pocos en abordar directamente el papel molecular de SLC7A5 en la progresión tumoral. Otros trabajos han descrito la participación de SLC7A5/SLC3A2 y ASCT2 en un complejo asociado a la activación metabólica y marcador pronóstico de un amplio número de tumores, el complejo CD147-CD98 (Weidle et al., 2010; Xu and Hemler, 2005). Dicho complejo también incluye los transportadores de monocarboxilatos MCT1 y MCT4, la molécula de adhesión de célula epitelial EpCAM, reguladora de la proliferación celular y la proteína CD147, que actúa conduciendo a MCT1 y MCT4 a la superficie celular. Este complejo por tanto captaría aminoácidos esenciales a través de SLC7A5 al mismo tiempo que expulsaría el lactato acumulado por la glicolisis a través de MCT1 y MCT4, coordinando el transporte de los distintos metabolitos para satisfacer las necesidades metabólicas y las señales de supervivencia de las células tumorales. Además también ha sido demostrado otro mecanismo adicional por el cual la cadena pesada SLC3A2 del heterodímero, promueve la expresión en membrana del transportador de glucosa GLUT1 y contribuye por tanto no sólo a la regulación del metabolismo de aminoácidos sino también al de la glucosa (Ohno et al., 2011). Por lo tanto la inducción de SLC7A5 por HIF2α podría repercutir en transportadores de otros metabolitos con los que se asocia y entender que HIF2α pudiera impactar en el transporte de otros metabolitos indirectamente vía HIF2α.

Regulación de SLC7A5

Como ya se ha mencionado, la expresión del transportador de aminoácidos SLC7A5 está aumentada en numerosos cánceres humanos, incluidos los carcinomas renales de célula clara deficientes para VHL analizados en el presente trabajo, y está implicado en el crecimiento celular y la supervivencia de numerosas líneas celulares cancerígenas. Sin embargo el mecanismo molecular implicado en su regulación se desconocía. En este trabajo hemos identificado *Slc7a5* como un nuevo gen de respuesta directa a la regulación transcripcional por HIF2, que puede por tanto inducirse tan pronto como HIF2α se estabiliza en las lesiones de ccRCC. Nuestro análisis muestra que la unión de HIF2α al promotor proximal de *Slc7a5* es específica de esta isoforma, ya que no se observa cuando HIF1α se encuentra estabilizado en las células WT8 HIF1α(P-A)^2. Estudios previos han mostrado que HIF2α, al contrario

que HIF1α, potencia la transcripción de genes dependientes de c-Myc mediante la estabilización de los complejos heterodiméricos c-Myc-Max, un proceso que no requiere la unión directa de HIF2α a los promotores de dichos genes. Este efecto activador de HIF2 sobre c-Myc ha servido para explicar en parte las propiedades pro-proliferativas de HIF2α. Existen dos estudios en los que se observa inducción de SLC7A5 debida a c-Myc en células P493-6 (Gao et al., 2009) y células MIA Paca-2 (Hayashi et al., 2012). Nuestros propios datos (no publicados) indican que c-Myc puede efectivamente unirse al promotor y que su unión se potencia incluso en presencia de la forma HIF2α(P-A)^{2}bHLH*, (sin capacidad para unirse a ADN), datos en concordancia con estos estudios previos comentados anteriormente. De hecho uno de los dos sitios de unión a ADN que en nuestro trabajo identificamos como un posible sitio de actuación de HIF2α tiene una secuencia nucleotídica que coincide con la descrita como canónica de las E-box, sitios de unión del factor c-Myc. Sin embargo, como mostramos en la Figura 12, HIF2α(P-A)^{2}bHLH* no es capaz de inducir la expresión de SLC7A5. Por lo tanto consideramos que este mecanismo de cooperación entre HIF2α y c-Myc (aunque parece operativo en el promotor de SLC7A5) no es lo suficientemente potente como para justificar la inducción de SLC7A5 vía HIF2α. Por el contario, en el presente trabajo mostramos que HIF2α se une a su promotor proximal y necesita de un dominio de unión a ADN intacto para promover su inducción. Por lo tanto la expresión de *Slc7a5* dependiente de HIF2α no puede explicarse mediante el modelo de transactivación de c-Myc, sino que parece más similar al caso del gen *Oct4*, descrito previamente como otro caso de unión directa específica de HIF2α a secuencias proximales del promotor. Como en el caso de *Oct4*, esta unión es especifica de HIF2α ya que HIF1α no es capaz de unirse a este promotor (Covello et al., 2006). A día de hoy estos dos genes constituyen en cierta manera una excepción, ya que estudios realizados en otros genes indican que la especificidad de HIF1α o HIF2α no reside en sus preferencias de unión a motivos de ADN (Mole et al., 2009; Schödel et al., 2011). Quizá todos estos aspectos de especificidad de reconocimiento en distintos promotores implican marcas epigenéticas de la cromatina o interacciones específicas con factores acompañantes y cercanos a los HRE en cada uno de los promotores regulados específicamente por HIF1α o HIF2α. En cualquier caso, aunque HIF1α no parece unirse al promotor de SLC7A5, sí parece inhibir moderadamente la expresión de SLC7A5 (Figura 12) lo cual podría explicarse por la capacidad de HIF1α (contraria a HIF2α) de desestabilizar la formación de los heterodímeros c-Myc-Max, promoviendo por tanto la represión de los genes dependientes de c-Myc.

Conclusiones finales

En resumen este trabajo describe un nuevo vínculo entre las vías reguladas por los factores de transcripción HIF y la activación de mTORC1 e identifica una nueva diana transcripcional y exclusiva de la isoforma HIF2α, el transportador de aminoácidos SLC7A5, como responsable de dicha activación. Con la descripción de este eje molecular aportamos las bases moleculares que explican las propiedades pro-proliferativas y pro-tumorales de HIF2α. Además en el trabajo se definen dos escenarios fisiológicos específicos, el pulmón y el hígado, en los cuales HIF2α promueve la activación de mTORC1, en contraste con lo descrito en otros contextos biológicos en los que la hipoxia conduce a la inhibición de mTORC1. En conclusión nuestros descubrimientos en este campo pueden explicar los efectos protumorales del factor HIF2α y ayudar a entender las bases de la proliferación autónoma de célula en determinadas situaciones fisiológicas en respuesta a la acción de la hipoxia así como nuevos ejes de acción vía HIF2α-mTORC1 implicados en funciones biológicas que no estén estrictamente relacionadas con proliferación celular.

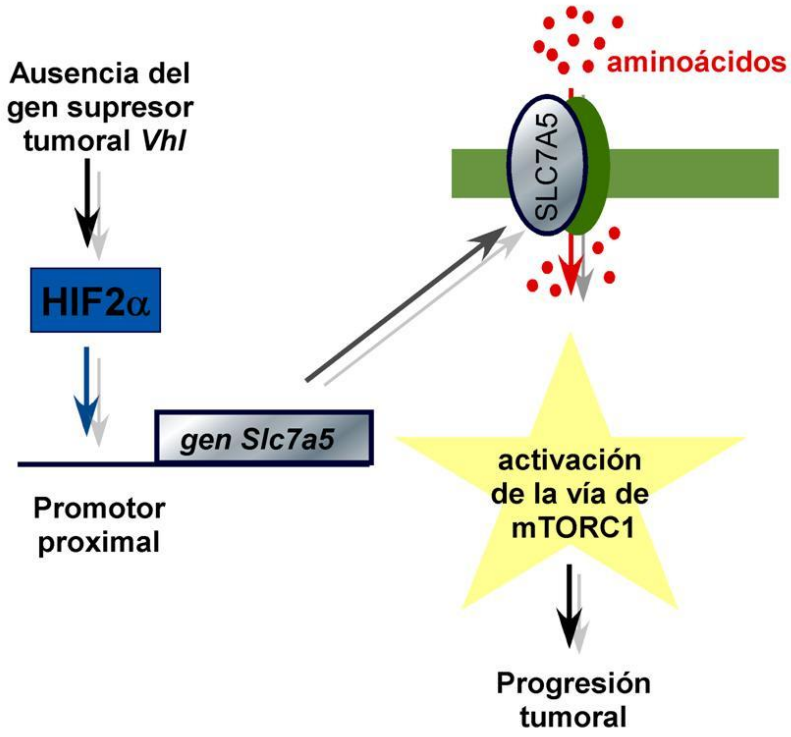

Figura 34. Mecanismo propuesto para la activación de mTORC1 a través del eje HIF2α-SLC7A5. La activación del factor de transcripción inducible por hipoxia HIF2α induce la expresión del transportador de aminoácidos SLC7A5, el cual facilita la activación de mTORC1 dependiente de aminoácidos, promoviendo la consecuente ventaja proliferativa para la célula.

CONCLUSIONES

CONCLUSIONES

1. El factor HIF2α, pero no HIF1α, activa mTORC1 en células de carcinoma renal WT8 y 786-O cuando el aporte de aminoácidos es limitante.

2. Esta inducción de mTORC1 dependiente de HIF2α requiere la inducción transcripcional específica del transportador de aminoácidos SLC7A5, un reconocido activador de mTORC1.

3. La inducción de SLC7A5 y la consecuente activación de mTORC1 por HIF2α requiere su unión a ADN y por lo tanto ocurre mediante la ruta canónica de activación de HIF2α.

4. La isoforma HIF2α, pero no HIF1α, se une específicamente al promotor proximal de SLC7A5 e induce la activación de su transcripción.

5. HIF2α induce la proliferación de células de carcinoma renal WT8 vía SLC7A5 y mTORC1 cuando el aporte de aminoácidos es limitante.

6. La inducción de SLC7A5 vía HIF2α es esencial para el crecimiento de tumores generados de células de carcinoma renal 786-O en ratones inmunodeficientes.

7. La expresión de SLC7A5 está aumentada en tumores humanos de carcinoma renal deficiente en VHL.

8. HIF2α induce la expresión de SLC7A5 y la activación de mTORC1 en otros escenarios *in vivo* no tumorales donde se activa el sistema de HIF como en pulmones e hígado de ratones deficientes en VHL.

9. HIF2α induce la activación de mTORC1 en epitelio bronquial de pulmones de ratones expuestos a hipoxia *in vivo* así como la expresión génica de *Slc7a5*, lo cual plantea un escenario hipóxico fisiológicamente relevante en el que la hipoxia no inhibe sino que induce la actividad de mTORC1.

BIBLIOGRAFÍA

REFERENCIAS

Acker, T., Diez-Juan, A., Aragones, J., Tjwa, M., Brusselmans, K., Moons, L., Fukumura, D., Moreno-Murciano, M.P., Herbert, J.-M., Burger, A., et al. (2005). Genetic evidence for a tumor suppressor role of HIF-2alpha. Cancer Cell *8*, 131–141.

Albiero, E., Ruggeri, M., Fortuna, S., Finotto, S., Bernardi, M., Madeo, D., and Rodeghiero, F. (2011). Isolated erythrocytosis: study of 67 patients and identification of three novel germ-line mutations in the prolyl hydroxylase domain protein 2 (PHD2) gene. Haematologica.

Alimov, A., Sundelin, B., Wang, N., Larsson, C., and Bergerheim, U. (2004). Loss of 14q31-q32.2 in renal cell carcinoma is associated with high malignancy grade and poor survival. International Journal of Oncology *25*, 179–185.

Aragonés, J., Schneider, M., Van Geyte, K., Fraisl, P., Dresselaers, T., Mazzone, M., Dirkx, R., Zacchigna, S., Lemieux, H., Jeoung, N.H., et al. (2008). Deficiency or inhibition of oxygen sensor Phd1 induces hypoxia tolerance by reprogramming basal metabolism. Nature Genetics *40*, 170–180.

Aragonés, J., Fraisl, P., Baes, M., and Carmeliet, P. (2009). Oxygen sensors at the crossroad of metabolism. Cell Metabolism *9*, 11–22.

Arany, Z. (1996). An essential role for p300/CBP in the cellular response to hypoxia. Proceedings of the National Academy of Sciences *93*, 12969–12973.

Arsham, A.M., Howell, J.J., and Simon, M.C. (2003). A novel hypoxia-inducible factor-independent hypoxic response regulating mammalian target of rapamycin and its targets. The Journal of Biological Chemistry *278*, 29655–29660.

Avruch, J., Long, X., Ortiz-Vega, S., Rapley, J., Papageorgiou, A., and Dai, N. (2009). Amino acid regulation of TOR complex 1. American Journal of Physiology Endocrinology and Metabolism *296*, E592–E602.

Bell, E.L., and Chandel, N.S. (2007). Mitochondrial oxygen sensing: regulation of hypoxia-inducible factor by mitochondrial generated reactive oxygen species. Essays in Biochemistry *43*, 17–27.

Bergers, G., and Benjamin, L.E. (2003). Tumorigenesis and the angiogenic switch. Nat Rev Cancer *3*, 401–410.

Bertout, J.A., Patel, S.A., and Simon, M.C. (2008). The impact of O2 availability on human cancer. Nature Reviews Cancer *8*, 967–975.

Biswas, S., Troy, H., Leek, R., Chung, Y.-L., Li, J., Raval, R.R., Turley, H., Gatter, K., Pezzella, F., Griffiths, J.R., et al. (2010). Effects of HIF-1α and HIF2α on Growth and Metabolism of Clear-Cell Renal Cell Carcinoma 786-0 Xenografts. Journal of Oncology *2010*, 757908.

Blouin, C.C., Pagé, E.L., Soucy, G.M., and Richard, D.E. (2004). Hypoxic gene activation by lipopolysaccharide in macrophages: implication of hypoxia-inducible factor 1alpha. Blood *103*, 1124–1130.

Blouw, B., Song, H., Tihan, T., Bosze, J., Ferrara, N., Gerber, H.P., Johnson, R.S., and Bergers, G. (2003). The hypoxic response of tumors is dependent on their microenvironment. Cancer Cell *4*, 133–146.

Bröer, S., and Palacín, M. (2011). The role of amino acid transporters in inherited and acquired diseases. The Biochemical Journal *436*, 193–211.

Bröer, A., Brookes, N., Ganapathy, V., Dimmer, K.S., Wagner, C.A., Lang, F., and Bröer, S. (1999). The astroglial ASCT2 amino acid transporter as a mediator of glutamine efflux. Journal of Neurochemistry *73*, 2184–2194.

Bröer, A., Wagner, C., Lang, F., and Bröer, S. (2000). Neutral amino acid transporter ASCT2 displays substrate-induced Na+ exchange and a substrate-gated anion conductance. The Biochemical Journal *346 Pt 3*, 705–710.

Bruick, R.K., and McKnight, S.L. (2001). A conserved family of prolyl-4-hydroxylases that modify HIF. Science *294*, 1337–1340.

Brusselmans, K., Compernolle, V., Tjwa, M., Wiesener, M.S., Maxwell, P.H., Collen, D., and Carmeliet, P. (2003). Heterozygous deficiency of hypoxia-inducible factor-2alpha protects mice against pulmonary hypertension and right ventricular dysfunction during prolonged hypoxia. J Clin Invest *111*, 1519–1527.

Bushuev, V.I., Miasnikova, G.Y., Sergueeva, A.I., Polyakova, L.A., Okhotin, D., Gaskin, P.R., Debebe, Z., Nekhai, S., Castro, O.L., Prchal, J.T., et al. (2006). Endothelin-1, vascular endothelial growth factor and systolic pulmonary artery pressure in patients with Chuvash polycythemia. Haematologica *91*, 744–749.

Cam, H., Easton, J.B., High, A., and Houghton, P.J. (2010). mTORC1 signaling under hypoxic conditions is controlled by ATM-dependent phosphorylation of HIF-1alpha. Mol Cell *40*, 509–520.

Carmeliet, P., Dor, Y., Herbert, J.M., Fukumura, D., Brusselmans, K., Dewerchin, M., Neeman, M., Bono, F., Abramovitch, R., Maxwell, P., et al. (1998). Role of HIF-1alpha in hypoxia-mediated apoptosis, cell proliferation and tumour angiogenesis. Nature *394*, 485–490.

Chen, T.-H., Wang, J.-F., Chan, P., and Lee, H.-M. (2005). Angiotensin II stimulates hypoxia-inducible factor 1alpha accumulation in glomerular mesangial cells. Annals Of The New York Academy Of Sciences *1042*, 286–293.

Covello, K.L., Simon, M.C., and Keith, B. (2005). Targeted replacement of hypoxia-inducible factor-1alpha by a hypoxia-inducible factor-2alpha knock-in allele promotes tumor growth. Cancer Research *65*, 2277–2286.

Covello, K.L., Kehler, J., Yu, H., Gordan, J.D., Arsham, A.M., Hu, C.J., Labosky, P.A., Simon, M.C., and Keith, B. (2006). HIF-2alpha regulates Oct-4: effects of hypoxia on stem cell function, embryonic development, and tumor growth. Genes Dev *20*, 557–570.

Crino, P., Nathanson, K., and Henske, E. (2006). The tuberous sclerosis complex. N Engl J Med. *28;355*, 1345–1356.

Cunningham, J.T., Rodgers, J.T., Arlow, D.H., Vazquez, F., Mootha, V.K., and Puigserver, P. (2007). mTOR controls mitochondrial oxidative function through a YY1-PGC-1alpha transcriptional complex. Nature *450*, 736–740.

Dahia, P.L.M., Ross, K.N., Wright, M.E., Hayashida, C.Y., Santagata, S., Barontini, M., Kung, A.L., Sanso, G., Powers, J.F., Tischler, A.S., et al. (2005). A HIF1alpha regulatory loop links hypoxia and mitochondrial signals in pheochromocytomas. PLoS Genetics *1*, 72–80.

Dayan, F., Roux, D., Brahimi-Horn, M.C., Pouyssegur, J., and Mazure, N.M. (2006). The oxygen sensor factor-inhibiting hypoxia-inducible factor-1 controls expression of distinct genes through the bifunctional transcriptional character of hypoxia-inducible factor-1alpha. Cancer Research *66*, 3688–3698.

Ehrismann, D., Flashman, E., Genn, D.N., Mathioudakis, N., Hewitson, K.S., Ratcliffe, P.J., and Schofield, C.J. (2007). Studies on the activity of the hypoxia-inducible-factor hydroxylases using an oxygen consumption assay. The Biochemical Journal *401*, 227–234.

Elorza, A., Soro-Arnáiz, I., Meléndez-Rodríguez, F., Rodríguez-Vaello, V., Marsboom, G., De Cárcer, G., Acosta-Iborra, B., Albacete-Albacete, L., Ordóñez, A., Serrano-Oviedo, L., et al. (2012). HIF2α acts as an mTORC1 activator through the amino acid carrier SLC7A5. Molecular Cell *48*, 681–691.

Ema, M., Hirota, K., Mimura, J., Abe, H., Yodoi, J., Sogawa, K., Poellinger, L., and Fujii-Kuriyama, Y. (1999). Molecular mechanisms of transcription activation by HLF and HIF1alpha in response to hypoxia: their stabilization and redox signal-induced interaction with CBP/p300. The The European Molecular Biology Organization Journal *18*, 1905–1914.

Epstein, A.C., Gleadle, J.M., McNeill, L.A., Hewitson, K.S., O'Rourke, J., Mole, D.R., Mukherji, M., Metzen, E., Wilson, M.I., Dhanda, A., et al. (2001). C. elegans EGL-9 and mammalian homologs define a family of dioxygenases that regulate HIF by prolyl hydroxylation. Cell *107*, 43–54.

Fan, X., Ross, D.D., Arakawa, H., Ganapathy, V., Tamai, I., and Nakanishi, T. (2010). Impact of system L amino acid transporter 1 (LAT1) on proliferation of human ovarian cancer cells: a possible target for combination therapy with anti-proliferative aminopeptidase inhibitors. Biochemical Pharmacology *80*, 811–818.

Ferlay, J., Shin, H.-R., Bray, F., Forman, D., Mathers, C., and Parkin, D.M. (2010). Estimates of worldwide burden of cancer in 2008: GLOBOCAN 2008. International Journal of Cancer Journal International Du Cancer *127*, 2893–2917.

Firth, J.D., Ebert, B.L., Pugh, C.W., and Ratcliffe, P.J. (1994). Oxygen-regulated control elements in the phosphoglycerate kinase 1 and lactate dehydrogenase A genes: similarities with the erythropoietin 3' enhancer. Proceedings of the National Academy of Sciences of the United States of America *91*, 6496–6500.

Franovic, A., Holterman, C.E., Payette, J., and Lee, S. (2009). Human cancers converge at the HIF-2alpha oncogenic axis. Proceedings of the National Academy of Sciences of the United States of America *106*, 21306–21311.

Fuchs, B.C., and Bode, B.P. (2005). Amino acid transporters ASCT2 and LAT1 in cancer: partners in crime? Semin Cancer Biol *15*, 254–266.

Fukuda, R., Zhang, H., Kim, J., Shimoda, L., Dang, C. V, and Semenza, G.L. (2007). HIF-1 regulates cytochrome oxidase subunits to optimize efficiency of respiration in hypoxic cells. Cell *129*, 111–122.

Gao, P., Tchernyshyov, I., Chang, T.-C., Lee, Y.-S., Kita, K., Ochi, T., Zeller, K.I., De Marzo, A.M., Van Eyk, J.E., Mendell, J.T., et al. (2009). c-Myc suppression of miR-23a/b enhances mitochondrial glutaminase expression and glutamine metabolism. Nature *458*, 762–765.

Gardner, L.B., Li, Q., Park, M.S., Flanagan, W.M., Semenza, G.L., and Dang, C. V (2001). Hypoxia inhibits G1/S transition through regulation of p27 expression. The Journal of Biological Chemistry *276*, 7919–7926.

Gasol, E., Jiménez-Vidal, M., Chillarón, J., Zorzano, A., and Palacín, M. (2004). Membrane topology of system xc- light subunit reveals a re-entrant loop with substrate-restricted accessibility. The Journal of Biological Chemistry *279*, 31228–31236.

Gordan, J.D., Bertout, J.A., Hu, C.J., Diehl, J.A., and Simon, M.C. (2007). HIF-2alpha promotes hypoxic cell proliferation by enhancing c-myc transcriptional activity. Cancer Cell *11*, 335–347.

Gordan, J.D., Lal, P., Dondeti, V.R., Letrero, R., Parekh, K.N., Oquendo, C.E., Greenberg, R.A., Flaherty, K.T., Rathmell, W.K., Keith, B., et al. (2008). HIF-alpha effects on c-Myc distinguish two subtypes of sporadic VHL-deficient clear cell renal carcinoma. Cancer Cell *14*, 435–446.

Gorlach, A., Diebold, I., Schini-Kerth, V.B., Berchner-Pfannschmidt, U., Roth, U., Brandes, R.P., Kietzmann, T., and Busse, R. (2001). Thrombin Activates the Hypoxia-Inducible Factor-1 Signaling Pathway in Vascular Smooth Muscle Cells : Role of the p22phox-Containing NADPH Oxidase. Circulation Research *89*, 47–54.

Green, S.L., Freiberg, R.A., and Giaccia, A.J. (2001). p21(Cip1) and p27(Kip1) regulate cell cycle reentry after hypoxic stress but are not necessary for hypoxia-induced arrest. Molecular and Cellular Biology *21*, 1196–1206.

Gu, Y.Z., Moran, S.M., Hogenesch, J.B., Wartman, L., and Bradfield, C.A. (1998). Molecular characterization and chromosomal localization of a third alpha-class hypoxia inducible factor subunit, HIF3alpha. Gene Expression *7*, 205–213.

Guertin, D.A., Stevens, D.M., Thoreen, C.C., Burds, A.A., Kalaany, N.Y., Moffat, J., Brown, M., Fitzgerald, K.J., and Sabatini, D.M. (2006). Ablation in mice of the mTORC components raptor, rictor, or mLST8 reveals that mTORC2 is required for signaling to Akt-FOXO and PKCalpha, but not S6K1. Developmental Cell *11*, 859–871.

Gunaratnam, L., Morley, M., Franovic, A., De Paulsen, N., Mekhail, K., Parolin, D.A.E., Nakamura, E., Lorimer, I.A.J., and Lee, S. (2003). Hypoxia inducible factor activates

the transforming growth factor-alpha/epidermal growth factor receptor growth stimulatory pathway in VHL(-/-) renal cell carcinoma cells. The Journal of Biological Chemistry *278*, 44966–44974.

Guzy, R.D., Mack, M.M., and Schumacker, P.T. (2007). Mitochondrial complex III is required for hypoxia-induced ROS production and gene transcription in yeast. Antioxidants Redox Signaling *9*, 1317–1328.

Gwinn, D.M., Shackelford, D.B., Egan, D.F., Mihaylova, M.M., Mery, A., Vasquez, D.S., Turk, B.E., and Shaw, R.J. (2008). AMPK phosphorylation of raptor mediates a metabolic checkpoint. Molecular Cell *30*, 214–226.

Haase, V.H., Glickman, J.N., Socolovsky, M., and Jaenisch, R. (2001). Vascular tumors in livers with targeted inactivation of the von Hippel-Lindau tumor suppressor. Proceedings of the National Academy of Sciences of the United States of America *98*, 1583–1588.

Hao, H.-X., Khalimonchuk, O., Schraders, M., Dephoure, N., Bayley, J.-P., Kunst, H., Devilee, P., Cremers, C.W.R.J., Schiffman, J.D., Bentz, B.G., et al. (2009). SDH5, a gene required for flavination of succinate dehydrogenase, is mutated in paraganglioma. Science *325*, 1139–1142.

Hara, K., Yonezawa, K., Weng, Q.P., Kozlowski, M.T., Belham, C., and Avruch, J. (1998). Amino acid sufficiency and mTOR regulate p70 S6 kinase and eIF-4E BP1 through a common effector mechanism. The Journal of Biological Chemistry *273*, 14484–14494.

Hayashi, K., Jutabha, P., Endou, H., and Anzai, N. (2012). c-Myc is crucial for the expression of LAT1 in MIA Paca-2 human pancreatic cancer cells. Oncol Rep. *28*, 862–866.

Hewitson, K.S., McNeill, L.A., Riordan, M. V, Tian, Y.-M., Bullock, A.N., Welford, R.W., Elkins, J.M., Oldham, N.J., Bhattacharya, S., Gleadle, J.M., et al. (2002). Hypoxia-inducible factor (HIF) asparagine hydroxylase is identical to factor inhibiting HIF (FIH) and is related to the cupin structural family. The Journal of Biological Chemistry *277*, 26351–26355.

Hickey, M.M., Richardson, T., Wang, T., Mosqueira, M., Arguiri, E., Yu, H., Yu, Q.-C., Solomides, C.C., Morrisey, E.E., Khurana, T.S., et al. (2010). The von Hippel–Lindau Chuvash mutation promotes pulmonary hypertension and fibrosis in mice. Journal of Clinical Investigation *120*, 827–839.

Hill, P., Shukla, D., Tran, M.G.B., Aragones, J., Cook, H.T., Carmeliet, P., and Maxwell, P.H. (2008). Inhibition of Hypoxia Inducible Factor Hydroxylases Protects Against Renal Ischemia-Reperfusion Injury. Journal of The American Society Of Nephrology *19*, 39–46.

Holmquist-Mengelbier, L., Fredlund, E., Löfstedt, T., Noguera, R., Navarro, S., Nilsson, H., Pietras, A., Vallon-Christersson, J., Borg, A., Gradin, K., et al. (2006). Recruitment of HIF-1alpha and HIF-2alpha to common target genes is differentially regulated in neuroblastoma: HIF-2alpha promotes an aggressive phenotype. Cancer Cell *10*, 413–423.

Hopfl, G., Wenger, R.H., Ziegler, U., Stallmach, T., Gardelle, O., Achermann, R., Wergin, M., Kaser-Hotz, B., Saunders, H.M., Williams, K.J., et al. (2002). Rescue of hypoxia-inducible factor-1a-deficient tumor growth by wild-type cells is independent of vascular endothelial growth factor. Cancer Research *62*, 2962–2970.

Hudes, G., Carducci, M., Tomczak, P., Dutcher, J., Figlin, R., Kapoor, A., Staroslawska, E., Sosman, J., McDermott, D., Bodrogi, I., et al. (2007). Temsirolimus, interferon alfa, or both for advanced renal-cell carcinoma. (Massachusetts Medical Society).

Inoki, K., Zhu, T., and Guan, K.-L. (2003). TSC2 mediates cellular energy response to control cell growth and survival. Cell *115*, 577–590.

Ivan, M., Kondo, K., Yang, H.F., Kim, W., Valiando, J., Ohh, M., Salic, A., Asara, J.M., Lane, W.S., Kaelin Jr., W.G., et al. (2001). HIFalpha targeted for VHL-mediated destruction by proline hydroxylation: implications for O2 sensing. Science *292*, 464–468.

Jaakkola, P., Mole, D.R., Tian, Y.M., Wilson, M.I., Gielbert, J., Gaskell, S.J., Von Kriegsheim, A., Hebestreit, H.F., Mukherji, M., Schofield, C.J., et al. (2001). Targeting of HIF-alpha to the von Hippel-Lindau ubiquitylation complex by O2-regulated prolyl hydroxylation. Science *292*, 468–472.

Jiang, B.-H., Rue, E., Wang, G.L., Roe, R., and Semenza, G.L. (1996). Dimerization, DNA Binding, and Transactivation Properties of Hypoxia-inducible Factor 1. Journal of Biological Chemistry *271*, 17771–17778.

Jung, Y., Isaacs, J.S., Lee, S., Trepel, J., Neckers, L., and Oncology, M. (2003). IL-1β mediated up-regulation of HIF-1α via an NFkB/COX- 2 pathway identifies HIF-1 as a critical link between inflammation and oncogenesis. The FASEB Journal *17*, 2115–2117.

Kaira, K., Oriuchi, N., Imai, H., Shimizu, K., Yanagitani, N., Sunaga, N., Hisada, T., Tanaka, S., Ishizuka, T., Kanai, Y., et al. (2008). l-type amino acid transporter 1 and CD98 expression in primary and metastatic sites of human neoplasms. Cancer Science *99*, 2380–2386.

Kaira, K., Oriuchi, N., Imai, H., Shimizu, K., Yanagitani, N., Sunaga, N., Hisada, T., Ishizuka, T., Kanai, Y., Nakajima, T., et al. (2009). Prognostic significance of L-type amino acid transporter 1 (LAT1) and 4F2 heavy chain (CD98) expression in stage I pulmonary adenocarcinoma. Lung Cancer Amsterdam Netherlands *66*, 120–126.

Kaira, K., Oriuchi, N., Takahashi, T., Nakagawa, K., Ohde, Y., Okumura, T., Murakami, H., Shukuya, T., Kenmotsu, H., Naito, T., et al. (2011). LAT1 expression is closely associated with hypoxic markers and mTOR in resected non-small cell lung cancer. American Journal of Translational Research *3*, 468–478.

Kaji, M., Kabir-Salmani, M., Anzai, N., Jin, C.J., Akimoto, Y., Horita, A., Sakamoto, A., Kanai, Y., Sakurai, H., and Iwashita, M. (2010). Properties of L-type amino acid transporter 1 in epidermal ovarian cancer. International Journal of Gynecological Cancer Official Journal of the International Gynecological Cancer Society *20*, 329–336.

Kaku, H., Ito, S., Ebara, S., Ouchida, M., Nasu, Y., Tsushima, T., Kumon, H., and Shimizu, K. (2004). Positive correlation between allelic loss at chromosome 14q24-31 and poor prognosis of patients with renal cell carcinoma. Urology *64*, 176–181.

Kim, J.E., and Chen, J. (2004). regulation of peroxisome proliferator-activated receptor-gamma activity by mammalian target of rapamycin and amino acids in adipogenesis. Diabetes *53*, 2748–2756.

Kim, E., Goraksha-Hicks, P., Li, L., Neufeld, T.P., and Guan, K.L. (2008). Regulation of TORC1 by Rag GTPases in nutrient response. Nat Cell Biol *10*, 935–945.

Kim, J.W., Tchernyshyov, I., Semenza, G.L., and Dang, C. V (2006a). HIF-1-mediated expression of pyruvate dehydrogenase kinase: a metabolic switch required for cellular adaptation to hypoxia. Cell Metab *3*, 177–185.

Kim, W.Y., Safran, M., Buckley, M.R., Ebert, B.L., Glickman, J., Bosenberg, M., Regan, M., and Kaelin Jr., W.G. (2006b). Failure to prolyl hydroxylate hypoxia-inducible factor alpha phenocopies VHL inactivation in vivo. EMBO J *25*, 4650–4662.

Kim, W.Y., Perera, S., Zhou, B., Carretero, J., Yeh, J.J., Heathcote, S.A., Jackson, A.L., Nikolinakos, P., Ospina, B., Naumov, G., et al. (2009). HIF2α cooperates with RAS to promote lung tumorigenesis in mice. Journal of Clinical Investigation *119*, 2160–2170.

Klatte, T., Rao, P.N., De Martino, M., LaRochelle, J., Shuch, B., Zomorodian, N., Said, J., Kabbinavar, F.F., Belldegrun, A.S., and Pantuck, A.J. (2009). Cytogenetic profile predicts prognosis of patients with clear cell renal cell carcinoma. Journal of Clinical Oncology *27*, 746–753.

Koivunen, P., Tiainen, P., Hyvärinen, J., Williams, K.E., Sormunen, R., Klaus, S.J., Kivirikko, K.I., and Myllyharju, J. (2007). An endoplasmic reticulum transmembrane prolyl 4-hydroxylase is induced by hypoxia and acts on hypoxia-inducible factor alpha. The Journal of Biological Chemistry *282*, 30544–30552.

Kondo, K., Klco, J., Nakamura, E., Lechpammer, M., and Kaelin Jr., W.G. (2002). Inhibition of HIF is necessary for tumor suppression by the von Hippel-Lindau protein. Cancer Cell *1*, 237–246.

Kondo, K., Kim, W.Y., Lechpammer, M., and Kaelin Jr., W.G. (2003). Inhibition of HIF2alpha is sufficient to suppress pVHL-defective tumor growth. PLoS Biol *1*, E83.

Koshiji, M., Kageyama, Y., Pete, E.A., Horikawa, I., Barrett, J.C., and Huang, L.E. (2004). HIF-1alpha induces cell cycle arrest by functionally counteracting Myc. EMBO J *23*, 1949–1956.

Koshiji, M., To, K.K.-W., Hammer, S., Kumamoto, K., Harris, A.L., Modrich, P., and Huang, L.E. (2005). HIF-1alpha induces genetic instability by transcriptionally downregulating MutSalpha expression. Molecular Cell *17*, 793–803.

Kucejova, B., Pena-Llopis, S., Yamasaki, T., Sivanand, S., Tran, T.A., Alexander, S., Wolff, N.C., Lotan, Y., Xie, X.J., Kabbani, W., et al. (2011). Interplay between pVHL and mTORC1 pathways in clear-cell renal cell carcinoma. Mol Cancer Res *9*, 1255–1265.

Lando, D., Peet, D.J., Gorman, J.J., Whelan, D.A., Whitelaw, M.L., and Bruick, R.K. (2002). FIH-1 is an asparaginyl hydroxylase enzyme that regulates the transcriptional activity of hypoxia-inducible factor. Genes Development *16*, 1466–1471.

Lee, C.-H., Inoki, K., Karbowniczek, M., Petroulakis, E., Sonenberg, N., Henske, E.P., and Guan, K.-L. (2007). Constitutive mTOR activation in TSC mutants sensitizes cells to energy starvation and genomic damage via p53. The The European Molecular Biology Organization Journal *26*, 4812–4823.

Lee, S., Kim, S., Seo, H., Shin, S., Kim, D., Park, C., Kim, K., Kim, Y., Jeong, J., and Kim, I. (2012). Over-expression of miR-145 enhances the effectiveness of HSVtk gene therapy for malignant glioma. Cancer Letters *320*, 72–80.

Liu, L., Cash, T.P., Jones, R.G., Keith, B., Thompson, C.B., and Simon, M.C. (2006). Hypoxia-induced energy stress regulates mRNA translation and cell growth. Mol Cell *21*, 521–531.

Lu, H., Dalgard, C.L., Mohyeldin, A., McFate, T., Tait, A.S., and Verma, A. (2005). Reversible inactivation of HIF-1 prolyl hydroxylases allows cell metabolism to control basal HIF-1. The Journal of Biological Chemistry *280*, 41928–41939.

Mack, F.A., Patel, J.H., Biju, M.P., Haase, V.H., and Simon, M.C. (2005). Decreased Growth of Vhl−/− Fibrosarcomas Is Associated with Elevated Levels of Cyclin Kinase Inhibitors p21 and p27. Molecular and Cellular Biology *25*, 4565–4578.

Mahon, P.C., Hirota, K., and Semenza, G.L. (2001). FIH-1: a novel protein that interacts with HIF-1alpha and VHL to mediate repression of HIF-1 transcriptional activity. Genes and Development *15*, 2675–2686.

Majmundar, A.J., Wong, W.J., and Simon, M.C. (2010). Hypoxia-inducible factors and the response to hypoxic stress. Molecular Cell *40*, 294–309.

Mandriota, S.J., Turner, K.J., Davies, D.R., Murray, P.G., Morgan, N. V, Sowter, H.M., Wykoff, C.C., Maher, E.R., Harris, A.L., Ratcliffe, P.J., et al. (2002). HIF activation identifies early lesions in VHL kidneys: evidence for site-specific tumor suppressor function in the nephron. Cancer Cell *1*, 459–468.

Maranchie, J.K., Vasselli, J.R., Riss, J., Bonifacino, J.S., Linehan, W.M., and Klausner, R.D. (2002). The contribution of VHL substrate binding and HIF1-α to the phenotype of VHL loss in renal cell carcinoma. Cancer Cell *1*, 247–255.

Mastrogiannaki, M., Matak, P., Keith, B., Simon, M.C., Vaulont, S., and Peyssonnaux, C. (2009). HIF-2α, but not HIF-1α, promotes iron absorption in mice. Journal of Clinical Investigation *119*, 1159–1166.

Maxwell, P.H., Wiesener, M.S., Chang, G.W., Clifford, S.C., Vaux, E.C., Cockman, M.E., Wykoff, C.C., Pugh, C.W., Maher, E.R., and Ratcliffe, P.J. (1999). The tumour suppressor protein VHL targets hypoxia-inducible factors for oxygen-dependent proteolysis. Nature *399*, 271–275.

McCracken, A.N., and Edinger, A.L. (2013). Nutrient transporters: the Achilles' heel of anabolism. Trends in Endocrinology and Metabolism TEM *24*, 200–208.

Meier, C., Ristic, Z., Klauser, S., and Verrey, F. (2002). Activation of system L heterodimeric amino acid exchangers by intracellular substrates. The The European Molecular Biology Organization Journal *21*, 580–589.

Miró-Murillo, M., Elorza, A., Soro-Arnáiz, I., Albacete-Albacete, L., Ordoñez, A., Balsa, E., Vara-Vega, A., Vázquez, S., Fuertes, E., Fernández-Criado, C., et al. (2011). Acute Vhl gene inactivation induces cardiac HIF-dependent erythropoietin gene expression. PLoS One *6*, e22589.

Mitsumori, K., Kittleson, J.M., Itoh, N., Delahunt, B., Heathcott, R.W., Stewart, J.H., McCredie, M.R.E., and Reeve, A.E. (2002). Chromosome 14q LOH in localized clear cell renal cell carcinoma. The Journal of Pathology *198*, 110–114.

Mole, D.R., Blancher, C., Copley, R.R., Pollard, P.J., Gleadle, J.M., Ragoussis, J., and Ratcliffe, P.J. (2009). Genome-wide association of hypoxia-inducible factor (HIF)-1alpha and HIF-2alpha DNA binding with expression profiling of hypoxia-inducible transcripts. The Journal of Biological Chemistry *284*, 16767–16775.

Mollenhauer, M., Kiss, J., Dudda, J., Kirchberg, J., Rahbari, N., Radhakrishnan, P., Niemietz, T., Rausch, V., Weitz, J., and Schneider, M. (2012). Deficiency of the oxygen sensor PHD1 augments liver regeneration after partial hepatectomy. Langenbecks Archives of Surgery Deutsche Gesellschaft Für Chirurgie *397*, 1313–1322.

Motzer, R.J., Escudier, B., Oudard, S., Hutson, T.E., Porta, C., Bracarda, S., Grünwald, V., Thompson, J.A., Figlin, R.A., Hollaender, N., et al. (2008). Efficacy of everolimus in advanced renal cell carcinoma: a double-blind, randomised, placebo-controlled phase III trial.

Nicklin, P., Bergman, P., Zhang, B., Triantafellow, E., Wang, H., Nyfeler, B., Yang, H., Hild, M., Kung, C., Wilson, C., et al. (2009). Bidirectional transport of amino acids regulates mTOR and autophagy. Cell *136*, 521–534.

Niedenzu, C., Grasedyck, K., Voelkel, N.F., Bittmann, S., and Lindner, J. (1981). Proliferation of lung cells in chronically hypoxic rats. An autoradiographic and radiochemical study. Int Arch Occup Environ Health *48*, 185–193.

Noda, T., and Ohsumi, Y. (1998). Tor, a phosphatidylinositol kinase homologue, controls autophagy in yeast. The Journal of Biological Chemistry *273*, 3963–3966.

Ohkawa, M., Ohno, Y., Masuko, K., Takeuchi, A., Suda, K., Kubo, A., Kawahara, R., Okazaki, S., Tanaka, T., Saya, H., et al. (2011). Oncogenicity of L-type amino-acid transporter 1 (LAT1) revealed by targeted gene disruption in chicken DT40 cells: LAT1 is a promising molecular target for human cancer therapy. Biochemical and Biophysical Research Communications *406*, 649–655.

Ohno, H., Nakatsu, Y., Sakoda, H., Kushiyama, A., Ono, H., Fujishiro, M., Otani, Y., Okubo, H., Yoneda, M., Fukushima, T., et al. (2011). 4F2hc stabilizes GLUT1 protein and increases glucose transport activity. American Journal of Physiology Cell Physiology *300*, C1047–C1054.

Page, E.L., Chan, D.A., Giaccia, A.J., Levine, M., and Richard, D.E. (2008). Hypoxia-inducible Factor-1 alpha Stabilization in Nonhypoxic Conditions : Role of Oxidation and Intracellular Ascorbate Depletion. Molecular Biology of the Cell *19*, 86–94.

Pagé, E.L., Robitaille, G.A., Pouysségur, J., and Richard, D.E. (2002). Induction of hypoxia-inducible factor-1alpha by transcriptional and translational mechanisms. The Journal of Biological Chemistry *277*, 48403–48409.

Pantuck, A.J., Seligson, D.B., Klatte, T., Yu, H., Leppert, J.T., Moore, L., O'Toole, T., Gibbons, J., Belldegrun, A.S., and Figlin, R.A. (2007). Prognostic relevance of the mTOR pathway in renal cell carcinoma: implications for molecular patient selection for targeted therapy. Cancer *109*, 2257–2267.

Papandreou, I., Cairns, R.A., Fontana, L., Lim, A.L., and Denko, N.C. (2006). HIF-1 mediates adaptation to hypoxia by actively downregulating mitochondrial oxygen consumption. Cell Metab *3*, 187–197.

Parry, L., Maynard, J.H., Patel, A., Clifford, S.C., Morrissey, C., Maher, E.R., Cheadle, J.P., and Sampson, J.R. (2001). Analysis of the TSC1and TSC2genes in sporadic renal cell carcinomas. British Journal of Cancer *85*, 1226–1230.

De Paulsen, N., Brychzy, A., Fournier, M.-C., Klausner, R.D., Gnarra, J.R., Pause, A., and Lee, S. (2001). Role of transforming growth factor-α in von Hippel– Lindau (VHL)−/− clear cell renal carcinoma cell proliferation: A possible mechanism coupling VHL tumor suppressor inactivation and tumorigenesis. Proceedings of the National Academy of Sciences of the United States of America *98*, 1387–1392.

Porstmann, T., Santos, C.R., Griffiths, B., Cully, M., Wu, M., Leevers, S., Griffiths, J.R., Chung, Y.-L., and Schulze, A. (2008). SREBP Activity Is Regulated by mTORC1 and Contributes to Akt-Dependent Cell Growth. Cell Metabolism *8*, 224–236.

Purdue, M.P., Johansson, M., Zelenika, D., Toro, J.R., Scelo, G., Moore, L.E., Prokhortchouk, E., Wu, X., Kiemeney, L.A., Gaborieau, V., et al. (2011). Genome-wide association study of renal cell carcinoma identifies two susceptibility loci on 2p21 and 11q13.3. Nature Genetics *43*, 60–65.

Rankin, E.B., Biju, M.P., Liu, Q., Unger, T.L., Rha, J., Johnson, R.S., Simon, M.C., Keith, B., and Haase, V.H. (2007). Hypoxia-inducible factor-2 (HIF-2) regulates hepatic erythropoietin in vivo. J Clin Invest *117*, 1068–1077.

Raval, R.R., Lau, K.W., Tran, M.G., Sowter, H.M., Mandriota, S.J., Li, J.L., Pugh, C.W., Maxwell, P.H., Harris, A.L., and Ratcliffe, P.J. (2005). Contrasting properties of hypoxia-inducible factor 1 (HIF-1) and HIF-2 in von Hippel-Lindau-associated renal cell carcinoma. Mol Cell Biol *25*, 5675–5686.

Reid, M.A., Wang, W.-I., Rosales, K.R., Welliver, M.X., Pan, M., and Kong, M. (2013). The B55α Subunit of PP2A Drives a p53-Dependent Metabolic Adaptation to Glutamine Deprivation. Molecular Cell *50*, 200–211.

Reig, N., Chillarón, J., Bartoccioni, P., Fernández, E., Bendahan, A., Zorzano, A., Kanner, B., Palacín, M., and Bertran, J. (2002). The light subunit of system bo,+ is fully functional in the absence of the heavy subunit. The The European Molecular Biology Organization Journal *21*, 4906–4914.

Richard, D.E., Berra, E., and Pouyssegur, J. (2000). Nonhypoxic pathway mediates the induction of hypoxia-inducible factor 1alpha in vascular smooth muscle cells. The Journal of Biological Chemistry *275*, 26765–26771.

Robb, V.A., Karbowniczek, M., Klein-Szanto, A.J., and Henske, E.P. (2007). Activation of the mTOR signaling pathway in renal clear cell carcinoma. The Journal of Urology *177*, 346–352.

Rolfs, A., Kvietikova, I., Gassmann, M., and Wenger, R.H. (1997). Oxygen-regulated transferrin expression is mediated by hypoxia-inducible factor-1. The Journal of Biological Chemistry *272*, 20055–20062.

Ruzankina, Y., Pinzon-Guzman, C., Asare, A., Ong, T., Pontano, L., Cotsarelis, G., Zediak, V.P., Velez, M., Bhandoola, A., and Brown, E.J. (2007). Deletion of the developmentally essential gene ATR in adult mice leads to age-related phenotypes and stem cell loss. Cell Stem Cell *1*, 113–126.

Ryan, H.E., Lo, J., and Johnson, R.S. (1998). HIF-1 alpha is required for solid tumor formation and embryonic vascularization. The The European Molecular Biology Organization Journal *17*, 3005–3015.

Sancak, Y., Peterson, T.R., Shaul, Y.D., Lindquist, R.A., Thoreen, C.C., Bar-Peled, L., and Sabatini, D.M. (2008). The Rag GTPases bind raptor and mediate amino acid signaling to mTORC1. Science *320*, 1496–1501.

Schneider, M., Van Geyte, K., Fraisl, P., Kiss, J., Aragonés, J., Mazzone, M., Mairbäurl, H., De Bock, K., Jeoung, N.H., Mollenhauer, M., et al. (2010). Loss or Silencing of the PHD1 Prolyl Hydroxylase Protects Livers of Mice Against Ischemia/Reperfusion Injury. Gastroenterology *138*, 1143–1154.e1–e2.

Schödel, J., Oikonomopoulos, S., Ragoussis, J., Pugh, C.W., Ratcliffe, P.J., and Mole, D.R. (2011). High-resolution genome-wide mapping of HIF-binding sites by ChIP-seq. Blood *117*, e207–e217.

Semenza, G.L. (2003a). Targeting HIF-1 for cancer therapy. Nature Reviews Cancer *3*, 721–732.

Semenza, G.L. (2003b). Angiogenesis in ischemic and neoplastic disorders. Annual Review of Medicine *54*, 17–28.

Shaw, R.J., and Cantley, L.C. (2006). Ras, PI(3)K and mTOR signalling controls tumour cell growth. Nature *441*, 424–430.

Shen, C., Beroukhim, R., Schumacher, S.E., Zhou, J., Chang, M., Signoretti, S., and Kaelin Jr., W.G. (2011). Genetic and functional studies implicate HIF1alpha as a 14q kidney cancer suppressor gene. Cancer Discov *1*, 222–235.

Shi, Y.-H., Bingle, L., Gong, L.-H., Wang, Y.-X., Corke, K.P., and Fang, W.-G. (2007). Basic FGF augments hypoxia induced HIF-1-alpha expression and VEGF release in T47D breast cancer cells. Pathology *39*, 396–400.

Shimoda, L.A., Fallon, M., Pisarcik, S., Wang, J., and Semenza, G.L. (2006). HIF-1 regulates hypoxic induction of NHE1 expression and alkalinization of intracellular pH in pulmonary arterial myocytes. American Journal of Physiology Lung Cellular and Molecular Physiology *291*, L941–L949.

Sinclair, L.V., Rolf, J., Emslie, E., Shi, Y.-B., Taylor, P.M., and Cantrell, D.A. (2013). Control of amino-acid transport by antigen receptors coordinates the metabolic reprogramming essential for T cell differentiation. Nat Immunol *14*, 500–508.

Smith, T.G., Brooks, J.T., Balanos, G.M., Lappin, T.R., Layton, D.M., Leedham, D.L., Liu, C., Maxwell, P.H., McMullin, M.F., McNamara, C.J., et al. (2008). Mutation of the von Hippel-Lindau gene alters human cardiopulmonary physiology. Advances in Experimental Medicine and Biology *605*, 51–56.

Sonenberg, N., and Hinnebusch, A.G. (2009). Regulation of translation initiation in eukaryotes: mechanisms and biological targets. Cell *136*, 731–745.

Sridharan, V., Guichard, J., Li, C.-Y., Muise-Helmericks, R., Beeson, C.C., and Wright, G.L. (2008). O2-sensing signal cascade: clamping of O2 respiration, reduced ATP utilization, and inducible fumarate respiration. American Journal of Physiology Cell Physiology *295*, C29–C37.

Stenmark, K.R., Fagan, K.A., and Frid, M.G. (2006). Hypoxia-induced pulmonary vascular remodeling: cellular and molecular mechanisms. Circulation Research *99*, 675–691.

Tello, D., Balsa, E., Acosta-Iborra, B., Fuertes-Yebra, E., Elorza, A., Ordóñez, A., Corral-Escariz, M., Soro, I., López-Bernardo, E., Perales-Clemente, E., et al. (2011). Induction of the Mitochondrial NDUFA4L2 Protein by HIF-1α Decreases Oxygen Consumption by Inhibiting Complex I Activity. Cell Metabolism *14*, 768–779.

Tian, H., McKnight, S.L., and Russell, D.W. (1997). Endothelial PAS domain protein 1 (EPAS1), a transcription factor selectively expressed in endothelial cells. Genes & Development *11*, 72–82.

Tomlinson, I.P.M., Alam, N.A., Rowan, A.J., Barclay, E., Jaeger, E.E.M., Kelsell, D., Leigh, I., Gorman, P., Lamlum, H., Rahman, S., et al. (2002). Germline mutations in FH predispose to dominantly inherited uterine fibroids, skin leiomyomata and papillary renal cell cancer. Nature Genetics *30*, 406–410.

Torrents, D., Pineda, M., Ferna, E., Lloberas, J., Shi, Y., Zorzano, A., and Palacı, M. (1998). Identification and Characterization of a Membrane Protein (y L Amino Acid Transporter-1) That Associates with 4F2hc to Encode the Amino Acid Transport Activity y L.A candidate gene for lysinuric protein intolerance. The Journal of Biological Chemistry *273*, 32437–32445.

Toschi, A., Lee, E., Gadir, N., Ohh, M., and Foster, D.A. (2008). Differential dependence of hypoxia-inducible factors 1 alpha and 2 alpha on mTORC1 and mTORC2. The Journal of Biological Chemistry *283*, 34495–34499.

Ullah, M.S., Davies, A.J., and Halestrap, A.P. (2006). The Plasma Membrane Lactate Transporter MCT4 , but Not MCT1 , Is Up-regulated by Hypoxia through. Journal of Biological Chemistry *281*, 9030–9037.

Verrey, F., Closs, E.I., Wagner, C.A., Palacin, M., Endou, H., and Kanai, Y. (2004). CATs and HATs: the SLC7 family of amino acid transporters. Pflugers Archiv European Journal of Physiology *447*, 532–542.

Wang, G.L., Jiang, B.H., Rue, E.A., and Semenza, G.L. (1995). Hypoxia-inducible factor 1 is a basic-helix-loop-helix-PAS heterodimer regulated by cellular O2 tension. Proc Natl Acad Sci U S A *92*, 5510–5514.

Wang, X., Campbell, L.E., Miller, C.M., and Proud, C.G. (1998). Amino acid availability regulates p70 S6 kinase and multiple translation factors. Biochem J *334 (Pt 1*, 261–267.

Ward, J.P.T. (2008). Oxygen sensors in context. Biochimica Et Biophysica Acta *1777*, 1–14.

Weidle, U.H., Scheuer, W., Eggle, D., Klostermann, S., and Stockinger, H. (2010). Cancer-related issues of CD147. Cancer Genomics Proteomics *7*, 157–169.

Wiesener, Turley, H., Allen, W., Willam, C., Eckardt, K., Talks, K., Wood, S., Gatter, K., Harris, A., Pugh, C., et al. (1998). Induction of endothelial PAS domain protein-1 by hypoxia: Characterization and comparison with hypoxia-inducible factor-1 alpha. Culture *92*, 2260–2268.

Wiesener, M.S., Jurgensen, J.S., Rosenberger, C., Scholze, C.K., Horstrup, J.H., Warnecke, C., Mandriota, S., Bechmann, I., Frei, U.A., Pugh, C.W., et al. (2003). Widespread hypoxia-inducible expression of HIF-2alpha in distinct cell populations of different organs. FASEB J *17*, 271–273.

Wise, D.R., Ward, P.S., Shay, J.E.S., Cross, J.R., Gruber, J.J., Sachdeva, U.M., Platt, J.M., DeMatteo, R.G., Simon, M.C., and Thompson, C.B. (2011). Hypoxia promotes isocitrate dehydrogenase-dependent carboxylation of α-ketoglutarate to citrate to support cell growth and viability. Proceedings of the National Academy of Sciences of the United States of America *108*, 19611–19616.

Wolff, N.C., Vega-Rubin-de-Celis, S., Xie, X.J., Castrillon, D.H., Kabbani, W., and Brugarolas, J. (2011). Cell-type-dependent regulation of mTORC1 by REDD1 and the tumor suppressors TSC1/TSC2 and LKB1 in response to hypoxia. Mol Cell Biol *31*, 1870–1884.

Wykoff, C.C., Sotiriou, C., Cockman, M.E., Ratcliffe, P.J., Maxwell, P., Liu, E., and Harris, A.L. (2004). Gene array of VHL mutation and hypoxia shows novel hypoxia-induced genes and that cyclin D1 is a VHL target gene. British Journal of Cancer *90*, 1235–1243.

Xu, D., and Hemler, M.E. (2005). Metabolic activation-related CD147-CD98 complex. Molecular Cellular Proteomics MCP *4*, 1061–1071.

Yanagida, O., Kanai, Y., Chairoungdua, A., Kim, D., Segawa, H., Nii, T., Cha, S., Matsuo, H., Fukushima, J., Fukasawa, Y., et al. (2001). Human L-type amino acid transporter 1 (LAT1): characterization of function and expression in tumor cell lines. Biochim Biophys Acta *1514*, 291–302.

Yoon, D., Okhotin, D. V, Kim, B., Okhotina, Y., Okhotin, D.J., Miasnikova, G.Y., Sergueeva, A.I., Polyakova, L.A., Maslow, A., Lee, Y., et al. (2010). Increased size of solid organs in patients with Chuvash polycythemia and in mice with altered expression of HIF-1alpha and HIF-2alpha. Journal of Molecular Medicine Berlin Germany *88*, 523–530.

Zelzer, E., Levy, Y., Kahana, C., Shilo, B.Z., Rubinstein, M., and Cohen, B. (1998). Insulin induces transcription of target genes through the hypoxia-inducible factor HIF-1alpha/ARNT. The The European Molecular Biology Organization Journal *17*, 5085–5094.

Zhang, H., Gao, P., Fukuda, R., Kumar, G., Krishnamachary, B., Zeller, K.I., Dang, C. V, and Semenza, G.L. (2007). HIF-1 inhibits mitochondrial biogenesis and cellular respiration in VHL-deficient renal cell carcinoma by repression of C-MYC activity. Cancer Cell *11*, 407–420.

Zhang, H., Zhang, G., Gonzalez, F.J., Park, S., and Cai, D. (2011). Hypoxia-Inducible Factor Directs POMC Gene to Mediate Hypothalamic Glucose Sensing and Energy Balance Regulation. PLoS Biology *9*, 16.

Zhou, J., Schmid, T., and Brüne, B. (2003). Tumor necrosis factor-alpha causes accumulation of a ubiquitinated form of hypoxia inducible factor-1alpha through a nuclear factor-kappaB-dependent pathway. Molecular Biology of the Cell *14*, 2216–2225.

Zimmer, M., Doucette, D., Siddiqui, N., and Iliopoulos, O. (2004). Inhibition of hypoxia-inducible factor is sufficient for growth suppression of VHL-/- tumors. Molecular Cancer Research MCR *2*, 89–95.

Zoncu, R., Efeyan, A., and Sabatini, D.M. (2011). mTOR: from growth signal integration to cancer, diabetes and ageing. Nat Rev Mol Cell Biol *12*, 21–35.

ANEXO I

ANEXO I

El trabajo presentado en esta tesis doctoral se haya fundamentalmente descrito en el siguiente artículo:

Elorza A, Soro-Arnáiz I, Meléndez-Rodríguez F, Rodríguez-Vaello V, Marsboom G, de Cárcer G, Acosta-Iborra B, Albacete-Albacete L, Ordóñez A, Serrano-Oviedo L, Giménez-Bachs JM, Vara-Vega A, Salinas A, Sánchez-Prieto R, Martín del Río R, Sánchez-Madrid F, Malumbres M, Landázuri MO, Aragonés J. **"HIF2α acts as an mTORC1 activator through the amino acid carrier SLC7A5"**. Mol Cell. 2012 Dec 14;48(5):681-91.

Durante su periodo de formación la doctorando ha participado además en los siguientes trabajos:

- Acosta-Iborra B*, **Elorza A***, Olazabal IM*, Martín-Cofreces NB, Martin-Puig S, Miró M, Calzada MJ, Aragonés J, Sánchez-Madrid F, Landázuri MO. **"Macrophage oxygen sensing modulates antigen presentation and phagocytic functions involving IFN-gamma production through the HIF-1 alpha transcription factor".** J Immunol. 2009 Mar 1;182(5):3155-64.

  ***** Primera posición de la autoría compartida.

- Aragonés J, **Elorza A**, Acosta-Iborra B, Landázuri MO. **"Myeloid hypoxia-inducible factors in inflammatory diseases".** Crit Rev Immunol. 2011;31(1):1-13. Review.

- Miró-Murillo M*, **Elorza A***, Soro-Arnáiz I*, Albacete-Albacete L, Ordoñez A, Balsa E, Vara-Vega A, Vázquez S, Fuertes E, Fernández-Criado C, Landázuri MO, Aragonés J. **"Acute Vhl gene inactivation induces cardiac HIF-dependent erythropoietin gene expression".** PLoS One. 2011;6(7):e22589.

  ***** Primera posición de la autoría compartida.

- Tello D, Balsa E, Acosta-Iborra B, Fuertes-Yebra E, **Elorza A**, Ordóñez Á, Corral-Escariz M, Soro I, López-Bernardo E, Perales-Clemente E, Martínez-Ruiz A, Enríquez JA, Aragonés J, Cadenas S, Landázuri MO**. "Induction of the mitochondrial NDUFA4L2 protein by HIF-1α decreases oxygen consumption by inhibiting Complex I activity".** Cell Metab. 2011 Dec 7;14(6):768-79.

ANEXO II

Macrophage Oxygen Sensing Modulates Antigen Presentation and Phagocytic Functions Involving IFN-γ Production through the HIF-1α Transcription Factor[1]

Bárbara Acosta-Iborra,[2]* Ainara Elorza,[2]* Isabel M. Olazabal,[2]* Noa B. Martín-Cofreces,* Silvia Martin-Puig,* Marta Miró,[†] María J. Calzada,* Julián Aragonés,* Francisco Sánchez-Madrid,*[‡] and Manuel O. Landázuri[3]*

Low oxygen tension areas are found in inflamed or diseased tissues where hypoxic cells induce survival pathways by regulating the hypoxia-inducible transcription factor (HIF). Macrophages are essential regulators of inflammation and, therefore, we have analyzed their response to hypoxia. Murine peritoneal elicited macrophages cultured under hypoxia produced higher levels of IFN-γ and IL-12 mRNA and protein than those cultured under normoxia. A similar IFN-γ increment was obtained with in vivo models using macrophages from mice exposed to atmospheric hypoxia. Our studies showed that IFN-γ induction was mediated through HIF-1α binding to its promoter on a new functional hypoxia response element. The requirement of HIF-α in the IFN-γ induction was confirmed in RAW264.7 cells, where HIF-1α was knocked down, as well as in resident HIF-1α null macrophages. Moreover, Ag presentation capacity was enhanced in hypoxia through the up-regulation of costimulatory and Ag-presenting receptor expression. Hypoxic macrophages generated productive immune synapses with CD8 T cells that were more efficient for activation of TCR/CD3ε, CD3ζ and linker for activation of T cell phosphorylation, and T cell cytokine production. In addition, hypoxic macrophages bound opsonized particles with a higher efficiency, increasing their phagocytic uptake, through the up-regulated expression of phagocytic receptors. These hypoxia-increased immune responses were markedly reduced in HIF-1α- and in IFN-γ-silenced macrophages, indicating a link between HIF-1α and IFN-γ in the functional responses of macrophages to hypoxia. Our data underscore an important role of hypoxia in the activation of macrophage cytokine production, Ag-presenting activity, and phagocytic activity due to an HIF-1α-mediated increase in IFN-γ levels. *The Journal of Immunology,* **2009, 182: 3155–3164.**

Inflamed and ischemic tissues contain areas of hypoxia or low oxygen tensions as a consequence of inadequate blood supply. The ability of cells to generate energy in a mitochondrial-dependent manner is compromised in a hypoxic environment, thus undergoing adaptation mechanisms of their metabolism for survival. This response is mediated through the hypoxia-inducible factors (HIF)[4] (1, 2), which regulate the transcription of genes involved in different processes such as angiogenesis (vascular endothelial growth factor (VEGF)) (3, 4), glycolysis (glucose transporter type-1 (Glut-1)) (5, 6), and HIF autoregulation (prolyl hydroxylases domains (PHDs)) (7). HIF is a basic helix-loop-helix transcription factor of the Per-ARNT-Sim superfamily composed of two subunits, namely, HIF-α and HIF-β (aryl hydrocarbon receptor nuclear translocator). The HIF complex is modulated in an oxygen-sensitive manner through the availability of HIF-α protein, which, in the presence of oxygen, is targeted for degradation through hydroxylation at specific prolyl residues by PHDs (8, 9). HIF-α is then recognized and ubiquitinated by the Von Hippel Lindau E3 ubiquitin ligase complex for its degradation by the proteasome (10). In contrast, at low oxygen tensions, PHD enzymes can no longer hydroxylate the HIF-α subunit, which is stabilized and freed to form an active transcription complex with HIF-β, and is able to migrate to the nucleus and to bind to hypoxic response elements (HREs) within the promoter of specific target genes.

Macrophages play an important role in the innate as well as the adaptive immune response through their specific functions of phagocytosis, Ag presentation, cytokine secretion, and tissue remodeling. As professional phagocytes, macrophages express a wide variety of receptors that participate in the phagocytic uptake of Ags, including those that recognize Ig Fc fragments (mainly FcγRs), and complement activation products such as C3b (CR3, CR4, CRI) (11, 12). Upon activation, macrophages are induced to produce cytokines such as IL-12, IL-18, IFN-γ, TNF-α, and IL-1β

*Servicio de Inmunología, Hospital Universitario de la Princesa, Universidad Autónoma de Madrid, Madrid; [†]Gabinete Veterinario, Facultad de Medicina, Universidad Autónoma de Madrid, Madrid; [‡]Departamento de Biología Vascular e Inflamación, Centro Nacional de Investigaciones Cardiovasculares, Madrid, Spain

Received for publication May 28, 2008. Accepted for publication December 27, 2008.

The costs of publication of this article were defrayed in part by the payment of page charges. This article must therefore be hereby marked *advertisement* in accordance with 18 U.S.C. Section 1734 solely to indicate this fact.

[1] This work was supported by the Migration and Inflammation Network UAMAD04 and Comision Interministerial de Ciencia y Tecnologia (to M.O.L.) and Red Temática de Enfermedades Cardiovasculares (RD06/0014/0031 to M.O.L., RD06/0014/0030 to F.S.-M., and fellowship for M.M.). B.A.-I. is an investigator from the Ministerio de Educación y Ciencia. A.E. is from the Ministerio de Salud y Consumo. I.M.O., M.J.C., and J.A. are investigators from the Ministerio de Ciencia y Tecnología Programa Ramón y Cajal.

[2] B.A.-I., A.E., and I.M.O. contributed equally to this work.

[3] Address correspondence and reprint requests to Dr. Manuel O. Landázuri, Servicio de Inmunología, Hospital de la Princesa, Universidad Autónoma de Madrid, C/ Diego de León, 62, E-28006, Madrid, Spain. E-mail address: mortiz.hlpr@salud.madrid.org

[4] Abbreviations used in this paper: HIF, hypoxia-inducible factor; PHD, prolyl hydroxylase domain; VEGF, vascular endothelial growth factor; IS, immune synapse; MTOC, microtubule-organizing center; HRE, hypoxia response element; LAT, linker for activation of T cells; MHC-I/II, MHC class I/II; RT, real time; siRNA, small interfering RNA; ChIP, chromatin immunoprecipitation; siSCR, scrambled siRNA; OVAp, OVA peptide; Glut-1, glucose transporter type-1; DMOG, dimethyloxalylglycine.

www.jimmunol.org/cgi/doi/10.4049/jimmunol.0801710

(13–20). Through these cytokines macrophages drive an inflammatory response by increasing their phagocytic capability. Moreover, these cytokines promote macrophage Ag processing and presentation and the differentiation and activation of Th1 IFN-γ-secreting cells, CTL, and NK cells (21–23). The goal of Ag presentation is to amplify the signal through T cell cytokine production and clonal expansion. Ag-loaded presenting cells (macrophages, dendritic cells, B cells) form stable conjugates with specific T cells and promote the relocalization of Ag recognition receptors, cell adhesion, and signaling molecules to the contact site, forming what has been termed the immune synapse (IS) (24, 25). During the formation of the IS, the TCR is engaged and activated for the recruitment of different signaling molecules, such as ZAP70 or linker for activation of T cells (LAT), the F-actin cytoskeleton is recruited to the contact site for the stabilization and reorganization of the IS, and the microtubule-organizing center (MTOC) is reoriented, increasing the efficient secretion of killing granules and cytokines (25–28).

Previous studies have documented that macrophages are involved in a number of inflammatory diseases such as atherosclerotic plaques, myocardial infarcts, rheumatoid arthritis, wound healing, bacterial infections, and malignant tumors, in which areas of hypoxia are present (29, 30). In these areas, macrophages express HIF protein abundantly and respond rapidly to hypoxia (31, 32). Moreover, HIF-1α is stabilized in macrophages activated by nonhypoxic stimulus, playing a role in the proper infiltration and activation of leukocytes during an inflammatory process and mediating the bactericidal capacity and the control of pathogen spreading during infection (31–34). In this work, we have studied the effect of hypoxia on macrophage functions in the absence of any other stimuli. We report herein that under hypoxia macrophages are able to form efficient IS with increased T cell cytokine production ability and enhanced phagocytic uptake. Furthermore, hypoxia increases macrophage IFN-γ secretion, which is dependent on HIF-1α binding to its promoter on a functional HRE site.

Materials and Methods

Mice

All experiments were performed in 6- to 12-wk-old mice. Mice were housed and bred in the Animal Unit of the School of Medicine (Universidad Autónoma, Madrid, Spain) in a pathogen-free facility. C57BL/6 mice (H-2^b) were used for macrophage isolation. OT-I mice, an H-$2K^b$ restricted anti-OVA TCR-transgenic mice under a C57BL/6 background, were used for T lymphocyte isolation (35). Mice with myeloid lineage-specific knockout of HIF-1α (HIF-1α flox-LysMCre) have been previously described (33). Experimental procedures were approved by the Committee for Research Ethics of the Universidad Autónoma de Madrid and conducted under the supervision of the Universidad Autónoma de Madrid Head of Animal Welfare and Health in accordance with Spanish and European guidelines.

Cell culture

Peritoneal thioglycolate-elicited macrophages depleted of granulocytes were isolated by adhesion to tissue culture plates and several washes. $CD8^+$ T cells were isolated from spleen and lymph nodes and were depleted from other populations using the AutoMACS magnetic sorter. Mice macrophages and T cells were maintained in RPMI 1640 medium with GLUTAMAX-I (Invitrogen) and RAW264.7 and J774A.1 cells were grown in DMEM (Cambrex). Both media were supplemented with 100 U/ml penicillin, 100 μg/ml streptomycin, and 2 or 10% FCS (Cambrex), respectively. Cells cultured in normoxia were incubated in the present or absence of 10 ng/ml LPS (Sigma-Aldrich) during 40 h. Dimethyloxalylglycine (DMOG) was purchased from BIOMOL.

Hypoxic conditions

The cells were routinely cultured in 21% O_2 and 5% CO_2 (normoxic conditions). To expose the cells to hypoxia, they were placed in an in vivo 400 hypoxia Work Station (Ruskinn Technology) that was infused with a mixture of 1% O_2, 5% CO_2, and 94% N_2 (S.E. Carburos Metalicos). For in vivo assays, mice were injected, when needed, with thioglycolate for 4 days, then exposed either to 21% (N) or 13% for 1 h and then 7.5% oxygen levels (Hx) for 40 h before macrophage isolation. Macrophages were isolated by peritoneal lavage and by adhesion to tissue-cultured plates.

Table I. *Primer sequences*

No.	Target	Direction	Sequence
1	28S	F	CAGTACGAATACAGACCG
2	28S	R	GGCAACAACACATCATCAG
3	HIF-1α	F	GTTTACTAAAGGACAAGTCACC
4	HIF-1α	R	TTCTGTTTGTTGAAGGGAG
5	PHD3	F	GATGCTGAAGAAAGGGC
6	PHD3	R	CTGGCAAAGAGAGTATCTG
7	VEGF	F	TGCCAAGTGGTCCCAG
8	VEGF	R	GTGAGGTCTTGATCCG
9	IFN-γ	F	TGGCTCTGCAGGATTTTCATG
10	IFN-γ	R	TCAAGTGGCATAGATGTGGAAGAA
11	IL-12p40	F	CAGATGACATGGTGAAGACG
12	IL-12p40	R	GTTGTGGAAGAAGTCTCTCTAGTA
13	IL-18	F	AATGGCTGCCATGTCA
14	IL-18	R	TCCGTATTACTGCGGTTG
15	IL-10	F	CCAAGCCTTATCGGAAATG
16	IL-10	R	TGGCCTTGTAGACACC
17	BNIP-3	F	GGCGTCTGACAACTTCC
18	BNIP-3	R	ACCGCATTTACAGAACAAATTAAC
19	IFN-γ promoter	F	ctcgagCCTTGGGTGTGTTGAGTGAA
20	IFN-γ promoter	R	aagcttAGGAGAAGCCCAGAACTTCT
21	IFN-γ mut	F	CTTGTGAAAATTAGCAATCCCGAGGA
22	IFN-γ mut	R	TCCTCGGGATTGCTAATTTTCACAAG
23	IFN-γ ChIP	F	CTCATCGTCAGAGAGCCCAA
24	IFN-γ ChIP	R	AGGATCAGCTGATGTGTCTT

Macrophage cytokine secretion and activation markers

For cytokine synthesis and secretion analysis, IL-12 and IFN-γ were detected by quantitative PCR (oligonucleotides in Table I) and by ELISA with BD Biosciences Abs at different time points under hypoxia exposure. For assessment of surface molecule expression on macrophages, cells were processed 40 h after hypoxia exposure with a cell dissociation buffer (Life Technologies). Cells were stained for CD11b, CD32/16, MHC class I (H-2^b), and MHC-II (I-A, I-B) using FITC-labeled Abs and for CD18, CD40, CD86, and F4/80 using biotin-labeled Abs and with allophycocyanin-streptavidin (BD Biosciences).

Immunoprecipitation and Western blot

Cells were processed with Laemmli buffer, resolved on 10% SDS-polyacrylamide gels, and immunoblotted with monoclonal HIF-1α (1/1000; R&D Systems), polyclonal PHD3 (1/2000; Bethyl Laboratories), or Glut-1 (Santa Cruz Biotechnology). For Ag presentation assays, macrophage and conjugates were processed for immunoprecipitations and Western blot as previously described (36) with the following Abs: monoclonal anti-CD3ζ 448 (1/100) (37), monoclonal anti-phosphotyrosine 4G10 Ab (1 μg/ml; Upstate Biotechnology), polyclonal anti-phospho-LAT Y191, and anti-total LAT (1 and 2 μg/ml respectively; Upstate Biotechnology). Immunolabeling was detected by ECL (Amersham Pharmacia Biotech) and visualized with a digital luminescent image analyzer (FUJI Film LAS-1000 CH).

Quantitative real-time (RT)-PCR

Cells were harvested in 1 ml of Ultraspec reagent (Biotecx) and RNA was reverse-transcribed to cDNA (Improm-II reverse transcriptase; Promega). The PCR were performed with the LC FastStart DNA master SYBR Green I kit (Roche Applied Science) and in a Light Cycler system (Roche Applied Science). Data were analyzed with Light Cycler software version 3.5.28 (Idaho Technology). For each sample, the gene copy number was normalized to the amount of ribosomal mRNA 28S. Primers used in Table I.

Small interfering RNA (siRNA) transfection

RAW264.7 cells were transfected according to the Lipofectamine 2000 (Invitrogen) protocol with 50 pmol of siRNA. HIF-1α siRNA (sc-44225) and control scrambled siRNA (sc-37007) were from Santa Cruz Biotechnology. Macrophage peritoneal cells were transfected following HiPerFect manufacturer instructions (Qiagen) with 5 nM siRNA: scrambled, HIF-1α, or IFN-γ. Transfected cells were incubated at 37°C and 5% CO_2 under normoxic or hypoxic conditions for 40 h.

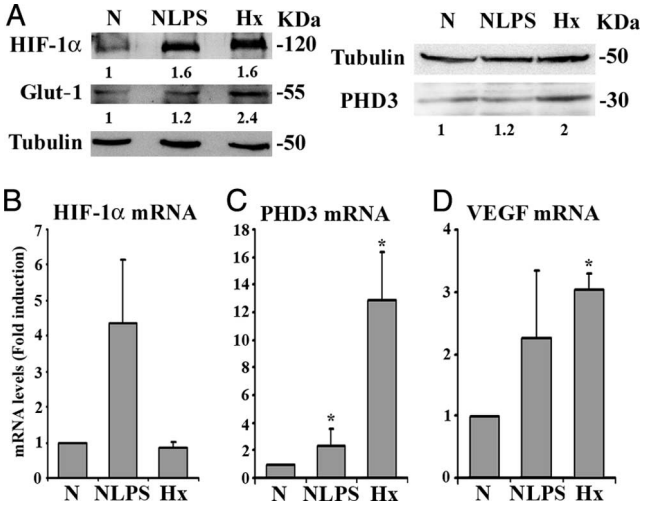

FIGURE 1. Expression of hypoxia-dependent genes in primary murine macrophages cultured in hypoxic conditions. *A*, Western blot analysis of HIF-1α, Glut-1, PHD3, and tubulin in macrophages cultured under normoxia (N), under normoxia with 10 ng/ml LPS (NLPS), or under 1% oxygen levels (hypoxia (Hx)) for 16 h. Densitometric analysis are represented as fold inductions compared with normoxia. Protein levels were normalized to tubulin. mRNA levels of HIF-1α (*B*), PHD3 (*C*), or VEGF (*D*) in macrophages treated as indicated in *A*.

Chromatin immunoprecipitation (ChIP)

For the ChIP assays, cells were exposed to hypoxia or normoxia for 6 h. Cells were processed as previously described (38). For immunoprecipitations, whole rabbit serum (IgG control) and polyclonal anti-HIF-1α antiserum (ab2185; Abcam) were used. The PCR primers used are indicated in Table I.

Generation of plasmid construct

The IFN-γ promoter region was cloned using the mouse genomic sequence: −848 to −22 containing putative hypoxia-inducible regulatory sequences, which were amplified by PCR (primers in Table I). The PCR products were cloned into *Xho*I and *Hin*dIII sites of the pGL3 basic luciferase plasmid (Promega). Genomic DNA was used as a template for the PCRs. The mutant HRE was generated by PCR.

Cell nucleofection and reporter assays

RAW264.7 cells were nucleofected in normoxia following Amaxa nucleofection protocols and 3 h later were exposed or not to hypoxia. The luciferase reporter plasmids used were: *Renilla* firefly luciferase vector, pGL3-Luc, pGL3-PHD3-Luc (38), pGL3-IFN-γ-Luc and their mutated constructs at the HRE core: pGL3-PHD3Mut-Luc and pGL3-IFN-γMut-Luc. After 24 h of hypoxic exposure, cells were harvested and the firefly luciferase activity was quantified using a dual luciferase system (Promega) in which the firefly luciferase activity was normalized to the *Renilla* luciferase activity.

Ag presentation assays, immunofluorescence staining, and intracellular cytokine staining

Macrophages cultured under normoxic or hypoxic conditions for 40 h were loaded or not with 100 ng/ml (1 nM) OVA peptide (257–264, SIINFEKL) 2 h before T cell addition. Then, $CD8^+$ T cells (1×10^6) were added in normoxia or hypoxia to macrophages during different time points depending on the assay. Immunofluorescence staining was performed using the monoclonal α-tubulin Ab FITC-labeled (Sigma-Aldrich) or the APA1/1 Ab, which detects the activated conformation of CD3 (39, 40). Intracellular cytokine T cell staining was performed as described previously by activation with PMA and ionomycin, inhibition of secretion with brefeldin A, and staining (41).

Opsonization and phagocytosis assays

Particles used were sheep RBC (SRBC) opsonized in normoxic conditions as previously described (42) for FcγR or CR-mediated phagocytosis using rabbit anti-SRBC IgG (MP Biomedicals) or IgM Abs (Accurate Chemical) and C5-deficient serum, respectively. Macrophages cultured under normoxic or hypoxic conditions for 40 h were starved for 2 h and were incubated with opsonized SRBC in a 1:20 ratio during 15 min. Cells were fixed and stained for Alexa Fluor 488-labeled anti-rabbit Abs (Molecular Probes) to detect the SRBC and with phalloidin labeled with Alexa Fluor 564 for F-actin staining. Internalized particles appeared big and swollen, while external particles appeared small and shrunken due to the fixation process.

Statistical analysis

Data were analyzed by the ANOVA Mann-Whitney *U* test followed by the Kruskal-Wallis test. The *p* values obtained are indicated in the text and figures.

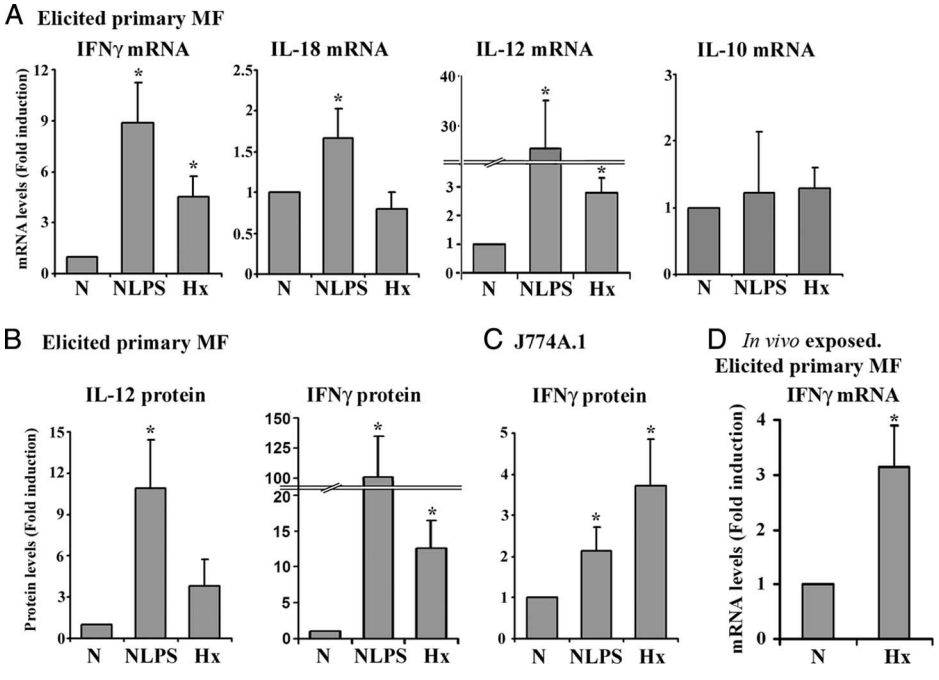

FIGURE 2. Increased IFN-γ and IL-12 production by macrophages cultured in hypoxia. *A*, Macrophages cultured under different conditions (as in Fig. 1) were processed for RNA isolation and quantitative RT-PCR assays were performed to quantify IFN-γ, IL-12, IL-18, and IL-10 mRNA levels. *B*, Supernatants from peritoneal-elicited macrophages were recovered and tested by ELISA for IL-12 and IFN-γ protein quantification and (*C*) for IFN-γ quantification in the macrophage cell line J774A.1. *D*, mRNA IFN-γ quantification from elicited macrophages isolated form mice exposed in vivo to normoxia or hypoxia for 40 h. *A–D*, mRNA and protein levels are expressed as fold inductions compared with macrophages cultured in normoxia. The arithmetic mean ± SEM from four different experiments is represented (∗, $p < 0.05$).

Results

Hypoxia induces macrophage proinflammatory cytokine production

Macrophages have been involved in inflammatory diseases where areas of hypoxia are present (29–32) Thus, we assessed whether hypoxia affected the cytokine production capacity in macrophages. We first characterized the response of macrophages to hypoxia by assessing the expression of several hypoxia-responsive genes (3–7) in peritoneal-elicited macrophages. HIF-1α protein and the hypoxia-dependent proteins Glut-1 (5, 6) and PHD3 (7) were analyzed by Western blotting and were found to be increased under hypoxic conditions as compared with normoxia (Fig. 1*A*). These proteins were also induced, although at lower levels, in macrophages treated with LPS as a control of macrophage activation (Fig. 1*A*) (43, 44). HIF-2α, another isoform of HIF-α (45), was undetected by Western blot and only detected at very low levels by quantitative RT-PCR (data not shown). HIF-1α mRNA remained constant after hypoxia exposure (Fig. 1*B*). LPS-treated macrophages, however, expressed higher levels of HIF-1α mRNA (43, 44). PHD3 and VEGF (3, 4) mRNA levels were induced both in macrophages under hypoxic conditions as well as in response to LPS (Fig. 1, *C* and *D*). These data indicate that primary macrophages respond to hypoxia by inducing hypoxia and HIF-1α target-dependent genes.

Next, we analyzed whether hypoxia affected the inflammatory response of macrophages through RT-PCR and ELISA. Our results indicated that elicited macrophages under hypoxia significantly induced IFN-γ and IL-12, but not IL-18. However, LPS-treated macrophages induced these three cytokines (Fig. 2*A*). In contrast, the anti-inflammatory cytokine IL-10 mRNA was not induced either by hypoxia or LPS (Fig. 2*A*). IFN-γ protein secretion was assayed in peritoneal-elicited macrophages, and similar effects were observed in resident macrophages or the macrophage cell line J774A.1 (Fig. 2, *B* and *C*, and data not shown). To corroborate these data, RNA was extracted from macrophages from mice exposed in vivo to hypoxia, and IFN-γ mRNA was also induced compared with normoxic mice (Fig. 2*D*). These results indicate that hypoxia stimulates macrophages to secrete the proinflammatory cytokines IFN-γ and IL-12, while IL-10 anti-inflammatory cytokine levels remained constant, suggesting that the fine modulation of cytokines may be involved in an activatory phenotype of macrophages under an hypoxic environment.

HIF-1α mediates IFN-γ production in hypoxia

To determine the involvement of the canonical hypoxia pathway in the proinflammatory response of macrophages, we used an inhibitor of PHDs, DMOG, that stabilizes HIF-1α in normoxic conditions, resembling the HIF-1α-mediated response to hypoxia (46, 47). Elicited peritoneal macrophages incubated with 100 μM DMOG increased both mRNA and protein levels of IFN-γ at 48 h (Fig. 3*A*). The direct role of HIF-1α in the induction of IFN-γ was also evidenced in macrophages transfected with HIF-1α siRNA and cultured under hypoxia. A clear reduction was observed in HIF-1α protein and a significant decrease in IFN-γ mRNA levels after interference, compared with macrophages transfected with scrambled siRNA (siSCR; $p < 0.05$) and to control (mock transfected) (Fig. 3, *B* and *C*). Moreover, resident peritoneal macrophages isolated from myeloid linage-specific HIF-1α knockout mice exposed to hypoxia did not induce the transcription of IFN-γ nor BNIP-3 (an HIF-1α-dependent gene (48, 49)), compared with macrophages from the corresponding control mice (Fig. 3*D*). Taking together, these evidences confirmed that HIF-1α plays an important role in the hypoxia-mediated production of the IFN-γ cytokine.

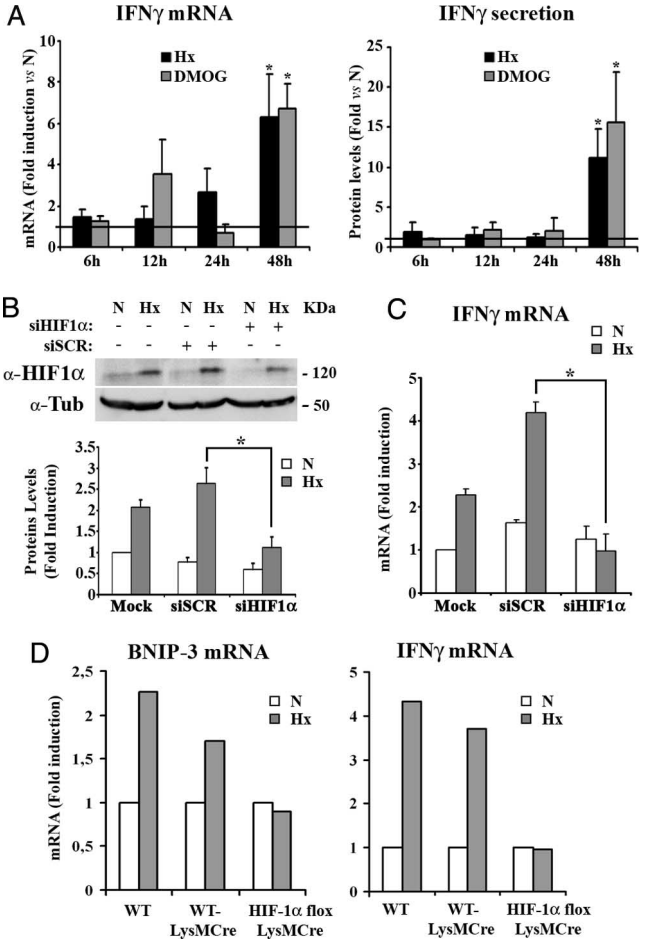

FIGURE 3. HIF-1α mediates the IFN-γ production in hypoxia. *A*, Kinetics of mRNA and protein levels of IFN-γ in macrophages in normoxia in the presence or absence of 100 μM DMOG or in hypoxia. Results are expressed as fold induction compared with normoxia (*, $p < 0.05$). *B* and *C*, RAW264.7 cells were either mock transfected or transfected with siRNA for HIF-1α (siHIF1α) or its scramble control (siSCR) and incubated under normoxia (N) or hypoxia (Hx). *Upper panel*, Representative Western blot analysis of HIF-1α and tubulin as loading control. *Lower panel*, Densitometric analyses are represented as fold inductions compared with normoxia in mock-transfected cells and normalized by tubulin. *C*, IFN-γ mRNA levels are expressed as fold inductions compared with normoxia. *D*, Resident macrophages isolated from control mice (WT and WT-LysMCre) or HIF-1α knockout mice (HIF-1α flox-LysMCre) exposed in vivo to hypoxia. IFN-γ mRNA levels are expressed as fold inductions of hypoxia vs normoxia. Data correspond to macrophages pooled from three different animals for each experimental condition.

Consequently, the search for HRE sites within the promoter of the IFN-γ gene rendered a putative HRE site conserved among different mammalian species (Fig. 4*A*). To ascertain whether this HRE site was a functional HIF binding site, the in vivo binding of HIF-1α to the IFN-γ promoter was tested by HIF-1α ChIP assay on elicited peritoneal macrophages cultured under normoxic or hypoxic conditions. Under hypoxic conditions, endogenous HIF-1α protein bound to HRE within the IFN-γ promoter, whereas no binding was observed under normoxic conditions (Fig. 4*B*).

To assess the functionality of this HRE site, the -848 to -22 sequence from the murine IFN-γ promoter was cloned in a luciferase reporter expression vector. RAW 264.7 cells were nucleofected and cultured under normoxia or hypoxia for 16 h. The luciferase expression of this IFN-γ construct was induced under

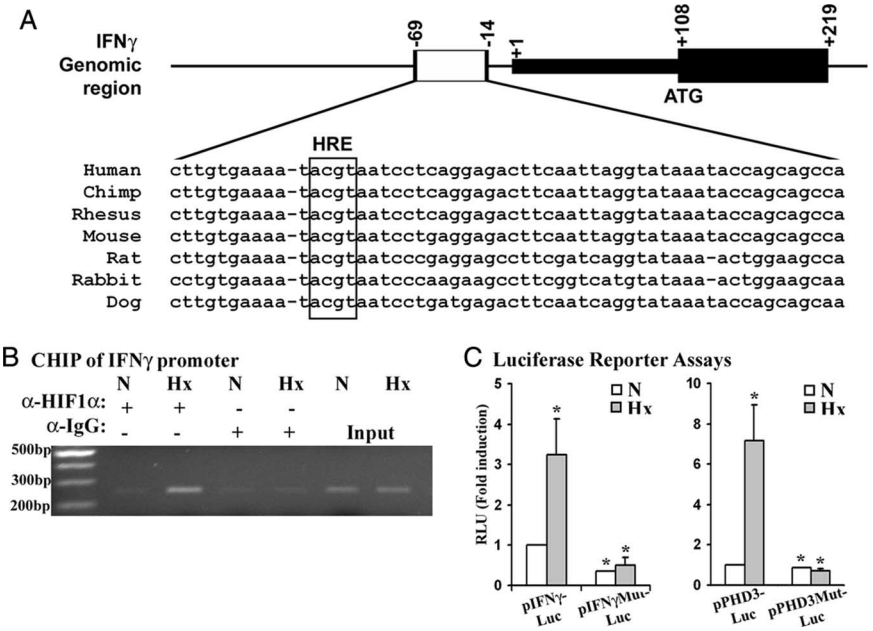

FIGURE 4. HIF-1α binds to a functional HRE site in the IFN-γ promoter. *A*, Blast sequence alignment of 1000 bp of the IFN-γ proximal promoter sequence of different mammalian species containing the conserved HRE site remarked by a box. *B*, ChIP of the DNA from primary macrophages cultured in normoxia (N) or hypoxia (Hx) during 6 h with either anti-HIF-1α Ab (*lanes 1* and *2*) or anti-IgG Ab (*lanes 3* and *4*); total lysate (input, *lanes 5* and *6*). *C*, RAW264.7 macrophage cell line was nucleofected with constructs expressing the IFN-γ or PHD3 promoter containing the wild-type HRE site (pIFN-γ-Luc, pPHD3-Luc) or a mutated HRE site (pIFN-γMut-Luc or pPHD3Mut-Luc). Results are expressed as the fold induction of relative luciferase units (RLU).

hypoxic conditions (Fig. 4*C*) compared with normoxic macrophages. As a positive control, the PHD3 promoter construct responded efficiently to hypoxia (Fig. 4*C*). To confirm that the hypoxia program in macrophages involves the HRE site of the IFN-γ promoter, a mutant construct was generated in which the central conserved ACGT core was mutated to TAGC. A similar PHD3 mutant construct was also used as control (38). These mutant constructs were no longer responsive to hypoxia, either in the IFN-γ promoter or in the PHD3 promoter (Fig. 4*C*). Altogether, these results indicate that the activatory response of macrophages in hypoxia is directly mediated through HIF-1α, which binds to the new, functional HRE site present in the IFN-γ promoter.

Hypoxia enhances macrophage expression of Ag-presenting molecules and the formation of productive IS

Since hypoxic macrophages induce proinflammatory cytokine production, we analyzed whether hypoxia affected elicited peritoneal macrophage functions such as Ag presentation. First, the expression of costimulatory and Ag presentation molecules was determined under hypoxic conditions. CD40, CD86, and MHC-I expression levels were enhanced in hypoxic macrophages compared with macrophages cultured in normoxia (Fig. 5*A*). In contrast, CD80 and MHC-II expression was not induced significantly (data not shown).

Next, the nature and characteristics of the IS were analyzed in macrophages cultured under hypoxic conditions. Since MHC-I expression was significantly up-regulated during hypoxia, we focused on MHC-I presentation. Thus, macrophages loaded with OVA peptide$_{257–264}$ (OVAp) were conjugated with CD8$^+$ T cells from OT-I mice and the number of conjugates formed was determined. No significant differences were observed in the number of conjugates formed in normoxic and hypoxic macrophages (data not shown). T cell activation during IS requires the translocation of the MTOC for the efficient secretion of cytokines (50). Therefore, T cell MTOC translocation toward the contact area was analyzed, showing a high translocation efficiency (70% positive T cells) in normoxia that was only slightly increased in the T cells cultivated with hypoxia- and LPS-treated macrophages (data not shown).

Since the number of IS was not altered in response to hypoxia, we next determined whether hypoxia increased the efficiency of these IS by analyzing the conformationally active CD3ε chain, staining with the specific Ab APA 1/1 (39, 40). Hypoxic macrophages induced a much higher percentage of active TCR/CD3ε conformation compared with normoxic macrophages (Fig. 5, *B* and *C*). To further confirm the effect of hypoxic macrophages on the TCR engagement regulation, different markers of the TCR proximal activation signals were analyzed. The phosphorylation of CD3ζ and of its downstream T cell-specific protein LAT on Y195 residue was assessed. Western blot analyses revealed that in the presence of OVAp, hypoxic macrophages (Hx$^+$) induced stronger TCR/CD3ζ and LAT phosphorylation signals, as well as LPS-treated macrophages (NLPS$^+$) compared with normoxic macrophages (N$^+$; Fig. 5, *D* and *E*).

Next, we assessed later events of T cell activation such as cytokine production. T cells conjugated under hypoxia conditions with macrophages loaded with OVAp (Hx$^+$) showed increased IL-2 and IFN-γ production compared with T cells conjugated in normoxia (N$^+$; Fig. 5*F*). To discard a possible effect of hypoxia on this T cell activation, macrophages cultured under normoxia or hypoxia were fixed, loaded or not with OVAp, and subsequently incubated with T cells under normoxia. A similar result was obtained, indicating that OVAp-loaded hypoxic macrophages induce T cells (normoxic or hypoxic) to produce cytokines more efficiently (supplemental Fig. 1S[5]).

Taken together, these results indicate that macrophages under hypoxia induced productive IS, with increased active TCR/CD3ε conformation, early signaling events, and proinflammatory cytokine production.

Hypoxia induces the phagocytic activity of macrophages

To further analyze the role of hypoxia on macrophage functions, macrophage phagocytosis assays were performed on elicited peritoneal macrophages. CR (CD11b (α_M)/CD18 (β_2))- and FcγR (CD32/CD16)-mediated phagocytosis were assessed as two different opsonic phagocytic pathways. Both the binding and the internalization of differently opsonized SRBC were increased in macrophages cultured in hypoxia compared with macrophages

[5] The online version of this article contains supplemental material.

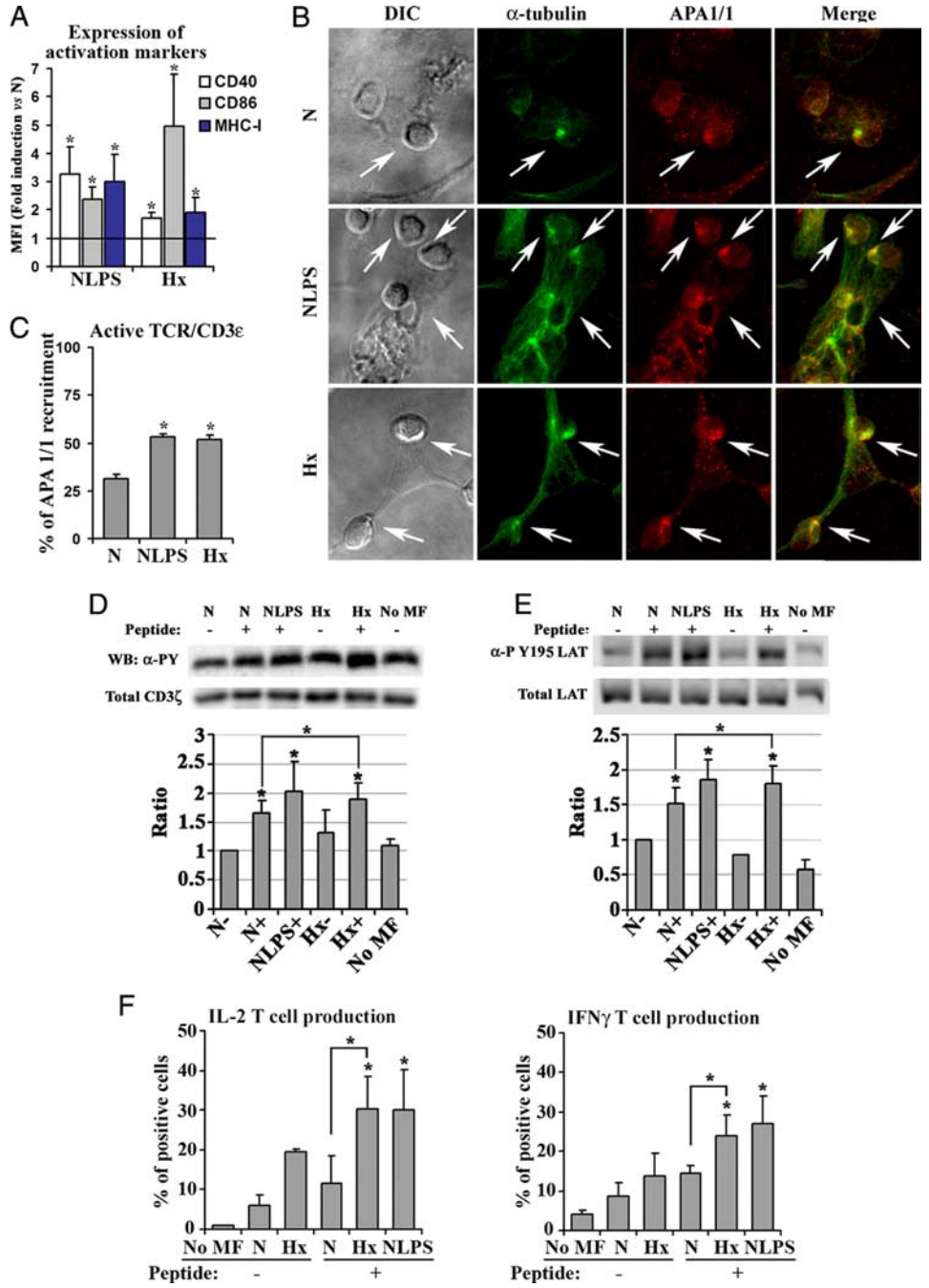

FIGURE 5. Macrophages form productive IS more efficiently in hypoxia. *A*, Cytometric analysis of CD40, CD86, and MHC-I, were performed in macrophages cultured in normoxia with or without LPS or in hypoxia. Results are expressed as the mean fluorescence intensity (MFI) normalized to normoxia expression and the mean of five different experiments is represented. *B*, Conjugates were formed during 20 min between the different cultured macrophages (as in Fig. 1) and $CD8^+$ T cells in the presence of OVAp in normoxia or hypoxia. Conjugates were then fixed and stained: differential interference contrast (DIC; *left panel*), MTOC is detected with α-tubulin Ab (green), active TCR/CD3ε conformation is detected with APA1/1 Ab (red), merged images (*right panel*). *C*, The number of T cells with active TCR/CD3ε recruited to the contact site was quantified and expressed as the percentage of the conjugates formed. Results correspond to arithmetic mean ± SEM of four independent experiments (∗, $p < 0.01$). *D*, Macrophage/T cell conjugates were processed and immunoprecipitated with anti-CD3ζ Ab and immunoblotted for anti-phosphotyrosine residues with 4G10 Ab (*upper panel*) or for total CD3ζ (*lower panel*) or *E*, immunoblotted for Y195-phosphorylated LAT (*upper panel*) or total LAT (*lower panel*). T cells without macrophages are represented as No MF. Graphs below *D* and *E* show the results of densitometric analysis, presented as the ratio of phosphorylated to total protein bands. Data are the arithmetic means ± SEM of four different experiments (∗, $p < 0.05$). *F*, Macrophages were cultured under normoxia with or without LPS or under hypoxia for 40 h. Conjugates were then formed under the same oxygen conditions for 40 h with $CD8^+$ T cells and in the presence or absence of 100 nM OVAp. T cells were analyzed for the intracellular production of IL-2 (*left*) and IFN-γ (*right*) by flow cytometry (see *Materials and Methods*). Data were quantified and expressed as the percentage of positive cells. The mean ± SEM of four different experiments is represented (∗, $p < 0.05$).

cultured in normoxia (2.5- to 3-fold and 1.5-fold for CR and FcγR, respectively; Fig. 6, *A* and *B*). LPS-treated macrophages, incubated in normoxia, also showed increased binding and internalization of opsonized SRBC (Fig. 6, *A* and *B*).

To determine whether the increased binding of particles to macrophages, after hypoxia treatment was mediated by regulating the expression of phagocytic receptors, flow cytometry analyses were performed. Both receptors CR (CD11b/CD18) and FcγR were

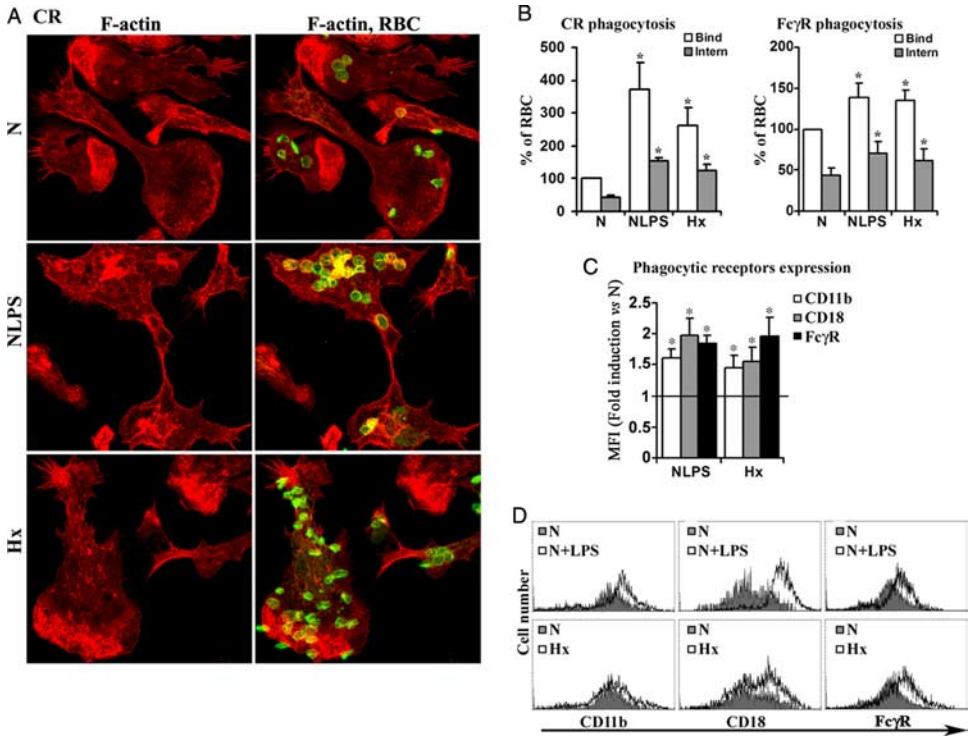

FIGURE 6. Phagocytosis through CR and FcγR is increased in primary macrophages cultured in hypoxia. *A*, Phagocytosis assays were performed in the different cultured macrophages as in Fig. 1, and cells were fixed and stained for F-actin (red, *left panel*) and for SRBC (green); merged images are shown in the *right panel*. *B*, Particle binding and internalization were quantified by counting 500 macrophages in duplicate per condition in each experiment. Results are expressed as the percentage of bound or internalized particles in macrophages (see *Materials and Methods*) cultured under the different conditions. Results were normalized compared with normoxia and are the mean of six different experiments. *C* and *D*, Cytometric analysis of CD11b, CD18, and FcγR were performed as in Fig. 1*A*. Results are expressed as the mean fluorescence intensity (MFI), normalized to normoxia expression, and are the mean of five different experiments. *B* and *C*, Error bars refer to SEM (*, $p < 0.05$). *D*, Representative overlay histograms comparing normoxia-cultured macrophages to LPS-treated macrophages (*upper histograms*) or to hypoxia-cultured macrophages (*lower histograms*).

up-regulated during hypoxia, as well as in LPS-treated macrophages (Fig. 6, *C* and *D*). These results indicate that hypoxia promotes increased binding and internalization of particles by up-regulating CR and FcγR expression levels, thus leading to a more efficient phagocytosis. Together with the data above, our results indicate that macrophage functions of inflammatory cytokine production, Ag presentation, and phagocytosis are induced upon low oxygen tensions.

HIF-1α through IFN-γ is responsible for the hypoxic-induced increment in productive IS formation and phagocytic activity

Taken into account that HIF-1α regulates IFN-γ production under hypoxia exposure, we assessed the direct role of either HIF-1α or IFN-γ in the IS response and the phagocytic activity of macrophages. Thus, mouse peritoneal-elicited macrophages were transfected with either HIF-1α or IFN-γ siRNAs, cultured under hypoxia, and their functionality was tested. IFN-γ siRNA notably reduced the transcription of IFN-γ as well as the siRNA to HIF-1α did (85–90% reduction approximately). The effect of HIF-1α interference was also confirmed with an ~60% reduction in the mRNA levels of BNIP-3 (a HIF-1α-dependent gene (48, 49)), compared with macrophages transfected with siSCR in hypoxia ($p < 0.05$; Fig. 7*A*). When Ag-loaded macrophages were conjugated with CD8 T cells, the recruitment of active TCR/CD3ε to the contact site was assessed. The induction levels in the recruitment observed with the siSCR in hypoxia compared with normoxia were almost completely lost with HIF-1α or IFN-γ interference (Fig. 7*B*). HIF-1α or IFN-γ siRNAs also decreased the CR or FcγR phagocytosis hypoxic induction (Fig. 7*C*). These data demonstrate that HIF-1α-mediated induction of IFN-γ in hypoxia is responsible for the increase in macrophage-dependent IS formation and phagocytic activity.

Discussion

In the present work, we have characterized the inflammatory phenotype of macrophages exposed to low oxygen tensions. We have shown that upon hypoxia macrophages increased the production of IFN-γ, which relies on HIF-1α binding to the new, functional HRE site on the IFN-γ promoter. Moreover, hypoxic macrophages were able to form IS and to phagocytose more efficiently than in normoxia and, more importantly, these effects were mediated through HIF-1α and IFN-γ.

Our results indicate that macrophages in hypoxia induced an increment in IFN-γ and IL-12 mRNA and protein secretion levels, while the anti-inflammatory cytokine IL-10 mRNA remained constant, suggesting that proinflammatory cytokines may be involved in the activated phenotype of macrophages. It has long been thought that only T cells or NK cells were responsible for IFN-γ secretion; however, several studies have described a role for macrophages and dendritic cells as IFN-γ-producing cells, in an autocrine or a paracrine manner (13–15, 17–20). These results were also corroborated by the increased IFN-γ mRNA transcription levels in macrophages from mice exposed in vivo to hypoxia. IL-12 and IL-18 induce macrophages to secrete IFN-γ (17), but it may occur that IFN-γ induces macrophages to secrete more IFN-γ as well as IL-12. These cytokines can induce signaling cascades that

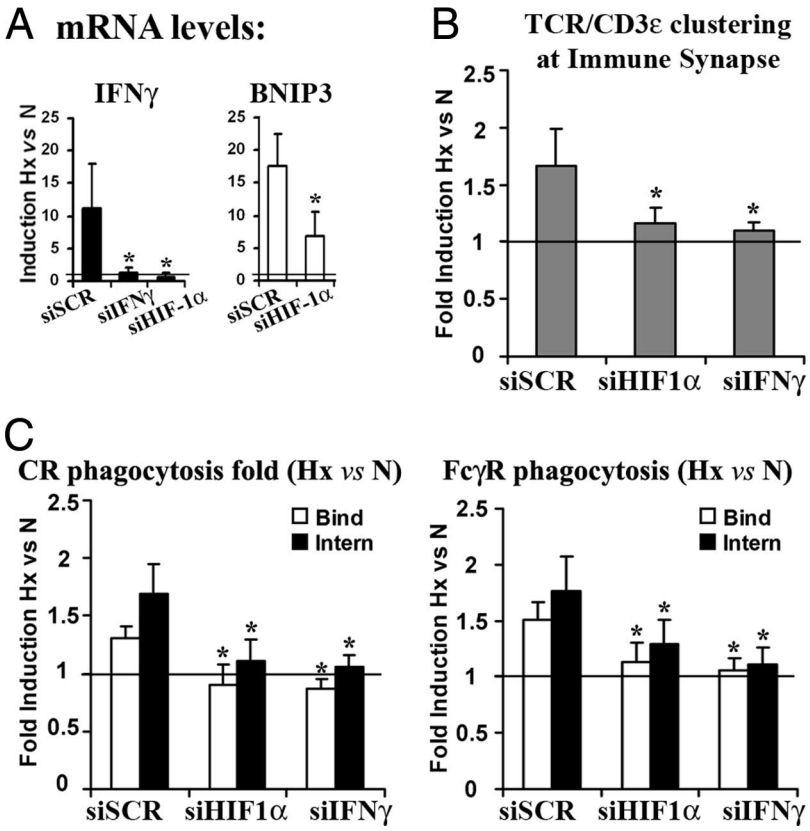

FIGURE 7. RNA interference of IFN-γ or HIF-1α inhibits the hypoxia-increased efficiency of IS and phagocytic activity. *A*, Mouse-elicited peritoneal macrophages were transfected with siRNA control (siSCR), siIFN-γ, or siHIF-1α and incubated in normoxia/hypoxia for 40 h. mRNA levels of IFN-γ and BNIP-3 after interference are shown. *B*, Conjugates were formed during 20 min between the different cultured macrophages (as in Fig. 5), fixed, and stained for active TCR/CD3ε conformation with APA1/1 Ab and for α-tubulin. The number of T cells with active TCR/CD3ε recruited to the contact site was quantified and expressed as the percentage of the conjugates formed. *C*, Phagocytosis assays were performed, and the percentage of binding and percentage of internalization were quantified (*A–C*). Data are represented as the fold induction of hypoxia vs normoxia and are the mean $\pm$ SEM of three experiments ($*$, $p < 0.01$).

increase the bactericidal capacity after phagocytosis, the costimulatory and Ag-presenting molecule expression, as well as the induction of $CD8^+$ T cell differentiation to CTLs (21–23, 51). Moreover, our RNA interference data demonstrate that IFN-γ mediates the hypoxia-induced increment in the formation of productive IS as well as the phagocytic binding and uptake.

The hypoxia-inducible transcription factor HIF-1α plays a direct role in macrophage activation, since RNA interference of HIF-1α correlated with an almost total reduction of the hypoxia-mediated enhancement of IFN-γ transcription, and, in addition, resident macrophages from HIF-1α flox-LysMCre mice were unable to induce IFN-γ levels. We herein describe a novel mechanism for HIF-1α involvement in macrophage IFN-γ production based on several experimental evidences: 1) the existence of a HRE in the IFN-γ promoter conserved among different mammalian species, 2) HIF-1α binds to the IFN-γ promoter in vivo, and 3) this promoter sequence is transcriptionally functional and depends on the HRE site, since when mutated the transcriptional activity is lost. Other cytokines secreted by macrophages have promoters that also contain HRE sites, such as TNF-α, IL-6, or IL-8 (52, 53); however, for TNF-α and IL-6 it is not known whether these sites are functional. Since HIF-1α binds to the IFN-γ promoter at early time points of hypoxia exposure (6 h; Fig. 4*B*), but mRNA induction is not detected until 24 h (Fig. 2*A*), it is conceivable that other hypoxia-dependent coactivators could be required for its transcription. In this regard, AP-1 and STAT-4 have been reported to regulate IFN-γ transcription, to interact with HIF1-α (20, 54, 55), and, in the case of AP-1, to be activated by hypoxia (56, 57). However, it is still unknown whether there is any correlation between STAT-4 activation by hypoxia and IFN-γ transcription. Therefore, hypoxia through HIF-1α may induce the secretion of different cytokines that are responsible for the inflammatory phenotype of macrophages and the up-regulation of Ag-presenting, costimulatory molecules and phagocytic receptors.

Macrophages play a key role in innate immunity since they can recognize, ingest, and destroy pathogens by themselves. Phagocytosis efficiency has been reported to be increased by hypoxia. On one hand, the bactericidal capacity of macrophages in hypoxia is increased (33, 58, 59). On the other hand, hypoxia reoxygenation treatments increased in vivo FcγR-mediated phagocytosis (60). In our model of hypoxic macrophages, we have also found an increased rate of not only FcγR phagocytosis, but also CR phagocytosis. We observed the up-regulation of the phagocytic receptor molecules expression on macrophages, CD11b, CD18, and FcγR, which may account, in part, for the increased particle binding detected in our assays. In contrast, other nonopsonized pathogens are internalized with the same efficiency independently of different oxygen levels, although it is not known whether the expression of the phagocytic receptors involved in this particular uptake could be regulated through hypoxia. Moreover, as stated above, HIF-1α regulation of IFN-γ is a key event in the phagocytic efficiency induced by hypoxia.

Our results show that hypoxia, without any other costimuli, primes macrophages to secrete proinflammatory cytokines and to present Ags efficiently. In this regard, hypoxia-activated macrophages increased the expression of the costimulatory and Ag-presenting molecules CD40, CD86, and MHC-I, which could prepare the macrophage for a prompt and efficient response. Therefore, when T cells contact with hypoxia-activated macrophages, in the presence of a specific Ag, a potent T cell cytokine response is achieved. These efficient cytokine-producing IS correlate with a high induction of the TCR/CD3ε active conformation, as well as the tyrosine phosphorylation of the TCR/CD3ζ chain and of the proximal TCR signaling molecule LAT. The up-regulation of macrophage costimulatory molecules as well as macrophage cytokine production (IFN-γ and IL-12) by hypoxia may explain the enhanced Ag-presenting capacity and efficient IS formation.

Macrophages can be differently activated through a variety of stimuli (61). Hypoxia-stimulated macrophages could mimic M1 classically activated macrophages in a similar manner as LPS-activated macrophages. In fact, the classical activation triggers proinflammatory cytokine secretion, which match our data on the increment of the proinflammatory cytokines IFN-γ and IL-12, together with the increase of IL-6, reactive oxygen species and NO synthesis previously described (53, 59, 62, 63). Therefore, hypoxia could be acting as a priming step preparing the macrophage for an active response. In addition to hypoxia, LPS or other inflammatory signals may act either synergistic or antagonistically inducing further activation or inhibition of the macrophage (18, 62, 64), in particular, in the development of LPS-induced sepsis (53), atheroma plaque formation or tissue remodeling. Further studies on these responses are needed to understand the cross-talk between the different pathways involved in macrophage modulation.

In summary, our data provide several pieces of evidence indicating that oxygen sensing by macrophages regulates their functions: Ag presentation, phagocytosis, and cytokine production. More importantly, a mechanism of activation has been proposed, in which HIF-1α binds to and activates IFN-γ promoter mediating IFN-γ production, which is involved in the acquisition of a macrophage-activated phenotype.

Acknowledgments

We thank Dr. L. del Peso for the use of HRE localization software, suggestions, and advise; A. Lamana for the RT-PCR primers, and J. Lazcano and B. Alarcón for providing us with OT-I mice. We also thank E. Fuertes and A. Vara Vega for technical advice and support.

Disclosures

The authors have no financial conflict of interest.

References

1. Maxwell, P. H., C. W. Pugh, and P. J. Ratcliffe. 2001. The pVHL-hIF-1 system: a key mediator of oxygen homeostasis. *Adv. Exp. Med. Biol.* 502: 365–376.
2. Semenza, G. L. 2001. HIF-1, O_2, and the 3 PHDs: how animal cells signal hypoxia to the nucleus. *Cell* 107: 1–3.
3. Levy, A. P., N. S. Levy, S. Wegner, and M. A. Goldberg. 1995. Transcriptional regulation of the rat vascular endothelial growth factor gene by hypoxia. *J. Biol. Chem.* 270: 13333–13340.
4. Liu, Y., S. R. Cox, T. Morita, and S. Kourembanas. 1995. Hypoxia regulates vascular endothelial growth factor gene expression in endothelial cells: identification of a 5′ enhancer. *Circ. Res.* 77: 638–643.
5. Ebert, B. L., J. D. Firth, and P. J. Ratcliffe. 1995. Hypoxia and mitochondrial inhibitors regulate expression of glucose transporter-1 via distinct *cis*-acting sequences. *J. Biol. Chem.* 270: 29083–29089.
6. Hayashi, M., M. Sakata, T. Takeda, T. Yamamoto, Y. Okamoto, K. Sawada, A. Kimura, R. Minekawa, M. Tahara, K. Tasaka, and Y. Murata. 2004. Induction of glucose transporter 1 expression through hypoxia-inducible factor 1α under hypoxic conditions in trophoblast-derived cells. *J. Endocrinol.* 183: 145–154.
7. del Peso, L., M. C. Castellanos, E. Temes, S. Martin-Puig, Y. Cuevas, G. Olmos, and M. O. Landazuri. 2003. The von Hippel Lindau/hypoxia-inducible factor (HIF) pathway regulates the transcription of the HIF-proline hydroxylase genes in response to low oxygen. *J. Biol. Chem.* 278: 48690–48695.
8. Bruick, R. K., and S. L. McKnight. 2001. A conserved family of prolyl-4-hydroxylases that modify HIF. *Science* 294: 1337–1340.
9. Epstein, A. C., J. M. Gleadle, L. A. McNeill, K. S. Hewitson, J. O'Rourke, D. R. Mole, M. Mukherji, E. Metzen, M. I. Wilson, A. Dhanda, et al. 2001. *C. elegans* EGL-9 and mammalian homologs define a family of dioxygenases that regulate HIF by prolyl hydroxylation. *Cell* 107: 43–54.
10. Maxwell, P. H., M. S. Wiesener, G. W. Chang, S. C. Clifford, E. C. Vaux, M. E. Cockman, C. C. Wykoff, C. W. Pugh, E. R. Maher, and P. J. Ratcliffe. 1999. The tumour suppressor protein VHL targets hypoxia-inducible factors for oxygen-dependent proteolysis. *Nature* 399: 271–275.
11. Bajtay, Z., E. Csomor, N. Sandor, and A. Erdei. 2006. Expression and role of Fc- and complement-receptors on human dendritic cells. *Immunol. Lett.* 104: 46–52.
12. Helmy, K. Y., K. J. Katschke, Jr., N. N. Gorgani, N. M. Kljavin, J. M. Elliott, L. Diehl, S. J. Scales, N. Ghilardi, and M. van Lookeren Campagne. 2006. CRIg: a macrophage complement receptor required for phagocytosis of circulating pathogens. *Cell* 124: 915–927.
13. Di Marzio, P., P. Puddu, L. Conti, F. Belardelli, and S. Gessani. 1994. Interferon γ upregulates its own gene expression in mouse peritoneal macrophages. *J. Exp. Med.* 179: 1731–1736.
14. Frucht, D. M., T. Fukao, C. Bogdan, H. Schindler, J. J. O'Shea, and S. Koyasu. 2001. IFN-γ production by antigen-presenting cells: mechanisms emerge. *Trends Immunol.* 22: 556–560.
15. Fultz, M. J., S. A. Barber, C. W. Dieffenbach, and S. N. Vogel. 1993. Induction of IFN-γ in macrophages by lipopolysaccharide. *Int. Immunol.* 5: 1383–1392.
16. Le Page, C., P. Genin, M. G. Baines, and J. Hiscott. 2000. Interferon activation and innate immunity. *Rev. Immunogenet.* 2: 374–386.
17. Munder, M., M. Mallo, K. Eichmann, and M. Modolell. 1998. Murine macrophages secrete interferon γ upon combined stimulation with interleukin (IL)-12 and IL-18: a novel pathway of autocrine macrophage activation. *J. Exp. Med.* 187: 2103–2108.
18. Murata, Y., T. Ohteki, S. Koyasu, and J. Hamuro. 2002. IFN-γ and pro-inflammatory cytokine production by antigen-presenting cells is dictated by intracellular thiol redox status regulated by oxygen tension. *Eur. J. Immunol.* 32: 2866–2873.
19. Puddu, P., L. Fantuzzi, P. Borghi, B. Varano, G. Rainaldi, E. Guillemard, W. Malorni, P. Nicaise, S. F. Wolf, F. Belardelli, and S. Gessani. 1997. IL-12 induces IFN-γ expression and secretion in mouse peritoneal macrophages. *J. Immunol.* 159: 3490–3497.
20. Schindler, H., M. B. Lutz, M. Rollinghoff, and C. Bogdan. 2001. The production of IFN-γ by IL-12/IL-18-activated macrophages requires STAT4 signaling and is inhibited by IL-4. *J. Immunol.* 166: 3075–3082.
21. Doody, G. M., S. Stephenson, C. McManamy, and R. M. Tooze. 2007. PRDM1/BLIMP-1 modulates IFN-γ-dependent control of the MHC class I antigen-processing and peptide-loading pathway. *J. Immunol.* 179: 7614–7623.
22. Giroux, M., M. Schmidt, and A. Descoteaux. 2003. IFN-γ-induced MHC class II expression: transactivation of class II transactivator promoter IV by IFN regulatory factor-1 is regulated by protein kinase C-α. *J. Immunol.* 171: 4187–4194.
23. Haring, J. S., G. A. Corbin, and J. T. Harty. 2005. Dynamic regulation of IFN-γ signaling in antigen-specific $CD8^+$ T cells responding to infection. *J. Immunol.* 174: 6791–6802.
24. Dustin, M. L., M. W. Olszowy, A. D. Holdorf, J. Li, S. Bromley, N. Desai, P. Widder, F. Rosenberger, P. A. van der Merwe, P. M. Allen, and A. S. Shaw. 1998. A novel adaptor protein orchestrates receptor patterning and cytoskeletal polarity in T-cell contacts. *Cell* 94: 667–677.
25. Monks, C. R., B. A. Freiberg, H. Kupfer, N. Sciaky, and A. Kupfer. 1998. Three-dimensional segregation of supramolecular activation clusters in T cells. *Nature* 395: 82–86.
26. Bunnell, S. C., V. Kapoor, R. P. Trible, W. Zhang, and L. E. Samelson. 2001. Dynamic actin polymerization drives T cell receptor-induced spreading: a role for the signal transduction adaptor LAT. *Immunity* 14: 315–329.
27. Dustin, M. L., and J. A. Cooper. 2000. The immunological synapse and the actin cytoskeleton: molecular hardware for T cell signaling. *Nat. Immunol.* 1: 23–29.
28. Grakoui, A., S. K. Bromley, C. Sumen, M. M. Davis, A. S. Shaw, P. M. Allen, and M. L. Dustin. 1999. The immunological synapse: a molecular machine controlling T cell activation. *Science* 285: 221–227.
29. Lewis, J. S., J. A. Lee, J. C. Underwood, A. L. Harris, and C. E. Lewis. 1999. Macrophage responses to hypoxia: relevance to disease mechanisms. *J. Leukocyte Biol.* 66: 889–900.
30. Murdoch, C., and C. E. Lewis. 2005. Macrophage migration and gene expression in response to tumor hypoxia. *Int. J. Cancer.* 117: 701–708.
31. Burke, B., N. Tang, K. P. Corke, D. Tazzyman, K. Ameri, M. Wells, and C. E. Lewis. 2002. Expression of HIF-1α by human macrophages: implications for the use of macrophages in hypoxia-regulated cancer gene therapy. *J. Pathol.* 196: 204–212.
32. Talks, K. L., H. Turley, K. C. Gatter, P. H. Maxwell, C. W. Pugh, P. J. Ratcliffe, and A. L. Harris. 2000. The expression and distribution of the hypoxia-inducible factors HIF-1α and HIF-2α in normal human tissues, cancers, and tumor-associated macrophages. *Am. J. Pathol.* 157: 411–421.
33. Cramer, T., Y. Yamanishi, B. E. Clausen, I. Forster, R. Pawlinski, N. Mackman, V. H. Haase, R. Jaenisch, M. Corr, V. Nizet, et al 2003. HIF-1α is essential for myeloid cell-mediated inflammation. *Cell* 112: 645–657.
34. Hollander, A. P., K. P. Corke, A. J. Freemont, and C. E. Lewis. 2001. Expression of hypoxia-inducible factor 1α by macrophages in the rheumatoid synovium: implications for targeting of therapeutic genes to the inflamed joint. *Arthritis Rheum.* 44: 1540–1544.
35. Hogquist, K. A., S. C. Jameson, W. R. Heath, J. L. Howard, M. J. Bevan, and F. R. Carbone. 1994. T cell receptor antagonist peptides induce positive selection. *Cell* 76: 17–27.
36. Olazabal, I. M., N. B. Martin-Cofreces, M. Mittelbrunn, G. Martinez Del Hoyo, B. Alarcon, and F. Sanchez-Madrid. 2008. Activation outcomes induced in naive CD8 T cells by macrophages primed via "phagocytic" and non-"phagocytic" pathways. *Mol. Biol. Cell* 19: 701–710.
37. Sahuquillo, A. G., A. Roumier, E. Teixeiro, R. Bragado, and B. Alarcon. 1998. T cell receptor (TCR) engagement in apoptosis-defective, but interleukin 2 (IL-2)-producing, T cells results in impaired ZAP70/CD3-ζ association. *J. Exp. Med.* 187: 1179–1192.
38. Pescador, N., Y. Cuevas, S. Naranjo, M. Alcaide, D. Villar, M. O. Landazuri, and L. Del Peso. 2005. Identification of a functional hypoxia-responsive element that regulates the expression of the egl nine homologue 3 (egln3/phd3) gene. *Biochem. J.* 390: 189–197.
39. Risueno, R. M., D. Gil, E. Fernandez, F. Sanchez-Madrid, and B. Alarcon. 2005. Ligand-induced conformational change in the T-cell receptor associated with productive immune synapses. *Blood* 106: 601–608.
40. Risueno, R. M., H. M. van Santen, and B. Alarcon. 2006. A conformational change senses the strength of T cell receptor-ligand interaction during thymic selection. *Proc. Natl. Acad. Sci. USA* 103: 9625–9630.

41. Casey, K. A., and M. F. Mescher. 2007. IL-21 promotes differentiation of naive CD8 T cells to a unique effector phenotype. *J. Immunol.* 178: 7640–7648.
42. Olazabal, I. M., E. Caron, R. C. May, K. Schilling, D. A. Knecht, and L. M. Machesky. 2002. Rho-kinase and myosin-II control phagocytic cup formation during CR, but not FcγR, phagocytosis. *Curr. Biol.* 12: 1413–1418.
43. Blouin, C. C., E. L. Page, G. M. Soucy, and D. E. Richard. 2004. Hypoxic gene activation by lipopolysaccharide in macrophages: implication of hypoxia-inducible factor 1α. *Blood* 103: 1124–1130.
44. Frede, S., C. Stockmann, P. Freitag, and J. Fandrey. 2006. Bacterial lipopolysaccharide induces HIF-1 activation in human monocytes via p44/42 MAPK and NF-κB. *Biochem. J.* 396: 517–527.
45. Wiesener, M. S., H. Turley, W. Allen, C. Willam, K. U. Eckardt, K. Talks, S. M. Wood, K. C. Gatter, A. L. Harris, C. W. Pugh, et al. 1998. Induction of endothelial PAS domain protein-1 by hypoxia: characterization and comparison with hypoxia-inducible factor-1α. *Blood* 92: 2260–2268.
46. Asikainen, T. M., B. K. Schneider, N. S. Waleh, R. I. Clyman, W. B. Ho, L. A. Flippin, V. Gunzler, and C. W. White. 2005. Activation of hypoxia-inducible factors in hyperoxia through prolyl 4-hydroxylase blockade in cells and explants of primate lung. *Proc. Natl. Acad. Sci. USA.* 102: 10212–10217.
47. Milkiewicz, M., C. W. Pugh, and S. Egginton. 2004. Inhibition of endogenous HIF inactivation induces angiogenesis in ischaemic skeletal muscles of mice. *J. Physiol.* 560: 21–26.
48. Guo, K., G. Searfoss, D. Krolikowski, M. Pagnoni, C. Franks, K. Clark, K. T. Yu, M. Jaye, and Y. Ivashchenko. 2001. Hypoxia induces the expression of the pro-apoptotic gene BNIP3. *Cell Death Differ.* 8: 367–376.
49. Sowter, H. M., P. J. Ratcliffe, P. Watson, A. H. Greenberg, and A. L. Harris. 2001. HIF-1-dependent regulation of hypoxic induction of the cell death factors BNIP3 and NIX in human tumors. *Cancer Res.* 61: 6669–6673.
50. Martin-Cofreces, N. B., J. Robles-Valero, J. R. Cabrero, M. Mittelbrunn, M. Gordon-Alonso, C. H. Sung, B. Alarcon, J. Vazquez, and F. Sanchez-Madrid. 2008. MTOC translocation modulates IS formation and controls sustained T cell signaling. *J. Cell Biol.* 182: 951–962.
51. Nguyen, V. T., and E. N. Benveniste. 2000. Involvement of STAT-1 and ets family members in interferon-γ induction of CD40 transcription in microglia/macrophages. *J. Biol. Chem.* 275: 23674–23684.
52. Kim, K. S., V. Rajagopal, C. Gonsalves, C. Johnson, and V. K. Kalra. 2006. A novel role of hypoxia-inducible factor in cobalt chloride- and hypoxia-mediated expression of IL-8 chemokine in human endothelial cells. *J. Immunol.* 177: 7211–7224.
53. Peyssonnaux, C., P. Cejudo-Martin, A. Doedens, A. S. Zinkernagel, R. S. Johnson, and V. Nizet. 2007. Cutting edge: essential role of hypoxia inducible factor-1α in development of lipopolysaccharide-induced sepsis. *J. Immunol.* 178: 7516–7519.
54. Khomenko, T., X. Deng, Z. Sandor, A. S. Tarnawski, and S. Szabo. 2004. Cysteamine alters redox state, HIF-1α transcriptional interactions and reduces duodenal mucosal oxygenation: novel insight into the mechanisms of duodenal ulceration. *Biochem. Biophys. Res. Commun.* 317: 121–127.
55. Lawless, V. A., S. Zhang, O. N. Ozes, H. A. Bruns, I. Oldham, T. Hoey, M. J. Grusby, and M. H. Kaplan. 2000. Stat4 regulates multiple components of IFN-γ-inducing signaling pathways. *J. Immunol.* 165: 6803–6808.
56. Kunz, M., and S. M. Ibrahim. 2003. Molecular responses to hypoxia in tumor cells. *Mol. Cancer* 2: 23–36.
57. Rupec, R. A., and P. A. Baeuerle. 1995. The genomic response of tumor cells to hypoxia and reoxygenation: differential activation of transcription factors AP-1 and NF-κB. *Eur. J. Biochem.* 234: 632–640.
58. Colhone, M. C., W. W. Arrais-Silva, C. Picoli, and S. Giorgio. 2004. Effect of hypoxia on macrophage infection by *Leishmania amazonensis*. *J. Parasitol.* 90: 510–515.
59. Peyssonnaux, C., V. Datta, T. Cramer, A. Doedens, E. A. Theodorakis, R. L. Gallo, N. Hurtado-Ziola, V. Nizet, and R. S. Johnson. 2005. HIF-1α expression regulates the bactericidal capacity of phagocytes. *J. Clin. Invest.* 115: 1806–1815.
60. Anand, R. J., S. C. Gribar, J. Li, J. W. Kohler, M. C. Branca, T. Dubowski, C. P. Sodhi, and D. J. Hackam. 2007. Hypoxia causes an increase in phagocytosis by macrophages in a HIF-1α-dependent manner. *J. Leukocyte Biol.* 82: 1257–1265.
61. Gordon, S. 2003. Alternative activation of macrophages. *Nat. Rev. Immunol.* 3: 23–35.
62. Nishi, K., T. Oda, S. Takabuchi, S. Oda, K. Fukuda, T. Adachi, G. L. Semenza, K. Shingu, and K. Hirota. 2008. LPS induces hypoxia-inducible factor 1 activation in macrophage-differentiated cells in a reactive oxygen species-dependent manner. *Antioxid. Redox Signal.* 10: 983–995.
63. Yoshida, K., K. Kirito, H. Yongzhen, K. Ozawa, K. Kaushansky, and N. Komatsu. 2008. Thrombopoietin (TPO) regulates HIF-1α levels through generation of mitochondrial reactive oxygen species. *Int. J. Hematol.* 88: 43–51.
64. Mi, Z., A. Rapisarda, L. Taylor, A. Brooks, M. Creighton-Gutteridge, G. Melillo, and L. Varesio. 2008. Synergistic induction of HIF-1α transcriptional activity by hypoxia and lipopolysaccharide in macrophages. *Cell Cycle* 7: 232–241.

Critical Reviews™ in Immunology, 31(1):1–13 (2011)

Myeloid Hypoxia-Inducible Factors in Inflammatory Diseases

Julián Aragonés*, Ainara Elorza, Bárbara Acosta-Iborra, & Manuel O. Landázuri

Servicio de Inmunología, Hospital Universitario de La Princesa, Madrid, Spain

*Address all correspondence to Dr. Julián Aragonés, Servicio de Inmunología, Hospital Universitario de La Princesa, Diego de León 62, 28006 Madrid, Spain; jaragones.hlpr@salud.madrid.org

ABSTRACT: Hypoxia inducible factors (HIF1 and HIF2) have emerged as central regulators of the activity of myeloid cells at inflammatory sites where O_2 is frequently limited. Novel insights in the field have revealed that the expression of HIFs by myeloid cells is not exclusively induced by hypoxia but also in response to central inflammatory mediators independently of O_2 shortage. This has substantially elevated the biological significance of HIFs in the context of inflammatory diseases. As a consequence, the loss of HIF1 or HIF2 in myeloid cells specifically compromises some of the processes driven by myeloid cells, such as bactericidal activity and myeloid invasion, as well as inflammation-associated detrimental consequences.

KEY WORDS: hypoxia-inducible factor (HIF), hypoxia, macrophages, inflammation

ABBREVIATIONS

HIF, hypoxia-inducible factor; **TAMs**, tumor-associated macrophages; **LPS**, lipopolysaccharide; **PHD**, prolyl hydroxylase domain; **FIH**, factor inhibiting HIF; **VHL**, Von Hippel-Lindau; **Glut**, glucose transporter; **PGK**, phosphoglycerate kinase; **GBS**, group B streptococcus; **GAS**, gram-positive pathogen group A Streptococcus; **CRAMP**, cathelicidin-related antimicrobial peptide; **NO**, nitric oxide; **iNOS**, inducible nitric oxide synthase; **MHC**, major histocompatibility complex; **NF-κB**, nuclear factor kB; **VEGF**, vascular endothelial growth factor; **TLR**, toll-like receptor; **ROS**, reactive oxygen species; **TNF**, tumor necrosis factor; **acLDL**, acetyl low density lipoprotein; **SPARC**, secreted protein acidic and rich in cysteine

I. INTRODUCTION

The normal inflammatory/immune response involves the recruitment of circulating monocytes and neutrophils to specific locations, such as bacterial entry sites, intratumoral areas or atherosclerotic plaques. These pathological sites are generally associated with abnormal vascularization, which subsequently compromises the O_2 supply. Therefore, myeloid cells need to be equipped with mechanisms to cope with low O_2 tensions (hypoxia), while efficiently fulfilling their effector functions.

Oxygen sensing pathways mediated by the hypoxia-inducible factors (HIF1 and HIF2) are essential for cellular adaptation to oxygen fluctuations. In this regard, genetic studies have revealed an essential role for the HIF pathway in myeloid cell function.[1] Here, we will discuss recent insights into the molecular mechanisms underlying the role of HIFs in bactericidal activity and sepsis, the role of HIFs in the biology of noninfectious (phlogistic) inflammation and tumor-associated macrophages (TAMs) biology, as well as the ability of inflammatory mediators to regulate the expression of distinct HIF isoforms expression independently of hypoxia.[1-3]

Macrophages recruited to inflammatory sites undergo distinct forms of activation in response to cytokines and microbial signals. For example, lipopolysaccharide (LPS) and Th1 cytokines (eg, IFN-γ) induce classic macrophage polarization (M1) that is characterized by enhanced intracellular bacterial killing, production of NO, tissue destruction and tumor resistance. By contrast, Th2 cytokines as well as other signals induce alternative macrophage polarization (M2) mainly oriented toward immunoregulation, tissue re-

Received: 9/29/2010 Accepted: 9/30/2010

modeling and tumor promotion.[4,5] Here we will also discuss some recent evidence suggesting possible contrasting roles of HIF1 and HIF2 in macrophage M1 and M2 polarization.

II. HYPOXIA-INDUCIBLE FACTORS PATHWAY

Hypoxia-inducible transcription factors (HIF1α, -2α, and -3α), prolyl hydroxylase domain proteins (PHD1, -2 and -3) and the factor inhibiting HIF (FIH) are essential molecular elements in the cellular response to hypoxia.

In normoxia, PHDs and FIH enzymes operate as O_2 sensors, and they use O_2 to hydroxylate prolyl or asparagyl residues in HIFα subunits, respectively.[6-10] When critical prolyl residues of HIFα subunits are hydroxylated by PHDs, these HIFα subunits are recognized by von Hippel-Lindau (VHL), a protein in the multiprotein E3 ubiquitin ligase complex, which marks them for subsequent degradation by the proteasome machinery.[11,12] FIH hydroxylates a C-terminal asparaginyl residue in HIF1α that impairs its interaction with the p300, a coactivator of HIF1α transcriptional activity.[13,14]

In conditions of hypoxia, when O_2 supply is limited, PHDs and FIH do not have enough O_2 to hydroxylate the prolyl and asparaginyl residues in HIFα, resulting in the stabilization of the HIFα subunit and its binding to the p300 coactivator. Subsequently, the HIFα isoforms travel to the nucleus and associate with the HIFß subunit to form heterodimers, enabling them to enhance the transcription of many genes, some of which have critical functions in macrophage biology (see below). Importantly, PHDs and FIH have a lower affinity for O_2 than other O_2-dependent enzymes and, therefore, the PHD/FIH/HIF system is extremely sensitive to physiological fluctuations in O_2.[8-10,15,16]

III. HYPOXIA-INDUCIBLE FACTORS IN MYELOID CELL BIOENERGETICS

As mentioned above, myeloid cells are recruited to inflammatory sites where hypoxia occurs. Upon O_2 deprivation, HIF1α stimulates glycolytic flux by upregulating the expression of glucose transporters 1 and 3 (Glut1 and Glut3) and glycolytic enzymes, to ensure intracellular ATP is available when O_2 is limited.[17] Indeed, when compared with WT myeloid cells, HIF1α-deficient macrophages and neutrophils express lowers levels of the glucose transporter 1 (Glut1) and phosphoglycerate kinase (PGK), release less lactate and suffer a dramatic drop in the intracellular ATP pool.[18] These metabolic changes are not observed in HIF2α -deficient macrophages,[19] consistent with the central role of HIF1 in the transcriptional control of glycolytic genes.[20] The drop in ATP observed in HIF1-deficient myeloid cells has an enormous impact on energy-requiring myeloid activities such as cell aggregation, invasion and motility.[18] Moreover, the capacity to kill intracellular pathogens is critically dependent on energy intensive processes that require ATP (eg, peroxide generation). In this regard, a first study of Cramer et al. showed that ATP-independent bacterial engulfment occurs normally in HIF1α -deficient macrophages exposed to Group B *Streptococcus* (GBS), whereas their intracellular killing capacity is severely impaired (see below). Recent studies have also shown that the intracellular ATP pool driven by HIF1-induced glycolysis is also used to maintain the mitochondrial membrane potential and to prevent apoptotic cell death.[21,22] However, it is important to consider that the role of HIF1 in myeloid cell function is not entirely dependent on its metabolic functions, and other essential macrophages responses are also directly controlled by HIF1 (see below, Fig. 1).

IV. THE ROLE OF HYPOXIA-INDUCIBLE FACTOR-1 IN PROTECTING AGAINST BACTERIAL INFECTIONS

A. HIF1 Induces Bactericidal Activity in Macrophages

As mentioned above, bacterial entry sites are associated with low O_2 supply. Indeed, as a surrogate marker of hypoxia, pimonidazole staining reveals insufficient O_2 supply in lesions generated after gram-positive pathogen group A *Streptococcus* (GAS) infection.[3] Importantly, intracellular killing of the gram-negative bacterium *P. aeruginosa* and the gram-positive group A *Streptococcus* pathogen

(GAS) is compromised in HIF1-deficient macrophages.[3] By sharp contrast, VHL deficient macrophages, which have constitutively upregulated HIF levels, exhibit a heightened capacity for intracellular killing.[3] The cell autonomous incapacity of HIF1α -deficient myeloid cells to combat intracellular pathogens results in larger necrotic skin lesions, as well as greater weight loss when myeloid-specific HIF1α -deficient mice are subcutaneously inoculated with GAS. Moreover, these mice experience widespread local dissemination of bacteria in skin ulcers, as well as in the blood and spleen. Therefore, tight control of bacterial dissemination requires adequate HIF1 activity in the myeloid cells recruited to bacterial entry sites. The role of HIF2 in these experimental models has not been evaluated and future experiments in myeloid HIF2 deficient mice will be required to examine its relative contribution to bactericide activity.

B. Molecular Mechanisms Downstream of HIF1 Involved in HIF1-Induced Bactericide Activity

Molecular studies exploring the mechanisms underlying bactericide activity have revealed that HIF1 does not regulate the oxidative burst,[3] although other essential bactericide properties are altered in HIF1 deficient macrophages (Fig. 1). Granule proteases, such as neutrophil elastase and cathepsin G, are essential phagolysosome serine proteases whose role in innate immunity is evident in the phenotype of elastase gene KO mice in which host defense against gram-negative bacterial sepsis is impaired and resistance to endotoxin is enhanced.[23] Moreover, a recurrent bacterial infection is associated with Chediak-Higashi syndrome (CHS).[24] CHS is the consequence of homozygous mutations in the CHS1 gene, which encodes a protein involved in the formation of azurophilic granules that are rich in elastase.[25] The activity of neutrophil elastase and cathepsine G is dramatically reduced in HIF1 deficient neutrophils, and it is significantly elevated in VHL-deficient neutrophils. Moreover, HIF1 also controls the expression of cathelicidin-related antimicrobial peptide (CRAMP), which is constitutively induced in VHL deficient neutrophils and remarkably elevated by hypoxia in a HIF1-dependent manner.[3] It is still unknown whether the elastase, cathepsine or cathelicidine genes contain hypoxia-response elements within their respective promoters or whether they are indirectly regulated by HIF1.

Furthermore, HIF1 affects the production of nitric oxide (NO), which has antimicrobial effects against a variety of bacterial species and is a marker of classic macrophage M1 polarization[3] (see introduction for M1 polarization definition). In this regard, nitrite production as well as inducible nitric oxide synthase (iNOS) gene expression, in which a hypoxia-response element has been identified in its promoter,[26] are dependent on HIF1 in the myeloid lineage in response to GAS. By contrast, HIF2-deficient macrophages do not exhibit altered iNOS expression in response to LPS/IFN-γ,[19] suggesting that this aspect of intracellular killing is mainly controlled by HIF1. Furthermore, a recent study showed that the HIF2 isoform controls in thioglycollate-elicited peritoneal macrophages the expression of arginase 1, which reduces the intracellular L-arginine pool required to produce NO.[27] In fact, arginase, which is highly expressed in M2 polarized macrophages,[28] shuts down the capacity for intracellular killing, in part by reducing NO production.[29] This could suggest opposite roles of HIF1 and HIF2 in NO generation and potentially in M1/M2 polarization. However, some controversy exists about the relative contribution of HIF2 in the regulation of arginase 1, since a recent study has found that arginase 1 remains unaltered in HIF2-deficient bone marrow-derived macrophages in response to hypoxia or IL-4.[19] This controversy might be explained by the distinct source of primary macrophages used in each study, since the study of Takeda et al. shows that thioglycollate-elicited peritoneal macrophages exhibit higher expression of arginase 1 than bone marrow-derived macrophages.[27] Furthermore, another essential function of macrophages in fighting external pathogens lies in the appropriate antigen presentation and T cell recognition. This process is also enhanced, at least to some extent, through HIF1. Indeed, HIF1 upregulates the expression of co-stimulatory and antigen-presenting receptors, such as major histocompatibility complex I (MHCI), CD40 and CD86, via IFN-γ upregulation (see cy-

tokines & HIF section below).[30] Furthermore, HIF1 augments the expression of the gene coding for the phagocytic solute carrier Slc11a1, which confers resistance by inducing the expression of MHCII molecules, cytokines and chemokines.[31,32] Interestingly, the strength of this effect is more pronounced in some particular allelic variations of the highly polymorphic Z-DNA-forming microsatellite within its proximal promoter.[31,32] HIF2 does not contribute to MHC-II and CD86 upregulation, which suggests that enhanced antigen presentation in response to hypoxia is mainly dependent on HIF1.[19]

The fundamental role of the PHD/HIF system in fighting exogenous pathogens generates new opportunities for pharmacological interventions to combat pathogen infection. Indeed, pharmacological inhibition of PHDs and subsequent HIF activation boosts the bactericide capacity of phagocytes.[33,34] In mice treated with L-mimosine, a PHD inhibitor with no recognized antibiotic properties, bacterial progression is attenuated in an *S. aureus* skin infection model. In this study, this improvement is not related to an increase of neutrophil infiltration or the potency of their respiratory burst but, rather, it seems

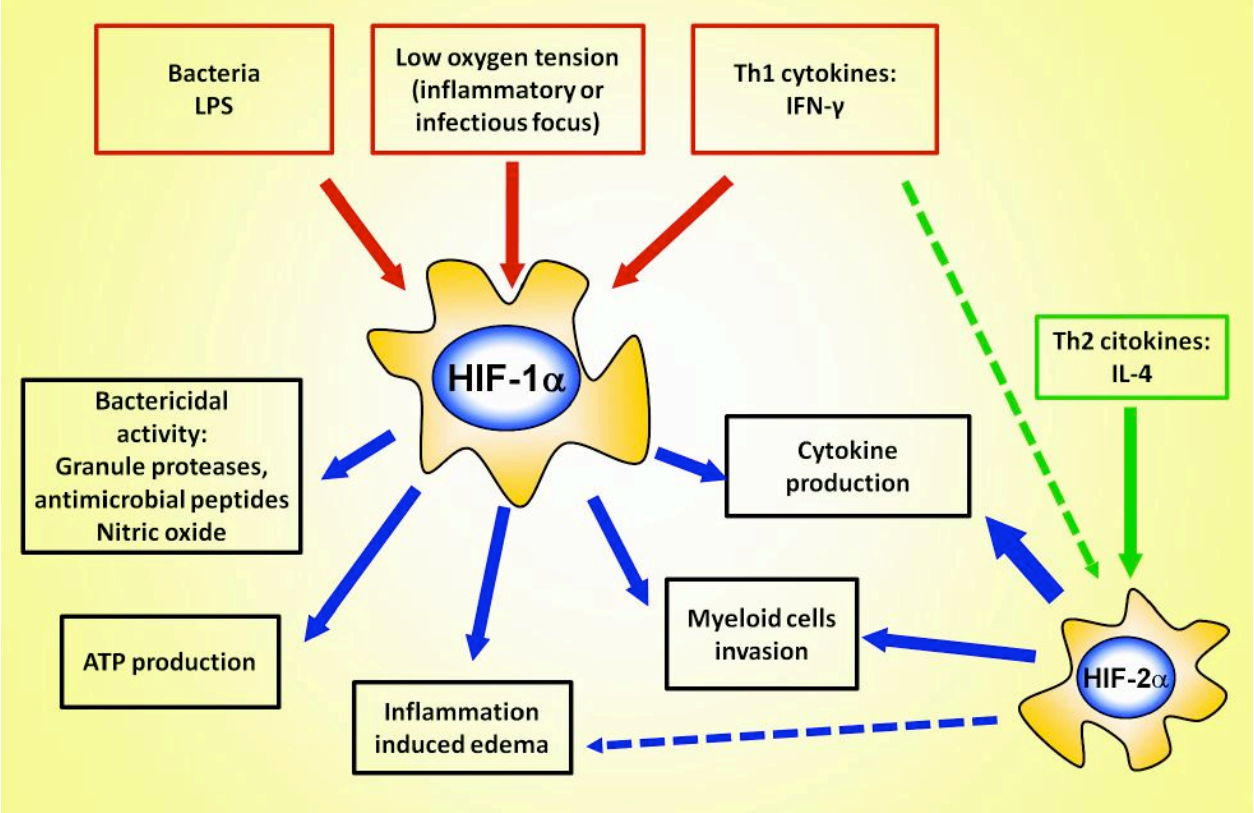

FIGURE 1. Regulators of HIF isoforms expression in myeloid cells and biological functions controlled by HIFs in inflammation.

Besides oxygen deprivation that takes place in inflammatory and infectious sites, other non-hypoxic stimuli (such as bacteria components as LPS) and some proinflammatory Th1 cytokines, such as IFN-γ can induce HIF1 expression in macrophages (red arrows). On the contrary, the Th2 cytokine IL-4 has been shown to induce HIF2 (green arrow). The role of Th1 cytokines such as IFN-γ and LPS on HIF2 regulation is still controversial (green dashed line). On the other hand, HIF1 increases macrophage microbicidal activity through the control of the expression of granule proteases, CRAMP and nitric oxide (NO). Furthermore, HIF1 controls intracellular ATP pool and inflammation associated edema (blue arrows). Other essential functions such as cytokine production and invasion capacity are regulated by both HIF isoforms. The role of myeloid HIF2 expression in vascular alteration at inflammatory sites (eg, edema) has not been explored (blue dashed line).

to be associated to an extracellular antimicrobial activity driven by HIF1.

C. HIF1 Induces Neutrophil Survival

In addition to its bactericide properties, the PHD/HIF system is critical for neutrophil survival. Indeed, hypoxia impairs naturally occurring neutrophil apoptosis through mechanisms independent of PI3K but involving HIF1α-induced nuclear factor -kappaB (NF-κB) activity.[35] Moreover, neutrophils from heterozygous VHL patients have moderate constitutive HIF1α activation, and they are more resistant to apoptosis.[36] In addition, L-gulono-γ-lactone oxidase $(Gulo)^{-/-}$ neutrophils, which cannot synthesize ascorbate (an essential metabolite to sustain PHD activity), show an impaired neutrophil apoptosis associated to HIF1 activation.[37] Concerning the role of HIF2 in this process, a recent study has shown that HIF2 is not detected in neutrophils, suggesting that HIF2 does not contribute to neutrophil survival.[19]

V. EXOGENOUS PATHOGENS INDUCE HIFS IN NORMOXIA

A. Bacterial Infection Induces HIF1 Under Normal Oxygen Conditions

HIF1 might be expected to regulate myeloid cell metabolism and bactericide activity exclusively and only in the hypoxic areas associated to bacterial entry sites and, therefore, would not operate in the well oxygenated areas surrounding these infection sites. However, several *in vitro* studies found that bacteria induce, to the same extent as hypoxia, the expression of HIF1 and its downstream genes in normoxia (see below). This clearly gives more protagonism to HIF1 as a principal component in the innate immune response, not restricting myeloid HIF activity to hypoxic areas. In this regard, two studies of Peyssonaux et al. found that GAS induces HIF1α expression to an even greater extent level than hypoxia in itself.[2,3] This was also observed with other gram-positive (*Staphylococcus aureus*) and gram-negative (*Pseudomonas aeruginosa and Salmonella typhimurium*) bacteria. Moreover, bacillary angiomatosis, characterized by lobulated proliferation of mainly capillary-sized vessels after *Bartonella henselae* infection, has been associated to HIF1 activation and the subsequent upregulation of HIF1-dependent angiogenic genes, such as VEGF-A.[38] Moreover, this HIF1α activation seems not to be restricted to the presence of bacteria since infection of cells by the obligate intracellular protozoan pathogen *Toxoplasma gondii* also induces HIF1α, which is essential for cell division of this parasite.[39] In addition, the Epstein-Barr virus latent membrane protein induces HIF1 synthesis.[40] HIF1α activation has also been found in macrophages and dendritic cells, as well as in skin lesions of mice infected with *Leishmania amazonensis*.[41,42]

Therefore, HIF1 activation does not seem to be exclusively restricted to hypoxic areas associated with inflammation, but it is also associated with the presence of infectious pathogens in themselves, irrespective of the O_2 supply (Fig. 1).

B. Molecular Mechanisms Involved in Bacteria-Induced HIF1 Activation

Importantly, gram-negative bacteria-induced HIF1 activation can be mimicked when macrophages are incubated with the lipopolysaccharide (LPS) found in the outer membrane of gram-negative bacteria.[2] Indeed, LPS potently induces, via its receptor TLR4, the expression of HIF1α in WT macrophages, yet only minimally in Toll-receptor-4 (TLR4) deficient macrophages.[3,43,44] Similarly, TLR4-deficient macrophages do not exhibit HIF1 activation in response to gram-negative *S. typhimurium* or *P. aeruginosa*. Moreover, it is notable that HIF1 also increases TLR4 expression reflecting the positive feedback loop that potentiates the close link between innate immunity and HIF1 expression.[45] Furthermore, the myeloid HIF1α-deficient mice display remarkable protection from the symptoms and lethality associated with LPS-induced sepsis.[2]

How can LPS induce HIF1α when oxygen is still present? LPS is a well recognized activator of the nuclear factor-kappaB (NF-κB) transcription factor[46] and indeed, LPS induces HIF1α gene expression in WT macrophages through a functional NF-κB DNA binding site in the HIF1α proximal promoter.[2,46,47] Ultimately, cytokine genes, iNOS as well as matrix metalloproteases (MMPs),[20] controlled by NF-κB or HIFs, are some lethal media-

tors in septic shock. The role of NF-κB subunits in LPS-induced HIF1 activation is also evident in LPS tolerant macrophages that only weakly induce HIF1 and show increased expression of p52, a NF-κB subunit that counteracts p65/p50 NF-κB activation of the HIF1α promoter.[2,46,47] However, other studies have shown that HIF1α upregulation in response to LPS may also be independent of NF-κB when mediated by reactive oxygen species (ROS).[48,49] Moreover, TLR4 signaling also represses the expression of PHD2 and PHD3 oxygen sensors, suggesting an effect of LPS on HIF1α stability.[2] However, this was not evident in a recent study that directly assessed HIF1α half-life in response to LPS.[27] Bacterial-induced HIF1α activation has also been linked to the inhibition of PHDs/FIH, as invading bacteria sequester iron, which is an essential cofactor of these enzymes. This mechanism could be especially relevant in M1 polarized macrophages that reprogram iron metabolism to favor iron sequestering by the reticuloendothelial system.[50] Indeed, the application of purified siderophores (iron-binding proteins of bacterial origin) activates HIF1α.[51] In summary, bacterial infection induces HIF1-gene expression through different strategies in normoxic conditions, subsequently inducing a HIF1-dependent bactericide activity.

VI. THE INTERPLAY BETWEEN CYTOKINES AND HIFS AND ITS POSSIBLE ROLE IN MACROPHAGE POLARIZATION

A. Cytokine-Regulated Expression of HIF Isoforms

As mentioned above, macrophages recruited to inflammatory sites are instructed by cytokines and microbial signals to undergo classic macrophage polarization (M1) or alternative macrophage polarization (M2) (see above).[4,5,52] M1 polarization is characterized by enhanced intracellular bacterial killing and tumor resistance, whereas alternative macrophage polarization (M2) is characterized by an immunoregulatory phenotype and tumor promotion. Studies on thioglycollate-elicited peritoneal macrophages have shown that HIF1 is induced when macrophages undergo M1 polarization in response to IFN-γ, whereas it is not altered when macrophages undergo M2 polarization in response to IL-4.[27,53] IFN-γ does not increase the stability of HIF1α, but rather, it produces an increase in HIF1 α mRNA levels that may involve NF-κB as it has been shown for LPS. The fact that NF-κB activation has been associated to M1 macrophage polarization in some contexts,[54] as well as the role of HIF1 in intracellular killing (see above), could further suggest a role of HIF1 in M1 macrophage polarization.

By contrast to HIF1α, HIF2 is induced when macrophages undergo M2 polarization in response to IL-4, whereas HIF2 is drastically repressed when macrophages undergo M1 polarization in response to LPS/IFN-γ. This shift would suggest that HIF1 and HIF2 fulfill opposite roles in macrophage polarization. However, certain controversy exists regarding this issue, since it was recently shown that LPS/IFN-γ also increases HIF2 expression in TPA-differentiated U-937 monocyte cell line.[19] Probably, this observation might simply reflect the distinct conditions of the *in vitro* models employed, and thus, future studies should explore the specific conditions leading to HIF2 repression or activation in response to M1 and M2 polarization (see additional discussion below).

B. Regulation of Cytokine Production Mediated by HIF Isoforms

There is evidence that HIF1-driven NO production controls TNF-α gene expression,[3] and hence, the ability of TNF-α to increase macrophage microbicidal activity. Thus, HIF1 could help combat pathogen infection through hypoxia-induced TNF-α expression. In addition to the indirect effects of NO on cytokine production, murine peritoneal elicited macrophages produce more IFN-γ in response to hypoxia, which is mediated by an HRE in the IFN-γ proximal promoter.[30] The HIF1/IFN-γ axis upregulates the expression of phagocyte receptors that mediate opsonized particle binding and phagocytic uptake. Moreover, IL-1 α as well as IL-1β expression is partially dependent on HIF1 activity.[2]

However, a recent study on HIF2-deficient myeloid cells has revealed that HIF2 is more relevant than HIF1 in regulating the expression of some proin-

flammatory Th1 cytokines (Fig. 1). Myeloid HIF2 deficient mice exhibit markedly reduced systemic serum elevation of IL-1β, IL-12 and TNF-α, and they survive longer than WT mice when challenged with LPS.[19] Furthermore, hypoxia exacerbates LPS/IFN-γ-induced IL1-β, IL-12 and IL-6 expression via HIF2, and indeed, HIF2 can bind directly to the IL-6 promoter.[19] In addition to the role of NF-κB on the HIF1 α promoter, HIF isoforms can also control NF-κB activity under some conditions.[48] However, the relative contribution of the HIF1-NF-κB pathway in the hypoxic induction of some NF-κB-dependent genes is not completely understood.

As mentioned above, HIF1 activity in myeloid lineage seems to facilitate M1 polarization markers (see above), whereas HIF2 could not contribute to this polarization fate. Moreover, the ability of Th2 cytokines to induce specifically HIF2 expression could suggest a possible role in M2 polarization. However, the recognized role of the Th1 cytokines IFN-γ, TNF-α, IL-12 and IL-1 in upregulating macrophage microbicide activity, as well as the ability of both HIF isoforms to regulate the expression of Th1 cytokines, suggest that both HIF1 and HIF2 facilitate classical macrophage activation (M1) to combat outside infectious pathogens (see above). This contrasts with the proposal that HIF2 could exclusively regulate events associated with M2, but not M1, polarization (see above). This novel information further emphasizes the need for future studies to explore to which extent HIF1 and HIF2 modify the balance between M1 and M2 polarization.

VII. HYPOXIA-INDUCIBLE FACTORS IN NON-INFECTIOUS INFLAMMATION

A. Myeloid HIF in Cutaneous and Joint Inflammation Models

In the previous sections we have considered the role of myeloid HIF isoforms in combating infectious pathogens. However, myeloid cells are frequently recruited to other locations where inflammation occurs, albeit in the absence of an overt infection. An initial study of Cramer et al. evaluated the role of myeloid HIF1 in mouse models of skin inflammation characterized by edema and massive leukocyte infiltration.[18] Indeed, an ear inflammation model in wild type mice induces skin inflammation and overt edema, as well as an increase of ear weight, skin CD45 staining and myeloperoxidase activity. All these inflammation markers are attenuated in myeloid HIF1-deficient mice.[18] In accordance with the central role of HIFs in this phenotype, these signs of inflammation and edema are more aggressive in myeloid VHL-deficient mice. Similar data were obtained in a second macrophage-driven model of skin inflammation, a skin irritation mouse model associated with extensive histological signs of edema, infiltration and epidermal hyperproliferation in wild-type mice that is absent in myeloid HIF1-deficient mice.[18] This anti-inflammatory scenario has also been found in a more specific and non-cutaneous model of joint inflammation in which the loss of myeloid HIF1α expression reduces the gross manifestations of ankle swelling and edema, as well as the histological signs of cartilage destruction.[18] The clinical value of these studies is supported by the fact that HIF1 is expressed by macrophages in the rheumatoid synovium of human patients.[55] Overall, myeloid HIF1 expression is essential for the inflammatory features associated with these non-infection inflammation models (Fig. 1).

Impaired leukocyte invasion in these models of inflammation can be explained by the central role of HIF1 in myeloid cell bioenergetics and the dramatic drop of intracellular ATP that compromises the aggregation, invasion and motility of HIF1-deficient myeloid cells (see above).[18] Moreover, NO causes macrophage migration through HIF1α-dependent GTPases, Cdc42 and Rac1 stimulation, which could to some extent explain the defects in cell motility of HIF1α-deficient macrophages (see above).[56] Furthermore, hypoxia also controls macrophage adhesion by inducing the expression of β2 integrins through HIF1.[30,57] In terms of the role of HIF1 in joint inflammation, the TNF-α converting enzyme (TACE) or ADAM17 (that is involved in the release of soluble form of TNF-α) is regulated through direct binding of HIF1 to its 5′ promoter region.[58] In addition, HIFs induce the expression of the proangiogenic factor VEGFA that is involved in the formation of edema associated to inflammation. Indeed,

myeloid VEGF̃A-deficient mice do not compromise leukocyte infiltration but they have severely reduced histological signs of edema,[18] indicating that myeloid cell-derived VEGF̃A is essential for vascular alterations at inflammatory sites.[18] Overall, myeloid HIF1 activity plays a substantial role in the tissue alterations associated to local phlogistic inflammation, and future studies will be required to assess the role of myeloid HIF2 in these models of inflammation (Fig. 1).

B. Myeloid HIF in Ischemic Diseases

Myeloid cells are recruited on a large scale to ischemic areas where tissue perfusion is compromised and therefore hypoxia develops. Several studies have shown that myeloid HIF expression participates in the acute tissue response to ischemia as well as in postischemic tissue recovery. Indeed, silencing of HIF1α gene expression in hematopoietic stem cells impairs neutrophil infiltration into the myocardial infarct zone, which can be at least explained by a decrease in CCR1, CCR2 and CCR4 gene expression.[59] Moreover, while infarct size is not altered, left ventricle remodeling and cardiac function is improved suggesting that HIF1 expressing infiltrating cells have detrimental consequences after acute cardiac ischemia.[59] In sharp contrast, myeloid HIF1 expression also appears to have beneficial effects on postischemic tissue remodeling. Indeed, the link between HIFs and cell adhesion through regulation of β2 integrin expression previously discussed above is thought to be involved in bone marrow-derived angiogenic cells (BMDACs) recruitment to ischemic/hypoxic areas.[60] The surface receptors of BMDACs suggest that they are similar to bone marrow myeloid cells although they express higher levels of VEGFR1 and VEGFR2. The HIF-dependent increase in cell surface expression of β2 integrins on BMDACs has been exploited therapeutically in mouse limb ischemia models to facilitate BMDACs homing to ischemic areas and facilitate perfusion, motor function and limb salvage.[60] Furthermore, oxygen-induced retinopathy leads to vascular obliteration and subsequent abnormal vessel growth. Myeloid progenitors differentiate into microglia and promote vascular repair in this model of ischemic retinopathy.[61] Importantly, myeloid progenitors lacking HIF1 expression do not repair these vascular alterations implicating myeloid HIF expression in the vascular remodeling of post-ischemic tissues. Therefore, future studies will be necessary to further explore the role of myeloid HIF1 in ischemic models and particularly its relative contribution to acute ischemia and postischemia tissue remodeling.

C. Myeloid HIF in Tumor Progression

Immune cells are highly represented in intratumoral environments and macrophages are frequently the most abundant of these cells. Tumor-associated macrophages (TAMs) normally contribute to tumor progression and malignancy.[62] Indeed, while the cytotoxicity of macrophages in the early immune response contributes to the death of tumor cells, the presence of macrophages has been also correlated with a poor prognosis for patients. In this regard, TAMs can express markers of M2 polarization, such as enhanced expression of anti-inflammatory mediators, matrix remodeling proteins, growth factors, and CD206 and stabilin-1 scavenger receptors (see below). In contrast to proinflammatory M1 macrophages, M2 macrophages reduce the expression of cytotoxic mediators and enhance tumor progression. Indeed, re-programming TAMs toward M1 polarization restores their capacity to kill tumor cells.[63] Moreover, HIF1$\alpha^{-/-}$ macrophages were recently shown to be unable to induce apoptosis and cytotoxicity of tumor-spheroid cells, in association with reduced iNOS, TNF-α and IL-6 expression. In addition, HIF1α represses some M2 polarization markers such as the mannose receptor (CD206), the multifunctional scavenger/sorting receptor stabilin-1, which mediates the clearance of acLDL and SPARC, and the macrophage-scavenger receptor-1.[64,65] Therefore, HIF1 could be responsible for driving TAMs toward a cytotoxic M1 polarization fate and impairing M2 macrophage polarization. However, the possible redirection toward M1 polarization by HIF1 seems to be inefficient given that the subset of TAMs located in perinecrotic and hypoxic tumor areas usually expresses M2 polarization markers.[66,67] Indeed, a recent study in an adenocarcinoma model showed that hypoxic TAMs are CD11b^{+} butwith low

expression of MHCII indicative of M2 polarization, whereas the majority of CD11b^{+} MHC-II^{high} TAMs, resembling a M1 phenotype, are in normoxic areas suggesting that hypoxia could be an environmental stimulus that would explain the intratumoral heterogeneity of TAMs.[66,68] The same study revealed that these CD11b^{+} MHC-II^{low} hypoxic TAMs have a superior proangiogenic activity.[66] Immunohistological studies have found a strong HIF2α expression in TAMs,[69] suggesting that HIF2 could drive M2 polarization of hypoxic TAMs and therefore contribute to the distinct subsets of TAMs associated to tumor microenvironment. Studies in myeloid HIF2-deficient mice show altered migratory properties of HIF2-deficient macrophages that were associated with reduced tumor progression in these mice.[19] Future studies in myeloid HIF1-deficient mice will be necessary to assess the relative contribution of both HIF isoforms to tumor progression and in particular to the generation of different subsets of TAMs.

Hypoxic areas can normally be encountered at the inner core of solid tumors when tumor growth is not accompanied by an efficient angiogenesis.[70] However, in this hypoxic tumor area angiogenic factors are produced (eg, VEGF̃A) via HIF transcription factors in an attempt to induce vessel formation and to restore the O_2 supply to the hypoxic tumor area. As mentioned above, TAMs are located in intratumoral hypoxic regions,[67] and they seem to at least partially contribute to VEGF̃A production by the tumor.[71] This intratumoral VEGF̃A production is supraphysiological and it over-activates endothelial cells, leading to vessel tortuosity and vascular leakage, which makes this angiogenic response partially effective in counteracting tumor hypoxia. Indeed, a recent study showed that VEGF̃A produced by TAMs contributes to vascular dysfunction of the tumor. Tumor growth in myeloid VEGF̃A-deficient mice is associated with tumor vessels that are less tortuous, with increased pericyte coverage and decreased vessel length, indicative of vascular normalization.[71] Furthermore, several recent studies have shown that attenuation but not complete abrogation of VEGF̃A signaling reduces vessel tortuosity and vascular alterations, leading to vascular normalization and the alleviation of intratumoral hypoxia.[72,73] Overall, myeloid derived VEGF̃A is critical for vascular dysfunction at these intratumoral sites to which myeloid cells are recruited. The strong HIF2 expression detected in TAMs, as mentioned above, suggests that a TAMs derived VEGF̃A expression might be mainly controlled by HIF2.

D. Other Inflammatory Scenarios

The role of myeloid HIF1 expression in wound healing was recently evaluated in myeloid HIF1- deficient mice. The absence of HIF1α in myeloid cells accelerates the early phase of secondary intention wound healing *in vivo*, which has been associated with reduced NO production, although the precise molecular mechanisms remain unknown.[74] In addition, human atherosclerotic plaques represent another inflammatory scenario in which hypoxia develops and is accompanied by the massive recruitment of inflammatory cells.[75] Immunohistological analysis detected intense HIF1 and HIF2 accumulation at sites of macrophage invasion. Furthermore, the hypoxia-inducible transcription factor pathway has been associated with progression from early to advanced atherosclerosis, which also correlates with intraplaque angiogenesis.[75] In this context, a study of carotid plaques in different patients showed that 15-lipooxygenase-2 (a critical inflammatory element) is regulated by HIF1 and strongly expressed in intraplaque macrophage plaques.[76] There are still no genetic studies in mice to explore the relative contribution of myeloid HIF1 and HIF2 to atherosclerosis, but it seems to be an attractive area of study based on the immunohistological information currently available.

VIII. CONCLUSIONS

The biology of HIF has been closely linked to oxygen sensing pathways restricted to hypoxic anatomical locations in health and disease. However, molecular studies of inflammation have extended the importance of HIF biology since these proteins are not only regulated by O_2 supply, but also by central inflammatory mediators irrespective of the O_2 tension. These studies have clearly elevated the biological significance of HIF in inflammation and inform us about biological strategies to upregulate

HIF1 expression when oxygen is still present. Genetic studies with myeloid HIF1-deficient mice have provided substantial insight into the specific functions of HIF in combating pathogens, as well as in inflammation (phlogistic) models. The relative contribution of HIF1 and HIF2 in myeloid cell biology has begun to be elucidated, although the specific contribution of HIF2 in some inflammation models, such as bactericide activity, remains unexplored and will require further studies. Moreover, the contrasting roles of HIF1 and HIF2 in the regulation of M1 and M2 macrophage polarization markers highlight the distinct biological functions of both isoforms in macrophage biology, but their relative contribution to macrophage polarization fates needs to be investigated in more detail. Overall, the role of HIFs in inflammation has a significant clinical value for pharmacological interventions to counteract the detrimental aspects of inflammation associated to HIF activation.

ACKNOWLEDGEMENTS

The authors thank Dr. Angel Corbí, Dr. Ignacio Melero and Dr. María Escribese for their critical reading of the manuscript. This work has been supported by grants from Ministerio de Educación y Ciencia (BFU2008-03407/BMC) and RECAVA.

REFERENCES

1. Cramer T, Johnson RS. A novel role for the hypoxia inducible transcription factor HIF-1alpha: critical regulation of inflammatory cell function. Cell Cycle. 2003;2:192-193.
2. Peyssonnaux C, Cejudo-Martin P, Doedens A, Zinkernagel AS, Johnson RS, Nizet V. Cutting edge: Essential role of hypoxia inducible factor-1alpha in development of lipopolysaccharide-induced sepsis. J Immunol. 2007;178:7516-7519.
3. Peyssonnaux C, Datta V, Cramer T, Doedens A, Theodorakis EA, Gallo RL, Hurtado-Ziola N, Nizet V, Johnson RS. HIF-1alpha expression regulates the bactericidal capacity of phagocytes. J Clin Invest. 2005;115:1806-1815.
4. Martinez FO, Sica A, Mantovani A, Locati M. Macrophage activation and polarization. Front Biosci. 2008;13:453-461.
5. Sica A, Larghi P, Mancino A, Rubino L, Porta C, Totaro MG, Rimoldi M, Biswas SK, Allavena P, Mantovani A. Macrophage polarization in tumour progression. Semin Cancer Biol. 2008;18:349-355.
6. Bruick RK, McKnight SL. A conserved family of prolyl-4-hydroxylases that modify HIF. Science. 2001;294:1337-1340.
7. Epstein AC, Gleadle JM, McNeill LA, Hewitson KS, O'Rourke J, Mole DR, Mukherji M, Metzen E, Wilson MI, Dhanda A, Tian YM, Masson N, Hamilton DL, Jaakkola P, Barstead R, Hodgkin J, Maxwell PH, Pugh CW, Schofield CJ, Ratcliffe PJ. C. elegans EGL-9 and mammalian homologs define a family of dioxygenases that regulate HIF by prolyl hydroxylation. Cell. 2001;107:43-54.
8. Hirsila M, Koivunen P, Gunzler V, Kivirikko KI, Myllyharju J. Characterization of the human prolyl 4-hydroxylases that modify the hypoxia-inducible factor. J Biol Chem. 2003;278:30772-30780.
9. Koivunen P, Hirsila M, Gunzler V, Kivirikko KI, Myllyharju J. Catalytic properties of the asparaginyl hydroxylase (FIH) in the oxygen sensing pathway are distinct from those of its prolyl 4-hydroxylases. J Biol Chem. 2004;279:9899-9904.
10. Koivunen P, Hirsila M, Kivirikko KI, Myllyharju J. The length of peptide substrates has a marked effect on hydroxylation by the hypoxia-inducible factor prolyl 4-hydroxylases. J Biol Chem 2006; 281: 28712-28720.
11. Ivan M, Kondo K, Yang H, Kim W, Valiando J, Ohh M, Salic A, Asara JM, Lane WS, Kaelin WG, Jr. HIFalpha targeted for VHL-mediated destruction by proline hydroxylation: implications for O_2 sensing. Science. 2001;292:464-468.
12. Jaakkola P, Mole DR, Tian YM, Wilson MI, Gielbert J, Gaskell SJ, Kriegsheim A, Hebestreit HF, Mukherji M, Schofield CJ, Maxwell PH, Pugh CW, Ratcliffe PJ. Targeting of HIF-alpha to the von Hippel-Lindau ubiquitylation complex by O_2-regulated prolyl hydroxylation. Science. 2001;292:468-472.
13. Lando D, Peet DJ, Gorman JJ, Whelan DA, Whitelaw ML, Bruick RK. FIH-1 is an asparaginyl hydroxylase enzyme that regulates the transcriptional activity of hypoxia-inducible factor. Genes Dev. 2002;16:1466-1471.
14. Mahon PC, Hirota K, Semenza GL. FIH-1: a novel protein that interacts with HIF-1alpha and VHL to mediate repression of HIF-1 transcriptional activity. Genes Dev. 2001;15:2675-2686.
15. Ehrismann D, Flashman E, Genn DN, Mathioudakis N, Hewitson KS, Ratcliffe PJ, Schofield CJ. Studies on the activity of the hypoxia-inducible-factor hydroxylases using an oxygen consumption assay. Biochem J. 2007;401:227-234.
16. Ward JP. Oxygen sensors in context. Biochim Biophys Acta. 2008;1777:1-14.
17. Aragones J, Fraisl P, Baes M, Carmeliet P. Oxygen sensors at the crossroad of metabolism. Cell Metab. 2009;9:11-22.
18. Cramer T, Yamanishi Y, Clausen BE, Forster I, Pawlinski R, Mackman N, Haase VH, Jaenisch R, Corr M, Nizet V, Firestein GS, Gerber HP, Ferrara N, Johnson RS. HIF-1alpha is essential for myeloid cell-mediated inflammation. Cell. 2003;112:645-657.
19. Imtiyaz HZ, Williams EP, Hickey MM, Patel SA, Durham AC, Yuan LJ, Hammond R, Gimotty PA, Keith B, Simon MC. Hypoxia-inducible factor 2alpha regulates macrophage function in mouse models of acute and tumor inflammation. J Clin Invest. 2010;120:2699-2714.

20. Hu CJ, Wang LY, Chodosh LA, Keith B, Simon MC. Differential roles of hypoxia-inducible factor 1alpha (HIF-1alpha) and HIF-2alpha in hypoxic gene regulation. Mol Cell Biol. 2003;23:9361-9374.
21. Garedew A, Henderson SO, Moncada S. Activated macrophages utilize glycolytic ATP to maintain mitochondrial membrane potential and prevent apoptotic cell death. Cell Death Differ. 2010;17(10):1540-50.
22. Roiniotis J, Dinh H, Masendycz P, Turner A, Elsegood CL, Scholz GM, Hamilton JA. Hypoxia prolongs monocyte/macrophage survival and enhanced glycolysis is associated with their maturation under aerobic conditions. J Immunol. 2009;182:7974-7981.
23. Tkalcevic J, Novelli M, Phylactides M, Iredale JP, Segal AW, Roes J. Impaired immunity and enhanced resistance to endotoxin in the absence of neutrophil elastase and cathepsin G. Immunity. 2000;12:201-210.
24. Reeves EP, Lu H, Jacobs HL, Messina CG, Bolsover S, Gabella G, Potma EO, Warley A, Roes J, Segal AW. Killing activity of neutrophils is mediated through activation of proteases by K+ flux. Nature. 2002;416:291-297.
25. Ganz T, Metcalf JA, Gallin JI, Boxer LA, Lehrer RI. Microbicidal/cytotoxic proteins of neutrophils are deficient in two disorders: Chediak-Higashi syndrome and "specific" granule deficiency. J Clin Invest. 1988;82:552-556.
26. Jung F, Palmer LA, Zhou N, Johns RA. Hypoxic regulation of inducible nitric oxide synthase via hypoxia inducible factor-1 in cardiac myocytes. Circ Res. 2000;86:319-325.
27. Takeda N, O'Dea EL, Doedens A, Kim JW, Weidemann A, Stockmann C, Asagiri M, Simon MC, Hoffmann A, Johnson RS. Differential activation and antagonistic function of HIF-{alpha} isoforms in macrophages are essential for NO homeostasis. Genes Dev. 2010;24:491-501.
28. Bansal V, Ochoa JB. Arginine availability, arginase, and the immune response. Curr Opin Clin Nutr Metab Care. 2003;6:223-228.
29. Bronte V, Zanovello P. Regulation of immune responses by L-arginine metabolism. Nat Rev Immunol. 2005;5:641-654.
30. Acosta-Iborra B, Elorza A, Olazabal IM, Martin-Cofreces NB, Martin-Puig S, Miro M, Calzada MJ, Aragones J, Sanchez-Madrid F, Landazuri MO. Macrophage oxygen sensing modulates antigen presentation and phagocytic functions involving IFN-gamma production through the HIF-1 alpha transcription factor. J Immunol. 2009;182:3155-3164.
31. Bayele HK, Peyssonnaux C, Giatromanolaki A, Arrais-Silva WW, Mohamed HS, Collins H, Giorgio S, Koukourakis M, Johnson RS, Blackwell JM, Nizet V, Srai SK. HIF-1 regulates heritable variation and allele expression phenotypes of the macrophage immune response gene SLC11A1 from a Z-DNA forming microsatellite. Blood. 2007;110:3039-3048.
32. Blackwell JM, Searle S, Mohamed H, White JK. Divalent cation transport and susceptibility to infectious and autoimmune disease: continuation of the Ity/Lsh/Bcg/Nramp1/Slc11a1 gene story. Immunol Lett. 2003;85:197-203.
33. Fraisl P, Aragones J, Carmeliet P. Inhibition of oxygen sensors as a therapeutic strategy for ischaemic and inflammatory disease. Nat Rev Drug Discov. 2009;8:139-152.
34. Zinkernagel AS, Peyssonnaux C, Johnson RS, Nizet V. Pharmacologic augmentation of hypoxia-inducible factor-1alpha with mimosine boosts the bactericidal capacity of phagocytes. J Infect Dis. 2008;197:214-217.
35. Walmsley SR, Print C, Farahi N, Peyssonnaux C, Johnson RS, Cramer T, Sobolewski A, Condliffe AM, Cowburn AS, Johnson N, Chilvers ER. Hypoxia-induced neutrophil survival is mediated by HIF-1alpha-dependent NF-kappaB activity. J Exp Med. 2005;201:105-115.
36. Walmsley SR, Cowburn AS, Clatworthy MR, Morrell NW, Roper EC, Singleton V, Maxwell P, Whyte MK, Chilvers ER. Neutrophils from patients with heterozygous germline mutations in the von Hippel Lindau protein (pVHL) display delayed apoptosis and enhanced bacterial phagocytosis. Blood. 2006;108:3176-3178.
37. Vissers MC, Wilkie RP. Ascorbate deficiency results in impaired neutrophil apoptosis and clearance and is associated with up-regulation of hypoxia-inducible factor 1alpha. J Leukoc Biol. 2007;81:1236-1244.
38. Kempf VA, Lebiedziejewski M, Alitalo K, Walzlein JH, Ehehalt U, Fiebig J, Huber S, Schutt B, Sander CA, Muller S, Grassl G, Yazdi AS, Brehm B, Autenrieth IB. Activation of hypoxia-inducible factor-1 in bacillary angiomatosis: evidence for a role of hypoxia-inducible factor-1 in bacterial infections. Circulation. 2005;111:1054-1062.
39. Wiley M, Sweeney KR, Chan DA, Brown KM, McMurtrey C, Howard EW, Giaccia AJ, Blader IJ. Toxoplasma gondii activates hypoxia inducible factor (HIF) by stabilizing the HIF-1 alpha subunit via type I activin-like receptor kinase receptor signaling. J Biol Chem. 2010;285(35):26852-60.
40. Wakisaka N, Kondo S, Yoshizaki T, Murono S, Furukawa M, Pagano JS. Epstein-Barr virus latent membrane protein 1 induces synthesis of hypoxia-inducible factor 1 alpha. Mol Cell Biol. 2004;24:5223-5234.
41. Arrais-Silva WW, Paffaro VA Jr, Yamada AT, Giorgio S. Expression of hypoxia-inducible factor-1alpha in the cutaneous lesions of BALB/c mice infected with Leishmania amazonensis. Exp Mol Pathol. 2005;78:49-54.
42. Degrossoli A, Bosetto MC, Lima CB, Giorgio S. Expression of hypoxia-inducible factor 1alpha in mononuclear phagocytes infected with Leishmania amazonensis. Immunol Lett. 2007;114:119-125.
43. Blouin CC, Page EL, Soucy GM, Richard DE. Hypoxic gene activation by lipopolysaccharide in macrophages: implication of hypoxia-inducible factor 1alpha. Blood. 2004;103:1124-1130.
44. Liu FQ, Liu Y, Lui VC, Lamb JR, Tam PK, Chen Y. Hypoxia modulates lipopolysaccharide induced TNF-alpha expression in murine macrophages. Exp Cell Res. 2008;314:1327-1336.

45. Kim SY, Choi YJ, Joung SM, Lee BH, Jung YS, Lee JY. Hypoxic stress up-regulates the expression of Toll-like receptor 4 in macrophages via hypoxia-inducible factor. Immunology. 2010;129:516-524.
46. Frede S, Berchner-Pfannschmidt U, Fandrey J. Regulation of hypoxia-inducible factors during inflammation. Methods Enzymol. 2007;435:405-419.
47. Rius J, Guma M, Schachtrup C, Akassoglou K, Zinkernagel AS, Nizet V, Johnson RS, Haddad GG, Karin M. NF-kappaB links innate immunity to the hypoxic response through transcriptional regulation of HIF-1alpha. Nature. 2008.
48. Fang HY, Hughes R, Murdoch C, Coffelt SB, Biswas SK, Harris AL, Johnson RS, Imityaz HZ, Simon MC, Fredlund E, Greten FR, Rius J, Lewis CE. Hypoxia-inducible factors 1 and 2 are important transcriptional effectors in primary macrophages experiencing hypoxia. Blood. 2009;114:844-859.
49. Nishi K, Oda T, Takabuchi S, Oda S, Fukuda K, Adachi T, Semenza GL, Shingu K, Hirota K. LPS induces hypoxia-inducible factor 1 activation in macrophage-differentiated cells in a reactive oxygen species-dependent manner. Antioxid Redox Signal. 2008;10:983-996.
50. Recalcati S, Locati M, Marini A, Santambrogio P, Zaninotto F, De Pizzol M, Zammataro L, Girelli D, Cairo G. Differential regulation of iron homeostasis during human macrophage polarized activation. Eur J Immunol. 2010;40:824-835.
51. Hartmann H, Eltzschig HK, Wurz H, Hantke K, Rakin A, Yazdi AS, Matteoli G, Bohn E, Autenrieth IB, Karhausen J, Neumann D, Colgan SP, Kempf VA. Hypoxia-independent activation of HIF-1 by enterobacteriaceae and their siderophores. Gastroenterology. 2008;134:756-767.
52. Puig-Kroger A, Sierra-Filardi E, Dominguez-Soto A, Samaniego R, Corcuera MT, Gomez-Aguado F, Ratnam M, Sanchez-Mateos P, Corbi AL. Folate receptor beta is expressed by tumor-associated macrophages and constitutes a marker for M2 anti-inflammatory/regulatory macrophages. Cancer Res. 2009;69:9395-9403.
53. Rodriguez-Prados JC, Traves PG, Cuenca J, Rico D, Aragones J, Martin-Sanz P, Cascante M, Bosca L. Substrate fate in activated macrophages: a comparison between innate, classic, and alternative activation. J Immunol. 2010;185:605-614.
54. Porta C, Rimoldi M, Raes G, Brys L, Ghezzi P, Di Liberto D, Dieli F, Ghisletti S, Natoli G, De Baetselier P, Mantovani A, Sica A. Tolerance and M2 (alternative) macrophage polarization are related processes orchestrated by p50 nuclear factor kappaB. Proc Natl Acad Sci U S A. 2009;106:14978-14983.
55. Hollander AP, Corke KP, Freemont AJ, Lewis CE. Expression of hypoxia-inducible factor 1alpha by macrophages in the rheumatoid synovium: implications for targeting of therapeutic genes to the inflamed joint. Arthritis Rheum. 2001;44:1540-1544.
56. Zhou J, Dehne N, Brune B. Nitric oxide causes macrophage migration via the HIF-1-stimulated small GTPases Cdc42 and Rac1. Free Radic Biol Med. 2009;47:741-749.
57. Kong T, Eltzschig HK, Karhausen J, Colgan SP, Shelley CS. Leukocyte adhesion during hypoxia is mediated by HIF-1-dependent induction of beta2 integrin gene expression. Proc Natl Acad Sci U S A. 2004;101:10440-10445.
58. Charbonneau M, Harper K, Grondin F, Pelmus M, McDonald PP, Dubois CM. Hypoxia-inducible factor mediates hypoxic and tumor necrosis factor alpha-induced increases in tumor necrosis factor-alpha converting enzyme/ADAM17 expression by synovial cells. J Biol Chem. 2007;282:33714-33724.
59. Dong F, Khalil M, Kiedrowski M, O'Connor C, Petrovic E, Zhou X, Penn MS. Critical role for leukocyte hypoxia inducible factor-1alpha expression in post-myocardial infarction left ventricular remodeling. Circ Res. 2010;106:601-610.
60. Rey S, Lee K, Wang CJ, Gupta K, Chen S, McMillan A, Bhise N, Levchenko A, Semenza GL. Synergistic effect of HIF-1alpha gene therapy and HIF-1-activated bone marrow-derived angiogenic cells in a mouse model of limb ischemia. Proc Natl Acad Sci U S A. 2009;106:20399-20404.
61. Ritter MR, Banin E, Moreno SK, Aguilar E, Dorrell MI, Friedlander M. Myeloid progenitors differentiate into microglia and promote vascular repair in a model of ischemic retinopathy. J Clin Invest. 2006;116:3266-3276.
62. Qian BZ, Pollard JW. Macrophage diversity enhances tumor progression and metastasis. Cell. 2010;141:39-51.
63. Hagemann T, Lawrence T, McNeish I, Charles KA, Kulbe H, Thompson RG, Robinson SC, Balkwill FR. "Re-educating" tumor-associated macrophages by targeting NF-kappaB. J Exp Med. 2008;205:1261-1268.
64. Shirato K, Kizaki T, Sakurai T, Ogasawara JE, Ishibashi Y, Iijima T, Okada C, Noguchi I, Imaizumi K, Taniguchi N, Ohno H. Hypoxia-inducible factor-1alpha suppresses the expression of macrophage scavenger receptor 1. Pflugers Arch. 2009;459:93-103.
65. Werno C, Menrad H, Weigert A, Dehne N, Goerdt S, Schledzewski K, Kzhyshkowska J, Brune B. Knockout of Hif-1alpha in tumor-associated macrophages enhances M2 polarization and attenuates their pro-angiogenic responses. Carcinogenesis. 2010;31(10):1863-72.
66. Movahedi K, Laoui D, Gysemans C, Baeten M, Stange G, Van den Bossche J, Mack M, Pipeleers D, In't Veld P, De Baetselier P, Van Ginderachter JA. Different tumor microenvironments contain functionally distinct subsets of macrophages derived from Ly6C(high) monocytes. Cancer Res. 2010;70:5728-5739.
67. Murdoch C, Giannoudis A, Lewis CE. Mechanisms regulating the recruitment of macrophages into hypoxic areas of tumors and other ischemic tissues. Blood. 2004;104:2224-2234.
68. Lewis CE, Pollard JW. Distinct role of macrophages in different tumor microenvironments. Cancer Res. 2006;66:605-612.

69. Talks KL, Turley H, Gatter KC, Maxwell PH, Pugh CW, Ratcliffe PJ, Harris AL. The expression and distribution of the hypoxia-inducible factors HIF-1alpha and HIF-2alpha in normal human tissues, cancers, and tumor-associated macrophages. Am J Pathol. 2000;157:411-421.
70. Bertout JA, Patel SA, Simon MC. The impact of O_2 availability on human cancer. Nat Rev Cancer. 2008;8:967-975.
71. Stockmann C, Doedens A, Weidemann A, Zhang N, Takeda N, Greenberg JI, Cheresh DA, Johnson RS. Deletion of vascular endothelial growth factor in myeloid cells accelerates tumorigenesis. Nature. 2008;456:814-818.
72. Jain RK. Normalization of tumor vasculature: an emerging concept in antiangiogenic therapy. Science. 2005;307:58-62.
73. Mazzone M, Dettori D, Leite de Oliveira R, Loges S, Schmidt T, Jonckx B, Tian YM, Lanahan AA, Pollard P, Ruiz de Almodovar C, De Smet F, Vinckier S, Aragones J, Debackere K, Luttun A, Wyns S, Jordan B, Pisacane A, Gallez B, Lampugnani MG, Dejana E, Simons M, Ratcliffe P, Maxwell P, Carmeliet P. Heterozygous deficiency of PHD2 restores tumor oxygenation and inhibits metastasis via endothelial normalization. Cell. 2009;136:839-851.
74. Owings RA, Boerma M, Wang J, Berbee M, Laderoute KR, Soderberg LS, Vural E, Jensen MH. Selective deficiency of HIF-1alpha in myeloid cells influences secondary intention wound healing in mouse skin. In Vivo. 2009;23:879-884.
75. Sluimer JC, Gasc JM, van Wanroij JL, Kisters N, Groeneweg M, Sollewijn Gelpke MD, Cleutjens JP, van den Akker LH, Corvol P, Wouters BG, Daemen MJ, Bijnens AP. Hypoxia, hypoxia-inducible transcription factor, and macrophages in human atherosclerotic plaques are correlated with intraplaque angiogenesis. J Am Coll Cardiol. 2008;51:1258-1265.
76. Hulten LM, Olson FJ, Aberg H, Carlsson J, Karlstrom L, Boren J, Fagerberg B, Wiklund O. 15-Lipoxygenase-2 is expressed in macrophages in human carotid plaques and regulated by hypoxia-inducible factor-1alpha. Eur J Clin Invest. 2009;40:11-17.

OPEN ACCESS Freely available online

PLoS one

Acute *Vhl* Gene Inactivation Induces Cardiac HIF-Dependent Erythropoietin Gene Expression

Marta Miró-Murillo[2☯], Ainara Elorza[1☯], Inés Soro-Arnáiz[1☯], Lucas Albacete-Albacete[1], Angel Ordoñez[1], Eduardo Balsa[1], Alicia Vara-Vega[1], Silvia Vázquez[1], Esther Fuertes[1], Carmen Fernández-Criado[2], Manuel O. Landázuri[1], Julián Aragonés[1]*

1 Department of Immunology, Hospital of La Princesa, Sanitary Research Institute Princesa (IP), Autonomous University of Madrid, Madrid, Spain, **2** Animal Facility, Autonomous University of Madrid, Madrid, Spain

Abstract

Von Hippel Lindau (*Vhl*) gene inactivation results in embryonic lethality. The consequences of its inactivation in adult mice, and of the ensuing activation of the hypoxia-inducible factors (HIFs), have been explored mainly in a tissue-specific manner. This mid-gestation lethality can be also circumvented by using a floxed *Vhl* allele in combination with an ubiquous tamoxifen-inducible recombinase Cre-ER^{T2}. Here, we characterize a widespread reduction in *Vhl* gene expression in Vhl^{floxed}-UBC-Cre-ER^{T2} adult mice after dietary tamoxifen administration, a convenient route of administration that has yet to be fully characterized for global gene inactivation. *Vhl* gene inactivation rapidly resulted in a marked splenomegaly and skin erythema, accompanied by renal and hepatic induction of the erythropoietin (*Epo*) gene, indicative of the in vivo activation of the oxygen sensing HIF pathway. We show that acute *Vhl* gene inactivation also induced *Epo* gene expression in the heart, revealing cardiac tissue to be an extra-renal source of EPO. Indeed, primary cardiomyocytes and HL-1 cardiac cells both induce *Epo* gene expression when exposed to low O_2 tension in a HIF-dependent manner. Thus, as well as demonstrating the potential of dietary tamoxifen administration for gene inactivation studies in UBC-Cre-ER^{T2} mouse lines, this data provides evidence of a cardiac oxygen-sensing VHL/HIF/EPO pathway in adult mice.

Citation: Miró-Murillo M, Elorza A, Soro-Arnáiz I, Albacete-Albacete L, Ordoñez A, et al. (2011) Acute *Vhl* Gene Inactivation Induces Cardiac HIF-Dependent Erythropoietin Gene Expression. PLoS ONE 6(7): e22589. doi:10.1371/journal.pone.0022589

Editor: Mauricio Rojas, University of Pittsburgh, United States of America

Received December 7, 2010; **Accepted** June 29, 2011; **Published** July 21, 2011

Funding: This work was supported by grants from Ministerio de Educación y Ciencia (BFU2008-03407/BMC), RECAVA (RD06/0014/0031), CICYT (SAF2007-60592) and CAM (SAL0311/2006). The funders had no role in study design, data collection and analysis, decision to publish, or preparation of the manuscript.

Competing Interests: The authors have declared that no competing interests exist.

* E-mail: jaragones.hlpr@salud.madrid.org

☯ These authors contributed equally to this work.

Introduction

The ability of cells to respond to low O_2 supply (hypoxia) is fundamental in numerous pathological scenarios [1]. Hypoxia-inducible transcription factors (HIF) 1α, 2α and 3α, prolyl hydroxylase domain proteins (PHDs) 1, 2 and 3 and the von Hippel-Lindau (VHL) protein are essential molecular elements in the cellular response to low O_2 supply. In normoxia, PHDs hydroxylate prolyl residues in the HIFα subunits that are then recognized by VHL, a protein of the multiprotein E3 ubiquitin ligase complex that marks them for degradation by the proteasome [2,3]. In conditions of hypoxia O_2 is limited and it is insufficient to hydroxylate prolyl residues in HIFα [4,5]. As a result, these HIFα isoforms are stabilized and form a heterodimer with the HIFβ subunit, promoting the expression of many genes involved in cellular adaptation to hypoxia [6]. This includes the expression of erythropoietin (*Epo*) in the kidney and liver in order to facilitate oxygen delivery to hypoxic tissues [7,8,9,10]. Global *Vhl* gene inactivation in mice, and the ensuing HIF activation, can be used as a strategy to explore hypoxia signalling *in vivo*. However, conventional global *Vhl* gene inactivation is lethal in embryos [11], although this can be circumvented by only inducing *Vhl* gene inactivation in adult mice.

Widespread and acute gene inactivation in adult mice can be achieved through the ubiquitous expression of an inducible Cre recombinase, which can be used to eliminate the *Vhl* allelic region flanked by two loxP sites (a floxed *Vhl* allele). The nuclear activity of Cre can be induced by fusing it to a mutant form of the human estrogen receptor (ER^{T2}) that does not recognize its natural ligand (17β-estradiol) at physiological concentrations but rather, it binds the synthetic estrogen receptor ligand 4-hydroxytamoxifen (4-HT) [12]. This Cre-ER^{T2} is retained in the cytoplasm and only enters the nucleus in the presence of 4-HT, where it binds to loxP sites of the corresponding floxed alleles. Like other ubiquitous promoters, widespread Cre-ER^{T2} expression can be achieved in mice using the human ubiquitin C (UBC) promoter (UBC-Cre-ER^{T2} mice) [13]. Several means of administering tamoxifen have been described in rodents, including intraperitoneal injections and gavage [13]. However, the addition of 4-HT to powdered food or drinking water is a more convenient and less stressful means of inducing Cre recombinase activity in adult mice [14,15,16]. While the administration of tamoxifen via drinking water is hampered by its poor solubility, its delivery in food has been successfully achieved in several mouse lines [14,15,16]. However, to date, the full potential of a tamoxifen diet and its efficacy in inducing global Cre-ER^{T2} activity in different organs of a Cre-ER^{T2} transgenic mouse line (e.g. UBC-Cre-ER^{T2} mice) has not been fully explored.

Here we have successfully employed diet-based tamoxifen administration, a timesaving and convenient mean of delivering

tamoxifen in order to induce widespread inactivation of the *Vhl* gene in a Vhl^{floxed}-UBC-Cre-ER^{T2} mouse line. After validating the efficiency of tamoxifen dietary administration, we characterized VHL/HIF oxygen-sensing dependent events that were rapidly induced by global *Vhl* inactivation *in vivo* (within just a few days) in contrast to other works that have mainly studied the *in vivo* consequences of *Vhl* gene inactivation over several weeks [17,18]. This study validates the use of the tamoxifen diet in UBC-Cre-ER^{T2} mouse lines for global gene inactivation, and it identifies an oxygen-sensing VHL/HIF pathway controlling extra-renal *Epo* gene expression in cardiac tissue.

Results

Postnatal tamoxifen diet-mediated *Vhl* gene inactivation

Global *Vhl* gene inactivation results in embryonic lethality, at least in part due to placental dysfunction [11], preventing the study of the global loss of this gene in adult mice. We were interested in the short-term effects of activating the oxygen-sensing HIF pathway *in vivo*, as a result of global *Vhl* gene inactivation in adult Vhl^{floxed}-UBC-Cre-ER^{T2} mice through dietary tamoxifen administration. Since the full potential of dietary tamoxifen administration for global gene inactivation has not been explored previously, we first validated the efficacy of the tamoxifen diet in reducing *Vhl* gene expression in the Vhl^{floxed}-UBC-Cre-ER^{T2} mouse line. Age-matched Vhl^{floxed}-UBC-Cre-ER^{T2} as well as control mice Vhl^{floxed} and Vhl^{wt}-UBC-Cre-ER^{T2} were maintained for 10 days on an *ad libitum* diet of tamoxifen pellets (containing 400 mg/kg tamoxifen), before they were switched to a diet of normal chow for a further 10 days and *Vhl* gene expression was analyzed by quantitative real-time PCR in the different mouse organs. Hereinafter, the terms Vhl^{floxed}, Vhl^{wt}-UBC-Cre-ER^{T2} and Vhl^{floxed}-UBC-Cre-ER^{T2} refer to mice that have been administered a tamoxifen diet as indicated above. The tamoxifen diet significantly reduced *Vhl* gene expression in the kidney, spleen, liver, skeletal muscle, brown adipose tissue (BAT), heart, lung and brain of Vhl^{floxed}-UBC-Cre-ER^{T2} mice, reflecting widespread *Vhl* gene inactivation (Figure 1A). No differences in tamoxifen intake were observed between Vhl^{floxed}-UBC-Cre-ER^{T2} and control mice (Figure 1B). Significantly, gene inactivation was not homogeneous and expression of the *Vhl* gene was more strongly downregulated in the kidney and spleen, and less so in other tissues such as the brain and lung (Figure 1A). To further validate the specificity of *Vhl* gene inactivation, we also quantified *Vhl* gene expression in another UBC-Cre-ER^{T2} system, the $Hif1\alpha^{floxed}$-UBC-Cre-ER^{T2} mouse line and their corresponding $Hif1\alpha^{floxed}$ and $Hif1\alpha^{wt}$-UBC-Cre-ER^{T2} control mice. While there were no significant differences in tamoxifen intake between the different lines (Figure 1D), *Hif1α* gene expression was dramatically and globally reduced, while *Vhl* gene expression was not affected in tamoxifen fed $Hif1\alpha^{floxed}$-UBC-Cre-ER^{T2} mice (Figure 1C, E).

As mice were transiently exposed to a different diet, we evaluated their body weight before and after tamoxifen treatment. Baseline body weight diminished in a similar way (~10%) in Vhl^{floxed}-UBC-Cre-ER^{T2} and control mice after 10 days on the tamoxifen diet (Figure 2). However, while the body weight of control mice returned to pre-tamoxifen levels just one day after switching back to a normal diet (Figure 2), that was not the case in Vhl^{floxed}-UBC-Cre-ER^{T2} mice following tamoxifen treatment (Figure 2), suggesting that body weight was rapidly compromised by *Vhl* gene inactivation.

Gross appearance of mice shortly after acute *Vhl* inactivation

To further evaluate the efficacy of the tamoxifen diet on *Vhl* gene inactivation, we studied the biological consequences of acute *Vhl* inactivation soon after the mice returned to a normal diet (10 days). We evaluated spleen size and skin erythema as macroscopic indicators of activation of the HIF oxygen-sensing pathway *in vivo* [19]. All tamoxifen-treated Vhl^{floxed}-UBC-Cre-ER^{T2} mice analyzed exhibited marked splenomegaly when compared with controls (Figure 3 A, B). Moreover, some mice displayed obvious reddening of their paws and snouts (Figure 3 C, D). These external signs of skin erythema appeared as early as the ninth day of tamoxifen administration (data not shown), suggesting that this phenotype represents an acute manifestation of *Vhl* gene inactivation. Overall, these data confirm that dietary administration of tamoxifen is an efficient and convenient mean to induce widespread and rapid gene inactivation of floxed alleles in UBC-Cre-ER^{T2} mice and in particular, to study the short-term biological consequences of *Vhl* inactivation.

Acute *Vhl* inactivation induces cardiac *Epo* gene expression

Splenomegaly and erythema are recognized signs of activation of the oxygen-VHL/HIF/EPO pathway, and they have been reported previously in transgenic mice overexpressing EPO [20,21]. Given that the kidney and liver are the main sites of EPO production in adults [7,22,23], we investigated *Epo* gene expression in these organs in Vhl^{floxed}-UBC-Cre-ER^{T2} mice shortly after *Vhl* gene inactivation. When we analyzed renal and hepatic *Epo* gene expression in tamoxifen-treated Vhl^{floxed}-UBC-Cre-ER^{T2} mice, we found a strong induction of this gene in the kidney (~200 fold, Figure 4A) and an even stronger increase in the liver when compared to control mice (Figure 4B). The marked difference between these two organs is probably due to the very low basal levels of hepatic *Epo* gene expression, which results in more marked differences when *Vhl* is inactivated. These differences cannot simply be attributed to differences in *Vhl* inactivation, as *Vhl* is inactivated to a greater extent in the kidney than in the liver (Figure 1A). Moreover, serum EPO levels were drastically elevated in tamoxifen-treated Vhl^{floxed}-UBC-Cre-ER^{T2} when compared with tamoxifen-treated control mice (pg of EPO/ml: 150.5 ± 22.6 in Vhl^{floxed} versus 49835.5 ± 21586 in Vhl^{floxed}-UBC-Cre-ER^{T2}; $n=4$, $p<0.05$). These mice showed a remarkable reticulocytosis. Indeed, the number of circulating reticulocytes as well as splenic reticulocytes increases in Vhl^{floxed}-UBC-Cre-ER^{T2} mice (*Circulating reticulocytes* $x10^6/ml$: 603.92 ± 437 in Vhl^{floxed} versus 6391.53 ± 1381 in Vhl^{floxed}-UBC-Cre-ER^{T2}; $n=3$, $p=0.018$) (*Splenic reticulocytes* $x10^6/ml$: 32 ± 6.08 in Vhl^{floxed} versus 269.08 ± 4.4 in Vhl^{floxed}-UBC-Cre-ER^{T2}; $n=3$, $p=0.01$). However, a parallel hemocytometry showed that hematocrit is not significantly elevated in tamoxifen-treated Vhl^{floxed}-UBC-Cre-ER^{T2} when compared with control mice (*hematocrit %*: 40.8 ± 2.02 in Vhl^{floxed} versus 43 ± 5.3 in Vhl^{floxed}-UBC-Cre-ER^{T2}; $n=5$, $p=$NS). Furthermore, a follow up of Vhl^{floxed}-UBC-Cre-ER^{T2} mice revealed that they started to show anemia after a longer time period upon *Vhl* gene inactivation (*hematocrit %*: 42.62 ± 2.22 in Vhl^{floxed} versus 33.2 ± 3.8 in Vhl^{floxed}-UBC-Cre-ER^{T2}; $n=7$, $p=0.041$). In addition, the proportion of Hoechst $33342^{negative}$ $CD71^{negative}$ cells decrease in the spleens of Vhl^{floxed}-UBC-Cre-ER^{T2} (% of total number of splenic cells: 27.10 ± 5.3 in Vhl^{floxed} versus 3.22 ± 1.25 in Vhl^{floxed}-UBC-Cre-ER^{T2}; $n=3$, $p<0.01$). This possibly reflects a specific VHL-dependent effect on mature red blood cells survival that will be further explored in futures studies.

In line with other studies, baseline *Epo* gene expression was particularly weak in the heart [8], although we found a remarkable elevation in cardiac *Epo* gene expression in tamoxifen fed Vhl^{floxed}-UBC-Cre-ER^{T2} mice (Figure 4D). Given that cardiac *Vhl*

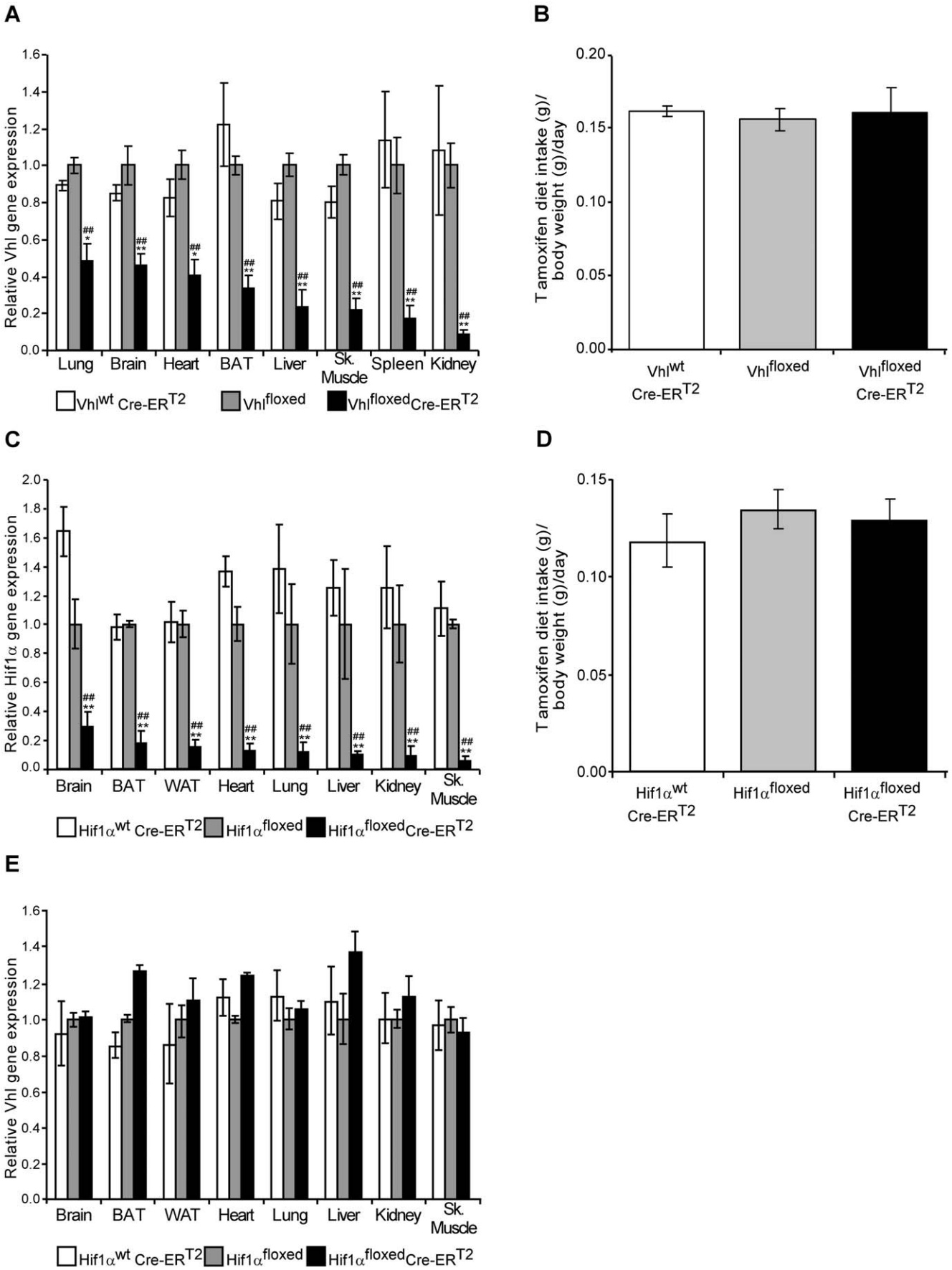
A
Relative Vhl gene expression
Lung
Brain
Heart
BAT
Liver
Sk. Muscle
Spleen
Kidney
Vhl^wt Cre-ER^T2
Vhl^floxed
Vhl^floxed Cre-ER^T2
B
Tamoxifen diet intake (g)/ body weight (g)/day
Vhl^wt Cre-ER^T2
Vhl^floxed
Vhl^floxed Cre-ER^T2
C
Relative Hif1α gene expression
Brain
BAT
WAT
Heart
Lung
Liver
Kidney
Sk. Muscle
Hif1α^wt Cre-ER^T2
Hif1α^floxed
Hif1α^floxed Cre-ER^T2
D
Tamoxifen diet intake (g)/ body weight (g)/day
Hif1α^wt Cre-ER^T2
Hif1α^floxed
Hif1α^floxed Cre-ER^T2
E
Relative Vhl gene expression
Brain
BAT
WAT
Heart
Lung
Liver
Kidney
Sk. Muscle
Hif1α^wt Cre-ER^T2
Hif1α^floxed
Hif1α^floxed Cre-ER^T2

Figure 1. *Vhl* and *Hif1α* gene expression in tamoxifen-fed Vhl^{floxed}-UBC-Cre-ER^{T2} and Hif1α^{floxed}-UBC-Cre-ER^{T2} mice. (A) Vhl^{wt}-UBC-Cre-ER^{T2} (n = 3), Vhl^{floxed} (n = 6) and Vhl^{floxed}-UBC-Cre-ER^{T2} (n = 6) mice were placed on a tamoxifen diet for ten days followed by ten additional days on a normal diet. Gene expression was assessed by RT-PCR in the tissues indicated, the expression of the *Vhl* gene was normalized to that of *Hprt* and it was expressed as the change relative to Vhl^{floxed} mice. (B) Tamoxifen intake was measured over the 10 days of tamoxifen administration in Vhl^{wt}-UBC-Cre-ER^{T2} (n = 3), Vhl^{floxed} (n = 6) and Vhl^{floxed}-UBC-Cre-ER^{T2} (n = 6) mice. (C,E) Hif1α^{wt}-UBC-Cre-ER^{T2} (n = 4), Hif1α^{floxed} (n = 3) and Hif1α^{floxed}-UBC-Cre-ER^{T2} (n = 5) mice were administered tamoxifen as indicated above. *Hif1α* (C) or *Vhl* (E) gene expression was normalized to that of *Hprt* and expressed as the change relative to Hif1α^{floxed} mice. (D) Tamoxifen intake in Hif1α^{wt}-UBC-Cre-ER^{T2} (n = 4), Hif1α^{floxed} (n = 3) and Hif1α^{floxed}-UBC-Cre-ER^{T2} (n = 5) mice was measured as in B. Total intake per day was expressed relative to the body weight at the end of the tamoxifen treatment and the values represent the mean ± SEM. Statistical significance was assessed using a two-tailed Student's t-test, (*, $p<0.05$; **, $p<0.01$) when comparing Vhl^{wt}-UBC-Cre-ER^{T2} or Hif1α^{wt}-UBC-Cre-ER^{T2} with Vhl^{floxed}-UBC-Cre-ER^{T2} or Hif1α^{floxed}-UBC-Cre-ER^{T2} respectively; ($^{\#\#}$, $p<0.01$) when comparing Vhl^{floxed} or Hif1α^{floxed} with Vhl^{floxed}-UBC-Cre-ER^{T2} or Hif1α^{floxed}-UBC-Cre-ER^{T2} respectively.
doi:10.1371/journal.pone.0022589.g001

expression is not fully ablated in tamoxifen-treated Vhl^{floxed}-UBC-Cre-ER^{T2} mice (Figure 1A), we presumed that cardiac *Epo* gene expression could be potentially higher if *Vhl* deletion were more prominent. Expression of glucose transporter-1 (*Glut1)*, a HIF-dependent gene [24], was also elevated in the hearts of tamoxifen treated Vhl^{floxed}-UBC-Cre-ER^{T2} mice (Figure 4D). In addition, *Epo* gene expression was markedly upregulated in the brain (Figure 4C), possibly reflecting oxygen-sensing VHL/HIF-dependent EPO production in glial cells, as described previously [25]. Induction of *Epo* gene expression was stronger in cardiac tissue than in the brain, perhaps due to the weak basal expression of the *Epo* gene in the heart. These data suggest that the oxygen-sensing VHL/HIF/EPO pathway is not restricted to classical EPO-producing tissues, and they demonstrate that the heart can express EPO upon *Vhl* inactivation. To determine whether cardiomyocytes could be contributing to this VHL-dependent response, *Epo* gene expression was analyzed in isolated primary rat cardiomyocytes exposed to low oxygen tension. While weak basal expression of the *Epo* gene was observed in normoxic cardiomyocytes, hypoxia (1% O_2) augmented markedly its expression (Figure 5A). Likewise, *Glut1* expression was also induced, which indicates an effective induction of the HIF pathway in these experimental conditions (Figure 5B). We further evaluated the role of the HIF system in hypoxia-induced *Epo* gene expression in cardiac cells in the HL-1 cell line, a well-recognized cardiac cell model that retains a differentiated cardiac myocyte phenotype and maintains contractile activity [26]. We specifically silenced expression of *Hif1α*, the main HIF isoform expressed at RNA level in this cardiomyocyte cell line (data not shown and Figure 6C). *Glut1* expression was induced by hypoxia in control scramble-transfected HL-1 cells but its expression was markedly attenuated in HL-1 cells transfected with siHIF1α (Figure 6B). Similarly, hypoxia-induced *Epo* gene expression was reduced when *Hif1α* was silenced in these cells (Figure 6A). These data indicate that hypoxia-induced *Epo* gene expression is an autonomous VHL/HIF-dependent cardiomyocyte response that occurs shortly after activation of this oxygen-sensing pathway. This response provides a molecular and cellular explanation for the elevated levels of cardiac *Epo* gene expression in Vhl^{floxed}-UBC-Cre-ER^{T2} mice.

Discussion

The oxygen-sensing VHL/HIF dependent pathway plays a central role in cellular adaptation to oxygen fluctuations [27,28]. This role has primarily been explored in mouse models in which HIF is chronically overactivated following tissue-specific *Vhl* inactivation [22,25,29]. Here, we characterize the short-term *in vivo* responses following global inactivation of *Vhl* in the Vhl^{floxed}-

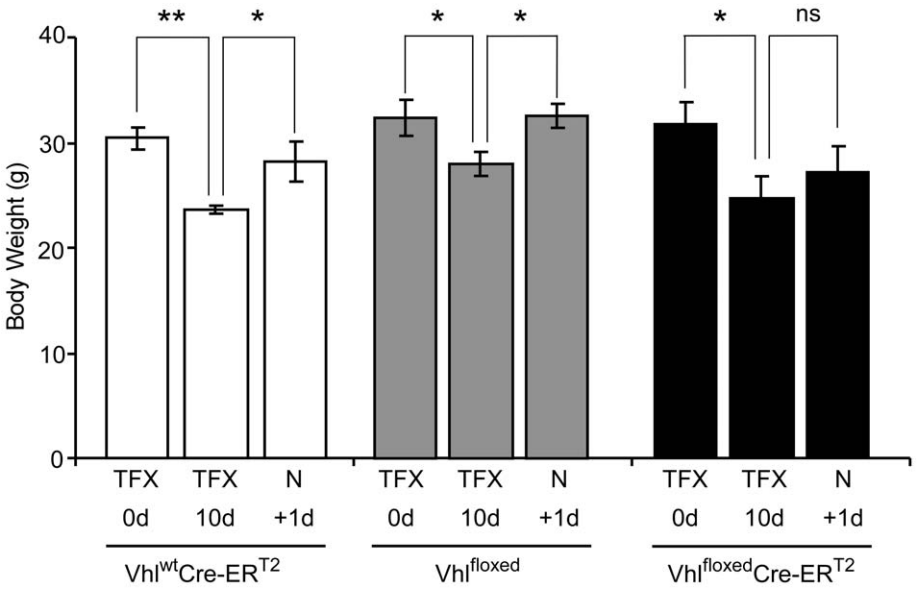

Figure 2. Body weight during and after tamoxifen diet administration in Vhl^{floxed}-UBC-Cre-ER^{T2} and control mice. Body weight of Vhl^{wt}-UBC-Cre-ER^{T2} (n = 3), Vhl^{floxed}-UBC-Cre-ER^{T2} (n = 6) control Vhl^{floxed} (n = 6) mice was measured before tamoxifen treatment (TFX 0d), at the end of 10 days on a tamoxifen diet (TFX 10d) and one day after returning to a normal diet (N +1d). Statistical significance was assessed using a two-tailed Student's t-test, (*, $p<0.05$; **, $p<0.01$; ns, no significant differences).
doi:10.1371/journal.pone.0022589.g002

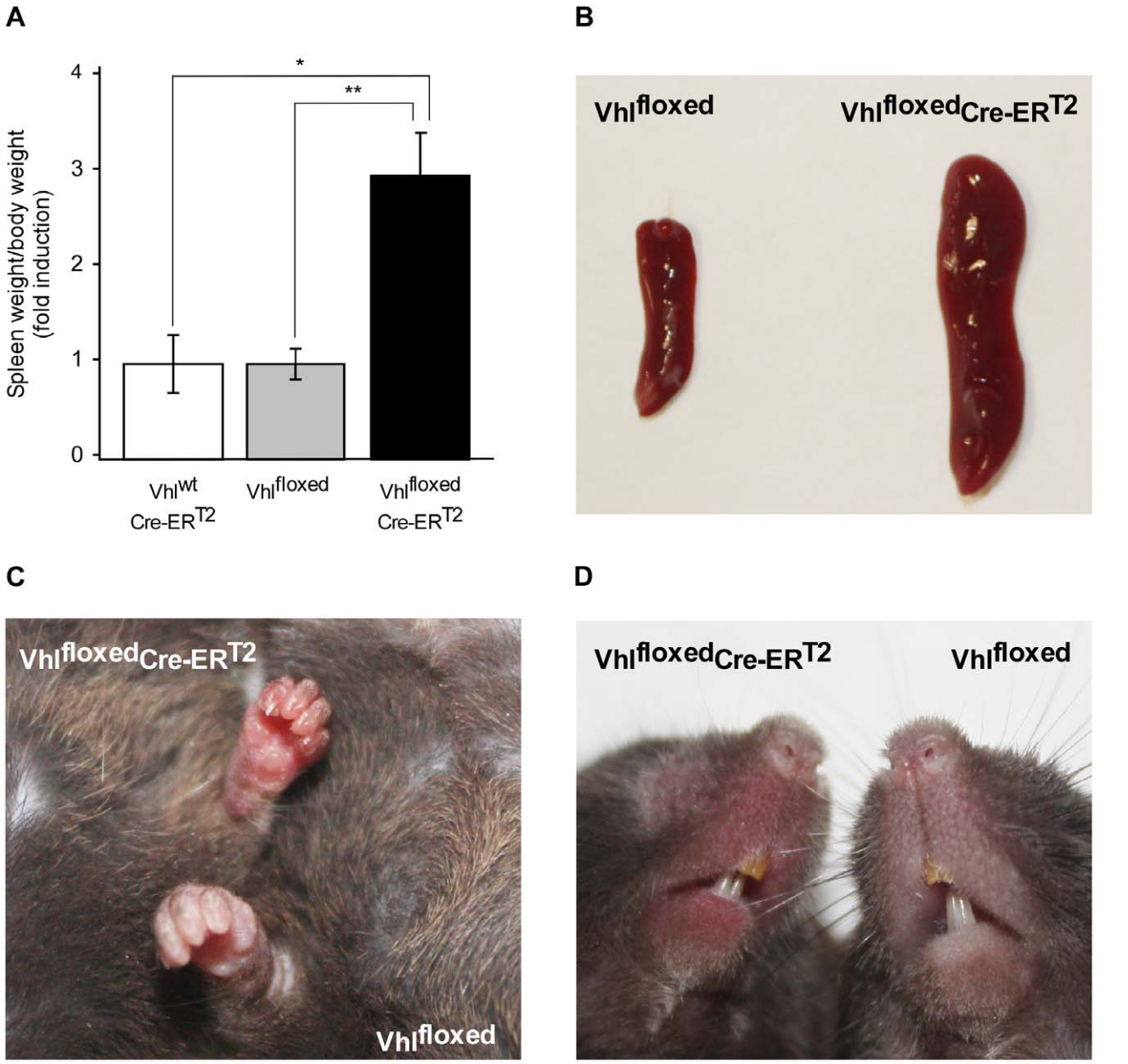

Figure 3. Gross appearance of tamoxifen-fed Vhl^{floxed}-Cre-ERT2 mice. (A) Vhl^{wt}-UBC-Cre-ER^{T2} (n = 3), Vhl^{floxed} (n = 9) and Vhl^{floxed}-UBC-Cre-ER^{T2} (n = 10) mice were administered tamoxifen as indicated in Figure 1 and the spleen/body weight ratio was then determined. Statistical significance was assessed using a two-tailed Student's t-test (*, $p<0.05$; **, $p<0.01$). Representative images of spleens (B), snouts (C) and paws (D) of Vhl^{floxed}-UBC-Cre-ER^{T2} and control Vhl^{floxed} mice are shown.
doi:10.1371/journal.pone.0022589.g003

UBC-Cre-ER^{T2} mouse line. For this purpose, we employed dietary administration of tamoxifen, a timesaving and convenient method of tamoxifen administration to induce Cre-ER^{T2} activity. The full potential for global gene inactivation was not previously explored. Indeed, dietary administration of tamoxifen has been characterized in mice with specific Cre-ER^{T2} expression in the heart, forebrain or in endothelial cells [14,15,16]. However, a comparative analysis of the efficiency of tamoxifen diet in different organs to determine its full potential to induce widespread gene inactivation has not been performed. Moreover, some of these studies have required several weeks on a tamoxifen diet. Here, we describe global gene inactivation in UBC-Cre-ER^{T2} mouse lines shortly (a few days) after tamoxifen administration.

In this first place, it appears that UBC-Cre-ER^{T2} is suitable to produce global gene inactivation in animals fed with a tamoxifen diet. However, tamoxifen-mediated *Vhl* gene inactivation was less pronounced in the Vhl^{floxed}-UBC-Cre-ER^{T2} line than *Hif1α* gene inactivation in Hif1α^{floxed}-UBC-Cre-ER^{T2} line, an effect that could not be attributed to differences in tamoxifen intake. This differential inactivation may reflect the specific efficacy of the Cre-ER^{T2} recombinase to act on the floxed region of the *Vhl* and *Hif1α* alleles. Thus, optimization of the tamoxifen diet may be necessary to achieve comparable effects in distinct UBC-Cre-ER^{T2} mouse lines. Nevertheless, the extent to which *Vhl* gene expression was reduced in these mice was sufficient to induce the activation of oxygen-sensing HIF pathways *in vivo*. Indeed, macroscopic

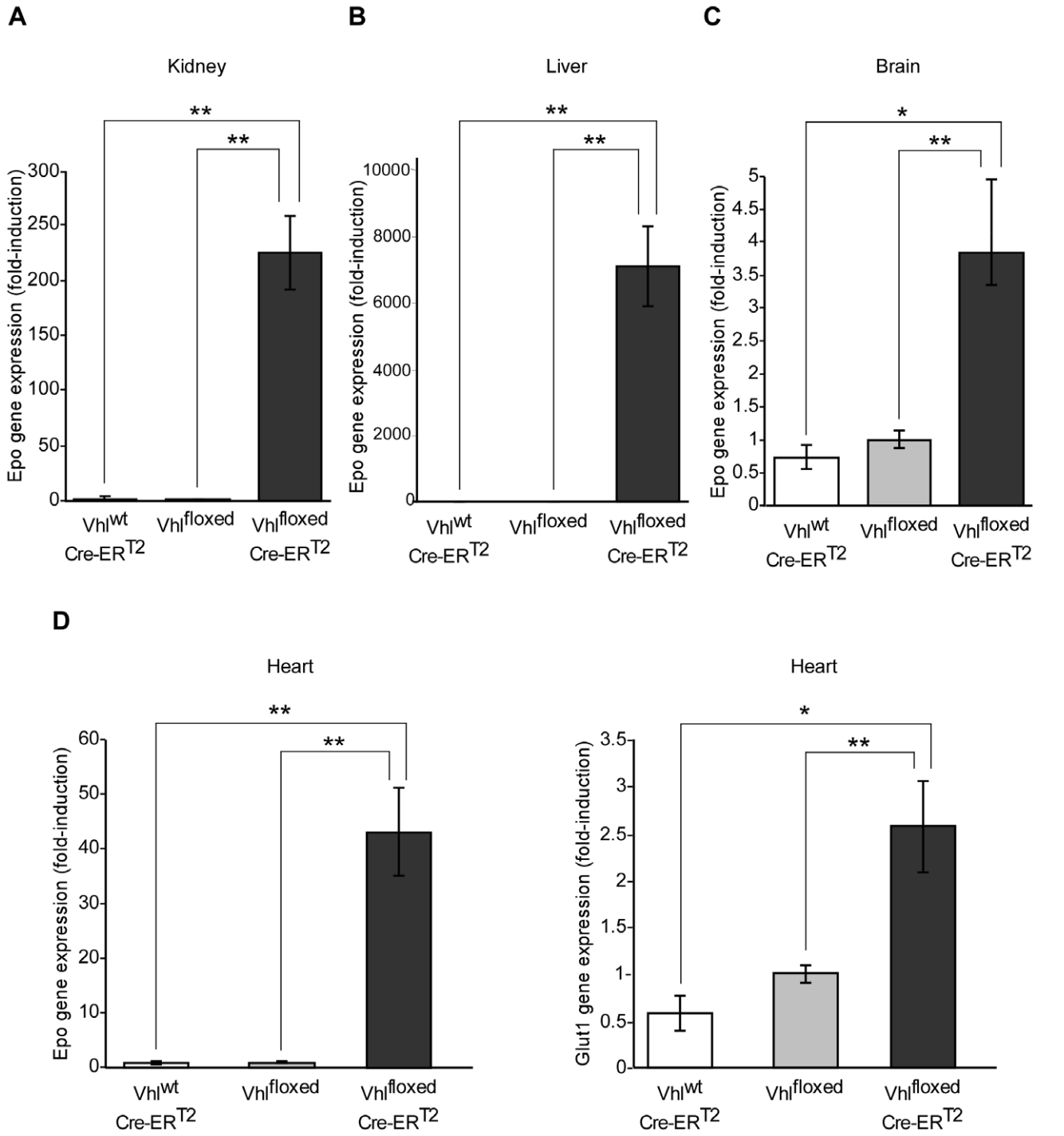

Figure 4. *Erythropoietin* gene expression in the kidney, liver, brain and heart of tamoxifen-fed Vhl^{floxed}-UBC-Cre-ER^{T2} mice. Vhl^{wt}-UBC-Cre-ER^{T2} (n = 3), Vhl^{floxed} (n = 6) and Vhl^{floxed}-UBC-Cre-ER^{T2} (n = 6) mice were administered tamoxifen as indicated in Figure 1. Gene expression was assessed by RT-PCR in the kidney (A), liver (B), brain (C) and heart (D). The expression of *Epo* and *Glut1* was normalized to that of *Hprt* and expressed as the change relative to Vhl^{floxed} mice. Statistical significance was assessed using a two-tailed Student's t-test (*, $p<0.05$; **, $p<0.01$).
doi:10.1371/journal.pone.0022589.g004

examination of tamoxifen-treated Vhl^{floxed}-UBC-Cre-ER^{T2} mice revealed marked splenomegaly, an indicator of increased activity of the oxygen-VHL/PHD/HIF sensing pathway, as seen in *Phd2* deficient and *Phd1:Phd3* double knock-out mice [19]. Tamoxifen-treated Vhl^{floxed}-UBC-Cre-ER^{T2} mice also rapidly show signs of skin erythema (Figure 3). Indeed, reddening of the paws and snouts can be apparent as early as the ninth day of tamoxifen administration (data not shown). This could reflect an increased blood flow to the skin as a consequence of local HIF-induced nitric oxide (NO) release and subsequent local vasodilatation as has been previously shown upon chronic epidermal *Vhl* deletion [30]. Boutin et al. also show that this increased cutaneous perfusion, as a consequence of epidermal *Vhl* gene inactivation, subsequently reduces liver/skin blood flow ratio leading to elevated hepatic *Epo*

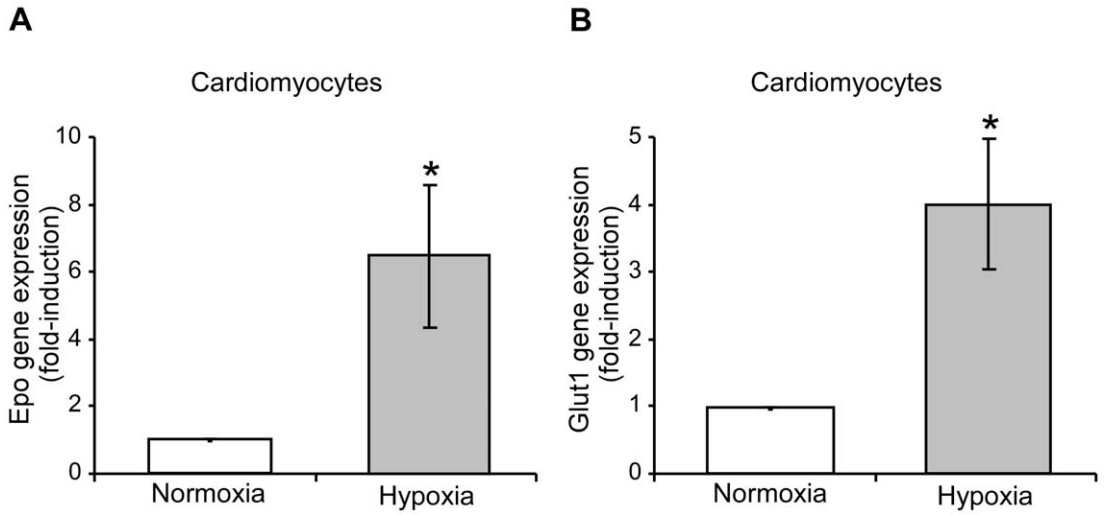

Figure 5. *Erythropoietin* and *glucose transporter-1* gene expression in isolated primary cardiomyocytes in response to hypoxia. Isolated rat cardiomyocyte cultures were subjected to basal normoxic conditions and/or hypoxia (1% O_2) for 24 hours. *Epo* (A) and *Glut1* (B) expression was then analyzed by RT-PCR and normalized to that of *Hprt*. The data from four independent experiments are expressed as the change relative to the normoxic values. Statistical significance was assessed using a two-tailed paired t-test (*, $p<0.05$).
doi:10.1371/journal.pone.0022589.g005

gene expression [30]. However, the increased hepatic *Epo* gene expression observed in tamoxifen-treated Vhl^{floxed}UBC-Cre-ER^{T2} mice is most likely a consequence of local *Vhl* gene deletion and HIF2α activation in liver.

It should be noted that other similar genetic systems have been developed to achieve inactivation of floxed alleles. Indeed, the tetracycline-dependent (Tet) system has been used for renal-specific Cre expression and subsequent inactivation of the tuberous sclerosis complex-1 (Tsc-1) when doxycycline is administered in the drinking water [31]. However, some difficulties in activating this doxycycline-dependent system in certain tissues have been reported [32,33,34]. By contrast, gene expression is significantly reduced in all the tissues analyzed from both Vhl^{floxed}-UBC-Cre-ER^{T2} and $Hif1\alpha^{floxed}$-UBC-Cre-ER^{T2} mouse lines exposed to tamoxifen diet.

Tamoxifen-treated Vhl^{floxed}-UBC-Cre-ER^{T2} mice have identified the heart as an additional site of EPO production upon *Vhl* inactivation. Indeed, the baseline expression of the *Epo* gene in the heart is weak but is elevated dramatically upon inactivation of *Vhl* gene expression. Experiments on isolated neonatal rat cardiomy-

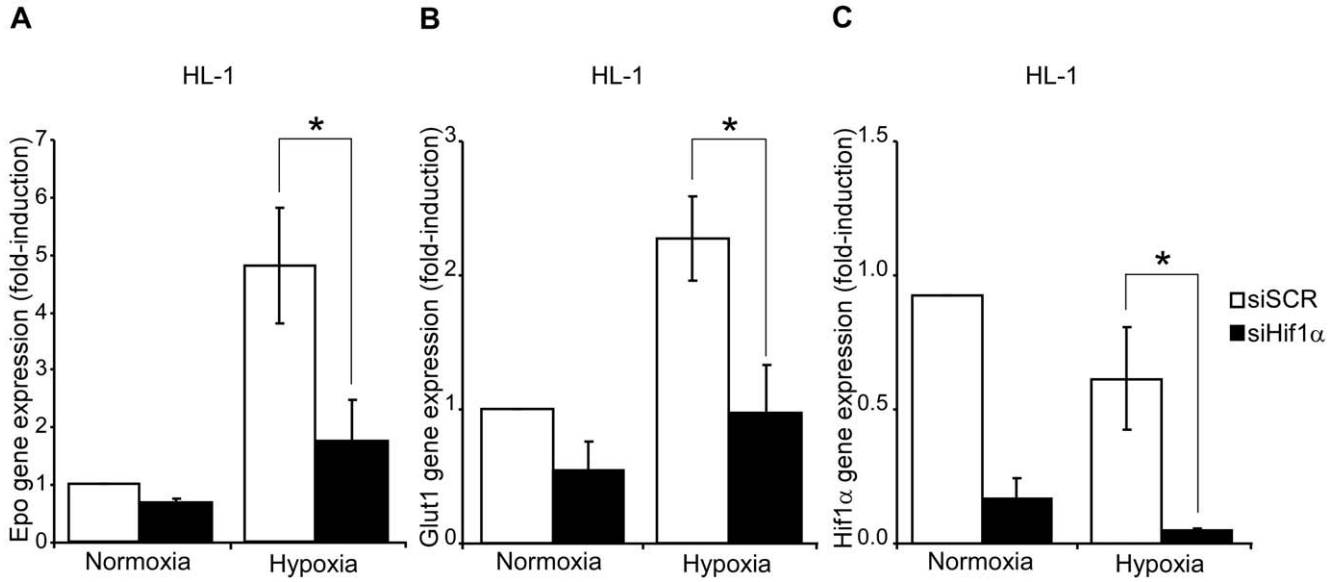

Figure 6. *Erythropoietin* and *glucose transporter-1* gene expression in HL-1 cardiomyocyte cell line in response to activation of the oxygen-sensing HIF pathway. (A,B,C) HL-1 cells were transfected with a siRNA for *Hif1α* (siHIF1α) or a scrambled siRNA control (siSCR) and 24 hours after transfection, the cells were exposed to normoxic or hypoxic (1% O_2) conditions. The expression of *Epo*, *Glut1* and *Hif1α* was measured as described above and the data from three independent experiments are expressed as the change relative to the normoxic values. Statistical significance was assessed using a two-tailed Student's t-test (*, $p<0.05$).
doi:10.1371/journal.pone.0022589.g006

ocytes revealed that EPO upregulation is an autonomous cardiomyocyte response to hypoxia that is mediated by the oxygen-sensing VHL/HIF pathway. This response is also observed in the HL-1 cardiac cell line, an experimental model suitable to study EPO production in adult cardiac cells. HL-1 is a cardiac cell line derived from the AT-1 adult mouse atrial cardiomyocyte tumor lineage, and these cells retain a differentiated cardiac myocyte phenotype and they maintain contractile activity [26]. Moreover, erythropoietin production has been demonstrated after myocardial infarction [35], which on the basis of our data could be mediated by cardiac HIF activation.

HIF1α gene expression is higher than HIF2α in HL-1 cells, which may explain the predominant contribution of HIF1α to hypoxia-induced *Epo* gene expression in these cardiac cells. However, the relative contribution of each isoform may differ *in vivo* and indeed, immunohistological studies have identified both HIF1α and HIF2α in cardiomyocytes of mice subjected to ischemia or atmospheric hypoxia [36,37,38,39,40]. Hif1α^{floxed} mice expressing Cre driven by myosin light chain 2v (MLC2v) cardiac promoter (Hif1α^{floxed}-MLC2v-Cre mice) markedly reduced HIF1α mRNA and protein expression in the heart, providing genetic evidence of *Hif1α* gene expression in cardiomyocytes [36]. Several studies have demonstrated a critical role for HIF1α in multiple cardiac oxygen-sensing pathways *in vivo* [29,36,41]. Thus, HIF1α could potentially drive cardiac *Epo* gene expression upon *Vhl* gene inactivation. However, HIF2α is the main contributor to HIF-induced *Epo* gene expression upon *Vhl* gene inactivation in the kidney, liver and glial cells [22,25,42,43]. Further studies will therefore be required to assess the relative contribution of these isoforms *in vivo*, and especially that of HIF2α to VHL/HIF-dependent cardiac EPO expression. It should be also noted that HIF1α and HIF2α are also found in cardiac stromal cells. Indeed, cardiac endothelial cells abundantly express both HIF isoforms when oxygen supply to myocardium becomes limited, as do cells in the vessel wall that are presumably smooth muscle cells, [36,37,38,39,40]. Therefore, cardiac *Epo* gene expression upon *Vhl* gene inactivation involves HIF activation in cardiomyocytes, although we cannot rule out the involvement of HIF activation in other cardiac cell types.

Elevation of cardiac *Epo* gene expression is very remarkable, although it occurs to a lesser extent than in the liver and kidney. Therefore, it is conceivable that cardiac EPO production serves a local autocrine or paracrine function when oxygen supply to cardiac tissue becomes limited. Indeed, several studies have shown that EPO protects cardiac tissue during ischemia and the ischemia-reperfusion insult, particularly by overactivating the serine threonine kinase AKT, as well as through other pathways involving sonic hedgehog [44,45,46]. Indeed, the myocardium of patients undergoing bypass is protected when pyruvate, a previously recognized suppressor of PHD activity, is used [47], which correlates with a remarkable upregulation of *Epo* gene expression [48]. However, the effect of pyruvate on *Epo* gene expression was not directly assessed in cardiac cells, nor was the direct contribution of HIF activity, as we have studied in this work. Furthermore, cardiac tolerance to ischemic damage induced by ischemic preconditioning in the heart involves HIF1α mediated upregulation of key cardioprotective molecules, such as ecto-5′-nucleotidase CD73 that generates adenosine, and the A2B adenosine receptor (A2BAR) [49]. Therefore, the cardiac oxygen-sensing VHL/HIF/EPO pathway may represent an endogenous cardioprotective response that works in tandem with other pathways (e.g. adenosine) to locally induce cardiomyocyte tolerance against ischemia or ischemia-reperfusion damage.

Materials and Methods

Ethics Statement

All the experimental procedures were approved by the Research Ethics Committee at the UAM (Autonomous University of Madrid) and they were carried out under the supervision of the Head of Animal Welfare and Health at the UAM in accordance with Spanish and European guidelines (B.O.E, 18 March 1988, and 86/609/EEC European Council Directives).

Cell culture and hypoxic conditions

The murine HL-1 cardiac cell line was cultured in Claycomb medium [26] containing 10% heat-inactivated Fetal Bovine Serum (FBS: Cambrex) and supplemented with 0.1 mM norepinephrine (Sigma) and 2 mM GLUTAMAX-I (Invitrogen). Cells were plated on gelatin (Difco) and fibronectin (Sigma) precoated surfaces, and cultured at 37°C for 16 hours. Neonatal rat cardiomyocytes were isolated from the hearts of 1 day-old Wistar rats using the Neomyt isolation system (Cellutron Life Technologies). To remove contaminating cardiac fibroblasts, dissociated cells were pre-plated for 1 hour on uncoated culture plates. The resulting suspension of cardiomyocytes was plated (2–3 million cells/60 mm plate) and cultured for 24 hours in medium supplemented with 10% FBS and 10 mM 5-bromo-2′-deoxyuridine (BrdU; Sigma, B5002), and then for an additional 24 hours in serum-free conditions. The cells were subjected to hypoxia in DMEM + 10% FBS. All media were supplemented with 100 U/ml penicillin, 100 µg/ml streptomycin and 1% HEPES buffer. Normoxic cells (21% O_2) were maintained at 37°C in an incubator with 5% CO_2. To induce hypoxia, cell culture dishes were placed into an Invivo$_2$ 400 humidified hypoxia workstation (Ruskinn Technologies, Bridgend, UK) with 1% O_2.

Mice

C;129S-*Vhlh*^{tm1Jae}/J mice (Jackson Laboratories, stock no. 4081) were used to generate the Vhl^{floxed}-UBC-Cre-ER^{T2} mice. These mice harbor two loxP sites flanking the promoter and exon 1 of the murine *Vhl* locus [50]. C;129S-*Vhlh*^{tm1Jae}/J mice were crossed with B6.Cg-Tg(UBC-Cre/ER^{T2})1Ejb/J mice (Jackson Laboratories, stock no. 008085) which ubiquitously express a tamoxifen-inducible Cre recombinase (Cre-ER^{T2}), [13]. Vhl^{floxed}-UBC-Cre-ER^{T2} mice were generated through the appropriate crosses, along with the corresponding controls, Vhl^{wt}-UBC-Cre-ER^{T2} and Vhl^{floxed}. Hif1α^{floxed}-UBC-Cre-ER^{T2} mice were generated from B6.129-Hif1a^{tm3Rsjo}/J mice (Jackson Laboratories, stock no. 007561), which harbor two loxP sites flanking exon 2 of the murine *Hif1α* locus [51]. These mice were crossed with Tg(UBC-Cre/ER^{T2})1Ejb/J mice as described above to generate Hif1α^{floxed}-UBC-Cre-ER^{T2} mice and their corresponding controls, Hif1α^{wt}-UBC-Cre-ER^{T2} and Hif1α^{floxed} mice.

The mice were bred and housed in a specific pathogen free (SPF) animal area of the animal facility at the Autonomous University of Madrid (UAM). For gene inactivation, Vhl^{wt}-UBC-Cre-ER^{T2}, Hif1α^{wt}-UBC-Cre-ER^{T2} and the corresponding control males (10–5 weeks old) were fed *ad libitum* for ten days with Teckland CRD TAM^{400}/CreER tamoxifen pellets (Harlan Teklad), which contain 400 mg tamoxifen citrate/kg. Subsequently, they were returned to a diet of standard mouse chow (Safe®, Augy, France) for an additional 10 days.

Reticulocyte counts and hematocrit measurement

The number of circulating or splenic reticulocytes was determined by counting total blood or splenic cells respectively followed by a flow cytometry analysis to determine the proportion of reticulocytes identified as CD71 positive cells (using the anti-

CD71-PE, Beckton-Dickinson) and low intracellular nucleic acid content (using the DNA dye Hoechst 33342) [52]. Similarly, splenic mature erythrocytes were identified as CD71 negative and Hoechst 33342 negative cells [52]. Hematocrit measurements were performed using a hemocytometer (apparatus SYSMEX KX-21N).

Quantitative real-time PCR analysis and primers

Mice were anaesthetized by intraperitoneal administration of ketamine (Ketolar® 50 mg/ml) and xylazine (Rompun® 20 mg/ml), and the tissues of interest were then removed and snap-frozen in liquid nitrogen. Subsequently, the tissue was homogenized in Trizol (Invitrogen) with two freeze/thaw cycles and total RNA was isolated using the RNeasy RNA extraction kit (Qiagen). cDNA was prepared by reverse transcription of RNA (1 μg) using Improm-II reverse transcriptase (Promega), and polymerase chain reaction (PCR) amplification was performed using a Power SYBR Green PCR Master Mix kit (Applied Biosystems). The following primer sets were used: mouse VHL (forward, 5′-TCAGCCCTACCCGATCTTACC-3′; reverse, 5′-ATCCCTGAAGAGCCAAAGATGA-3′); mouse HIF-1α (forward, 5′-CACCGATTCGCCATGGA-3′; reverse, 5′-TCGACGTTCAGAACTCATCTTTTTT-3′); rat HIF-1α (forward, 5′-GTCCTGTGGTGACTTGTCCTT-3′; reverse, 5′-TGGACTC TGATCATCTGACCAAA-3′); mouse erythropoietin (EPO) (forward, 5′-TCATCTGCGACAGTCGAGTTCT-3′; reverse, 5′-TTTTCACTCAGTCTGGGACCTTCT-3′); rat erythropoietin (EPO) (forward, 5′-CAAGGAGGCAGAAAATGTCACA-3′; reverse, 5′-TTTCCAAGCGTAG AAGTTGACTTTG-3′); mouse glucose transporter 1 (GLUT1) (forward, 5′-CGCAACGAGGAGAACC-3′; reverse, 5′-GCCGTG TTGACGATACC-3′); hypoxanthine-guanine phosphoribosyltransferase (HPRT) (forward, 5′-GTTAAGCAGTACAGCCCCAAA-3′; reverse, 5′-AGGGCATATCCAACAAC AAACTT-3′). The data were analyzed using StepOne Software version 2.0 (Applied Biosystems).

siRNA transfection

HL-1 cells were transfected with a siRNA targeting mouse HIF-1α (50 nM, sc-44225: Santa Cruz) or a scrambled control siRNA (sc-37007), using Lipofectamine 2000 (Invitrogen) according to the manufacturer's instructions. 24 hours after transfection the cells were exposed to normoxic or hypoxic conditions for an additional 24 hours.

Statistical analysis

The data are presented as the mean ± SEM. Statistical significance was assessed using a two-tailed Student's t-test in all figures, except in Figures 6A and B in which a two-tailed paired t-test was used.

Acknowledgments

The authors would like to thank Dr. L. del Peso, Dr. M.J. Calzada and Victoria Rodriguez for critical reading of the manuscript. The HL-1 cardiomyocyte cell line was kindly provided by Dr. Wiliam C. Claycomb (LSU Health Science Center, New Orleans, LA, USA).

Author Contributions

Conceived and designed the experiments: MM-M AE IS-A LA-A JA. Performed the experiments: MM-M AE IS-A LA-A AV-V SV. Analyzed the data: MM-M AE IS-A MOL JA. Contributed reagents/materials/analysis tools: AO EB AV-V SV EF CF-C. Wrote the paper: MM-M AE IS-A LA-A MOL JA.

References

1. Giaccia A, Siim BG, Johnson RS (2003) HIF-1 as a target for drug development. Nat Rev Drug Discov 2: 803–811.
2. Ivan M, Kondo K, Yang H, Kim W, Valiando J, et al. (2001) HIFalpha targeted for VHL-mediated destruction by proline hydroxylation: implications for O2 sensing. Science 292: 464–468.
3. Jaakkola P, Mole DR, Tian YM, Wilson MI, Gielbert J, et al. (2001) Targeting of HIF-alpha to the von Hippel-Lindau ubiquitylation complex by O2-regulated prolyl hydroxylation. Science 292: 468–472.
4. Bruick RK, McKnight SL (2001) A conserved family of prolyl-4-hydroxylases that modify HIF. Science 294: 1337–1340.
5. Epstein AC, Gleadle JM, McNeill LA, Hewitson KS, O'Rourke J, et al. (2001) C. elegans EGL-9 and mammalian homologs define a family of dioxygenases that regulate HIF by prolyl hydroxylation. Cell 107: 43–54.
6. Semenza GL (2007) Hypoxia-inducible factor 1 (HIF-1) pathway. Sci STKE 2007: cm8.
7. Eckardt KU, Kurtz A (2005) Regulation of erythropoietin production. Eur J Clin Invest 35(Suppl 3): 13–19.
8. Fandrey J, Bunn HF (1993) In vivo and in vitro regulation of erythropoietin mRNA: measurement by competitive polymerase chain reaction. Blood 81: 617–623.
9. Goldberg MA, Imagawa S, Strair RK, Bunn HF (1991) Regulation of the erythropoietin gene in Hep 3B cells. Semin Hematol 28: 35–40; discussion 40-31: .
10. Imagawa S, Goldberg MA, Bunn HF (1989) Regulation of the erythropoietin gene. Adv Exp Med Biol 271: 75–85.
11. Gnarra JR, Ward JM, Porter FD, Wagner JR, Devor DE, et al. (1997) Defective placental vasculogenesis causes embryonic lethality in VHL-deficient mice. Proc Natl Acad Sci U S A 94: 9102–9107.
12. Feil R, Wagner J, Metzger D, Chambon P (1997) Regulation of Cre recombinase activity by mutated estrogen receptor ligand-binding domains. Biochem Biophys Res Commun 237: 752–757.
13. Ruzankina Y, Pinzon-Guzman C, Asare A, Ong T, Pontano L, et al. (2007) Deletion of the developmentally essential gene ATR in adult mice leads to age-related phenotypes and stem cell loss. Cell Stem Cell 1: 113–126.
14. Casanova E, Fehsenfeld S, Lemberger T, Shimshek DR, Sprengel R, et al. (2002) ER-based double iCre fusion protein allows partial recombination in forebrain. Genesis 34: 208–214.
15. Forde A, Constien R, Grone HJ, Hammerling G, Arnold B (2002) Temporal Cre-mediated recombination exclusively in endothelial cells using Tie2 regulatory elements. Genesis 33: 191–197.
16. Kiermayer C, Conrad M, Schneider M, Schmidt J, Brielmeier M (2007) Optimization of spatiotemporal gene inactivation in mouse heart by oral application of tamoxifen citrate. Genesis 45: 11–16.
17. Ma W, Tessarollo L, Hong SB, Baba M, Southon E, et al. (2003) Hepatic vascular tumors, angiectasis in multiple organs, and impaired spermatogenesis in mice with conditional inactivation of the VHL gene. Cancer Res 63: 5320–5328.
18. Young AP, Schlisio S, Minamishima YA, Zhang Q, Li L, et al. (2008) VHL loss actuates a HIF-independent senescence programme mediated by Rb and p400. Nat Cell Biol 10: 361–369.
19. Takeda K, Aguila HL, Parikh NS, Li X, Lamothe K, et al. (2008) Regulation of adult erythropoiesis by prolyl hydroxylase domain proteins. Blood 111: 3229–3235.
20. Heinicke K, Baum O, Ogunshola OO, Vogel J, Stallmach T, et al. (2006) Excessive erythrocytosis in adult mice overexpressing erythropoietin leads to hepatic, renal, neuronal, and muscular degeneration. Am J Physiol Regul Integr Comp Physiol 291: R947–956.
21. Vogel J, Kiessling I, Heinicke K, Stallmach T, Ossent P, et al. (2003) Transgenic mice overexpressing erythropoietin adapt to excessive erythrocytosis by regulating blood viscosity. Blood 102: 2278–2284.
22. Rankin EB, Biju MP, Liu Q, Unger TL, Rha J, et al. (2007) Hypoxia-inducible factor-2 (HIF-2) regulates hepatic erythropoietin in vivo. J Clin Invest 117: 1068–1077.
23. Zanjani ED, Ascensao JL, McGlave PB, Banisadre M, Ash RC (1981) Studies on the liver to kidney switch of erythropoietin production. J Clin Invest 67: 1183–1188.
24. Chen C, Pore N, Behrooz A, Ismail-Beigi F, Maity A (2001) Regulation of glut1 mRNA by hypoxia-inducible factor-1. Interaction between H-ras and hypoxia. J Biol Chem 276: 9519–9525.
25. Weidemann A, Kerdiles YM, Knaup KX, Rafie CA, Boutin AT, et al. (2009) The glial cell response is an essential component of hypoxia-induced erythropoiesis in mice. J Clin Invest 119: 3373–3383.
26. White SM, Constantin PE, Claycomb WC (2004) Cardiac physiology at the cellular level: use of cultured HL-1 cardiomyocytes for studies of cardiac muscle cell structure and function. Am J Physiol Heart Circ Physiol 286: H823–829.

27. Mole DR, Ratcliffe PJ (2008) Cellular oxygen sensing in health and disease. Pediatr Nephrol 23: 681–694.
28. Semenza GL (2002) Involvement of hypoxia-inducible factor 1 in human cancer. Intern Med 41: 79–83.
29. Lei L, Mason S, Liu D, Huang Y, Marks C, et al. (2008) Hypoxia-inducible factor-dependent degeneration, failure, and malignant transformation of the heart in the absence of the von Hippel-Lindau protein. Mol Cell Biol 28: 3790–3803.
30. Boutin AT, Weidemann A, Fu Z, Mesropian L, Gradin K, et al. (2008) Epidermal sensing of oxygen is essential for systemic hypoxic response. Cell 133: 223–234.
31. Traykova-Brauch M, Schonig K, Greiner O, Miloud T, Jauch A, et al. (2008) An efficient and versatile system for acute and chronic modulation of renal tubular function in transgenic mice. Nat Med 14: 979–984.
32. Hochedlinger K, Yamada Y, Beard C, Jaenisch R (2005) Ectopic expression of Oct-4 blocks progenitor-cell differentiation and causes dysplasia in epithelial tissues. Cell 121: 465–477.
33. Hsiao EC, Nguyen TD, Ng JK, Scott MJ, Chang WC, et al. (2011) Constitutive Gs activation using a single-construct tetracycline-inducible expression system in embryonic stem cells and mice. Stem Cell Res Ther 2: 11.
34. Katsantoni EZ, Anghelescu NE, Rottier R, Moerland M, Antoniou M, et al. (2007) Ubiquitous expression of the rtTA2S-M2 inducible system in transgenic mice driven by the human hnRNPA2B1/CBX3 CpG island. BMC Dev Biol 7: 108.
35. Mengozzi M, Latini R, Salio M, Sfacteria A, Piedimonte G, et al. (2006) Increased erythropoietin production after myocardial infarction in mice. Heart 92: 838–839.
36. Huang Y, Hickey RP, Yeh JL, Liu D, Dadak A, et al. (2004) Cardiac myocyte-specific HIF-1alpha deletion alters vascularization, energy availability, calcium flux, and contractility in the normoxic heart. Faseb J 18: 1138–1140.
37. Jurgensen JS, Rosenberger C, Wiesener MS, Warnecke C, Horstrup JH, et al. (2004) Persistent induction of HIF-1alpha and -2alpha in cardiomyocytes and stromal cells of ischemic myocardium. Faseb J 18: 1415–1417.
38. Kim CH, Cho YS, Chun YS, Park JW, Kim MS (2002) Early expression of myocardial HIF-1alpha in response to mechanical stresses: regulation by stretch-activated channels and the phosphatidylinositol 3-kinase signaling pathway. Circ Res 90: E25–33.
39. Stroka DM, Burkhardt T, Desbaillets I, Wenger RH, Neil DA, et al. (2001) HIF-1 is expressed in normoxic tissue and displays an organ-specific regulation under systemic hypoxia. Faseb J 15: 2445–2453.
40. Wiesener MS, Jurgensen JS, Rosenberger C, Scholze CK, Horstrup JH, et al. (2003) Widespread hypoxia-inducible expression of HIF-2alpha in distinct cell populations of different organs. Faseb J 17: 271–273.
41. Cai Z, Zhong H, Bosch-Marce M, Fox-Talbot K, Wang L, et al. (2008) Complete loss of ischaemic preconditioning-induced cardioprotection in mice with partial deficiency of HIF-1 alpha. Cardiovasc Res 77: 463–470.
42. Kapitsinou PP, Liu Q, Unger TL, Rha J, Davidoff O, et al. (2010) Hepatic HIF-2 regulates erythropoietic responses to hypoxia in renal anemia. Blood 116: 3039–3048.
43. Warnecke C, Zaborowska Z, Kurreck J, Erdmann VA, Frei U, et al. (2004) Differentiating the functional role of hypoxia-inducible factor (HIF)-1alpha and HIF-2alpha (EPAS-1) by the use of RNA interference: erythropoietin is a HIF-2alpha target gene in Hep3B and Kelly cells. Faseb J 18: 1462–1464.
44. Camici GG, Stallmach T, Hermann M, Hassink R, Doevendans P, et al. (2007) Constitutively overexpressed erythropoietin reduces infarct size in a mouse model of permanent coronary artery ligation. Methods Enzymol 435: 147–155.
45. Burger D, Xenocostas A, Feng QP (2009) Molecular basis of cardioprotection by erythropoietin. Curr Mol Pharmacol 2: 56–69.
46. Ueda K, Takano H, Niitsuma Y, Hasegawa H, Uchiyama R, et al. (2010) Sonic hedgehog is a critical mediator of erythropoietin-induced cardiac protection in mice. J Clin Invest 120: 2016–2029.
47. Lu H, Dalgard CL, Mohyeldin A, McFate T, Tait AS, et al. (2005) Reversible inactivation of HIF-1 prolyl hydroxylases allows cell metabolism to control basal HIF-1. J Biol Chem 280: 41928–41939.
48. Ryou MG, Flaherty DC, Hoxha B, Sun J, Gurji H, et al. (2009) Pyruvate-fortified cardioplegia evokes myocardial erythropoietin signaling in swine undergoing cardiopulmonary bypass. Am J Physiol Heart Circ Physiol 297: H1914–1922.
49. Eckle T, Kohler D, Lehmann R, El Kasmi K, Eltzschig HK (2008) Hypoxia-inducible factor-1 is central to cardioprotection: a new paradigm for ischemic preconditioning. Circulation 118: 166–175.
50. Haase VH, Glickman JN, Socolovsky M, Jaenisch R (2001) Vascular tumors in livers with targeted inactivation of the von Hippel-Lindau tumor suppressor. Proc Natl Acad Sci U S A 98: 1583–1588.
51. Ryan HE, Lo J, Johnson RS (1998) HIF-1 alpha is required for solid tumor formation and embryonic vascularization. Embo J 17: 3005–3015.
52. Chen SY, Wang Y, Telen MJ, Chi JT (2008) The genomic analysis of erythrocyte microRNA expression in sickle cell diseases. PLoS One 3: e2360.

Cell Metabolism
Article

Induction of the Mitochondrial NDUFA4L2 Protein by HIF-1α Decreases Oxygen Consumption by Inhibiting Complex I Activity

Daniel Tello,[1,5] Eduardo Balsa,[1,5] Bárbara Acosta-Iborra,[1] Esther Fuertes-Yebra,[1] Ainara Elorza,[1] Ángel Ordóñez,[1] María Corral-Escariz,[1] Inés Soro,[1] Elia López-Bernardo,[1] Ester Perales-Clemente,[2] Antonio Martínez-Ruiz,[1] José Antonio Enríquez,[2,3] Julián Aragonés,[1] Susana Cadenas,[1,4] and Manuel O. Landázuri[1,*]

[1]Servicio de Inmunología, Hospital Universitario de La Princesa, Universidad Autónoma de Madrid, Instituto de Investigación Sanitaria Princesa (IIS-IP), Madrid, 28006, Spain
[2]Centro Nacional de Investigaciones Cardiovasculares Carlos III (CNIC), Madrid, 28029, Spain
[3]Departamento de Bioquímica y Biología Molecular y Celular, Facultad de Ciencias, Universidad de Zaragoza, Zaragoza, 50013, Spain
[4]Departamento de Biología Molecular, Facultad de Ciencias, Universidad Autónoma de Madrid, Madrid, 28049, Spain
[5]These authors contributed equally to this work
*Correspondence: mortiz.hlpr@salud.madrid.org
DOI 10.1016/j.cmet.2011.10.008

SUMMARY

The fine regulation of mitochondrial function has proved to be an essential metabolic adaptation to fluctuations in oxygen availability. During hypoxia, cells activate an anaerobic switch that favors glycolysis and attenuates the mitochondrial activity. This switch involves the hypoxia-inducible transcription factor-1 (HIF-1). We have identified a HIF-1 target gene, the mitochondrial *NDUFA4L2* (NADH dehydrogenase [ubiquinone] 1 alpha subcomplex, 4-like 2). Our results, obtained employing NDUFA4L2-silenced cells and NDUFA4L2 knockout murine embryonic fibroblasts, indicate that hypoxia-induced NDUFA4L2 attenuates mitochondrial oxygen consumption involving inhibition of Complex I activity, which limits the intracellular ROS production under low-oxygen conditions. Thus, reducing mitochondrial Complex I activity via NDUFA4L2 appears to be an essential element in the mitochondrial reprogramming induced by HIF-1.

INTRODUCTION

Aerobic organisms have developed specific systems to deliver oxygen to cells in different anatomical locations. However, insufficient oxygen supply and the ensuing hypoxia is a hallmark of different pathological situations. In response to hypoxia, cells activate a metabolic program that reduces oxygen consumption by actively lowering mitochondrial oxidative phosphorylation (OXPHOS) activity, the main oxygen-consuming process in most cell types, accompanied by an increase in glucose uptake and the rate of glycolysis (Aragonés et al., 2008; Iyer et al., 1998; Kim et al., 2006; Papandreou et al., 2006). This hypoxic adaptation is due to the expression of genes triggered by hypoxia-inducible factors (HIFs) (Aragonés et al., 2009). HIFs are master transcription factors regulated in an O_2-dependent manner by a family of prolyl hydroxylases (PHDs), which use O_2 as a substrate to hydroxylate HIF-α subunits in conditions of normoxia (Kaelin and Ratcliffe, 2008). These hydroxylated substrates are then ubiquitinated after recognition by VHL, and they are degraded by the proteasome. By contrast, PHD activity is inhibited in hypoxic conditions, and accordingly, HIF-α subunits accumulate, heterodimerize with HIF-β, and activate the expression of HIF-dependent target genes (Schofield and Ratcliffe, 2004; Semenza, 2004, 2009).

Among the genes whose expression is upregulated by HIFs are glucose transporters, like *GLUT1*, as well as key enzymes involved in glycolysis (Iyer et al., 1998). The *PDK1* and *PDK3* genes that code for pyruvate dehydrogenase (PDH) kinases are also upregulated, which results in increased phosphorylation and inactivation of PDH, the enzyme that converts pyruvate to acetyl-CoA (Kim et al., 2006; Lu et al., 2008; Papandreou et al., 2006). This process limits the substrate available for the tricarboxylic acid cycle (TCA) and thus for OXPHOS activity. Mitochondrial respiration is also regulated by additional mechanisms that maximize respiratory efficiency under conditions of reduced O_2 availability. Genes that regulate cytochrome *c* oxidase (the ETC Complex IV that reduces O_2 to H_2O) are also regulated by HIFs, including *COX4-2* isoform and the *LON* protease, which produces a switch from isoform COX4-1 to COX4-2 that optimizes the efficiency of respiration under hypoxic conditions (Fukuda et al., 2007).

Complex I (NADH:ubiquinone oxidoreductase) is the largest and least understood component of the respiratory chain. This complex catalyzes the first step in the electron transport chain (ETC), transferring electrons from NADH to a noncovalently bound flavin mononucleotide (FMN) and then, via a series of iron-sulfur clusters (FeS), to the final ubiquinone acceptor. Complex I consists of 45 different subunits that are assembled into a structure of ~1 MDa, and while 7 subunits are encoded by mitochondrial DNA, the remaining 38 are coded for by the nuclear genome (Carroll et al., 2006). The activity of the Complex I is affected by hypoxia, either through posttranslational modification (Frost et al., 2005) or the reduced expression of mitochondrial genes (Chan et al., 2009). Here we report that HIF-1 induces the expression of the NADH dehydrogenase (ubiquinone) 1 alpha subcomplex subunit 4-like 2 gene (*NDUFA4L2*, also called

NADH-ubiquinone oxidoreductase MLRQ subunit homolog [*NUOMS*]), cataloged as a component of ETC Complex I due to its high sequence identity with *NDUFA4*. It was previously described using mRNA array technology that NDUFA4L2 is overexpressed in VHL-deficient cell lines and tumors (Favier et al., 2009; Papandreou et al., 2006), as well as in neuroblastoma cells in hypoxia (Fredlund et al., 2008) and in pathophysiological conditions like rheumatoid arthritis (Andreas et al., 2009). Although the physiological function of this protein remains unclear, we show here that it is involved in lowering mitochondrial oxygen consumption and Complex I activity, thereby reducing ROS production. This provides a point in the regulation of mitochondrial activity that can reprogram Complex I activity under low-oxygen conditions.

RESULTS

Hypoxia Induces the Mitochondrial Protein NDUFA4L2 in Primary Cultures and Tumor Cells In Vitro as well as In Vivo

We hypothesized that, as the principal electron acceptor, Complex I could be a key regulatory point in the control of the ETC during hypoxia. To identify Complex I components that might be regulated by moderate hypoxia, we used an mRNA array to analyze the expression of genes in HeLa cells maintained for short periods of time (6 hr) in 1% O_2. We detected the expression of 44 genes of Complex I in the array: 40 genes encoded by nuclear DNA and 4 encoded in the mitochondria (*ND1*, *ND2*, *ND3*, and *ND6*). Of all these genes, only *NDUFA4L2* was clearly induced by hypoxia, whereas the other genes encoded by nuclear DNA remained unchanged (Table S1). By contrast and as described previously (Piruat and López-Barneo, 2005), the other mitochondrially encoded genes underwent a marked downregulation in these hypoxic conditions (Table S1). It is important to note that *NDUFA4L2* gene is strongly induced by hypoxia. In fact, it appears among the first 12 genes more induced by hypoxia in the mRNA study (Table S2).

These microarray data were validated by RT-PCR on mRNA isolated from HeLa and PC-12 cells exposed to hypoxia. Indeed, RT-PCR assays confirmed that NDUFA4L2 expression was strongly upregulated in response to hypoxia (Figure 1A), while such conditions did not change the levels of other Complex I genes encoded in the nucleus, such as *NDUFA4*, *NDUFAB1*, or *NDUFB4*, although *ND1* and *ND6* expression was downregulated (Figure S1A). Upregulation of *NDUFA4L2* expression was also observed in HUVEC and cardiomyocytes subjected to hypoxia and after treatment with PHD inhibitors such as dimethyloxaloylglycine (DMOG) and deferroxamine (Figure 1B). The efficacy of hypoxia and DMOG in these experiments was corroborated by the marked upregulation of previously recognized HIF target genes such as *PHD3*, *BNIP3*, and *GLUT1* (Figure S1B). In addition, NDUFA4L2 expression was induced in brain tissue of mice exposed to 7.5% O_2 for 18 hr (Figure 1C). An increase in NDUFA4L2 protein was also evident in response to hypoxia in different cell types and brain tissue (Figure 1D) with an antibody specific to this protein that did not recognize the homologous NDUFA4 protein (Figure S1C). Moreover, the increase in NDUFA4L2 protein induced by hypoxia was evident in cardiomyocytes when assessed by immunofluorescence (Figure 1E).

We analyzed the cellular localization of NDUFA4L2 in normoxic and hypoxic conditions. A bioinformatics approach predicted that NDUFA4L2 would be localized in mitochondria (Table S3), and this prediction was then confirmed experimentally by analyzing mitochondrial and cytoplasmic fractions from HeLa cells. NDUFA4L2 was clearly enriched in the mitochondrial fraction under hypoxic conditions (Figure 1F), and immunofluorescence showed a clear colocalization of NDUFA4L2 and cytochrome *c* in HL-1 cells (Figure 1G), as well as the colocalization of NDUFA4L2 and the mitochondria-selective dye MitoTracker in HeLa cells (Figure S1D). These results confirmed the mitochondrial location of NDUFA4L2.

HIF-1α Regulates NDUFA4L2 Induction

To investigate whether hypoxia-induced *NDUFA4L2* expression was mediated by HIF transcription factors, we first silenced HIF-1β, the common partner of HIF-1α and HIF-2α, thereby impairing the canonical HIF transcriptional response. Interference of HIF-1β expression abolished the induction of *NDUFA4L2* during hypoxia (Figure 2A), as well as the response of *PHD3* (included as a control of HIF-target gene) (Figure S2A), indicating that HIF transcriptional activity is essential for *NDUFA4L2* induction.

To study the specific role of HIF-1α and HIF-2α in the response of *NDUFA4L2* to hypoxia, we performed RNA interference assays in human renal carcinoma RCC4 cells that constitutively stabilize HIF-1α and HIF-2α through the absence of VHL. Likewise, the response of NDUFA4L2 was also assessed in RCC4/VHL cells in which VHL expression was restored, and hence both HIF-1α and HIF-2α were exclusively upregulated in response to hypoxia. In line with the role of HIF activity in *NDUFA4L2* regulation, there was a robust upregulation of *NDUFA4L2* in hypoxic RCC4/VHL cells, whereas there was marked and constitutive *NDUFA4L2* expression in normoxic RCC4 cells that was only minimally upregulated in hypoxic conditions (Figure 2B). HIF-1α interference abrogated the expression of *NDUFA4L2* in both normoxic and hypoxic RCC4 cells (Figure 2B), as well as hypoxia-driven *NDUFA4L2* expression in RCC4/VHL cells (Figure 2B). By contrast, HIF-2α interference did not affect the expression of *NDUFA4L2* in RCC4/VHL cells exposed to hypoxia, and no significant effect was observed in RCC4 cells in either normoxic or hypoxic conditions (Figure 2B). The control experiments for the interference assays showed a specific reduction of *HIF-1α* or *HIF-2α* mRNA expression (Figure S2B).

We further confirmed these data in mouse embryonic fibroblasts (MEFs) from Hif-$1\alpha^{+f/+f}$/Cre conditional mice in which HIF-1α was lost after tamoxifen treatment. As a control, we employed tamoxifen Hif-$1\alpha^{+/+}$/Cre MEFs that lacked the CRE recombination sites required for HIF-1α ablation. The hypoxic induction of *Ndufa4l2* expression as well as that of the HIF target gene *Phd3* were only abrogated in Hif-$1\alpha^{+f/+f}$/Cre conditional MEFs following tamoxifen exposure, whereas they were still expressed in Hif-$1\alpha^{+/+}$/Cre MEFs (Figures 2C and S2C). Hence, the hypoxic induction of *Ndufa4l2* appeared to be mostly mediated by HIF-1α.

To identify possible hypoxia response elements (HREs) responsible for the induction of *NDUFA4L2*, the proximal promoter region (intron 1) of *NDUFA4L2* was analyzed, identifying

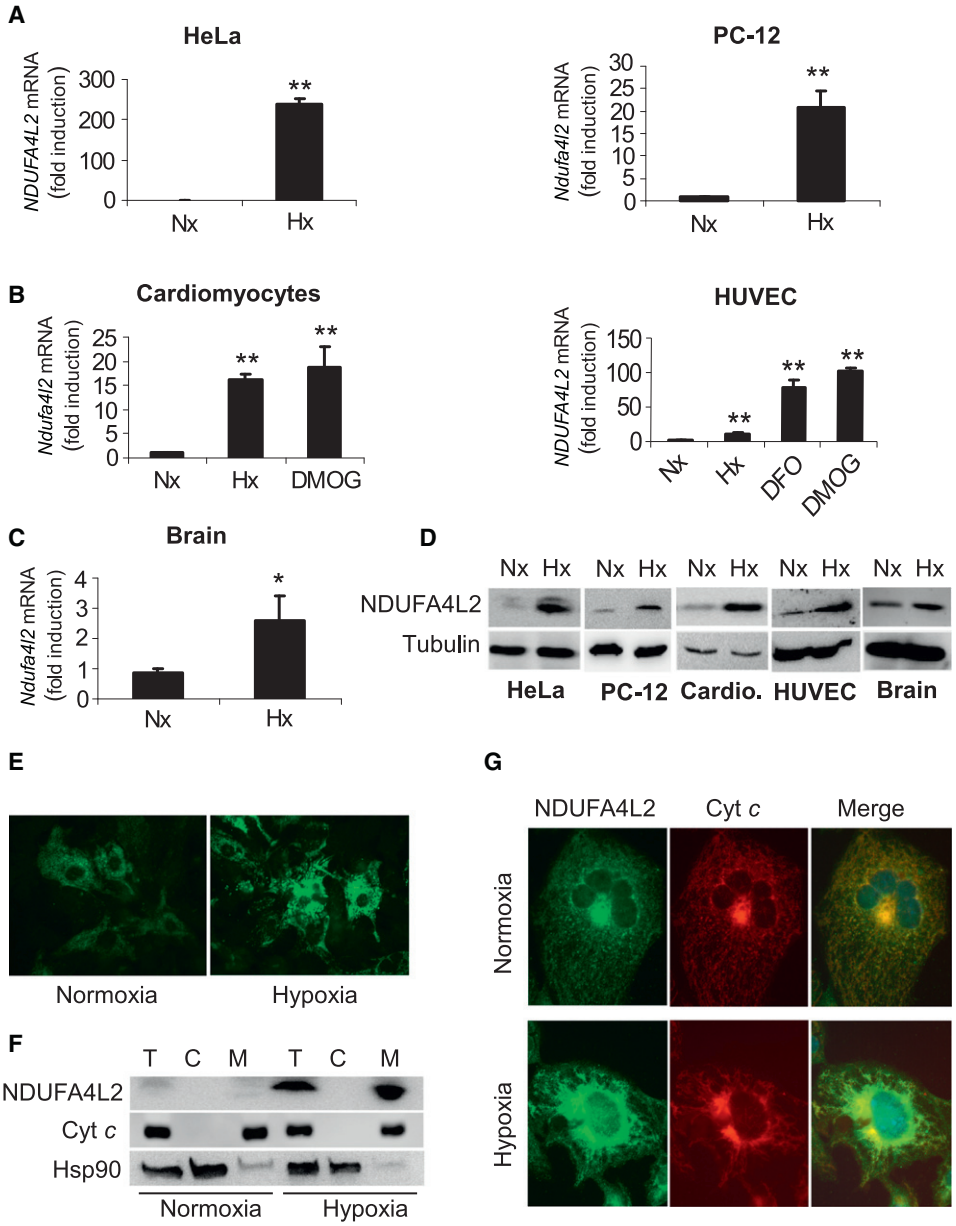

Figure 1. NDUFA4L2 Localizes to Mitochondria and Is Induced in Tumor Cells, in Primary Cultures, and In Vivo by Hypoxia

(A–C) Quantitative RT-PCR analysis of *NDUFA4L2* mRNA expression relative to the values in normoxia. HeLa, PC-12, cardiomyocytes, and HUVEC were cultured under conditions of normoxia or hypoxia (1% O_2) for 6 (HeLa) or 18 hr (PC-12, cardiomyocytes, HUVEC) (A and B). DMOG was added at 1 mM (cardiomyocytes) or 0.1 mM (HUVEC), and deferroxamine (DFO) was added at 0.2 mM in HUVEC (n = 3). Brain tissue from mice exposed to normoxic (n = 8) or hypoxic (7.5% O_2; n = 7) conditions for 18 hr is shown in (C).

(D) Immunoblot assay of NDUFA4L2 protein in HeLa, PC-12, HUVEC, or rat cardiomyocytes cultured under normoxic or hypoxic conditions (1% O_2 for cell cultures), as well as in brain tissue of mice subjected to hypoxia (7.5% O_2) for 18 hr. Tubulin is shown as a loading control. The images are representative of at least three experiments.

(E) Immunofluorescence showing the increase in NDUFA4L2 protein levels in rat cardiomyocytes exposed to normoxia or hypoxia (1% O_2) for 18 hr, with respect to those maintained in normoxic conditions. The images shown are representative of three experiments.

(F) Immunoblot assay of NDUFA4L2 in total cell (T), cytoplasmic (C), and mitochondrial (M) protein extracts from HeLa cells cultured under normoxic or hypoxic conditions (1% O_2) for 18 hr. Cytochrome *c* was assayed as a mitochondrial marker. The images shown are representative of three experiments.

(G) Immunofluorescence of HL-1 cells exposed to normoxia or hypoxia (1% O_2) for 18 hr. Images show staining for NDUFA4L2 (left panel, green) and cytochrome *c* (middle panel, red) and an overlay of the two signals (right panel). The images shown are representative of three experiments. See also Figure S1. n > 3; mean ± SEM; *p < 0.05; **p < 0.01.

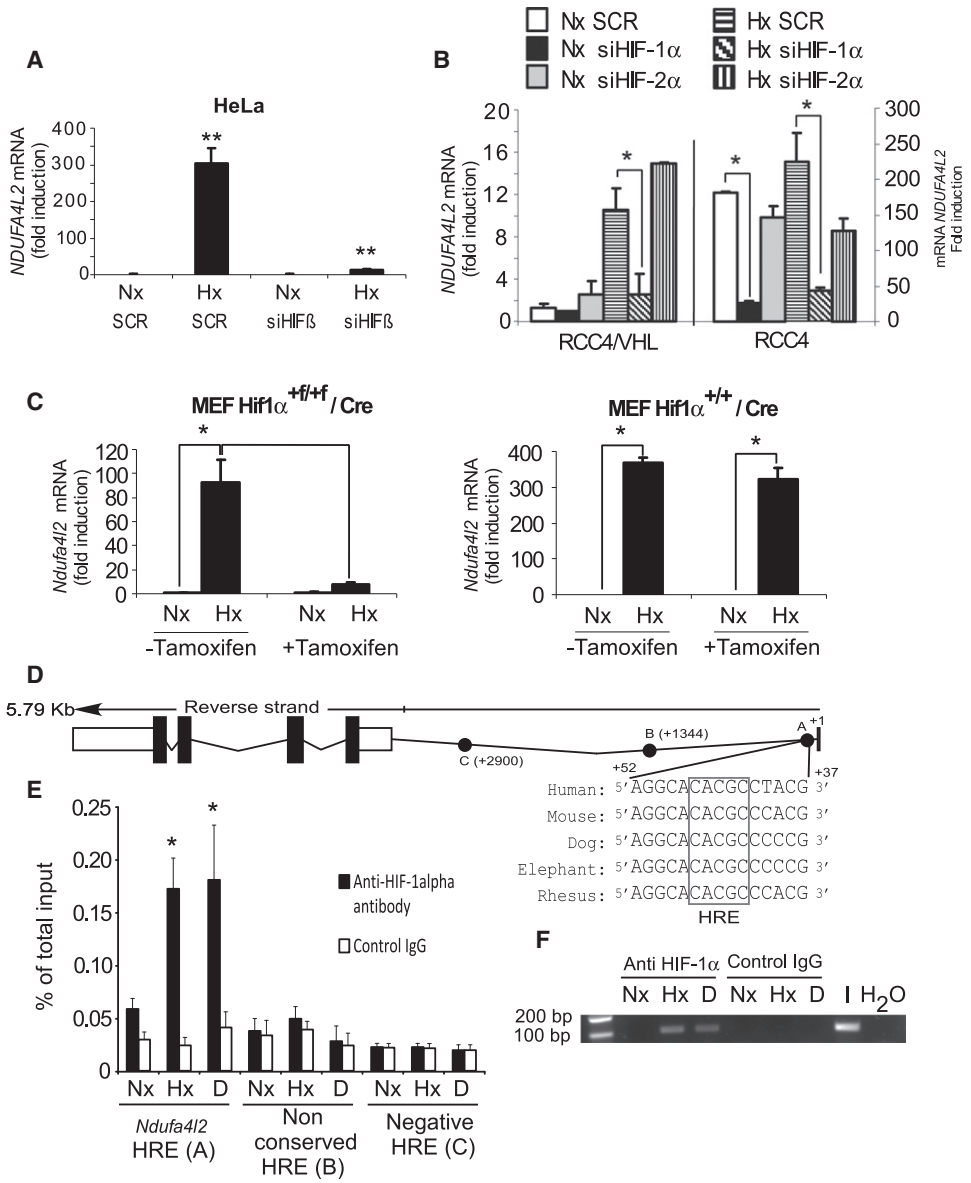

Figure 2. *NDUFA4L2* Induction Is Mediated by HIF-1α

(A) HeLa cells transfected with siRNA against HIF-β or a scramble control were cultured under normoxic or hypoxic (1% O_2) conditions for 24 hr. *NDUFA4L2* mRNA levels were quantified by real-time RT-PCR.

(B) VHL-deficient RCC4 cells or RCC4/VHL cells were transfected with siRNA against HIF-1α, HIF-2α, or a scramble control and exposed under normoxic or hypoxic conditions (1% O_2) for 24 hr. *NDUFA4L2* mRNA levels were quantified by real-time RT-PCR and are expressed relative to normoxic RCC4/VHL.

(C) Hif-1$\alpha^{+/+}$/Cre MEFs and Hif-1$\alpha^{+f/+f}$/Cre MEFs in the presence or absence of tamoxifen (1 μM) were cultured under normoxic or hypoxic conditions (1% O_2) for 18 hr. *NDUFA4L2* mRNA levels were quantified by real-time RT-PCR.

(D) Schematic representation of the human *NDUFA4L2* gene and the nucleotide sequences matching the consensus hypoxia response element (HRE) from five mammalian genes, indicating the regions A-B-C analyzed in the ChIP assay.

(E) ChIP assay of HIF-1α binding to the human *NDUFA4L2* gene in HeLa cells cultured in normoxic or hypoxic conditions (1% O_2) or exposed to DMOG (0.1 mM) for 6 hr. RT-PCR quantification is shown of regions A (putative NDUFA4L2 HRE), B (nonconserved HRE), and C (negative HRE) after immunoprecipitation with HIF-1α or a control antibody, represented as the percentage of that quantified in the total input DNA.

(F) Representative gel of DNA amplified in the ChIP assays shown in (E). See also Figure S2. n > 3; mean ± SEM; *p < 0.05; **p < 0.01.

two putative HREs at +43 and +1344 (Figure 2D). The +43 site is highly conserved between different species, unlike the +1344 site. Chromatin immunoprecipitation (ChIP) assays were performed on HeLa cells grown under normoxic or hypoxic conditions and after treatment with DMOG. To evaluate HIF-1α binding to *NDUFA4L2* regulatory sequences, quantitative PCR (qPCR) was performed using specific primers for the putative HRE site (A), the nonconserved HRE site (B), and a negative site (C). ChIP assays for *PDK1*, a well-known HIF-1α target, were also performed as a positive control (Figure S2D). HIF-1α

binding to the *NDUFA4L2* proximal promoter containing conserved HRE site (A) was strongly induced by hypoxia and DMOG treatment (Figure 2E), but not to the nonconserved HRE site (B) or the negative control region (C). The sequence amplified by qPCR had the expected size (Figure 2F). Taken together, these results suggest that *NDUFA4L2* is a direct HIF-1 target gene.

NDUFA4L2 Is Involved in the Hypoxia-Induced Decrease in Oxygen Consumption and Prevents Increases in Membrane Potential and ROS Production during Hypoxia

To test whether NDUFA4L2 is involved in the regulation of mitochondrial activity in hypoxia, we first determined the oxygen consumption in HeLa cells in which NDUFA4L2 was silenced by specific siRNA. In these experiments, *NDUFA4L2* expression was typically reduced by 80% in hypoxic conditions (Figure S3A) while *NDUFA4* mRNA levels were not affected by the siNDUFA4L2 (Figure S3B), highlighting the specificity of the interference of NDUFA4L2. Indeed, NDUFA4L2 interference reduced its protein expression in both normoxic and hypoxic conditions (Figure 3A), whereas the expression levels of proteins from other ETC complexes were unaffected by NDUFA4L2 interference (Figure S3C). Oxygen consumption decreased approximately 42% in hypoxic conditions when compared to normoxia in control HeLa cells (Figure 3B). However, oxygen consumption only decreased by 27% in hypoxic conditions when NDUFA4L2 was silenced in HeLa cells and when compared to control cells in normoxic conditions (Figure 3B). In normoxia, NDUFA4L2 silencing increased oxygen consumption by only 10%, probably due to the low normoxic levels of NDUFA4L2. We also tested whether transient overexpression of NDUFA4L2 might decrease oxygen consumption by using a pCMV-NDUFA4L2 vector to achieve expression levels similar to those obtained in hypoxia (Figures 3C and S3D). Transient overexpression of NDUFA4L2 decreased oxygen consumption in HeLa cells by approximately 20% (Figure 3D). Hence, we conclude that during hypoxia, NDUFA4L2 induction decreases oxygen consumption.

Since attenuation of mitochondrial activity in hypoxia may be a compensatory mechanism to keep mitochondrial ROS under control, we wondered whether hypoxia-driven NDUFA4L2 upregulation could also participate in this antioxidant response. Previous studies used the fluorescent dye H_2DCFDA and flow cytometry to demonstrate an increase of mitochondrial ROS production when cells are exposed to low O_2 tensions (Brunelle et al., 2005; Guzy et al., 2005; Mansfield et al., 2005). Accordingly, we observed increased H_2DCFDA fluorescence in HeLa cells exposed to hypoxia (1% O_2) that was exacerbated when NDUFA4L2 was silenced (Figure 3E). Similar data were obtained using the mitochondrial superoxide indicator MitoSOX (Figure 3F), which points to the mitochondrial origin of this increased superoxide production, probably from respiratory complexes. Increased ROS production in the absence of NDUFA4L2 during hypoxia correlated with an increased mitochondrial membrane potential in these conditions (Figure 3G). Conversely, NDUFA4L2 overexpression significantly decreased membrane potential compared to cells expressing the empty vector (Figure 3H).

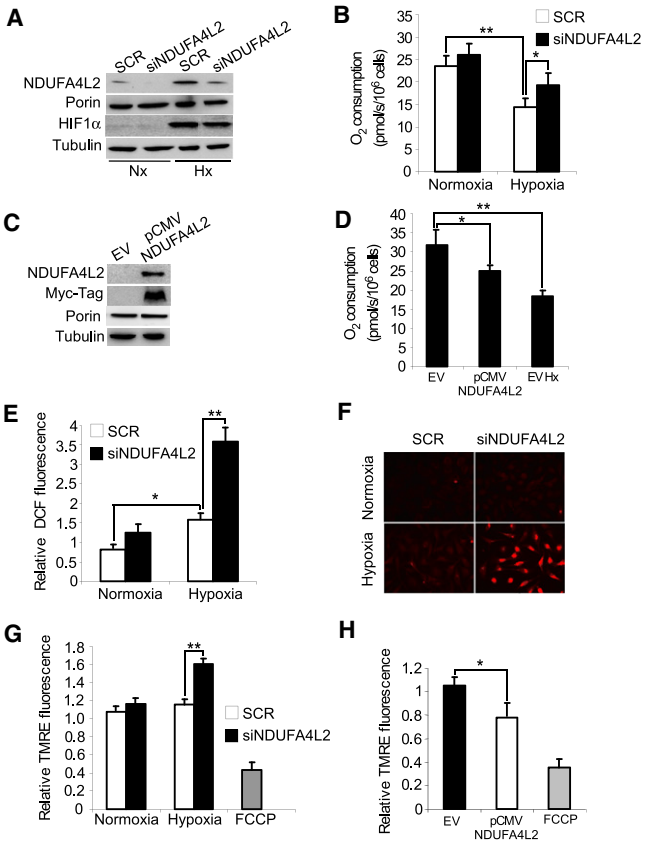

Figure 3. NDUFA4L2 Decreases Oxygen Consumption, Membrane Potential, and ROS Production in Hypoxia

(A–D) HeLa cells were transfected with a scramble control or NDUFA4L2 siRNA and exposed to normoxic or hypoxic (1% O_2) conditions for 18–24 hr. Immunoblot analysis of NDUFA4L2 and HIF-1α protein levels using tubulin and mitochondrial porin as loading controls is shown in (A). The images are representative of four independent experiments. Oxygen consumption rates were measured by high-resolution respirometry (B). HeLa cells were transfected with the empty vector (EV) or pCMV-NDUFA4L2 and then exposed to normoxic or hypoxic (1% O_2) conditions for 24 hr (C and D). Immunoblot analysis of NDUFA4L2 and myc-tagged protein levels using tubulin and mitochondrial porin as loading controls are shown (C). The images are representative of four independent experiments. Oxygen consumption rates were measured by high-resolution respirometry (D).

(E) Relative DCF fluorescence as a measure of intracellular hydrogen peroxide levels.

(F) Representative images of four independent experiments showing MitoSOX intensity as a measure of mitochondrial superoxide levels.

(G and H) Mitochondrial membrane potential was determined with the fluorescent probe TMRE and expressed relative to the control cells in normoxia. FCCP was used as a positive control of mitochondrial membrane depolarization (n > 3; mean ± SEM; *p < 0.05; **p < 0.01).

The Hypoxia-Induced Decrease in Oxygen Consumption via NDUFA4L2 Occurs through Complex I Inhibition

Given that NDUFA4L2 appears to be a mitochondrial protein involved in the downregulation of hypoxia-induced oxygen consumption, and that it likely belongs to the NDUFA4 subunit family of Complex I, we wondered whether NDUFA4L2 might be involved in actively regulating Complex I activity. We found that, when compared to normoxic conditions, Complex I activity

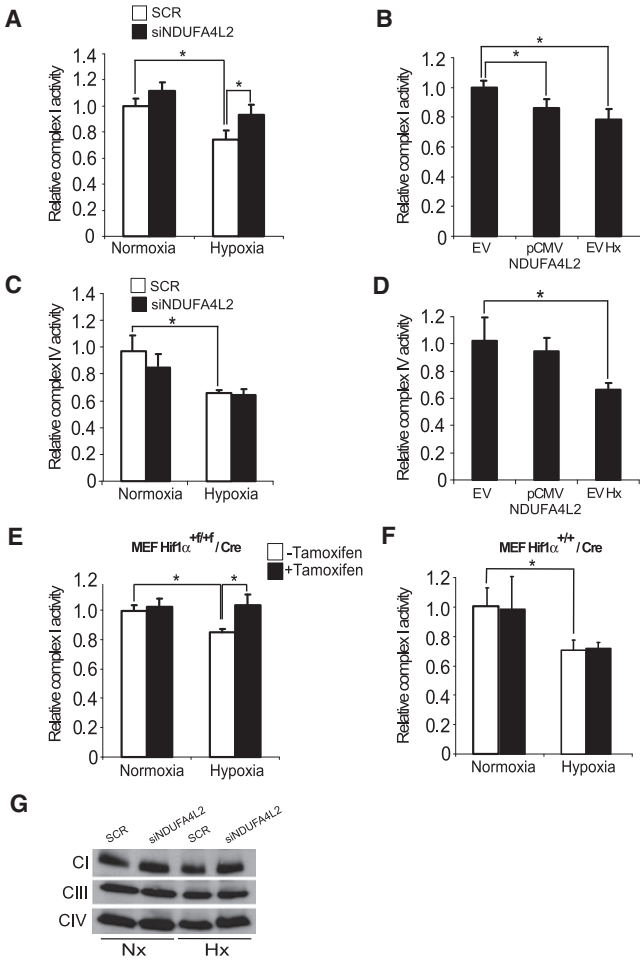

Figure 4. NDUFA4L2 Decreases Complex I Activity in Hypoxia

(A and B) Complex I activity was measured in HeLa cells transfected with a scramble control or NDUFA4L2 siRNA (A) or with the empty or pCMV-NDUFA4L2 vector (B), then exposed to normoxic or hypoxic (1% O_2) conditions for 24 hr.

(C and D) Complex IV activity was measured in HeLa cells transfected with a scramble control or NDUFA4L2 siRNA (C) and the empty or pCMV-NDUFA4L2 vector (D), then exposed to normoxic or hypoxic (1% O_2) conditions for 24 hr.

(E and F) Complex I activity was measured in Hif-1$\alpha^{+f/+f}$/Cre (E) or Hif-1$\alpha^{+/+}$/Cre MEFs (F) maintained in the presence or absence of tamoxifen (1 μM) for 48 hr and cultured under normoxic or hypoxic (1% O_2) conditions for 18 hr.

(G) Blue native PAGE (BN-PAGE) analysis of the mitochondrial OXPHOS Complex I (NDUFA9), Complex III (Core 2), and Complex IV (Col) from scramble and NDUFA4L2 siRNA HeLa cells exposed to normoxic or hypoxic (1% O_2) conditions for 24 hr (n > 3; mean ± SEM; *p < 0.05; **p < 0.01).

decreased ~20% in HeLa cells exposed to hypoxia (1% O_2 for 24 hr), although it did not when NDUFA4L2 expression was silenced (Figure 4A). Moreover, transient overexpression of NDUFA4L2 decreased Complex I activity in normoxic conditions (Figure 4B), demonstrating that NDUFA4L2 regulates Complex I under low-oxygen conditions.

To study the specificity of the effects of NDUFA4L2 on Complex I, we also measured Complex IV activity. Hypoxia (1% O_2 for 24 hr) induced a 38% decrease in Complex IV activity in HeLa cells (Figure 4C), but the silencing of NDUFA4L2 expression in hypoxia or its overexpression in normoxia did not affect Complex IV activity (Figures 4C and 4D). Similar results were obtained when Complex IV activity was determined spectrophotometrically (data not shown). Hence, NDUFA4L2 appears to affect ETC activity by specifically inhibiting Complex I. Since our results indicate that *NDUFA4L2* is a HIF-1α-dependent gene involved in the downregulation of Complex I activity in hypoxia, we further studied the role of HIF-1 in regulating Complex I. As expected, there was no decrease in Complex I activity following hypoxia in tamoxifen-treated Hif-1$\alpha^{+f/+f}$/Cre MEFs in which HIF-1α was ablated (Figure 4E). By contrast, a decrease in Complex I activity similar to that seen in HeLa cells was evident in tamoxifen-treated Hif-1$\alpha^{+/+}$/Cre MEFs (~20%) (Figure 4F). These results suggest that the HIF-1α-induced increase in NDUFA4L2 expression decreased oxygen consumption through the specific inhibition of mitochondrial Complex I activity.

Complex I activity can be modulated by its assembly (Vogel et al., 2005). We hypothesized that hypoxia-induced NDUFA4L2 could affect Complex I assembly. To test this possibility, we performed Blue native PAGE (BN-PAGE) in order to analyze the status of mitochondrial complexes. Neither hypoxia nor NDUFA4L2 silencing modified Complex I content, thus ruling out the involvement of NDUFA4L2 in the Complex I assembly process (Figure 4G).

Silencing of NDUFA4L2 Impairs Cell Proliferation in Hypoxia by Increasing Mitochondrial ROS Generation

While the absence of NDUFA4L2 does not significantly affect cell proliferation in normoxic conditions (Figure 5A), viable hypoxic NDUFA4L2-silenced HeLa cells proliferated at a slower rate than hypoxic control cells (Figure 5B). This slower proliferation was evident by both cell counting and by direct observation under the microscope (Figure 5C); it was also observed in other cell types such as HUVEC, UCD-Mel-N, and SKOV3 cells (Figure S4A). NDUFA4L2-silenced cells did not show either increased caspase-3 cleavage (Figure 5D) or changes in propidium iodide incorporation (Figure 5E), excluding the possibility that NDUFA4L2 silencing impaired cell proliferation by activating apoptosis. Additional studies showed that the capacity of hypoxic HeLa cells to form colonies in soft agar was affected when NDUFA4L2 was silenced, with a decrease in both the size and the number of colonies (Figure 5F). In order to investigate whether ROS overproduction in NDUFA4L2-silenced HeLa cells during hypoxia was responsible for the impairment in cell proliferation, we tested the effects of two different antioxidants, N-acetylcysteine (NAC) and MitoQ (an antioxidant targeted to mitochondria), on cell proliferation. Cell proliferation was restored when NDUFA4L2-silenced HeLa cells were treated with MitoQ in hypoxia (Figure 5G). This effect was also observed with NAC (Figure S4B), suggesting that exacerbated ROS production may be involved in the impairment of cell viability under hypoxia. Indeed, an increase in ROS production was detected in NDUFA4L2-silenced cells exposed to hypoxia using the mitochondrial superoxide indicator MitoSOX (Figure 5H). This increase was completely prevented by incubation with MitoQ (Figure 5H).

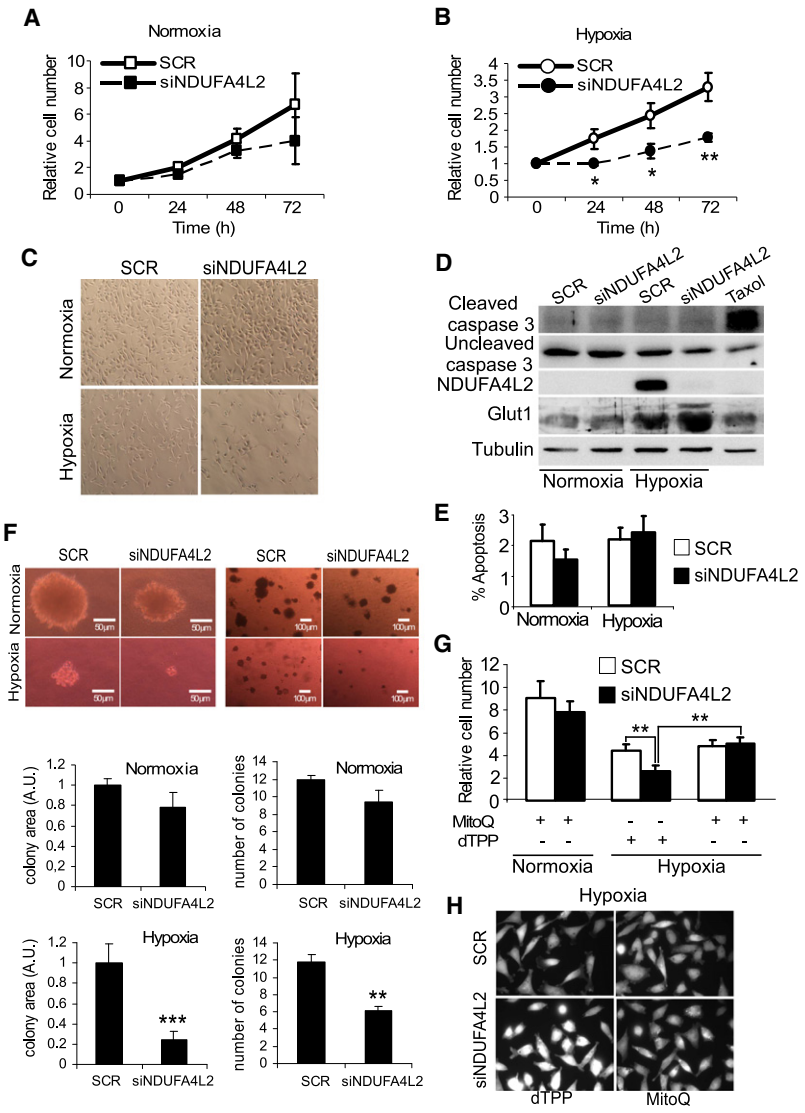

Figure 5. Reduced Hypoxic Levels of NDUFA4L2 Impair Cell Proliferation

(A and B) Growth curves of HeLa cells transfected with a scramble control or NDUFA4L2 siRNA in normoxic (A) and hypoxic (0.5% O_2) (B) conditions for different periods of time.

(C) Microscope images showing the density of HeLa cell cultures transfected with a scramble control or NDUFA4L2 siRNA and maintained under normoxic (21% O_2) or hypoxic (0.5% O_2) conditions for 72 hr.

(D) HeLa cells were transfected with either a scramble control or NDUFA4L2 siRNA and cultured under normoxic (21% O_2) or hypoxic (0.5% O_2) conditions for 72 hr, and the cell lysates were assayed in immunoblots that were probed with antibodies against NDUFA4L2, uncleaved caspase-3, and cleaved caspase-3. Glut1 was used as a positive control of hypoxic gene induction and tubulin as a loading control. Taxol was used as positive control of apoptosis.

(E) Scramble control or NDUFA4L2 siRNA HeLa cells maintained in normoxic (21% O_2) or hypoxic (0.5% O_2) conditions for 72 hr. The absolute value of apoptosis was measured by flow cytometry in cells stained with propidium iodide, as described in the Experimental Procedures.

(F) Image of colony formation by HeLa cells transfected with a scramble control or NDUFA4L2 siRNA in normoxic and hypoxic (0.5% O_2) conditions in soft agar for 15 days. Both size and number of colonies were quantified.

(G) Growth of HeLa cells transfected with a scramble control or NDUFA4L2 siRNA in normoxic and hypoxic (0.5% O_2) conditions with or without 0.5 μM MitoQ (0.5 μM dTPP was used as control of MitoQ) at 72 hr.

(H) Fluorescence microscopy images of hypoxic (0.5% O_2) cultured scramble and siNDUFA4L2 HeLa cells treated either with 0.5 μM MitoQ or 0.5 μM dTPP ($n > 3$; mean ± SEM; *$p < 0.05$; **$p < 0.01$).

Cell-cycle analysis showed that hypoxic NDUFA4L2-silenced HeLa cells had increased early S phase and decreased late S phase compared to scramble control cells (Figure S4C). Since NDUF4L2-silenced HeLa cells present ROS overproduction in hypoxia, and ROS can increase the phosphorylation of histone H2AX, a marker of cell stress (Driessens et al., 2009), we then analyzed the phosphorylation of H2AX histone. We observed increased phosho-H2AX levels in hypoxia when NDUFA4L2 was interfered (Figure S4D), suggesting that the lack of NDUFA4L2 in hypoxia produces cell stress.

It has been described that both the downregulation of the iron-sulfur cluster assembly proteins (ISCU1/2) via miR-210 and the upregulation of PDK1 are implicated in ROS control and cell viability in hypoxia (Chan et al., 2009; Chen et al., 2010; Favaro et al., 2010; Kim et al., 2006; Papandreou et al., 2006). To investigate the relative contribution of these effects to HeLa hypoxic adaptation, we performed cell proliferation assays. We only observed a decrease in ISCU1/2 protein at times over 24 hr at 0.5% (Figure S5A) but not in the milder hypoxic conditions (1% O_2). Furthermore, the overexpression of ISCU1/2 did not affect HeLa cell proliferation in hypoxia (0.5% O_2) at 72 hr (Figure S5B). In addition, HeLa cells in which PDK1 was silenced by specific siRNA (Figure S5C) showed a decrease in proliferation under hypoxia (0.5% O_2) at 72 hr (Figure S5D) similar to that observed in NDUFA4L2-silenced cells, suggesting that both NDUFA4L2 and PDK1 play an important role in ROS control and cell proliferation in our system conditions.

MEFs Obtained from NDUFA4L2 Knockout Mice Exhibit Higher Oxygen Consumption and Complex I Activity in Hypoxia Than Wild-Type MEFs

In order to gain further insight into the role of NDUFA4L2 on hypoxia-induced mitochondrial reprogramming, we generated NDUFA4L2 knockout (KO) mice. We initially planned to isolate primary cell cultures from NDUFA4L2-deficient adult mice. However, we found that homozygous *Ndufa4l2* gene inactivation results in perinatal lethality, which demonstrates an essential biological role of NDUFA4L2 in development that will be further explored in future studies. Therefore, we isolated NDUFA4L2-deficient MEFs and the corresponding wild-type controls from E12.5–14.5 embryos generated from NDUFA4L2$^{+/-}$ breeding pairs. In order to validate these MEF cultures, we analyzed the

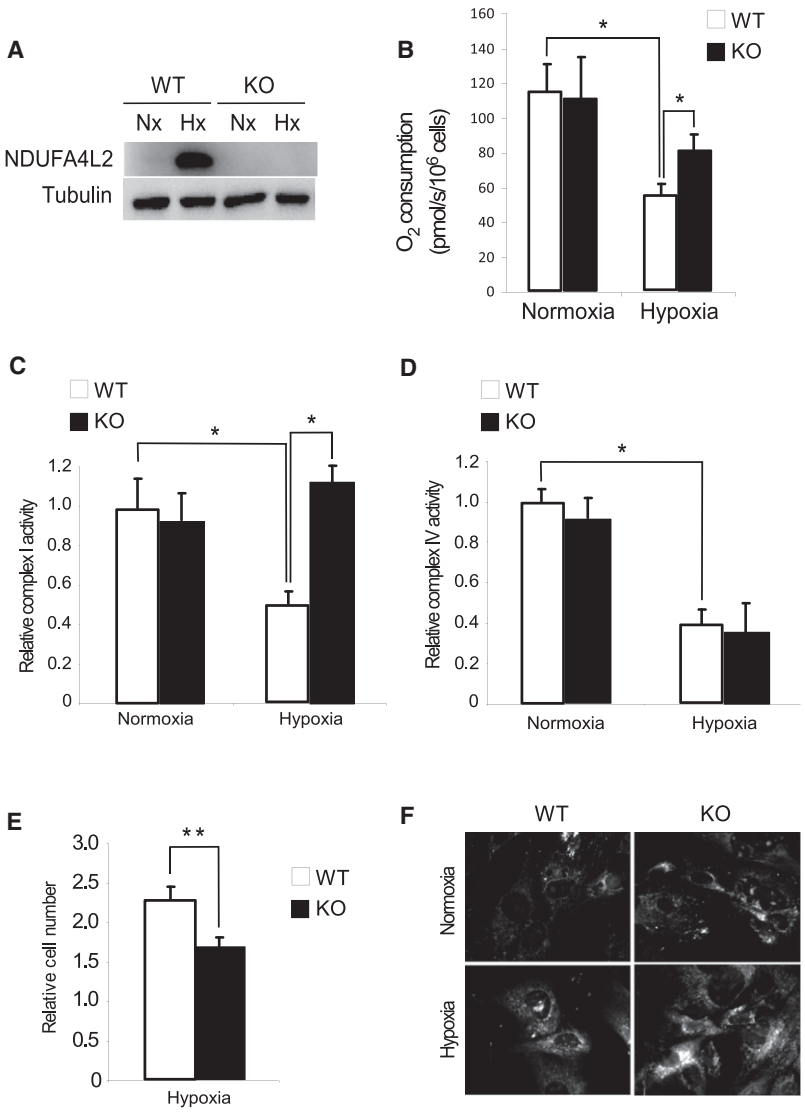

Figure 6. Analysis of NDUFA4L2-Deficient MEFs

(A–D) WT and KO MEFs were exposed to 0.5% hypoxia 24 hr prior to subsequent analysis. Immunoblot analysis showing the total deficiency of NDUFA4L2 is shown in (A). Tubulin was used as a loading control. Oxygen consumption rates were measured by high-resolution respirometry (Oxygraph 2k) (B). Complex I (C) and Complex IV (D) activities were measured spectrophotometrically and expressed relative to citrate synthase values.

(E) Relative growth rates of WT and KO NDUFA4L2 MEFs cultured in hypoxia (0.5% O_2).

(F) Representative images of three independent experiments showing MitoSOX intensity as a measure of mitochondrial superoxide levels (n > 3 mean ± SEM; *p < 0.05, **p < 0.01).

expression of NDUFA4L2. Western blot analysis confirmed that NDUFA4L2 increased in hypoxia in MEFs from wild-type mice only (Figure 6A). We determined oxygen consumption in MEFs obtained from NDUFA4L2 KO and wild-type mice (Figure 6B). Confirming results obtained in HeLa cells, MEFs from NDUFA4L2 KO mice showed increased respiration rate in hypoxia compared to wild-type mice (Figure 6B). The activity of Complex I in hypoxia was higher in MEFs from KO mice than in those from wild-type mice, confirming the results obtained in HeLa cells (Figure 6C). In contrast, the activity of Complex IV in hypoxia was similarly decreased in both types of MEFs (Figure 6D). The expression level of respiratory complexes was studied by BN-PAGE using DDM (n-dodecyl beta-D-maltoside), obtaining the same result as in HeLa cells (data not shown). In addition, MEFs from NDUFA4L2 KO mice exhibited a lower proliferation rate than those from wild-type mice when cultured under hypoxia (Figure 6E), and this lower proliferation correlated with increased ROS production under hypoxic conditions (Figure 6F).

NDUFA4 Paralogue Is Repressed under Hypoxia at the Protein Level

It is established that a COX4-2 to COX4-1 subunit substitution takes place at Complex IV during hypoxia (Fukuda et al., 2007). The paralogue proteins NDUFA4L2 and NDUFA4 derive from the same ancestral gene, share more than 65% in their amino acid sequence, and have been suggested to be part of mitochondrial Complex I (Walker et al., 1992). Since *NDUFA4* mRNA levels do not change in hypoxia up to 48 hr (Figure 7A), we investigated the fate of the protein under hypoxia. We found that NDUFA4 protein decreases in hypoxic cells while NDUFA4L2 protein expression increases in hypoxic conditions (Figure 7B). We also explored whether NDUFA4L2 levels would be responsible for the downregulation of NDUFA4. NDUFA4 protein levels decreased in hypoxia even when NDUFA4L2 was silenced (Figure 7C), and its expression in normoxia was unaffected by NDUFA4L2 overexpression (Figure 7D). NDUFA4 protein decreases to the same extent in NDUFA4L2 KO MEFs, demonstrating that both events occur independently (Figure 7E). Collectively, all these data indicate that NDUFA4L2 KO MEFs markedly repress NDUFA4 protein levels in hypoxia while Complex I activity is not affected, ruling out the possibility that Complex I activity is repressed in hypoxia via NDUFA4. These data stress the specific role of hypoxia-dependent NDUFA4L2 upregulation in Complex I activity inhibition.

DISCUSSION

The influence of fluctuations in oxygen concentration on mitochondrial activity has raised a great interest due to its broad impact on pathophysiology. Mitochondrial respiration is only compromised when the oxygen concentration drops below 0.1% O_2 because of the high affinity of mitochondrial cytochrome *c* oxidase (Complex IV) for oxygen (Aguirre et al., 2010; Gnaiger et al., 1998; Smolenski et al., 1991; Stumpe and Schrader, 1997). However, during moderate hypoxia (1%–2% O_2), cells

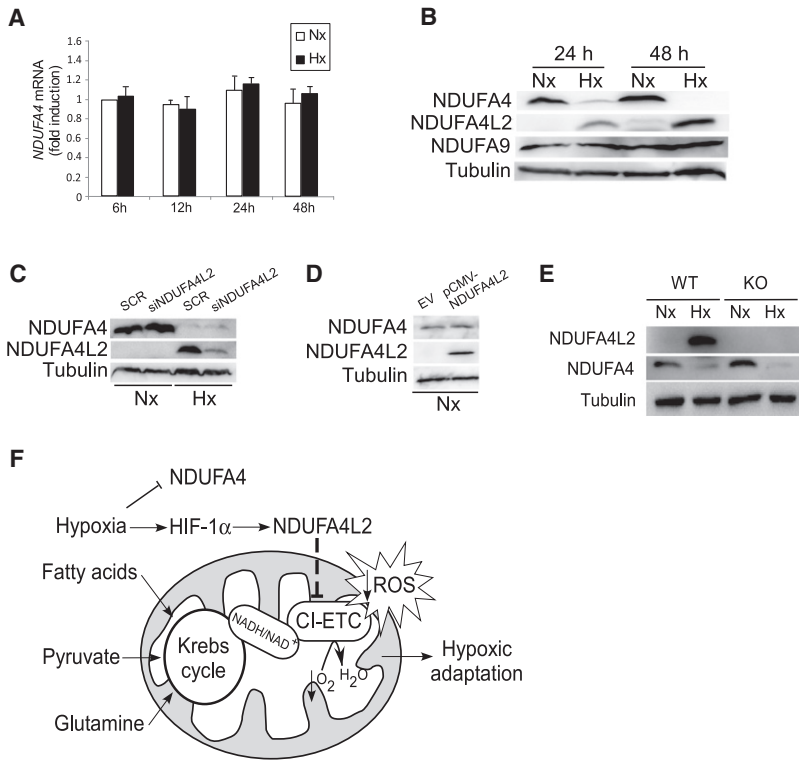

Figure 7. Opposite Regulation of NDUFA4 and NDUFA4L2 under Hypoxia

(A) HeLa cells were cultured under hypoxia (1% O_2) for 6, 12, 24, and 48 hr, and *NDUFA4* mRNA levels were analyzed.

(B) Immunoblot analysis of HeLa cells subjected to either 24 or 48 hr of hypoxia and proved against NDUFA4 and NDUFA4L2 antibodies. NDUFA9 was used as a loading control for Complex I, and tubulin was used as a total loading control.

(C and D) HeLa cells were transfected with a scramble control or NDUFA4L2 siRNA and then exposed to normoxic or hypoxic (1% O_2) conditions for 24 hr (C) or transfected with the empty or pCMV-NDUFA4L2 vector (D). Cell lysates were analyzed against NDUFA4, NDUFA4L2, and tubulin antibodies.

(E) Immunoblot analysis of MEFs WT and KO for NDUFA4L2 showing the total deficiency of NDUFA4L2 and the decrease of NDUFA4 under hypoxic (1% O_2) conditions for 24 hr. Tubulin was used as a loading control.

(F) Model showing the involvement of NDUFA4L2 induction by HIF-1α in hypoxic adaptation. HIF-1α stabilization by hypoxia upregulates NDUFA4L2, which inhibits ETC Complex I activity. As a result, oxygen consumption decreases and ROS production is abrogated, thereby allowing cells to adapt to the hypoxic conditions. In contrast, hypoxia decreases NDUFA4 protein levels ($n > 3$; mean ± SEM; $^*p < 0.05$; $^{**}p < 0.01$).

express a large number of genes, dependent on HIFs, that reprogram the metabolism to attenuate mitochondrial O_2 consumption, which also protects cells against excessive mitochondrial ROS formation (Aragonés et al., 2009; Kim et al., 2006; Papandreou et al., 2006).

At the molecular level, we show here that moderate hypoxia decreases oxygen consumption and Complex I activity via the HIF-1-dependent upregulation of NDUFA4L2. Our data indicate that *NDUFA4L2* is a HIF-1-dependent gene, emphasizing the role of HIF-1 in mitochondrial reprogramming and revealing NDUFA4L2 as an important element in metabolic adaptation to hypoxia. We have observed this induction in different cell types, as well as in tissue from animals subjected to hypoxia, suggesting a role in physiological adaptation to hypoxia. In this regard, NDUFA4L2 KO homozygous mice, which could be a presumed mouse model of Complex I gain of function based on our own data, show perinatal lethality, stressing the high relevance of this protein in vivo. Similarly, mouse models of Complex I deficiency (Kruse et al., 2008) also die shortly after birth, which indicates that Complex I activity needs to be tightly controlled to assure an adequate development early after birth.

The PHD oxygen-sensing pathway is also known to upregulate the PDH kinase isoforms PDK1, PDK3, and PDK4 (Aragonés et al., 2008; Kim et al., 2006; Lu et al., 2008; Papandreou et al., 2006). PDK overactivation reduces PDH activity, slowing down the conversion of pyruvate into acetyl-CoA and ultimately repressing the TCA cycle and the supply of NADH to the mitochondrial ETC. Therefore, PDKs could potentially cooperate with NDUFA4L2 to reduce mitochondrial Complex I activity under moderate hypoxic conditions, but it is also conceivable that NDUFA4L2 has other biological functions that cannot be accomplished by PDKs. For example, when metabolites that fuel the TCA cycle originate from pathways different from glycolysis (e.g., glutaminolysis or fatty acid oxidation), it would be necessary to reduce ETC activity in order to decrease mitochondrial function (Wheaton and Chandel, 2011). Hypoxia-induced NDUFA4L2 expression could fulfill this role, reducing oxygen consumption due to its strategic position downstream of the TCA cycle, possibly at Complex I (Figure 7F). Likewise, hypoxia induces the upregulation of microRNA-210, which represses ISCU1/2 (Chan et al., 2009; Chen et al., 2010; Favaro et al., 2010). These proteins facilitate the assembly of iron-sulfur clusters, including those in Complex I, Complex III, and aconitase, which are critical for electron transport and mitochondrial redox reactions. As a result, microRNA-210 represses mitochondrial respiration. In our model, and in line with previous studies, ISCU1/2 protein does not decrease prior to 48 hr and only under 0.5% O_2, while NDUFA4L2 becomes functional as early as 24 hr at 1% O_2. Moreover, ISCU1/2 recovery in hypoxic HeLa cells did not disturb proliferation. In this sense, it has been described that an anti-miR-210 affects HeLa cell proliferation at times longer than 48 hr and at very low oxygen tensions (0.01% O_2) (Favaro et al., 2010).

Very intriguingly, however, Complex I inhibition in HeLa cells takes place at milder hypoxia (1% O_2) (Figure 4), and this oxygen tension does not seem to be enough to decrease ISCU1/2 (Figure S5A). Furthermore, ISCU1/2 downregulation is not observed before 48 hr, but Complex I is inhibited as early as 24 hr. This opened a 24 hr window during which NDUFA4L2 could be acting before ISCU induction takes place. As demonstrated, NDUFA4L2 Complex I inhibition occurs without affecting Complex I quantity, but probably by a direct or indirect

interaction that remains to be elucidated. However, miRNA-210-targeted ISCU1/2 presumably fulfills its function by decreasing Complex I content. This early NDUFA4L2-dependent qualitative modulation followed by a later miR210-dependent quantitative repression of Complex I represents a possible model by which HIF-1 guarantees a fine control of Complex I under hypoxic conditions. In summary, we propose that, although NDUFA4L2 upregulation and miR-210-induced ISCU1/2 repression could act synergistically to decrease Complex I activity and oxygen consumption in chronic hypoxia, we should underscore that primary (1% O_2) Complex I inhibition can be only accomplished by early NDUFA4L2 induction.

Altered subunit content during hypoxia has also been reported for other ETC complexes. Thus, physiological hypoxia induces a COX4-1 to COX4-2 subunit switch, an effect mediated by HIF-1 that is thought to optimize the efficiency of respiration during conditions of reduced oxygen availability (Fukuda et al., 2007). Since we have found that NDUFA4 is downregulated at the protein level in hypoxia, we could speculate that NDUFA4L2 induction is taking over NDUFA4's place at Complex I and reducing in some way its activity. However, NDUFA4L2 KO MEFs markedly repress NDUFA4 protein levels in hypoxia, while Complex I activity is not affected, ruling out the possibility that Complex I activity is repressed in hypoxia via NDUFA4. In this regard, the role and location of NDUFA4 within Complex I are not yet well understood.

The ETC produces superoxide when single electrons are transferred to O_2 during electron transport. There are different sites of ROS production in mammalian mitochondria (Murphy, 2009), but the greatest maximum capacity of ROS production is the ubiquinone reduction site of Complex I and the outer quinone-binding site of the Q cycle in Complex III (Liu et al., 2002; Raha and Robinson, 2000; St-Pierre et al., 2002; Votyakova and Reynolds, 2001). Although superoxide production in isolated mitochondria correlates with oxygen tension (Liu et al., 2002), it is generally accepted that ROS production in cells increases during short periods of hypoxia (Brunelle et al., 2005; Guzy et al., 2005; Mansfield et al., 2005). In agreement with this, we detected increased ROS in hypoxia using the fluorescent probes DCFDA and MitoSOX. The hypoxia-induced ROS increase was exacerbated in the absence of NDUFA4L2, indicating that the expression of this protein keeps ROS production under control and hence could protect the cell against oxidative stress. Whether the effects of NDUFA4L2 on ROS production are direct or occur through the modulation of other mitochondrial proteins requires further research. However, the fact that mitochondrial membrane potential increases simultaneously with increased ROS in the absence of NDUFA4L2 suggests that both events might be closely associated, as has been demonstrated elsewhere (Korshunov et al., 1997; Votyakova and Reynolds, 2001).

Hypoxia-exposed cell cultures accumulate intracellular ROS, but most probably at lower sublethal concentrations. As shown in Figure 5, and in line with previous studies, hypoxia slows down proliferation (Gardner et al., 2001; Goda et al., 2003). However, NDUFA4L2-silenced cells and MEFs from NDUFA4L2 KO mice showed a more profound inhibition of cell proliferation in parallel to a higher ROS accumulation and DNA stress/damage (H2AX phosphorylation) than control cells or MEFs from wild-type mice. NDUFA4L2-silenced cells did not show signs of cellular apoptosis, probably because of the high-resistance nature of these tumor cells. Therefore, it is reasonable to think that the PHD-HIF system counteracts ROS overproduction that impairs cell growth.

Several in vivo and in vitro studies have revealed that the reduction of mitochondrial oxygen consumption through PHD and HIF activities prepares cells to tolerate more extreme lethal hypoxic/ischemic conditions, saving oxygen and reducing mitochondrial ROS formation. We hypothesize that NDUFA4L2 induction during hypoxia helps keep intracellular ROS production in check, consistent with the fact that NDUFA4L2 limits Complex I activity and prevents increases in membrane potential. It is therefore reasonable to speculate that NDUFA4L2 could participate in ischemic preconditioning. Indeed, several in vivo studies have shown that partial inhibition of Complex I with sublethal doses of amobarbital (a reversible inhibitor at the rotenone site of Complex I) prevents reperfusion-induced cardiac damage (Aldakkak et al., 2008; Chen et al., 2006a, 2006b).

Our studies indicate that mitochondrial Complex I activity is controlled by NDUFA4L2 during hypoxia. In conjunction with previous data on PHD- and HIF-regulated mitochondrial activity, we add further elements to the strategic armory used by HIFs to ensure that mitochondrial oxygen consumption is repressed in mild hypoxic conditions, highlighting the biological relevance of the regulation of this cellular response.

EXPERIMENTAL PROCEDURES

Cell Lines and Cultures

HeLa, RCC4, RCC4/VHL, PC-12, HL-1, neonatal rat cardiomyocytes, Hif-1$\alpha^{+/+}$/Cre or Hif-1$\alpha^{+f/+f}$/Cre MEFs, and human umbilical vein endothelial cells (HUVEC) were used. See Supplemental Experimental Procedures for details.

Microarray Analysis

Total RNA was extracted using Ultraspec reagent (Biotecx, Houston, TX). One-Color Microarray-Based Gene Expression Analysis Protocol (Agilent Technologies, Palo Alto, CA) was used to amplify and label RNA. Briefly, 200–700 ng of total RNA was reverse transcribed using T7 promoter Primer and MMLV-RT. Then cDNA was converted to aRNA using T7 RNA polymerase, which simultaneously amplifies target material and incorporates cyanine 3-labeled CTP. Samples were hybridized to Whole Human Genome Microarray 4 × 44K (G4112F, Agilent Technologies). Cy3-labeled aRNA (1.65 g) was hybridized for 17 hr at 65°C in a hybridization oven (G2545A, Agilent) set to 10 rpm in a final concentration of 1× GEx Hybridization Buffer HI-RPM, according to manufacturer's instructions (One-Color Microarray-Based Gene Expression Analysis, Agilent Technologies). Arrays were washed according to manufacturer's instructions (One-Color Microarray-Based Gene Expression Analysis, Agilent Technologies) and dried out using a centrifuge. Finally, arrays were scanned at 5 μm resolution on an Agilent DNA Microarray Scanner (G2565BA, Agilent Technologies) using the default settings for 4 × 44K format one-color arrays. Images provided by the scanner were analyzed using Feature Extraction software version 9.5.3.1 (Agilent Technologies).

In Vivo Hypoxia Experiments

Eight-week-old male C57BL/6 mice were exposed to hypoxic (7.5% O_2) or normoxic (21% O_2) conditions for 18 hr. After treatment mice were sacrificed under the same conditions to avoid tissue reoxygenation following hypoxia. The brain and heart were then excised, frozen in liquid nitrogen, and stored at −80°C. Organs were homogenized in liquid nitrogen and resuspended in RIPA buffer (1% NP40, 0.5% sodium deoxycholate, and 0.1% SDS in PBS buffer) for protein extraction or Ultraspec reagent (Biotecx, Houston, TX) for mRNA isolation.

Oxygen Consumption

Oxygen consumption was determined by high-resolution respirometry (Oxygraph-2k, Oroboros Instruments, Innsbruck, Austria). Cells were trypsinized after the indicated treatments and then resuspended at 2×10^6 cells/ml in HBSS containing 25 mM HEPES. The instrumental background flux was calculated as a linear function of the oxygen concentration, and the experimental data were corrected using DatLab software (Oroboros Instruments). The oxygen concentration in air-saturated culture medium at 37°C was 175.7 μM (Rodríguez-Juárez et al., 2007). Measurements were taken at 37°C in parallel Oxygraph-2k chambers for cells incubated in normoxic and hypoxic (1% O_2) conditions with the indicated treatments.

Mitochondria Isolation

The isolation of an enriched mitochondrial fraction from $2–5 \times 10^7$ HeLa cells was performed using the Mitochondria Isolation Kit MITOISO2 (Sigma) according to the manufacturer's instructions.

Complex I and IV Activity

The activities of Complex I and Complex IV were measured using the Complex I Enzyme Activity Microplate Assay Kit or the Complex IV Human Duplexing Microplate Assay Kit, both from MitoSciences, according to the manufacturer's instructions.

Mitochondrial Membrane Potential

Mitochondrial membrane potential was determined by incubating the cells with the fluorescent dye tetramethylrhodamine ethyl ester (TMRE; Sigma). Cells were incubated with 2.5 nM TMRE for 30 min at 37°C and subsequently analyzed by FACScan flow cytometer (Becton Dickinson, Lincoln Park, NJ).

Cell Proliferation and Apoptosis

For the cell proliferation assay, 2×10^5 HeLa, HUVEC, UCD-mel-N, and SKOV3 cells were planted in a 10 cm dish 1 day before exposure to hypoxic conditions (0.5% O_2). Either 0.1 mM NAC or 0.5 μM Mito-Q (0.5 μM DTPP was used as control of Mito-Q) was added to HeLa cells to determinate the effect of the antioxidants on NDUFA4L2-interfered cell proliferation in hypoxia. At the times indicated, the cells were trypsinized and the viable cells were counted using trypan blue. Apoptosis was determined by flow cytometry analysis of the cell cycle after DNA staining with propidium iodide (PI) and by analysis of cleaved caspase-3 with a specific antibody (Cell Signaling). Positive controls for apoptosis were performed by incubating HeLa cells with taxol (Calbiochem) at 1 μg/ml for 18 hr.

Soft Agar Assay

HeLa cells were seeded into 0.35% agar Noble (Difco) in DMEM containing 10% heat-inactivated FBS on top of a bed of 0.5% agar in 60 mm dishes at 5×10^3 cells per dish. Immobilized cells were grown for 15 days in a humidified chamber at 37°C and exposed to normoxic or hypoxic conditions (0.5% O_2). Colonies were then photographed using a DS-Fi1 camera (Nikon) and counted and measured using ImageJ software.

Analysis of ETC Complexes by Blue Native Electrophoresis Gel

Mitochondrial membrane proteins (100–150 mg) were applied and run on a 3%–13% first-dimension gradient Blue native electrophoresis gel as described elsewhere (Schägger, 1995). After electrophoresis, the complexes were electroblotted onto PVDF filters and sequentially probed with the following specific antibodies: anti-NDUFA9 (complex I), anti-core2 (complex III), anti-COI (complex IV), and anti-70 kDa subunit (complex II). All antibodies were obtained from Molecular Probes.

Ndufa4l2 Gene Inactivation in Mice

NDUFA4L2 chimeric males were obtained from Velocigene Regeneron Pharmaceuticals, Inc. (Reference number: 13661) through the KOMP repository. These chimeric mice were crossed with wild-type C57BL/6 females to generate NDUFA4L2 heterozygous mice. NDUFA4L2 heterozygous mice were used to generate NDUFA4L2-deficient embryos and the subsequent murine embryonic fibroblast isolation. The mice were bred and housed in a specific pathogen free (SPF) animal area of the animal facility at the Universidad Autónoma de Madrid (UAM).

Statistical Analysis

The data are presented as the means ± SEM of at least three independent experiments. Statistical significance *$p < 0.05$ or **$p < 0.01$ was assessed by the Wilcoxon test.

ACCESSION NUMBERS

The microarray data of HeLa cells are deposited at GEO DataSets with the accession number GSE33521.

SUPPLEMENTAL INFORMATION

Supplemental Information includes five figures, five tables, Supplemental Experimental Procedures, and Supplemental References and can be found with this article online at doi:10.1016/j.cmet.2011.10.008.

ACKNOWLEDGMENTS

This work was supported by Ministerio de Ciencia e Innovación (SAF 2007-06592, SAF 2010-14851), Comunidad Autónoma de Madrid (SAL 2006/0311), Metoxia Project-Health (F2 2009-222741), and Recava Network (RD 06/0014/0031) to M.O.L.; PS09/00101 and CP07/00143 to A.M.-R.; PI060701, PS09/00116, and CP08/00204 to S.C.; BFU2008-03407/BMC to J.A.; SAF2009-08007 to J.A.E.; and CSD2007-00020 to A.M.-R. and J.A.E. The CNIC is supported by the Instituto de Salud Carlos III-MICINN and the Pro-CNIC Foundation. We are grateful to Mike Murphy (Mitochondrial Biology Unit, MRC, Cambridge, UK) for the gift of MitoQ. We also thank Stephen Y. Chan and Joseph Loscalzo (Harvard Medical School, Boston, MA) for providing us ISCU expression vectors.

Received: April 12, 2010
Revised: July 21, 2011
Accepted: October 7, 2011
Published online: November 17, 2011

REFERENCES

Aguirre, E., Rodríguez-Juárez, F., Bellelli, A., Gnaiger, E., and Cadenas, S. (2010). Kinetic model of the inhibition of respiration by endogenous nitric oxide in intact cells. Biochim. Biophys. Acta *1797*, 557–565.

Aldakkak, M., Stowe, D.F., Chen, Q., Lesnefsky, E.J., and Camara, A.K. (2008). Inhibited mitochondrial respiration by amobarbital during cardiac ischaemia improves redox state and reduces matrix Ca2+ overload and ROS release. Cardiovasc. Res. *77*, 406–415.

Andreas, K., Häupl, T., Lübke, C., Ringe, J., Morawietz, L., Wachtel, A., Sittinger, M., and Kaps, C. (2009). Antirheumatic drug response signatures in human chondrocytes: potential molecular targets to stimulate cartilage regeneration. Arthritis Res. Ther. *11*, R15.

Aragonés, J., Schneider, M., Van Geyte, K., Fraisl, P., Dresselaers, T., Mazzone, M., Dirkx, R., Zacchigna, S., Lemieux, H., Jeoung, N.H., et al. (2008). Deficiency or inhibition of oxygen sensor Phd1 induces hypoxia tolerance by reprogramming basal metabolism. Nat. Genet. *40*, 170–180.

Aragonés, J., Fraisl, P., Baes, M., and Carmeliet, P. (2009). Oxygen sensors at the crossroad of metabolism. Cell Metab. *9*, 11–22.

Brunelle, J.K., Bell, E.L., Quesada, N.M., Vercauteren, K., Tiranti, V., Zeviani, M., Scarpulla, R.C., and Chandel, N.S. (2005). Oxygen sensing requires mitochondrial ROS but not oxidative phosphorylation. Cell Metab. *1*, 409–414.

Carroll, J., Fearnley, I.M., Skehel, J.M., Shannon, R.J., Hirst, J., and Walker, J.E. (2006). Bovine complex I is a complex of 45 different subunits. J. Biol. Chem. *281*, 32724–32727.

Chan, S.Y., Zhang, Y.Y., Hemann, C., Mahoney, C.E., Zweier, J.L., and Loscalzo, J. (2009). MicroRNA-210 controls mitochondrial metabolism during hypoxia by repressing the iron-sulfur cluster assembly proteins ISCU1/2. Cell Metab. *10*, 273–284.

Chen, Q., Hoppel, C.L., and Lesnefsky, E.J. (2006a). Blockade of electron transport before cardiac ischemia with the reversible inhibitor amobarbital protects rat heart mitochondria. J. Pharmacol. Exp. Ther. *316*, 200–207.

Chen, Q., Moghaddas, S., Hoppel, C.L., and Lesnefsky, E.J. (2006b). Reversible blockade of electron transport during ischemia protects mitochondria and decreases myocardial injury following reperfusion. J. Pharmacol. Exp. Ther. *319*, 1405–1412.

Chen, Z., Li, Y., Zhang, H., Huang, P., and Luthra, R. (2010). Hypoxia-regulated microRNA-210 modulates mitochondrial function and decreases ISCU and COX10 expression. Oncogene *29*, 4362–4368.

Driessens, N., Versteyhe, S., Ghaddhab, C., Burniat, A., De Deken, X., Van Sande, J., Dumont, J.E., Miot, F., and Corvilain, B. (2009). Hydrogen peroxide induces DNA single- and double-strand breaks in thyroid cells and is therefore a potential mutagen for this organ. Endocr. Relat. Cancer *16*, 845–856.

Favaro, E., Ramachandran, A., McCormick, R., Gee, H., Blancher, C., Crosby, M., Devlin, C., Blick, C., Buffa, F., Li, J.L., et al. (2010). MicroRNA-210 regulates mitochondrial free radical response to hypoxia and krebs cycle in cancer cells by targeting iron sulfur cluster protein ISCU. PLoS ONE *5*, e10345.

Favier, J., Brière, J.J., Burnichon, N., Rivière, J., Vescovo, L., Benit, P., Giscos-Douriez, I., De Reyniès, A., Bertherat, J., Badoual, C., et al. (2009). The Warburg effect is genetically determined in inherited pheochromocytomas. PLoS ONE *4*, e7094.

Fredlund, E., Ovenberger, M., Borg, K., and Påhlman, S. (2008). Transcriptional adaptation of neuroblastoma cells to hypoxia. Biochem. Biophys. Res. Commun. *366*, 1054–1060.

Frost, M.T., Wang, Q., Moncada, S., and Singer, M. (2005). Hypoxia accelerates nitric oxide-dependent inhibition of mitochondrial complex I in activated macrophages. Am. J. Physiol. Regul. Integr. Comp. Physiol. *288*, R394–R400.

Fukuda, R., Zhang, H., Kim, J.W., Shimoda, L., Dang, C.V., and Semenza, G.L. (2007). HIF-1 regulates cytochrome oxidase subunits to optimize efficiency of respiration in hypoxic cells. Cell *129*, 111–122.

Gardner, L.B., Li, Q., Park, M.S., Flanagan, W.M., Semenza, G.L., and Dang, C.V. (2001). Hypoxia inhibits G1/S transition through regulation of p27 expression. J. Biol. Chem. *276*, 7919–7926.

Gnaiger, E., Lassnig, B., Kuznetsov, A.V., and Margreiter, R. (1998). Mitochondrial respiration in the low oxygen environment of the cell. Effect of ADP on oxygen kinetics. Biochim. Biophys. Acta *1365*, 249–254.

Goda, N., Ryan, H.E., Khadivi, B., McNulty, W., Rickert, R.C., and Johnson, R.S. (2003). Hypoxia-inducible factor 1alpha is essential for cell cycle arrest during hypoxia. Mol. Cell. Biol. *23*, 359–369.

Guzy, R.D., Hoyos, B., Robin, E., Chen, H., Liu, L., Mansfield, K.D., Simon, M.C., Hammerling, U., and Schumacker, P.T. (2005). Mitochondrial complex III is required for hypoxia-induced ROS production and cellular oxygen sensing. Cell Metab. *1*, 401–408.

Iyer, N.V., Kotch, L.E., Agani, F., Leung, S.W., Laughner, E., Wenger, R.H., Gassmann, M., Gearhart, J.D., Lawler, A.M., Yu, A.Y., and Semenza, G.L. (1998). Cellular and developmental control of O2 homeostasis by hypoxia-inducible factor 1 alpha. Genes Dev. *12*, 149–162.

Kaelin, W.G., Jr., and Ratcliffe, P.J. (2008). Oxygen sensing by metazoans: the central role of the HIF hydroxylase pathway. Mol. Cell *30*, 393–402.

Kim, J.W., Tchernyshyov, I., Semenza, G.L., and Dang, C.V. (2006). HIF-1-mediated expression of pyruvate dehydrogenase kinase: a metabolic switch required for cellular adaptation to hypoxia. Cell Metab. *3*, 177–185.

Korshunov, S.S., Skulachev, V.P., and Starkov, A.A. (1997). High protonic potential actuates a mechanism of production of reactive oxygen species in mitochondria. FEBS Lett. *416*, 15–18.

Kruse, S.E., Watt, W.C., Marcinek, D.J., Kapur, R.P., Schenkman, K.A., and Palmiter, R.D. (2008). Mice with mitochondrial complex I deficiency develop a fatal encephalomyopathy. Cell Metab. *7*, 312–320.

Liu, Y., Fiskum, G., and Schubert, D. (2002). Generation of reactive oxygen species by the mitochondrial electron transport chain. J. Neurochem. *80*, 780–787.

Lu, C.W., Lin, S.C., Chen, K.F., Lai, Y.Y., and Tsai, S.J. (2008). Induction of pyruvate dehydrogenase kinase-3 by hypoxia-inducible factor-1 promotes metabolic switch and drug resistance. J. Biol. Chem. *283*, 28106–28114.

Mansfield, K.D., Guzy, R.D., Pan, Y., Young, R.M., Cash, T.P., Schumacker, P.T., and Simon, M.C. (2005). Mitochondrial dysfunction resulting from loss of cytochrome c impairs cellular oxygen sensing and hypoxic HIF-alpha activation. Cell Metab. *1*, 393–399.

Murphy, M.P. (2009). How mitochondria produce reactive oxygen species. Biochem. J. *417*, 1–13.

Papandreou, I., Cairns, R.A., Fontana, L., Lim, A.L., and Denko, N.C. (2006). HIF-1 mediates adaptation to hypoxia by actively downregulating mitochondrial oxygen consumption. Cell Metab. *3*, 187–197.

Piruat, J.I., and López-Barneo, J. (2005). Oxygen tension regulates mitochondrial DNA-encoded complex I gene expression. J. Biol. Chem. *280*, 42676–42684.

Raha, S., and Robinson, B.H. (2000). Mitochondria, oxygen free radicals, disease and ageing. Trends Biochem. Sci. *25*, 502–508.

Rodríguez-Juárez, F., Aguirre, E., and Cadenas, S. (2007). Relative sensitivity of soluble guanylate cyclase and mitochondrial respiration to endogenous nitric oxide at physiological oxygen concentration. Biochem. J. *405*, 223–231.

Schägger, H. (1995). Native electrophoresis for isolation of mitochondrial oxidative phosphorylation protein complexes. Methods Enzymol. *260*, 190–202.

Schofield, C.J., and Ratcliffe, P.J. (2004). Oxygen sensing by HIF hydroxylases. Nat. Rev. Mol. Cell Biol. *5*, 343–354.

Semenza, G.L. (2004). Hydroxylation of HIF-1: oxygen sensing at the molecular level. Physiology (Bethesda) *19*, 176–182.

Semenza, G.L. (2009). Regulation of oxygen homeostasis by hypoxia-inducible factor 1. Physiology (Bethesda) *24*, 97–106.

Smolenski, R.T., Schrader, J., de Groot, H., and Deussen, A. (1991). Oxygen partial pressure and free intracellular adenosine of isolated cardiomyocytes. Am. J. Physiol. *260*, C708–C714.

St-Pierre, J., Buckingham, J.A., Roebuck, S.J., and Brand, M.D. (2002). Topology of superoxide production from different sites in the mitochondrial electron transport chain. J. Biol. Chem. *277*, 44784–44790.

Stumpe, T., and Schrader, J. (1997). Phosphorylation potential, adenosine formation, and critical PO2 in stimulated rat cardiomyocytes. Am. J. Physiol. *273*, H756–H766.

Vogel, R.O., Janssen, R.J., Ugalde, C., Grovenstein, M., Huijbens, R.J., Visch, H.J., van den Heuvel, L.P., Willems, P.H., Zeviani, M., Smeitink, J.A., and Nijtmans, L.G. (2005). Human mitochondrial complex I assembly is mediated by NDUFAF1. FEBS J. *272*, 5317–5326.

Votyakova, T.V., and Reynolds, I.J. (2001). DeltaPsi(m)-Dependent and -independent production of reactive oxygen species by rat brain mitochondria. J. Neurochem. *79*, 266–277.

Walker, J.E., Arizmendi, J.M., Dupuis, A., Fearnley, I.M., Finel, M., Medd, S.M., Pilkington, S.J., Runswick, M.J., and Skehel, J.M. (1992). Sequences of 20 subunits of NADH:ubiquinone oxidoreductase from bovine heart mitochondria. Application of a novel strategy for sequencing proteins using the polymerase chain reaction. J. Mol. Biol. *226*, 1051–1072.

Wheaton, W.W., and Chandel, N.S. (2011). Hypoxia. 2. Hypoxia regulates cellular metabolism. Am. J. Physiol. Cell Physiol. *300*, C385–C393.

Molecular Cell
Article

HIF2α Acts as an mTORC1 Activator through the Amino Acid Carrier SLC7A5

Ainara Elorza,[1,7] Inés Soro-Arnáiz,[1,7] Florinda Meléndez-Rodríguez,[1] Victoria Rodríguez-Vaello,[1] Glenn Marsboom,[1] Guillermo de Cárcer,[3] Bárbara Acosta-Iborra,[1] Lucas Albacete-Albacete,[1] Angel Ordóñez,[1] Leticia Serrano-Oviedo,[5] Jose Miguel Giménez-Bachs,[6] Alicia Vara-Vega,[2] Antonio Salinas,[6] Ricardo Sánchez-Prieto,[5] Rafael Martín del Río,[4] Francisco Sánchez-Madrid,[2] Marcos Malumbres,[3] Manuel O. Landázuri,[1] and Julián Aragonés[1,*]

[1]Research Unit, Hospital Universitario Santa Cristina, Research Institute Princesa, Autonomous University of Madrid, 28009 Madrid, Spain
[2]Immunology Department, Hospital Universitario de La Princesa, Research Institute Princesa, Autonomous University of Madrid, 28006 Madrid, Spain
[3]Cell Division and Cancer Group, Spanish National Cancer Research Centre (CNIO), E-28029 Madrid, Spain
[4]Departamento de Investigación, Hospital Universitario Ramón y Cajal, 28034 Madrid, Spain
[5]Laboratorio de Oncología Molecular, Centro Regional de Investigaciones Biomédicas, Parque Científico y Tecnológico de Castilla-La Mancha (PCYTA)/Universidad de Castilla-La Mancha (UCLM), 02008 Albacete, Spain
[6]Servicio de Urología, Complejo Hospitalario Universitario de Albacete, Facultad de Medicina de la UCLM, 02006 Albacete, Spain
[7]These authors contributed equally to this work
*Correspondence: jaragones.hlpr@salud.madrid.org
http://dx.doi.org/10.1016/j.molcel.2012.09.017

SUMMARY

The mammalian target of rapamycin (mTOR) pathway, which is essential for cell proliferation, is repressed in certain cell types in hypoxia. However, hypoxia-inducible factor 2α (HIF2α) can act as a proliferation-promoting factor in some biological settings. This paradoxical situation led us to study whether HIF2α has a specific effect on mTORC1 regulation. Here we show that activation of the HIF2α pathway increases mTORC1 activity by upregulating expression of the amino acid carrier SLC7A5. At the molecular level we also show that HIF2α binds to the *Slc7a5* proximal promoter. Our findings identify a link between the oxygen-sensing HIF2α pathway and mTORC1 regulation, revealing the molecular basis of the tumor-promoting properties of HIF2α in von Hippel-Lindau-deficient cells. We also describe relevant physiological scenarios, including those that occur in liver and lung tissue, wherein HIF2α or low-oxygen tension drive mTORC1 activity and SLC7A5 expression.

INTRODUCTION

Cells are equipped with oxygen-sensing systems for mounting an adaptive-programmed response in situations wherein oxygen availability is limited. Hypoxia-inducible factors (HIF1, HIF2, and HIF3) are central regulators of this cellular response. Indeed, when oxygen is available, prolyl hydroxylases (PHD-1, PHD-2, and PHD-3) act as O_2 sensors, using O_2 to hydroxylate critical prolyl residues in HIFα subunits (Bruick and McKnight, 2001; Epstein et al., 2001; Wang et al., 1995). Upon hydroxylation by PHDs, these HIFα subunits are recognized by the von Hippel-Lindau (VHL) factor, a component in the multiprotein E3 ubiquitin ligase complex, which marks them for subsequent degradation by the proteasome machinery (Ivan et al., 2001; Jaakkola et al., 2001). In conditions of hypoxia, PHDs do not have enough O_2 to hydroxylate these prolyl residues, thereby stabilizing the HIFα subunits and activating the HIF-dependent transcriptional program.

The mammalian target of rapamycin (mTOR) is a serine-threonine kinase that senses and integrates signals from extracellular stimuli. By responding to oxygen and amino acid availability and energy status of the cell, mTOR plays a central role in cell growth and proliferation (Schmelzle and Hall, 2000; Sonenberg and Hinnebusch, 2009). The mTORC1 complex mediates the phosphorylation of 4EBP1 (eukaryotic initiation factor 4E-binding protein) and p70-S6K (ribosomal protein 6 kinase), and these two axes of the mTORC1 pathway are essential regulators of protein translation (Hara et al., 2002; Kim et al., 2002; Sonenberg and Hinnebusch, 2009). Phosphorylation of 4EBP1 by mTORC1 prevents its interaction with eIF4E, allowing assembly of the eIF4 complex and thereby promoting 5′-cap-mRNA translation (Sonenberg and Hinnebusch, 2009). Phosphorylation of p70-S6K by mTORC1 drives phosphorylation of its target, the ribosomal protein S6 (rpS6), an integral component of the 40S subunit of the ribosome (Ma and Blenis, 2009; Sonenberg and Hinnebusch, 2009). The activity of mTORC1 is usually inhibited when oxygen availability is limited, a mechanism thought to save ATP by limiting energy-consuming events such as protein translation. Such hypoxia-induced mTORC1 repression is mediated by HIF-driven gene expression of *Redd1* (Brugarolas et al., 2004; Cam et al., 2010; DeYoung et al., 2008; Wolff et al., 2011). Indeed, mTORC1 is inhibited by the GTPase-activating protein tuberous sclerosis complex (TSC1-TSC2) (Kwiatkowski, 2003; Li et al., 2004; Ma and Blenis, 2009; Manning and Cantley, 2003), and it is proposed that REDD1 directly binds to and sequesters 14-3-3 proteins from TSC2, resulting in TSC activation and subsequent mTORC1 inhibition (DeYoung et al., 2008). Another HIF1-dependent gene, *bNIP3*, has also been implicated in hypoxia-dependent mTORC1 inhibition, because

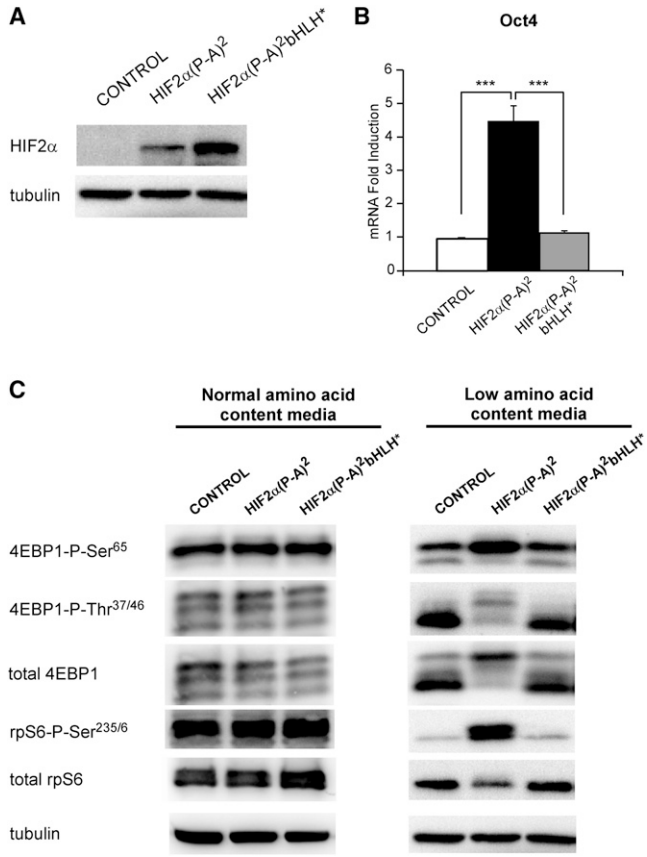

Figure 1. Effects of HIF2α Activity on mTORC1 Activation in WT8 Cells

(A) Western blot analysis of HIF2α and tubulin protein in HIF2α $(P\text{-}A)^2$, HIF2α $(P\text{-}A)^2$bHLH*, and WT8 control cells.

(B) Relative *Oct4* gene expression in HIF2α $(P\text{-}A)^2$, HIF2α $(P\text{-}A)^2$bHLH*, and WT8 control cells. The mean is shown; error bars represent SEM (n = 6, ***$p < 0.001$).

(C) Cell lysates from control, HIF2α $(P\text{-}A)^2$, and HIF2α $(P\text{-}A)^2$bHLH* WT8 cells cultured for 72 hr in normal culture media (left panel) or in media with 50% of the normal amino acid content (right panel) were analyzed by western blot with antibodies as shown.

See also Figure S1.

it decreases the activity of RHEB (Li et al., 2007), a small GTPase necessary for mTORC1 activity and negatively regulated by the TSC1-TSC2 complex (Kwiatkowski, 2003; Li et al., 2004; Ma and Blenis, 2009; Manning and Cantley, 2003). In addition to these HIF-dependent mechanisms, other essential HIF-independent pathways have been shown to drive mTORC1 repression during hypoxia, such as those involving AMP-activated protein kinase (AMPK) (Liu et al., 2006; Wolff et al., 2011).

HIF1α attenuates cell proliferation (Carmeliet et al., 1998; Goda et al., 2003; Gordan et al., 2007; Koshiji et al., 2004), and this effect is partially mediated by this TSC-dependent mTORC1 inhibition (Liu et al., 2006) but also involves a HIF1α-dependent repression of the proliferation-promoting transcription factor c-myc (Gordan et al., 2007; Koshiji et al., 2004). A recent study identified homozygous deletions of the *HIF1α* locus in 14q in many clear cell renal cell carcinoma (CCRCC) cell lines, specifically identifying *HIF1α* as a kidney cancer suppressor gene (Shen et al., 2011). However, recent studies of VHL-deficient cells that constitutively induce HIF isoforms in normoxic conditions have demonstrated the proliferation and tumor-promoting properties of the HIF2α isoform (Gordan et al., 2007; Gordan et al., 2008; Kondo et al., 2003; Kondo et al., 2002; Raval et al., 2005). A study of human renal cell carcinoma samples also revealed that VHL-deficient carcinomas can be categorized as those expressing both isoforms HIF1α and HIF2α and those expressing HIF2α alone after loss of HIF1α (Gordan et al., 2007). Those exclusively expressing HIF2α are larger in size and grow more rapidly, in agreement with the proproliferative properties of the HIF2α isoform (Gordan et al., 2007; Mandriota et al., 2002; Raval et al., 2005). Constitutive HIF2α activation also induces signs of proliferation in vivo in other biological systems, such as in liver tissue (Kim et al., 2006). A recent study in renal cell carcinoma demonstrated that, in contrast to HIF1α, HIF2α regulates the expression of several c-myc-dependent genes, such as *p21* and *cyclinD2*, by promoting c-myc and Max heterodimerization independently of HIF2α DNA binding activity (Gordan et al., 2007).

These proliferation-promoting properties of HIF2α are difficult to reconcile with the aforementioned mTORC1 repression induced by HIF1α and HIF-independent pathways. Here we show that activation of the HIF2α pathway in VHL-deficient tumor cells increases mTORC1 activity by upregulating the expression of SLC7A5, an amino acid carrier critical for its activity. This HIF2α-SLC7A5 molecular axis is essential for explaining the tumor-promoting properties of HIF2α in VHL-deficient tumor cells. Moreover, we found that upon *Vhl* gene inactivation in mice, endogenous HIF2α also drives both mTORC1 activation and SLC7A5 expression in other biological contexts in vivo. Importantly, we show that in lung tissue, both hypoxia and HIF2α activation increase mTORC1 activity and SLC7A5 expression, describing a hypoxic scenario leading to mTORC1 activation rather than the repression found in some other hypoxic contexts. We have thus shown that HIF2α increases mTORC1 activity in different biological systems, defining a link between the oxygen-sensing HIF2α pathway and mTORC1 regulation.

RESULTS

The HIF2α Pathway Induces mTORC1 Activity

To assess the role of HIF2α in the regulation of mTORC1 activity, we used ectopically expressed active and inactive forms of HIF2α in WT8 cells, a cellular model widely used for exploring the biological functions of HIF2α in tumor cells derived from renal cell carcinomas (Kondo et al., 2003; Kondo et al., 2002; Raval et al., 2005). We generated transfectants in WT8 cells that expressed a transcriptionally active and stable form of HIF2α (HIF2α $(P\text{-}A)^2$) or its corresponding DNA binding domain mutant (HIF2α $(P\text{-}A)^2$bHLH*) (see Supplemental Experimental Procedures available online). Both HIF2α forms were efficiently expressed in HIF2α $(P\text{-}A)^2$ WT8 and HIF2α $(P\text{-}A)^2$bHLH* WT8 cells compared with WT8 control cells (Figure 1A). *Oct4*, a well-recognized HIF2α-dependent gene (Covello et al., 2006), was regulated as expected (Figure 1B). The activity of mTORC1 was

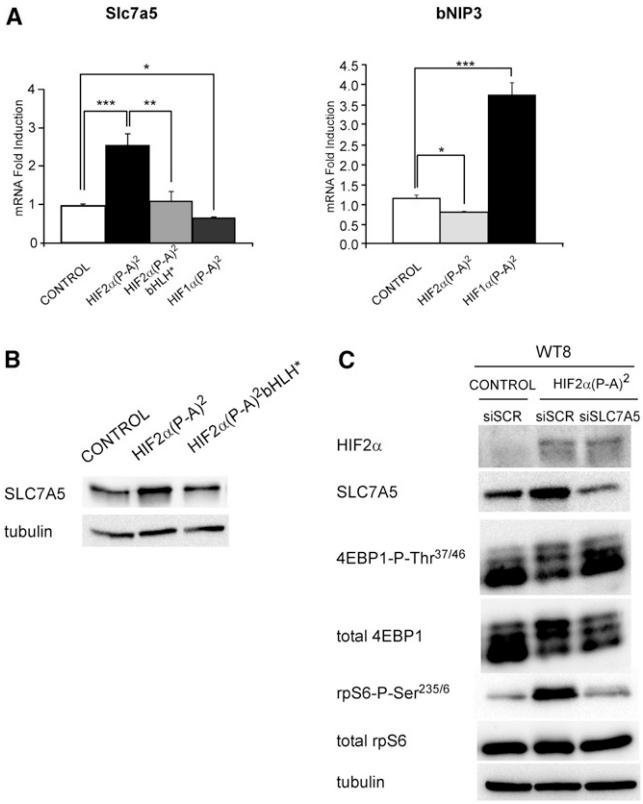

Figure 2. Contribution of SLC7A5 Expression to HIF2α-Dependent mTORC1 Activation

(A) Left panel, relative *Slc7a5* gene expression in HIF2α $(P\text{-}A)^2$, HIF2α $(P\text{-}A)^2$bHLH*, HIF1α $(P\text{-}A)^2$, and WT8 cells. The mean is shown, and error bars represent SEM (n = 6, *p < 0.05, **p < 0.01, ***p < 0.001). Right panel, relative *bNIP3* gene expression in HIF2α $(P\text{-}A)^2$, HIF1α $(P\text{-}A)^2$, and WT8 control cells (n = 4). The mean is shown; error bars represent SEM (n = 4, *p < 0.05, ***p < 0.001).

(B) Western blot analyses of SLC7A5 and tubulin protein levels in HIF2α $(P\text{-}A)^2$, HIF2α $(P\text{-}A)^2$bHLH*, and WT8 control cells.

(C) WT8 control cells were transfected with scrambled control small interfering RNA (siSCR), and HIF2α $(P\text{-}A)^2$ WT8 cells were transfected with either siSCR or siRNA against *Slc7a5* (siSLC7A5). The cells were subsequently cultured for 72 hr in media with 50% of the normal amino acid content. Whole-cell extracts were analyzed by western blot with antibodies indicated.

See also Figure S2.

then evaluated with two commonly used markers, the phosphorylated forms of 4EBP1 and rpS6 (Cam et al., 2010; Sonenberg and Hinnebusch, 2009). In normal culture media, the phosphorylation levels of 4EBP1 (assessed with antibodies for phospho-4EBP1^{Ser65} and phospho-4EBP1$^{Thr37/46}$) and rpS6 (assessed with an antibody for phospho-rpS6$^{Ser235/6}$) were similar in HIF2α $(P\text{-}A)^2$ WT8, HIF2α $(P\text{-}A)^2$bHLH* WT8, and control WT8 cells (Figure 1C). We then investigated whether HIF2α $(P\text{-}A)^2$ could induce mTORC1 activity in WT8 control cells when basal mTORC1 activity was decreased. As mTORC1 activity is dependent on extracellular amino acid concentration (Hara et al., 2002; Nicklin et al., 2009; Wang et al., 1998), we included an additional condition in these experiments: cells were cultured in media containing 50% of the normal amino acid concentration. Assessment of total 4EBP1 protein under these limiting amino acid conditions revealed that the majority of 4EBP1 in WT8 control cells was present in the lower band, indicative of hypophosphorylation and 4EBP1 inactivation. By contrast, the majority of 4EBP1 was present in the upper band in HIF2α $(P\text{-}A)^2$ WT8 cells, indicative of hyperphosphorylation and 4EBP1 activation. Moreover, anti-p4EBP1^{Ser65} revealed a more marked 4EBP1 phosphorylation of this Ser65 position in WT8 cells expressing HIF2α $(P\text{-}A)^2$. These upper bands were also detected when the membranes were probed with a p4EBP1$^{Thr37/46}$ antibody. This effect was entirely dependent on HIF2α DNA-binding activity, as the phospho-4EBP1 levels in WT8 cells expressing HIF2α $(P\text{-}A)^2$bHLH* were similar to those of WT8 control cells (Figure 1C). Likewise, phospho-rpS6$^{Ser235/6}$ levels were markedly higher in HIF2α $(P\text{-}A)^2$ WT8 cells compared with control and HIF2α $(P\text{-}A)^2$bHLH* WT8 cells (Figure 1C). This effect was specifically driven by HIF2α $(P\text{-}A)^2$, because mTORC1 activity was not induced in HIF1α $(P\text{-}A)^2$ WT8 cells that express a constitutively active form of HIF1α (Figure S1). Collectively, these data indicate that HIF2α sustains mTORC1 activity when amino acid supply is a limiting factor.

SLC7A5, an Activator of mTORC1, Is Specifically Induced by HIF2α

Based on these results, we investigated the molecular mechanisms linking HIF2α activity with mTORC1 activation. The amino acid carriers SLC1A5 (ASCT2) and SLC7A5 (LAT1) are critical in sustaining mTORC1 activity (Fuchs and Bode, 2005; Nicklin et al., 2009). We investigated whether HIF2α could alter the expression of these mTORC1 activators and found that *Slc7a5* gene expression was markedly induced in HIF2α $(P\text{-}A)^2$ WT8 cells compared with either WT8 control cells or HIF2α $(P\text{-}A)^2$bHLH* WT8 cells (Figure 2A). By contrast, ASCT2 RNA levels were minimally affected in HIF2α $(P\text{-}A)^2$ cells (data not shown). This effect was specifically driven by HIF2α, because HIF1α $(P\text{-}A)^2$ WT8 cells showed a modest inhibition of *Slc7a5* gene expression in parallel to the expected induction of *bNIP3* (Figure 2A), which is a well-recognized HIF1α-dependent gene (Raval et al., 2005). Western blots also revealed an increase in SLC7A5 protein levels in HIF2α $(P\text{-}A)^2$ WT8 cells (Figure 2B). To determine whether elevated SLC7A5 expression is responsible for HIF2α-dependent mTORC1 activation, we next silenced *Slc7a5* gene expression in HIF2α $(P\text{-}A)^2$ WT8 cells. This resulted in a marked repression of mTORC1 activity in HIF2α $(P\text{-}A)^2$ WT8 cells to near-control levels in WT8 control cells (Figure 2C). Indeed, total 4EBP1 and p4EBP1$^{Thr37/46}$ western blot analysis showed that *Slc7a5* gene silencing markedly increased the proportion of the lower 4EBP1 band, indicative of the hypophosphorylation and 4EBP1 inactivation (Figure 2C). Similarly, HIF2α $(P\text{-}A)^2$ was much less efficient in promoting rpS6 hyperphosphorylation when *Slc7a5* gene expression was reduced (Figure 2C). This partial silencing of SLC7A5 expression did not inhibit mTORC1 when cells were cultured in media with normal amino acid content (Figure S2A). In line with the involvement of SLC7A5 on HIF2α-dependent mTORC1 activity, HIF2α $(P\text{-}A)^2$ WT8 cells also preserved mTORC1 activity when cultured in media with a specifically reduced content of essential amino acids and glutamine (data not shown), which are those amino

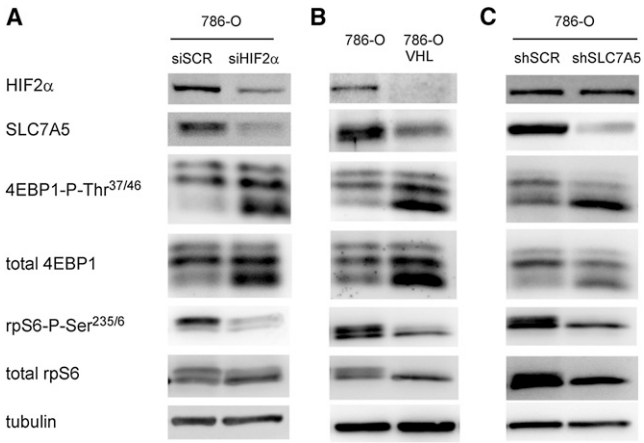

Figure 3. Effect of Endogenous HIF2α on mTORC1 Activity and SLC7A5 Expression in 786-O VHL-Deficient Cells

Western blot analysis with antibodies as shown in (A) HIF2α-silenced 786-O cells and their corresponding control siSCR-transfected 786-O cells 72 hr after transfection, (B) 786-O and their counterparts in which VHL expression was restored (786-O-VHL), and (C) SLC7A5-silenced 786-O cells and their corresponding control 786-O-shSCR cells. All these experiments were performed by culturing 786-O cells for 48 hr in media with 5% of the normal content of essential amino acids and glutamine.

acids more specifically involved in mTORC1 activity via SLC7A5 (Fuchs and Bode, 2005; Nicklin et al., 2009). Furthermore, silencing of RagA and RagB, previously identified as central mediators of essential-amino-acid-dependent mTORC1 activity (Kim et al., 2008; Sancak et al., 2008), also compromised mTORC1 activity in HIF2α $(P\text{-}A)^2$ WT8 cells (Figure S2B). All these data suggest that below a certain threshold of extracellular amino acid content, HIF2α-dependent SLC7A5 expression becomes a limiting factor for mTORC1 activity. This may reflect the fact that amino acid levels in normal culture media exceed those normally encountered by cells in vivo.

We next studied the role of endogenous HIF2α on the mTORC1 pathway and SLC7A5 expression using the VHL-deficient renal cell carcinoma cell line 786-O, which constitutively expresses endogenous HIF2α in normoxia (Kondo et al., 2002). Importantly, silencing of endogenous HIF2α resulted in a marked repression of mTORC1 activity and SLC7A5 expression in 786-O VHL-deficient cells when cells were cultured specifically in media with reduced content of essential amino acids and glutamine (Figure 3A), but not in media with normal amino acid content (data not shown). Indeed, silencing of HIF2α markedly increased the predominance of the lower 4EBP1 band, indicative of 4EBP1 inactivation, and also reduced rpS6 hyperphosphorylation levels (Figure 3A). Similar effects on mTORC1 activity and SLC7A5 expression were observed when HIF2α was repressed by restoring VHL expression in 786-O cells (Figure 3B). To assess the relative contribution of the HIF2α-dependent increase in SLC7A5 expression to mTORC1 activity in 786-O cells, we generated the 786-O-shSLC7A5 cell line, in which SLC7A5 expression was silenced to levels similar to those obtained after HIF2α silencing (see Figures 3A and 3C). Importantly, the levels of phospho-rpS6 decreased markedly following SLC7A5 silencing compared with their corresponding control 786-O-shSCR cells (Figure 3C). Moreover, 786-O-shSLC7A5 also showed a predominance of the lower 4EBP1 band, indicative of 4EBP1 inactivation, compared with 786-O-shSCR cells (Figure 3C). Collectively, these data indicate that endogenous HIF2α expression in 786-O cells also regulates mTORC1 activity via SLC7A5 when the amino acid supply is limited.

HIF2α Binds to the *Slc7a5* Proximal Promoter

The above results led us to explore whether SLC7A5 was a direct target of HIF2α. We next investigated whether HIF2α binds to the regulatory DNA sequences at the *Slc7a5* locus. Sequence analysis revealed that the human proximal promoter of *Slc7a5* contains two potential HIF binding sites at positions −112 and −458 (Figure 4A). Chromatin immunoprecipitation (ChIP) assay with HIF2α $(P\text{-}A)^2$ WT8, HIF2α $(P\text{-}A)^2$bHLH* WT8, and WT8 control cells showed that HIF2α binding activity to the *Slc7a5* proximal promoter, but not to *Slc7a5* intron 1, was augmented in HIF2α $(P\text{-}A)^2$ WT8 cells compared with HIF2α $(P\text{-}A)^2$bHLH* and WT8 control cells (Figure 4B). Moreover, constitutive binding of endogenous HIF2α to the *Slc7a5* proximal promoter, but not to *Slc7a5* intron 1, was observed in 786-O control cells when compared with 786-O-VHL cells (Figure 4C). A parallel analysis under identical experimental conditions in HIF1α $(P\text{-}A)^2$ WT8 cells revealed no binding of HIF1α to the *Slc7a5* proximal promoter, whereas binding was observed to the promoter of pyruvate dehydrogenase kinase 1 (*Pdk1*), a well-recognized HIF1α-responsive gene (Supplemental Experimental Procedures and Figure S3). Taken together, these findings indicate that HIF2α specifically binds directly to the *Slc7a5* proximal promoter through its DNA binding domain, and it therefore contributes to *Slc7a5* gene expression.

HIF2α Induces Renal Cell Carcinoma Cell Proliferation and Xenograft Growth via SLC7A5

HIF2α expression in renal cell VHL-deficient carcinoma has been shown to accelerate tumor growth (Kondo et al., 2003; Kondo et al., 2002; Raval et al., 2005). Thus, we first investigated the contribution of the HIF2α-SLC7A5 pathway to cell proliferation in HIF2α $(P\text{-}A)^2$ WT8 cells. These cells did not proliferate more rapidly than WT8 control cells or HIF2α $(P\text{-}A)^2$bHLH* WT8 cells when cultured in media with normal amino acid content. Indeed, a trend toward decreased proliferation was observed, although this did not differ significantly compared with HIF2α $(P\text{-}A)^2$bHLH* WT8 cells (Figure 5A). Given the role of SLC7A5 as an amino acid carrier, we investigated whether HIF2α can confer a proliferative advantage when cells are grown in conditions of limited amino acid availability. In media with 5% of the normal amino acid concentration, HIF2α $(P\text{-}A)^2$ WT8 cells showed a higher proliferation rate than WT8 control cells or HIF2α $(P\text{-}A)^2$bHLH* WT8 cells (Figure 5A). Moreover, none of the cell lines analyzed exhibited signs of apoptosis in these conditions (data not shown), and proliferation was maintained, although at a lower rate than in normal amino acid media. Importantly, both silencing of *Slc7a5* gene expression and pharmacological inhibition of mTORC1 by rapamycin diminished the proliferative advantage of HIF2α $(P\text{-}A)^2$ WT8 cells in media with low amino acid content (Figures 5B and 5C). This supports the role of the HIF2α-SLC7A5-mTORC1 molecular axis in this

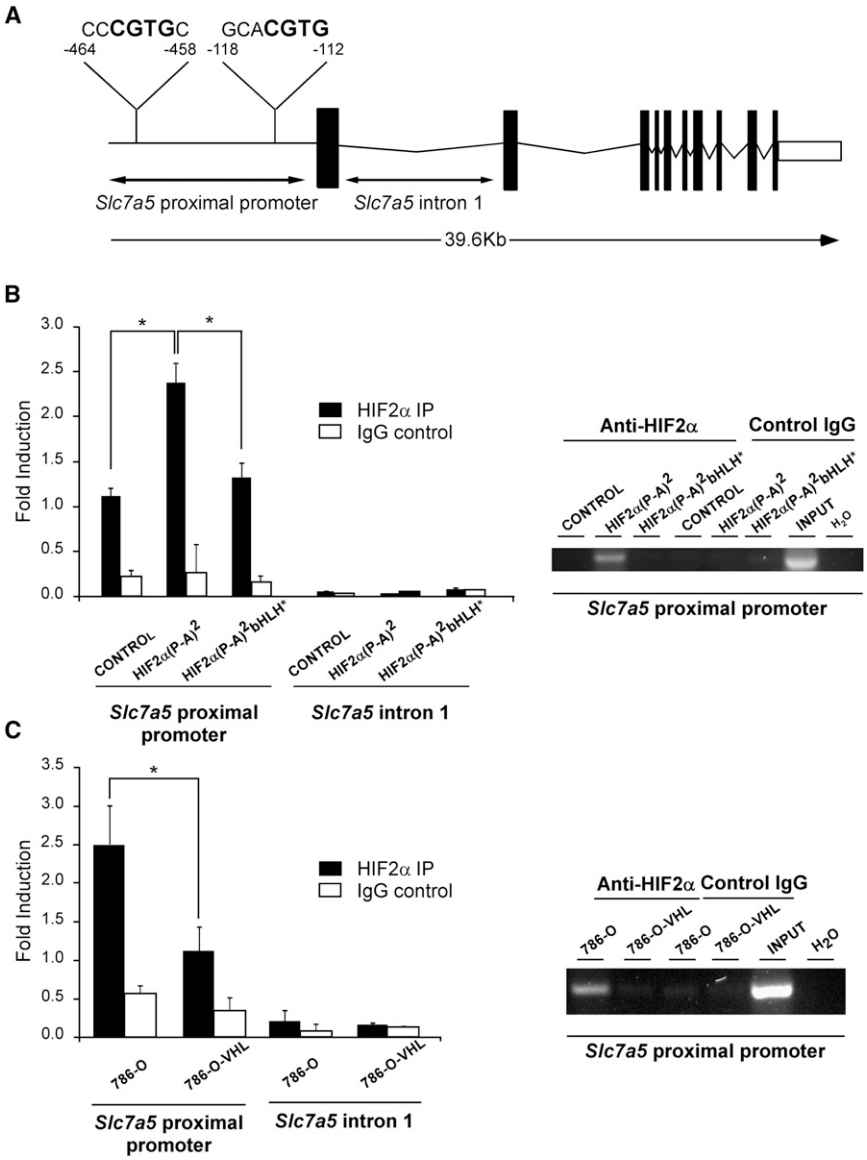

Figure 4. HIF2α Binds to the *Slc7a5* Proximal Promoter

(A) Schematic representation of the human *Slc7a5* gene indicating the positions of the proximal promoter and intron 1 and the nucleotide sequences corresponding to the putative hypoxia-response elements highlighted in bold.

(B and C) ChIP assay to assess the relative HIF2α binding activity to the human *Slc7a5* proximal promoter or intron 1 in (B) HIF2α $(P\text{-}A)^2$, HIF2α $(P\text{-}A)^2$bHLH*, and WT8 control cells or (C) 786-O and their counterparts in which VHL expression was restored (786-O-VHL). Representative gel showing DNA amplified in the ChIP assays is shown. The mean is shown; error bars represent SEM (n = 5, *p < 0.05). IgG, immunoglobulin G. See also Figure S3.

cell-autonomous proliferation advantage when amino acid supply is limited, a scenario thought to mimic the intratumoral environment during tumor growth (Marjon et al., 2004).

To address the role of the HIF2α-SLC7A5 pathway in tumor growth in vivo, we used the 786-O cellular model that has been widely used for assessing the protumoral properties of HIF2α in renal cell carcinoma (Kondo et al., 2003; Raval et al., 2005). For this purpose, we used 786-O-shSLC7A5 cells in which SLC7A5 expression was reduced to similar levels found upon HIF2α silencing in 786-O cells (see Figures 3A and 3C). Importantly, the xenograft growth capability of 786-O-shSLC7A5 cells was markedly suppressed compared with 786-O-shScrambled control cells (Figure 5D). Indeed, after 45 days of subcutaneous injection, the 786-O-shSLC7A5 xenograft size (mm^3) was markedly reduced (345.6 ± 89 in 786-O-shScrambled xenografts versus 56.62 ± 16 in 786-O-shSLC7A5 xenografts; n = 18; p = 0.0039). These findings indicate that HIF2α-dependent SLC7A5 expression is critical for explaining the tumor-promoting properties of HIF2α in 786-O cells when these cells encounter the intratumoral environment, presumably with a limited supply of amino acids (Marjon et al., 2004).

To pursue a possible clinical value for our data, we also investigated SLC7A5 expression in nephrectomy samples from patients with VHL-deficient CCRCCs or patients with non-clear cell renal cell carcinomas (NCRCCs). All CCRCCs (n = 5) showed elevated expression of carbonic anhydrase IX (*Caix*) (Figure S4), a previously identified HIF-dependent gene markedly elevated in CCRCCs as compared with healthy tissue (Mandriota et al., 2002; Raval et al., 2005). A parallel western blot analysis showed that total SLC7A5 signal, present as two bands, was increased in CCRCCs compared with healthy renal tissue and correlated with the CAIX signal (Figure S4). These two bands were identified as SLC7A5 via probing with four different antibodies for SLC7A5 (data not shown). CCRCC sample #4 did not show induction of SLC7A5 expression, which is in line with a much weaker elevation of CAIX expression in this particular sample. Moreover, neither CAIX expression nor SLC7A5 western blot signal was markedly altered in NCRCCs analyzed (n = 3), as observed in CCRCCs (Figure S4). Taken together with the aforementioned xenograft data, these findings show the importance of the HIF2α-SLC7A5 pathway in the CCRCC progression underlying the tumoral and proliferative properties of HIF2α.

HIF2α Regulates *Slc7a5* Gene Expression and mTORC1 Activity in Mice upon *Vhl* Gene Inactivation or Hypoxic Exposure In Vivo

We next explored whether the HIF2α-mTORC1 activatory pathway is present in other biological scenarios. We reasoned

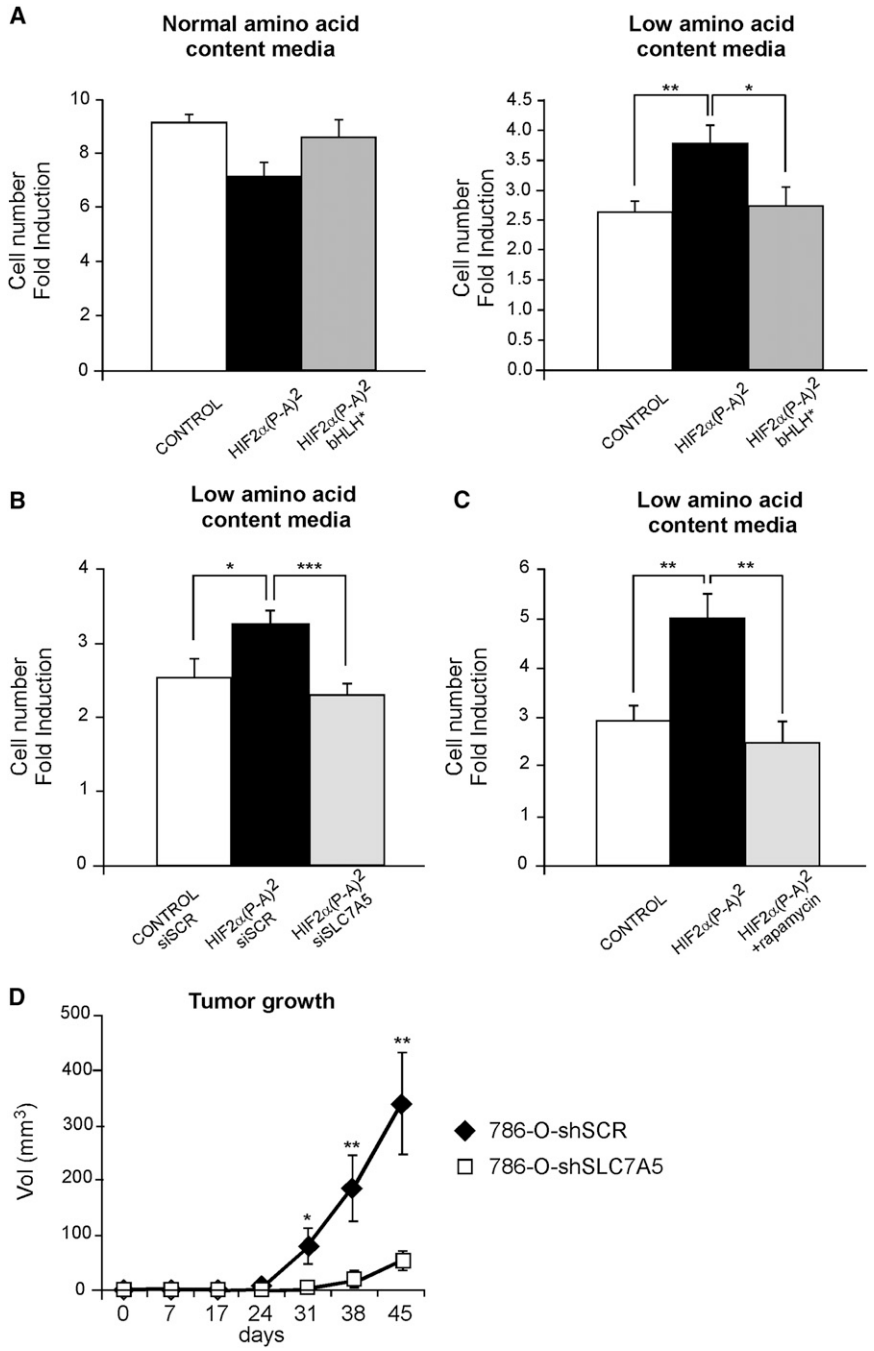

Figure 5. Role of the HIF2α-Dependent SLC7A5 Pathway in Cell Proliferation and Xenograft Growth

(A) Cell number fold induction in control, HIF2α $(P\text{-}A)^2$, and HIF2α $(P\text{-}A)^2$bHLH* WT8 cells cultured for 72 hr in normal media (left panel) or in media containing 5% of the normal amino acid concentration (right panel). Statistical significance was indicated only when HIF2α $(P\text{-}A)^2$ proliferation differed significantly from that of both HIF2α $(P\text{-}A)^2$bHLH* WT8 and control WT8 cells. The mean is shown; error bars represent SEM (n = 4, *p < 0.05, **p < 0.01.

(B) WT8 control cells were transfected with scrambled control siRNA (siSCR), and HIF2α $(P\text{-}A)^2$ WT8 cells were transfected with either siSCR or siRNA for *Slc7a5* (siSLC7A5). Twenty-four hours after transfection, cells were seeded at the same cell density in media containing 5% of the regular amino acid concentration, and the increase in cell number was analyzed after 72 hr. The mean is shown; error bars represent SEM (n = 4, *p < 0.05, ***p < 0.001).

(C) WT8 control cells and HIF2α $(P\text{-}A)^2$ WT8 cells were treated with rapamycin (20 nM) and cultured in media containing 5% of the regular amino acid concentration. The increase in cell number was analyzed after 72 hr. The mean is shown; error bars represent SEM (n = 8, **p < 0.01).

(D) Tumor-volume evolution (Vol) over a 45 day period of SLC7A5-silenced 786-O cells (white squares) and their corresponding control 786-O-shSCR cells (black squares) injected subcutaneously in the dorsal flanks of immunosuppressed severe combined immunodeficiency mice, as detailed in the Experimental Procedures section. The mean is shown; error bars represent SEM (n = 18, *p < 0.05, **p < 0.01).

See also Figure S4.

that this pathway may be especially relevant in the pulmonary response to hypoxia for two reasons: first, the lung exhibits the highest levels of *HIF2α* gene expression in rodents (Wiesener et al., 2003), and second, hypoxia promotes pro-proliferative responses in the lung (Brusselmans et al., 2003; Niedenzu et al., 1981). Mice were exposed for 4 days to hypoxic conditions (10% O_2), a widely used experimental protocol for studying pulmonary HIF2α-dependent biological responses in hypoxia in vivo that lead to HIF2α protein expression in the lung (Brusselmans et al., 2003). Western blot analysis revealed that levels of phosphorylated rpS6 were markedly increased in the lungs of hypoxic mice (Figure 6A). Moreover, hypoxia resulted in 4EBP1 activation, as demonstrated by the increased in phospho-4EBP1 levels assessed with the anti-p4EBP1^{Ser65} and p4EBP1$^{Thr37/46}$ antibodies, preferentially in the upper band when p4EBP1$^{Thr37/46}$ antibody was used (Figure 6A). An rpS6-Ser$^{235/6}$ immunostaining to localize mTORC1 activation in lung tissue revealed that hypoxia-induced mTORC1 was markedly increased in the bronchial epithelium of hypoxic mice (Figure 6B), resulting in a significant increase in the number of rpS6-Ser$^{235/6\ positive}$ bronchial epithelial cells (Figure 6B). We then asked whether HIF2α activation was enough to mimic this localized mTORC1 activation in the lungs. For this purpose, we used adult Vhl^{fl}-UBC-Cre-ER^{T2} mice in which the expression of *Vhl*, a central repressor of HIF activity, can be acutely inactivated (Miró-Murillo et al., 2011), as well as Vhl^{fl}HIF2α^{fl}-UBC-Cre-ER^{T2} mice in which *Vhl* and *HIF2α* can be simultaneously inactivated

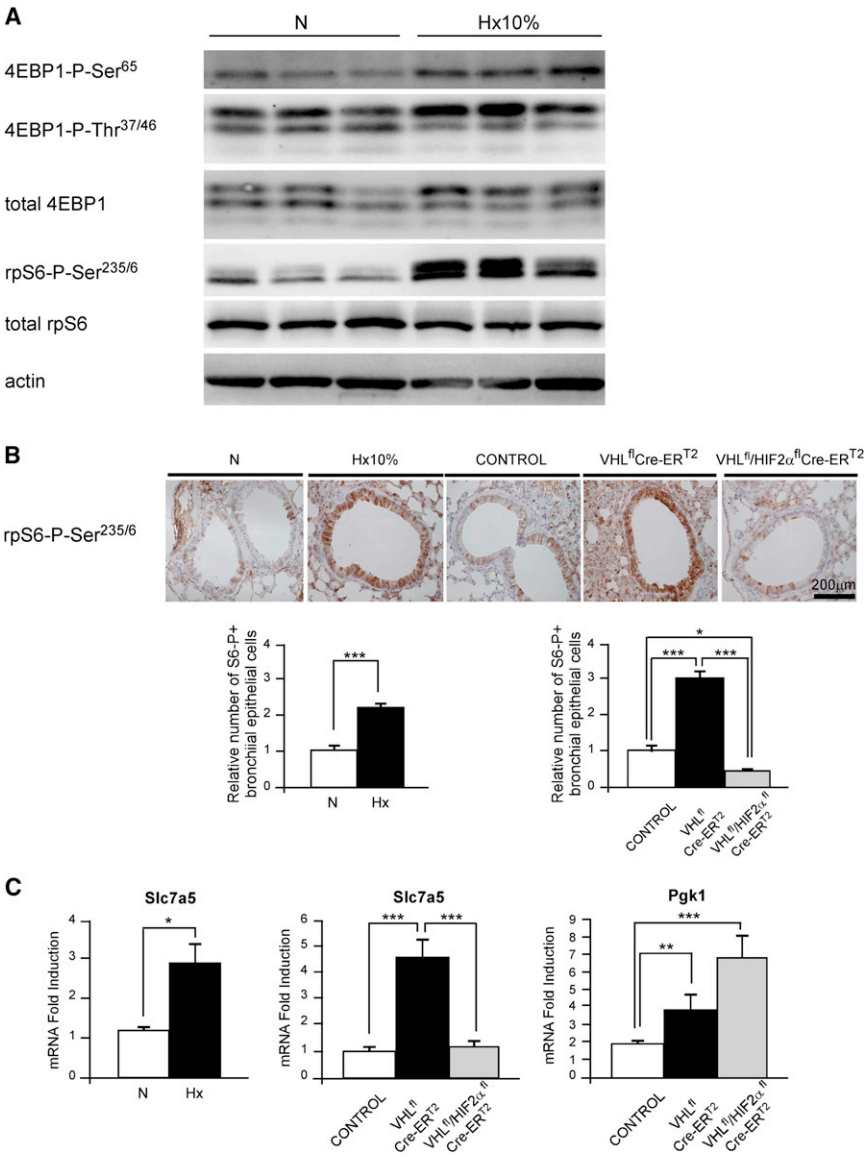

Figure 6. Hypoxia and HIF2α-Dependent mTORC1 Activity and *Slc7a5* Expression in Lung Tissue

(A) Wild-type mice were exposed to hypoxia (10% O_2) (Hx10%) or normoxia (N) for 4 days. Protein extracts from the lungs were analyzed by western blots with antibodies as shown.

(B) Lung phospho-rpS6$^{Ser235/6}$ immunostaining of mice exposed to normoxia or hypoxia (10% O_2) for 4 days and in Vhl^{fl}-UBC-Cre-ER^{T2}, Vhl^{fl}HIF2α^{fl}-UBC-Cre-ER^{T2}, and the corresponding control mice. Quantification of the number of bronchial epithelial cells positive for phospho-rpS6$^{Ser235/6}$ staining in wild-type mice exposed to hypoxia (n = 4) or normoxia (n = 4) as well as Vhl^{fl}-UBC-Cre-ER^{T2} (n = 4), Vhl^{fl}HIF2α^{fl}-UBC-Cre-ER^{T2} (n = 4), and the corresponding control mice (n = 3). Five airways were analyzed for each animal, and >1500 cells were analyzed for each group.

(C) Relative expression of *Slc7a5* gene in the lungs of normoxic (n = 7) and hypoxic mice (n = 6), and *Slc7a5* and *Pgk1* in Vhl^{fl}-UBC-Cre-ER^{T2} mice (n = 5), Vhl^{fl}HIF2α^{fl}-UBC-Cre-ER^{T2} mice (n = 5), and the corresponding controls (n = 6).

See also Figure S5. For (B) and (C), the mean is shown, and error bars represent SEM (*p < 0.05, **p < 0.01, ***p < 0.001).

(Figure S5A). Indeed, HIF2α protein levels were markedly elevated in the lungs of Vhl^{fl}-UBC-Cre-ER^{T2} mice, but not Vhl^{fl}HIF2α^{fl}-UBC-Cre-ER^{T2} mice (Figure S5B). HIF1α protein levels were induced in both Vhl^{fl}-UBC-Cre-ER^{T2} and Vhl^{fl}HIF2α^{fl}-UBC-Cre-ER^{T2} mice (Figure S5B). Importantly, the localized hypoxia-induced mTORC1 activation in bronchial epithelium was nicely mimicked when HIF2α was activated in the lung (Figure 6B). Indeed, the number of rpS6-Ser$^{235/6\ positive}$ bronchial epithelial cells was increased in the lungs of Vhl^{fl}-UBC-Cre-ER^{T2} mice, and this effect was dependent on HIF2α because it was not observed when *Vhl* and *HIF2α* were simultaneously inactivated in the Vhl^{fl}HIF2α^{fl}-UBC-Cre-ER^{T2} mice (Figure 6B). A further analysis showed that *Slc7a5* gene expression was markedly induced in the lungs of mice exposed to low-oxygen tension, as well as upon *Vhl* gene inactivation in Vhl^{fl}-UBC-Cre-ER^{T2} mice, but not in Vhl^{fl}HIF2α^{fl}-UBC-Cre-ER^{T2} mice (Figure 6C). This effect on *Slc7a5* gene expression was specific, in that elevation of phosphoglycerate kinase 1 (*Pgk1*), a well-recognized HIF1α-dependent gene in vivo (Rankin et al., 2007), was not reduced in Vhl^{fl}HIF2α^{fl}-UBC-Cre-ER^{T2} mice (Figure 6C). These data indicate that low-oxygen tension as well as HIF2α induction drive mTORC1 activation and increased *Slc7a5* expression in lung tissue and, importantly, define a hypoxic setting triggering mTORC1 activation.

Constitutive HIF2α activation has also been associated with signs of cell proliferation in liver tissue in vivo (Kim et al., 2006). We then investigated whether HIF2α also drives mTORC1 activation in the liver. Upon *Vhl* gene inactivation in Vhl^{fl}-UBC-Cre-ER^{T2} mice, HIF2α was elevated in the liver, whereas HIF1α was more modestly induced (Figure 7A). As expected, when *Vhl* and *HIF2α* were inactivated simultaneously in Vhl^{fl}HIF2α^{fl}-UBC-Cre-ER^{T2} mice (Figure S6A), HIF2α protein levels were undetectable, whereas modest HIF1α expression was still present (Figure 7A). Western blot analysis showed that both 4EBP1 and p70-S6K phosphorylation levels were induced in Vhl^{fl}-UBC-Cre-ER^{T2} mice, but not in Vhl^{fl}HIF2α^{fl}-UBC-Cre-ER^{T2} mice (Figure 7A), demonstrating the role of HIF2α in the activation of the mTORC1 pathway in the liver. A more detailed analysis in hepatocytes showed that basal hepatocyte rpS6-Ser$^{235/6}$ and SLC7A5 signal intensities were increased upon *Vhl* gene inactivation, and this increase was markedly suppressed when *Vhl* and *HIF2α* were simultaneously inactivated (Figures S6B and 7B). In a parallel analysis, *Slc7a5* gene expression, as well as

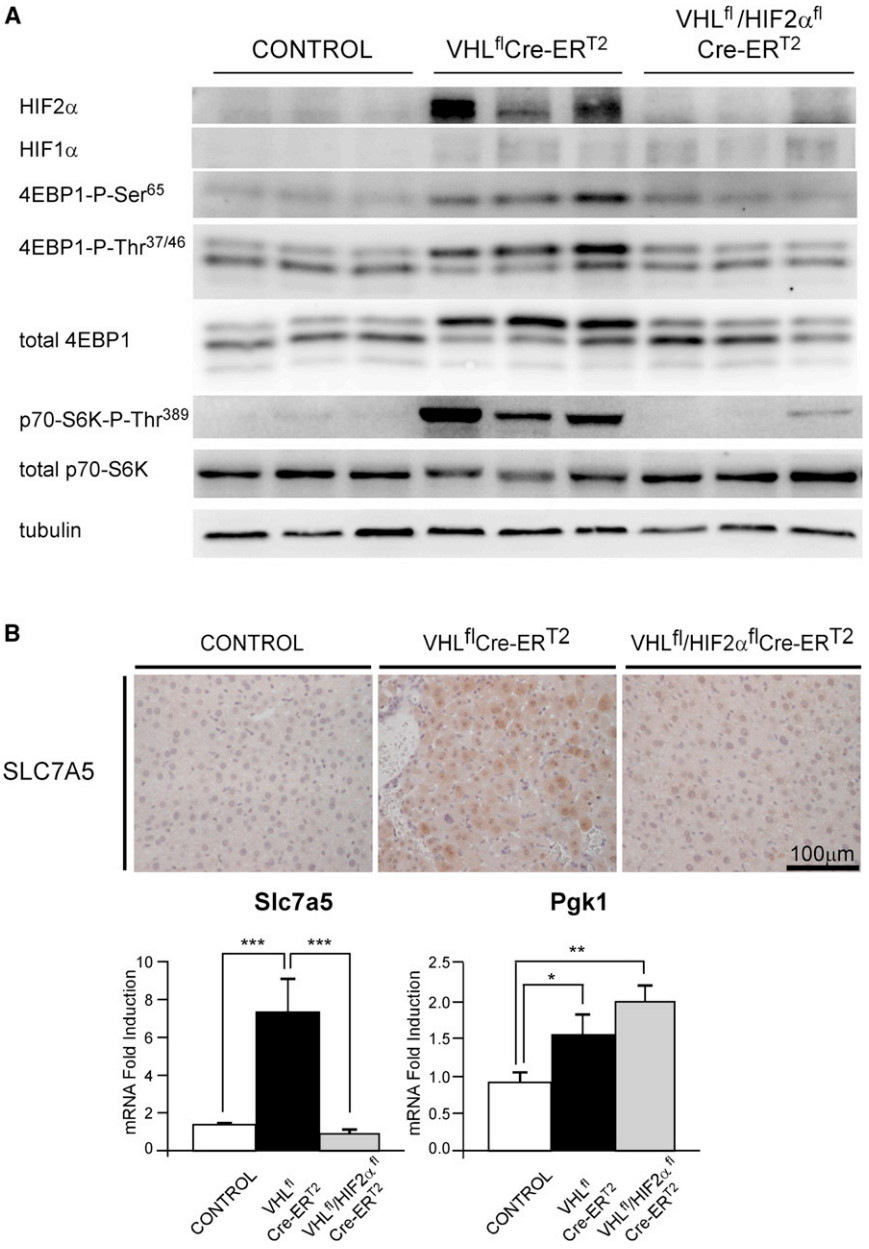

Figure 7. HIF2α-Dependent mTORC1 Activity and SLC7A5 Expression in VHL-Deficient Liver Tissue

(A) Protein extracts from the livers of Vhl^{fl}-UBC-Cre-ER^{T2}, Vhl^{fl}HIF2α^{fl}-UBC-Cre-ER^{T2}, and the corresponding control mice were analyzed by western blots with the indicated antibodies.

(B) SLC7A5 immunostaining of liver tissue (hepatocytes) from Vhl^{fl}-UBC-Cre-ER^{T2}, Vhl^{fl}HIF2α^{fl}-UBC-Cre-ER^{T2}, and corresponding control mice. Relative expression of *Slc7a5* and *Pgk-1* genes in the livers of Vhl^{fl}-UBC-Cre-ER^{T2} (n = 7), Vhl^{fl}HIF2α^{fl}-UBC-Cre-ER^{T2} (n = 6), and corresponding control mice (n = 7).

The mean is shown; error bars represent SEM (*p < 0.05, **p < 0.01, ***p < 0.001). See also Figure S6.

DISCUSSION

Cell-autonomous proliferation can be repressed when oxygen is scarce, limiting energy-consuming processes through HIF-dependent or -independent pathways (Koshiji et al., 2004; Liu et al., 2006). Conversely, the HIF2α isoform has emerged as a proliferation-promoting factor in VHL-deficient tumor cells, although the underlying molecular mechanisms and the nontumoral scenarios in which this occurs remain poorly understood (Gordan et al., 2007; Gordan et al., 2008; Shen et al., 2011). Here we show that HIF2α acts as a potent mTORC1 activator via the amino acid carrier *Slc7a5*, a HIF2-dependent gene, thus describing a molecular basis for the proliferation- and tumor-promoting properties of HIF2α in VHL- deficient cells (see the model in Figure S7).

Previous studies have established that hypoxia represses mTORC1 activity via both HIF1-dependent and HIF-independent pathways (Brugarolas et al., 2004; Liu et al., 2006). Remarkably, our present study reveals an opposite effect of HIF2α, which promotes mTORC1 activation via SLC7A5. Importantly, we found that in mice, HIF2α activation (upon *Vhl* gene inactivation) or hypoxia exposure (10% O_2) lead to mTORC1 activation in lung tissue without the apparent competition of the aforementioned HIF1-dependent and -independent mTORC1 inhibitory responses. Moreover, this mTORC1 activation upon HIF2α induction in lung tissue, as well as in liver tissue, takes place with a concomitant HIF1α activation. These observations suggest that mTORC1 activation via the HIF2α-SLC7A5 pathway overrides other possible pathways mediating hypoxia-induced mTORC1 inhibition that could be executed simultaneously in lungs or livers. Previous studies have shown that the HIF1α-REDD1 pathway does not lead to mTORC1 inhibition in certain tissues, that of the HIF1α-dependent gene *Pgk1*, was elevated upon *Vhl* gene inactivation (Figure 7B). In Vhl^{fl}HIF2α^{fl}-UBC-Cre-ER^{T2} mice, this elevation of *Slc7a5* expression was impaired, whereas *Pgk1* gene expression was not repressed (Figure 7B). Taken together, these findings indicate that HIF2α activation also increases mTORC1 activity and SLC7A5 expression in liver tissue, demonstrating therefore that this HIF2α-dependent pathway is present in different relevant physiological scenarios.

Our data indicate that HIF2α drives mTORC1 activity and SLC7A5 expression in different tumoral and nontumoral scenarios and, importantly, define the hypoxic lung as a relevant physiological context leading to hypoxia-induced mTORC1 activation instead of mTORC1 inhibition, as occurs in other hypoxic settings.

including the liver (Wolff et al., 2011) and possibly also including the lung tissue, in line with our findings. This may explain why mTORC1 activation is observed in the liver and lung upon *Vhl* gene inactivation despite the observed parallel induction of HIF1α activity in Vhl^{fl}-UBC-Cre-ER^{T2} mice. Taken together, the contrasting effects of the different oxygen-sensing pathways on mTORC1 activity indicate that hypoxia can drive mTORC1 activation or inhibition depending on the cell type or tissue and possibly also on the severity and duration of hypoxic challenge, among other variables. Another context in which the HIF2-SLC7A5 pathway is operative is in VHL-deficient renal cell carcinoma cells, in which expression of the HIF2α isoform is constitutively elevated and critical for the progression of these carcinomas. Importantly, HIF2α is activated in normoxic conditions in these cells, and thus HIF2α-dependent mTORC1 activation cannot be counteracted by the HIF1-dependent and HIF-independent pathways that repress mTORC1. In addition, a recent study reported that mTORC1 activity is not affected by REDD1 in VHL-deficient 786-O renal cell carcinoma cells (Kucejova et al., 2011). This study is in line with our observations showing that HIF1α does not repress mTORC1 in WT8 cells, as described here for HIF1α $(P\text{-}A)^2$ WT8 cells.

When discussing the mechanisms by which HIF2α exerts its protumoral activities in these cells, it should be noted that silencing of endogenous HIF2α in VHL-deficient cells, such as 786-O cells, markedly suppresses their tumor growth capability without altering their in vitro cell proliferation in normal culture media (Kondo et al., 2003; Raval et al., 2005). These observations indicate that HIF2α favors renal cell carcinoma cell proliferation in the tumor microenvironment. Silencing of SLC7A5 expression in 786-O cells also results in a marked suppression of their xenograft growth capability, whereas cell proliferation is unchanged when cells are cultured in normal culture media (data not shown). HIF2α-dependent SLC7A5 expression is therefore critical for the proliferation of 786-O cells in the intratumoral context. Indeed, our findings demonstrate that the HIF2α-induced cell proliferation advantage, via SLC7A5, occurs when amino acid availability is more limited than in normal in vitro cell culture conditions, a situation thought to mimic the environment of the inner core of tumors (Marjon et al., 2004). In light of the biological significance of SLC7A5 as an amino acid carrier, our findings indicate that the HIF2α-SLC7A5-mTORC1 pathway is not a limiting factor when extracellular amino acid supply is abundant, yet it is essential for preserving mTORC1 activity when amino acid supply is reduced. Moreover, it should be noted that the amino acid levels encountered in vivo by normal cells such as bronchial epithelial cells and hepatocytes may also be limiting when compared with those of normal culture media. Accordingly, these cells would also require the induction of SLC7A5 via HIF2α to accelerate amino-acid-dependent mTORC1 activation.

Our data show that SLC7A5 expression is induced in human samples of VHL-deficient CCRCCs. Previous studies reported that HIF2α is present in all CCRCCs analyzed (Gordan et al., 2008), and therefore SLC7A5 regulation can occur as soon as CCRCCs express HIF2α, considering that *Slc7a5* is a direct HIF2α target gene. Expression of the amino acid transporter SLC7A5 is upregulated in numerous human cancers and is implicated in the growth and survival of several cancer cell lines (reviewed in Fuchs and Bode, 2005). However, the molecular mechanisms that regulate this carrier remain largely unknown. Here, we describe a molecular mechanism that regulates *Slc7a5* transcription, identifying *Slc7a5* as a HIF2-responsive gene. Our analysis shows that the binding of HIF2α to the proximal promoter of the *Slc7a5* gene is specific because it is not observed when HIF1α is constitutively present in HIF1α $(P\text{-}A)^2$ WT8 cells. Further investigation will be required for understanding how the *Slc7a5* proximal promoter specifically favors the binding of the HIF2α isoform.

In summary, we describe a link between HIF pathways and mTORC1 activation involving the HIF2α-SLC7A5-mTORC1 axis, thus providing a molecular basis for the proliferation- and tumor-promoting properties of HIF2α. Moreover, we define relevant physiological scenarios, including those that occur in lung and liver tissue, in which HIF2α drives mTORC1 activation, in contrast to other hypoxic pathways that lead to mTORC1 inhibition.

EXPERIMENTAL PROCEDURES

Cells and Reagents

Retroviral vectors encoding HIF2α $(P\text{-}A)^2$, HIF2α $(P\text{-}A)^2$bHLH*, and HIF1α $(P\text{-}A)^2$ were used to generate stable transfectants in WT8 cells (see Supplemental Information). WT8 cells infected with the pBABE empty vector were used as WT8 control cells. Retroviral vectors pRV-VHL and pRV control were also used to generate stable transfectants in 786-O-pRV (control 786-O cells) and 786-O-pRV-VHL (786-O-VHL cells) (Kondo et al., 2003).

SLC7A5 (sc-62555-V) and control (sc-108080) small hairpin RNA (shRNA) lentiviral particles (from Santa Cruz Biotechnology) were used to generate stable transfectants in the 786-O cells, 786-O-shSLC7A5 cells, and their corresponding control 786-O-shSCR cells. All cells were maintained in RPMI 1640 with GlutaMAX-I (GIBCO) supplemented with 100 units/ml penicillin, 100 μg/ml streptomycin, and 10% fetal bovine serum (FBS, Cultek). To prepare mediums with lower amino acid content, normal RPMI media was diluted with the corresponding volume of amino-acid-free RPMI. Mediums with reduced content of essential amino acids and glutamine were prepared by adding the corresponding volumes of both essential and nonessential amino acids to amino-acid-free RPMI. All amino-acid-deprived mediums were supplemented with 10% dialyzed FBS (Sigma-Aldrich). Cells were routinely cultured in 21% O_2 and 5% CO_2 (normoxic conditions). Rapamycin was purchased from Sigma-Aldrich.

Mice

Vhl^{fl}-UBC-Cre-ER^{T2} mice and gene inactivation by exposure to tamoxifen diet were described previously (Miró-Murillo et al., 2011). $Vhl^{fl}HIF2\alpha^{fl}$-UBC-Cre-ER^{T2} mice were generated through the appropriate crosses using Epas1tm1Mcs/J mice (Jackson Laboratories, stock no. 008407). To induce hypoxia in vivo, mice were placed in an airtight chamber with inflow and outflow valves, which was infused with a mixture of 10% O_2 and 90% N_2 (Carburos Metálicos).

Ethics Statements

All mouse experimental procedures were approved by the research ethics committee at the UAM (Autonomous University of Madrid) and were carried out under the supervision of the Head of Animal Welfare and Health at the UAM, in accordance with Spanish and European guidelines (B.O.E, 18 March 1988, and 86/609/EEC European Council Directives).

Fresh human samples were obtained from patients diagnosed and surgically treated in the Urology Department of the University Complex of Albacete, under the supervision of the local ethical committee and the pathologist, with the purpose of not interfering in the histological evaluation.

Statistical Analysis

Data were expressed as the mean ± SEM, and the differences between groups were analyzed using a two-tailed Student's t test.

SUPPLEMENTAL INFORMATION

Supplemental Information includes seven figures and Supplemental Experimental Procedures and can be found with this article online at http://dx.doi.org/10.1016/j.molcel.2012.09.017.

ACKNOWLEDGMENTS

We thank Dr.Manuel Palacin for scientific advice. We also thank Dr. W.G. Kaelin (Medical Oncology/Molecular and Cellular Department, Dana-Farber Cancer Institute, Harvard Medical School, Boston) for providing the vectors encoding the HIF1α and HIF2α forms. This work was supported by grants from the Ministerio de Educación y Ciencia (BFU2008-03407/BMC and SAF2011-29716), RECAVA (RD06/0014/0031), CICYT (SAF2007-60592), CAM (SAL0311/2006), and the FP7-Health European Commission grant (282551, EpoCan).

Received: August 24, 2011
Revised: July 2, 2012
Accepted: September 11, 2012
Published online: October 25, 2012

REFERENCES

Brugarolas, J., Lei, K., Hurley, R.L., Manning, B.D., Reiling, J.H., Hafen, E., Witters, L.A., Ellisen, L.W., and Kaelin, W.G., Jr. (2004). Regulation of mTOR function in response to hypoxia by REDD1 and the TSC1/TSC2 tumor suppressor complex. Genes Dev. *18*, 2893–2904.

Bruick, R.K., and McKnight, S.L. (2001). A conserved family of prolyl-4-hydroxylases that modify HIF. Science *294*, 1337–1340.

Brusselmans, K., Compernolle, V., Tjwa, M., Wiesener, M.S., Maxwell, P.H., Collen, D., and Carmeliet, P. (2003). Heterozygous deficiency of hypoxia-inducible factor-2alpha protects mice against pulmonary hypertension and right ventricular dysfunction during prolonged hypoxia. J. Clin. Invest. *111*, 1519–1527.

Cam, H., Easton, J.B., High, A., and Houghton, P.J. (2010). mTORC1 signaling under hypoxic conditions is controlled by ATM-dependent phosphorylation of HIF-1α. Mol. Cell *40*, 509–520.

Carmeliet, P., Dor, Y., Herbert, J.M., Fukumura, D., Brusselmans, K., Dewerchin, M., Neeman, M., Bono, F., Abramovitch, R., Maxwell, P., et al. (1998). Role of HIF-1alpha in hypoxia-mediated apoptosis, cell proliferation and tumour angiogenesis. Nature *394*, 485–490.

Covello, K.L., Kehler, J., Yu, H., Gordan, J.D., Arsham, A.M., Hu, C.J., Labosky, P.A., Simon, M.C., and Keith, B. (2006). HIF-2alpha regulates Oct-4: effects of hypoxia on stem cell function, embryonic development, and tumor growth. Genes Dev. *20*, 557–570.

DeYoung, M.P., Horak, P., Sofer, A., Sgroi, D., and Ellisen, L.W. (2008). Hypoxia regulates TSC1/2-mTOR signaling and tumor suppression through REDD1-mediated 14-3-3 shuttling. Genes Dev. *22*, 239–251.

Epstein, A.C., Gleadle, J.M., McNeill, L.A., Hewitson, K.S., O'Rourke, J., Mole, D.R., Mukherji, M., Metzen, E., Wilson, M.I., Dhanda, A., et al. (2001). C. elegans EGL-9 and mammalian homologs define a family of dioxygenases that regulate HIF by prolyl hydroxylation. Cell *107*, 43–54.

Fuchs, B.C., and Bode, B.P. (2005). Amino acid transporters ASCT2 and LAT1 in cancer: partners in crime? Semin. Cancer Biol. *15*, 254–266.

Goda, N., Ryan, H.E., Khadivi, B., McNulty, W., Rickert, R.C., and Johnson, R.S. (2003). Hypoxia-inducible factor 1alpha is essential for cell cycle arrest during hypoxia. Mol. Cell. Biol. *23*, 359–369.

Gordan, J.D., Bertout, J.A., Hu, C.J., Diehl, J.A., and Simon, M.C. (2007). HIF-2alpha promotes hypoxic cell proliferation by enhancing c-myc transcriptional activity. Cancer Cell *11*, 335–347.

Gordan, J.D., Lal, P., Dondeti, V.R., Letrero, R., Parekh, K.N., Oquendo, C.E., Greenberg, R.A., Flaherty, K.T., Rathmell, W.K., Keith, B., et al. (2008). HIF-alpha effects on c-Myc distinguish two subtypes of sporadic VHL-deficient clear cell renal carcinoma. Cancer Cell *14*, 435–446.

Hara, K., Maruki, Y., Long, X., Yoshino, K., Oshiro, N., Hidayat, S., Tokunaga, C., Avruch, J., and Yonezawa, K. (2002). Raptor, a binding partner of target of rapamycin (TOR), mediates TOR action. Cell *110*, 177–189.

Ivan, M., Kondo, K., Yang, H., Kim, W., Valiando, J., Ohh, M., Salic, A., Asara, J.M., Lane, W.S., and Kaelin, W.G., Jr. (2001). HIFalpha targeted for VHL-mediated destruction by proline hydroxylation: implications for O2 sensing. Science *292*, 464–468.

Jaakkola, P., Mole, D.R., Tian, Y.M., Wilson, M.I., Gielbert, J., Gaskell, S.J., Kriegsheim Av, Hebestreit, H.F., Mukherji, M., Schofield, C.J., et al. (2001). Targeting of HIF-alpha to the von Hippel-Lindau ubiquitylation complex by O2-regulated prolyl hydroxylation. Science *292*, 468–472.

Kim, D.H., Sarbassov, D.D., Ali, S.M., King, J.E., Latek, R.R., Erdjument-Bromage, H., Tempst, P., and Sabatini, D.M. (2002). mTOR interacts with raptor to form a nutrient-sensitive complex that signals to the cell growth machinery. Cell *110*, 163–175.

Kim, W.Y., Safran, M., Buckley, M.R., Ebert, B.L., Glickman, J., Bosenberg, M., Regan, M., and Kaelin, W.G., Jr. (2006). Failure to prolyl hydroxylate hypoxia-inducible factor alpha phenocopies VHL inactivation in vivo. EMBO J. *25*, 4650–4662.

Kim, E., Goraksha-Hicks, P., Li, L., Neufeld, T.P., and Guan, K.L. (2008). Regulation of TORC1 by Rag GTPases in nutrient response. Nat. Cell Biol. *10*, 935–945.

Kondo, K., Klco, J., Nakamura, E., Lechpammer, M., and Kaelin, W.G., Jr. (2002). Inhibition of HIF is necessary for tumor suppression by the von Hippel-Lindau protein. Cancer Cell *1*, 237–246.

Kondo, K., Kim, W.Y., Lechpammer, M., and Kaelin, W.G., Jr. (2003). Inhibition of HIF2alpha is sufficient to suppress pVHL-defective tumor growth. PLoS Biol. *1*, E83.

Koshiji, M., Kageyama, Y., Pete, E.A., Horikawa, I., Barrett, J.C., and Huang, L.E. (2004). HIF-1alpha induces cell cycle arrest by functionally counteracting Myc. EMBO J. *23*, 1949–1956.

Kucejova, B., Peña-Llopis, S., Yamasaki, T., Sivanand, S., Tran, T.A., Alexander, S., Wolff, N.C., Lotan, Y., Xie, X.J., Kabbani, W., et al. (2011). Interplay between pVHL and mTORC1 pathways in clear-cell renal cell carcinoma. Mol. Cancer Res. *9*, 1255–1265.

Kwiatkowski, D.J. (2003). Tuberous sclerosis: from tubers to mTOR. Ann. Hum. Genet. *67*, 87–96.

Li, Y., Corradetti, M.N., Inoki, K., and Guan, K.L. (2004). TSC2: filling the GAP in the mTOR signaling pathway. Trends Biochem. Sci. *29*, 32–38.

Li, Y., Wang, Y., Kim, E., Beemiller, P., Wang, C.Y., Swanson, J., You, M., and Guan, K.L. (2007). Bnip3 mediates the hypoxia-induced inhibition on mammalian target of rapamycin by interacting with Rheb. J. Biol. Chem. *282*, 35803–35813.

Liu, L., Cash, T.P., Jones, R.G., Keith, B., Thompson, C.B., and Simon, M.C. (2006). Hypoxia-induced energy stress regulates mRNA translation and cell growth. Mol. Cell *21*, 521–531.

Ma, X.M., and Blenis, J. (2009). Molecular mechanisms of mTOR-mediated translational control. Nat. Rev. Mol. Cell Biol. *10*, 307–318.

Mandriota, S.J., Turner, K.J., Davies, D.R., Murray, P.G., Morgan, N.V., Sowter, H.M., Wykoff, C.C., Maher, E.R., Harris, A.L., Ratcliffe, P.J., and Maxwell, P.H. (2002). HIF activation identifies early lesions in VHL kidneys: evidence for site-specific tumor suppressor function in the nephron. Cancer Cell *1*, 459–468.

Manning, B.D., and Cantley, L.C. (2003). Rheb fills a GAP between TSC and TOR. Trends Biochem. Sci. *28*, 573–576.

Marjon, P.L., Bobrovnikova-Marjon, E.V., and Abcouwer, S.F. (2004). Expression of the pro-angiogenic factors vascular endothelial growth factor and interleukin-8/CXCL8 by human breast carcinomas is responsive to nutrient deprivation and endoplasmic reticulum stress. Mol. Cancer *3*, 4.

Miró-Murillo, M., Elorza, A., Soro-Arnáiz, I., Albacete-Albacete, L., Ordoñez, A., Balsa, E., Vara-Vega, A., Vázquez, S., Fuertes, E., Fernández-Criado, C., et al. (2011). Acute Vhl gene inactivation induces cardiac HIF-dependent erythropoietin gene expression. PLoS ONE *6*, e22589.

Nicklin, P., Bergman, P., Zhang, B., Triantafellow, E., Wang, H., Nyfeler, B., Yang, H., Hild, M., Kung, C., Wilson, C., et al. (2009). Bidirectional transport of amino acids regulates mTOR and autophagy. Cell *136*, 521–534.

Niedenzu, C., Grasedyck, K., Voelkel, N.F., Bittmann, S., and Lindner, J. (1981). Proliferation of lung cells in chronically hypoxic rats. An autoradiographic and radiochemical study. Int. Arch. Occup. Environ. Health *48*, 185–193.

Rankin, E.B., Biju, M.P., Liu, Q., Unger, T.L., Rha, J., Johnson, R.S., Simon, M.C., Keith, B., and Haase, V.H. (2007). Hypoxia-inducible factor-2 (HIF-2) regulates hepatic erythropoietin in vivo. J. Clin. Invest. *117*, 1068–1077.

Raval, R.R., Lau, K.W., Tran, M.G., Sowter, H.M., Mandriota, S.J., Li, J.L., Pugh, C.W., Maxwell, P.H., Harris, A.L., and Ratcliffe, P.J. (2005). Contrasting properties of hypoxia-inducible factor 1 (HIF-1) and HIF-2 in von Hippel-Lindau-associated renal cell carcinoma. Mol. Cell. Biol. *25*, 5675–5686.

Sancak, Y., Peterson, T.R., Shaul, Y.D., Lindquist, R.A., Thoreen, C.C., Bar-Peled, L., and Sabatini, D.M. (2008). The Rag GTPases bind raptor and mediate amino acid signaling to mTORC1. Science *320*, 1496–1501.

Schmelzle, T., and Hall, M.N. (2000). TOR, a central controller of cell growth. Cell *103*, 253–262.

Shen, C., Beroukhim, R., Schumacher, S.E., Zhou, J., Chang, M., Signoretti, S., and Kaelin, W.G., Jr. (2011). Genetic and functional studies implicate HIF1α as a 14q kidney cancer suppressor gene. Cancer Discov. *1*, 222–235.

Sonenberg, N., and Hinnebusch, A.G. (2009). Regulation of translation initiation in eukaryotes: mechanisms and biological targets. Cell *136*, 731–745.

Wang, G.L., Jiang, B.H., Rue, E.A., and Semenza, G.L. (1995). Hypoxia-inducible factor 1 is a basic-helix-loop-helix-PAS heterodimer regulated by cellular O2 tension. Proc. Natl. Acad. Sci. USA *92*, 5510–5514.

Wang, X., Campbell, L.E., Miller, C.M., and Proud, C.G. (1998). Amino acid availability regulates p70 S6 kinase and multiple translation factors. Biochem. J. *334*, 261–267.

Wiesener, M.S., Jürgensen, J.S., Rosenberger, C., Scholze, C.K., Hörstrup, J.H., Warnecke, C., Mandriota, S., Bechmann, I., Frei, U.A., Pugh, C.W., et al. (2003). Widespread hypoxia-inducible expression of HIF-2alpha in distinct cell populations of different organs. FASEB J. *17*, 271–273.

Wolff, N.C., Vega-Rubin-de-Celis, S., Xie, X.J., Castrillon, D.H., Kabbani, W., and Brugarolas, J. (2011). Cell-type-dependent regulation of mTORC1 by REDD1 and the tumor suppressors TSC1/TSC2 and LKB1 in response to hypoxia. Mol. Cell. Biol. *31*, 1870–1884.

Molecular Cell, Volume *48*

Supplemental Information

HIF2α Acts as an mTORC1 Activator through the Amino Acid Carrier SLC7A5

Ainara Elorza, Inés Soro-Arnaiz, Florinda Meléndez-Rodriguez, Victoria Rodriguez-Vaello, Glenn Marsboom, Guillermo de Cárcer, Bárbara Acosta-Iborra, Lucas Albacete-Albacete, Angel Ordoñez, Leticia Serrano-Oviedo, Jose Miguel Gimenez-Bachs, Alicia Vara-Vega, Antonio Salinas, Ricardo Sánchez-Prieto, Rafael Martin del Rio, Francisco Sanchez-Madrid, Marcos Malumbres, Manuel O. Landázuri, and Julián Aragonés

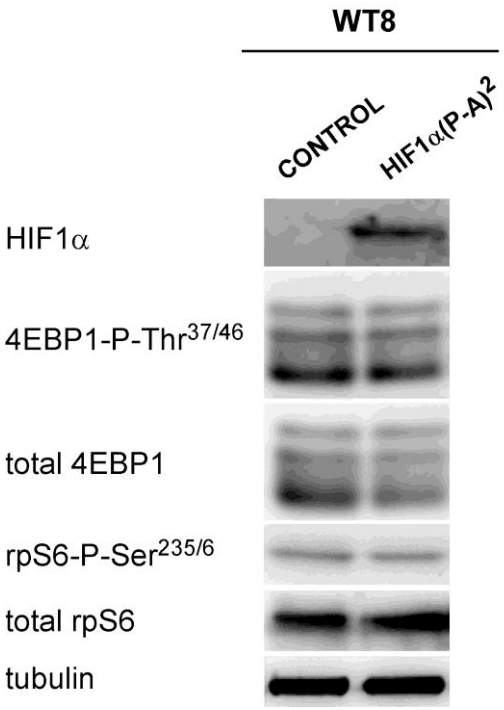

Figure S1. Effects of HIF1α Activity on mTORC1 Activation in WT8 Cells, Related to Figure 1

Western blot analysis of HIF1α, tubulin, total 4EBP1 and total rpS6, as well as phosphorylated 4EBP1 and rpS6 residues indicated in HIF1α $(P\text{-}A)^2$ WT8 and WT8 control cells cultured for 72 hours in media with 50% of the normal amino acid content.

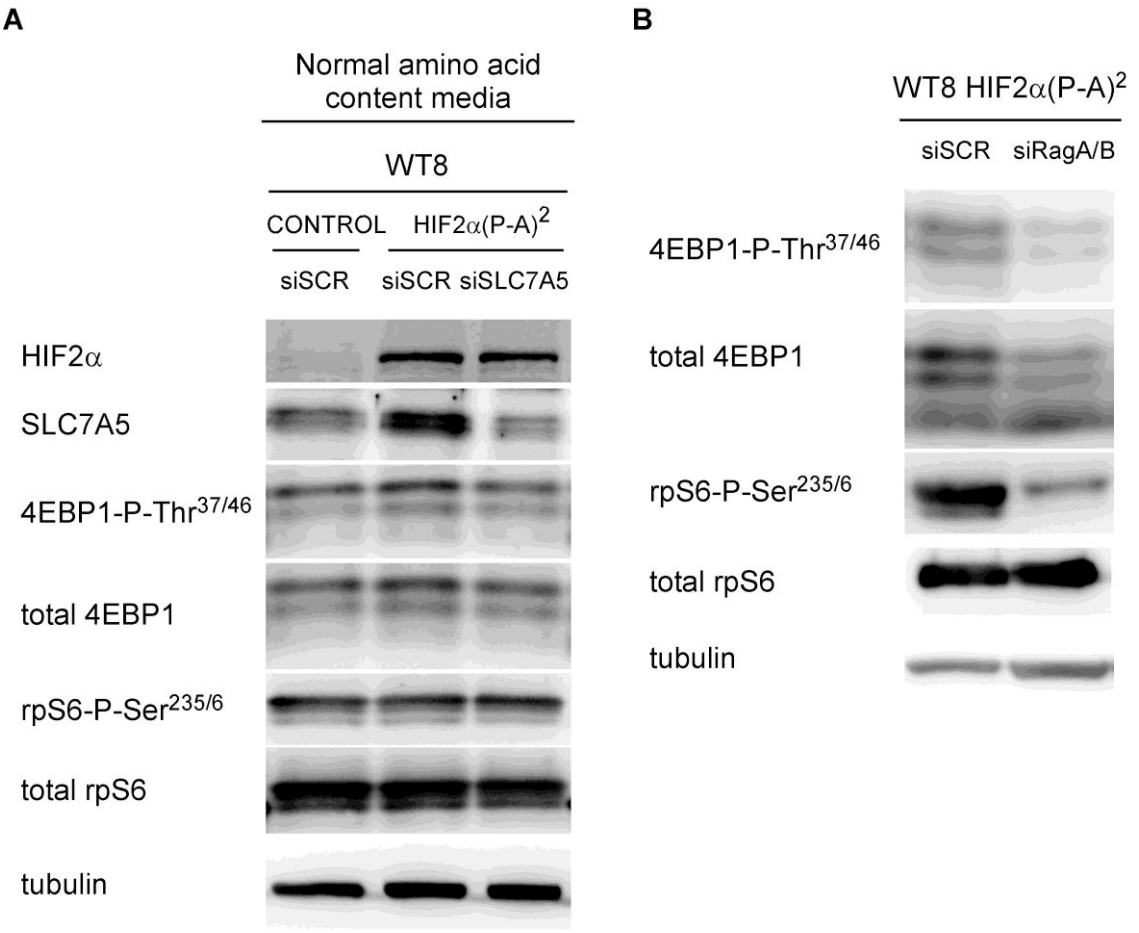

Figure S2. Contribution of SLC7A5 Expression to mTORC1 Activation in Normal Media, and mTORC1 Activity in RagA- and RagB-Silenced HIF2α (P-A)^2 WT8 cells in Low-Amino-Acid Media, Related to Figure 2

(A) WT8 control cells were transfected with scrambled siRNA control (siSCR) and HIF2α (P-A)^2 WT8 cells were transfected with either siSCR or siRNA against *Slc7a5* (siSLC7A5), and subsequently cultured for 72 hours in media with normal amino acid content. Whole cell extracts were analyzed by Western blot using antibodies against HIF2α, SLC7A5, tubulin, total and phospho-4EBP-1 indicated as well as total and phospho-rpS6 indicated. (B) HIF2α (P-A)^2 WT8 cells were transfected with either siSCR or siRNAs against *RagA* and *RagB*, and subsequently cultured for 72 hours in media with 50% of the normal amino acid content. *RagA* and *RagB* gene expression was silenced by 86% and 71% respectively. Whole cell extracts were analyzed by Western blot using antibodies against tubulin, total and phospho-4EBP1 indicated as well as total and phospho-rpS6 indicated.

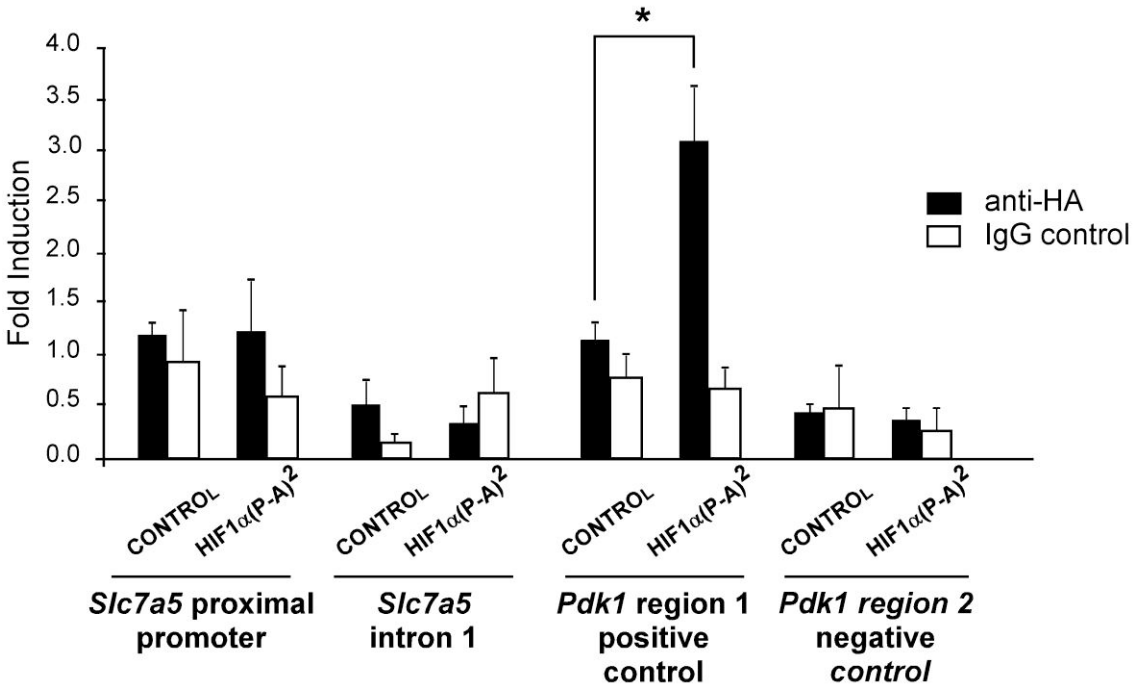

Figure S3. ChIP Assay Analysis of HIF1α Binding to the Human *Slc7a5* Promoter, Related to Figure 4

ChIP assay analysis of HIF1α binding to the human *Slc7a5* proximal promoter, intron 1 and the *Pdk1* regulatory sequences in HIF1α $(P\text{-}A)^2$ WT8 and WT8 control cells. Anti-HA antibodies were used for these ChIP assays as HIF1α $(P\text{-}A)^2$ is a HA-tagged version. After immunoprecipitation with anti-HA or anti-IgG antibodies, RT-PCR was quantified using oligos that amplify a region of the *Slc7a5* proximal promoter, *Slc7a5* intron 1 or the *Pdk1* region 1 and region 2. Data are represented as the change relative to WT8 control cells. The mean is shown; error bar represents SEM (n = 3;* $p<0.05$).

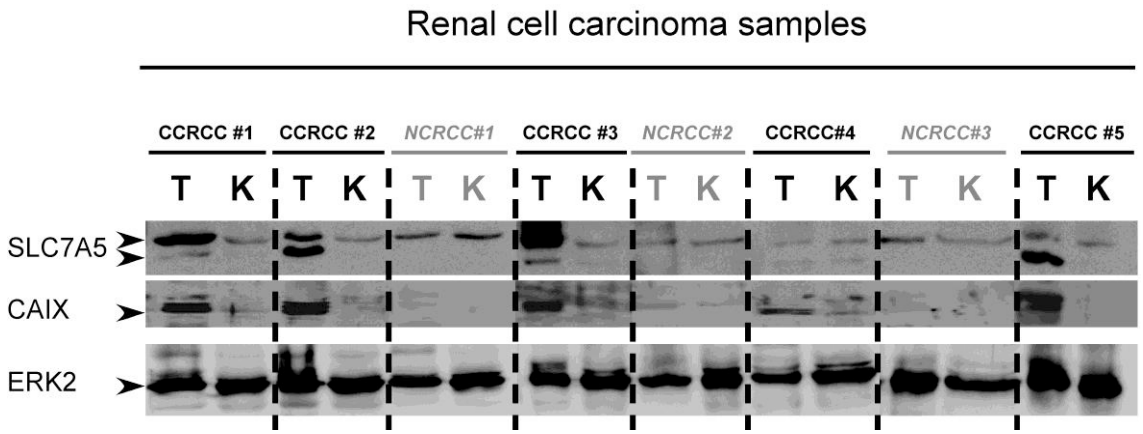

Figure S4. SLC7A5 Protein Expression in Renal Cell Carcinomas and the Corresponding Paired Unaffected Kidney Tissue, Related to Figure 5

Western blot analysis of SLC7A5 expression of 5 sporadic VHL-defective CCRCCs and 3 non-clear renal cell carcinomas (NCRCCs), including corresponding paired unaffected kidney tissue. NCRCC samples #1 and #2 were diagnosed as oncocytoma renal cell carcinoma and NCRCC sample #3 corresponds to a cromophobe renal cell carcinoma. T=Tumor and K= unaffected kidney tissue. The two bands indicated (arrowheads) were identified as SLC7A5. All CCRCCs used in this analysis (n = 5) were positive for the expression of carbonic anydrase IX (CAIX). ERK2 was used as a loading control.

A

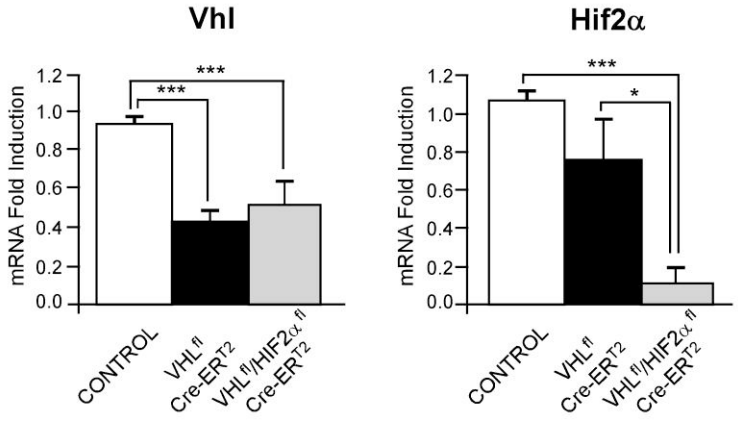

B

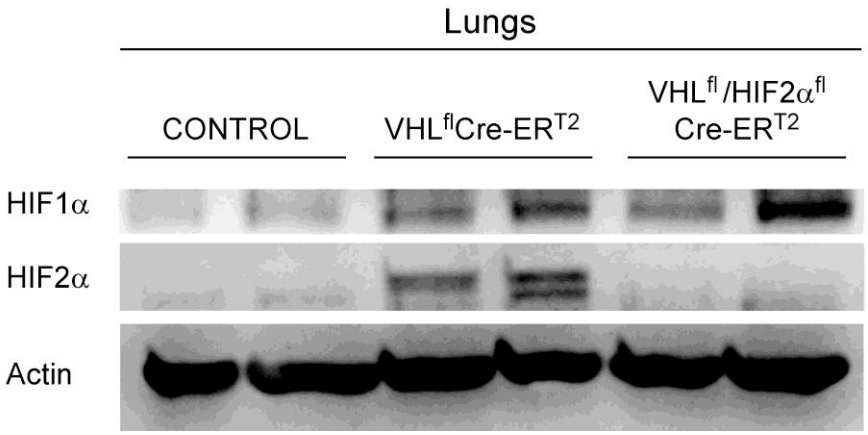

Figure S5. HIF1α and HIF2α Protein Expression in the Lungs upon *Vhl* Gene Inactivation, Related to Figure 6

(A) *Vhl* and *HIF2α* gene expression in the lungs of Vhl^{fl}-UBC-Cre-ER^{T2} mice (n = 5), Vhl^{fl}HIF2α^{fl}-UBC-Cre-ER^{T2} mice (n = 5) and the corresponding controls (n = 6), normalized to that of *Hprt*. The mean is shown; error bars represent SEM (*p<0.05; ***p<0.001). (B) Protein extracts from the lungs were analyzed by Western blots for HIF1α, HIF2α protein levels and actin as loading control.

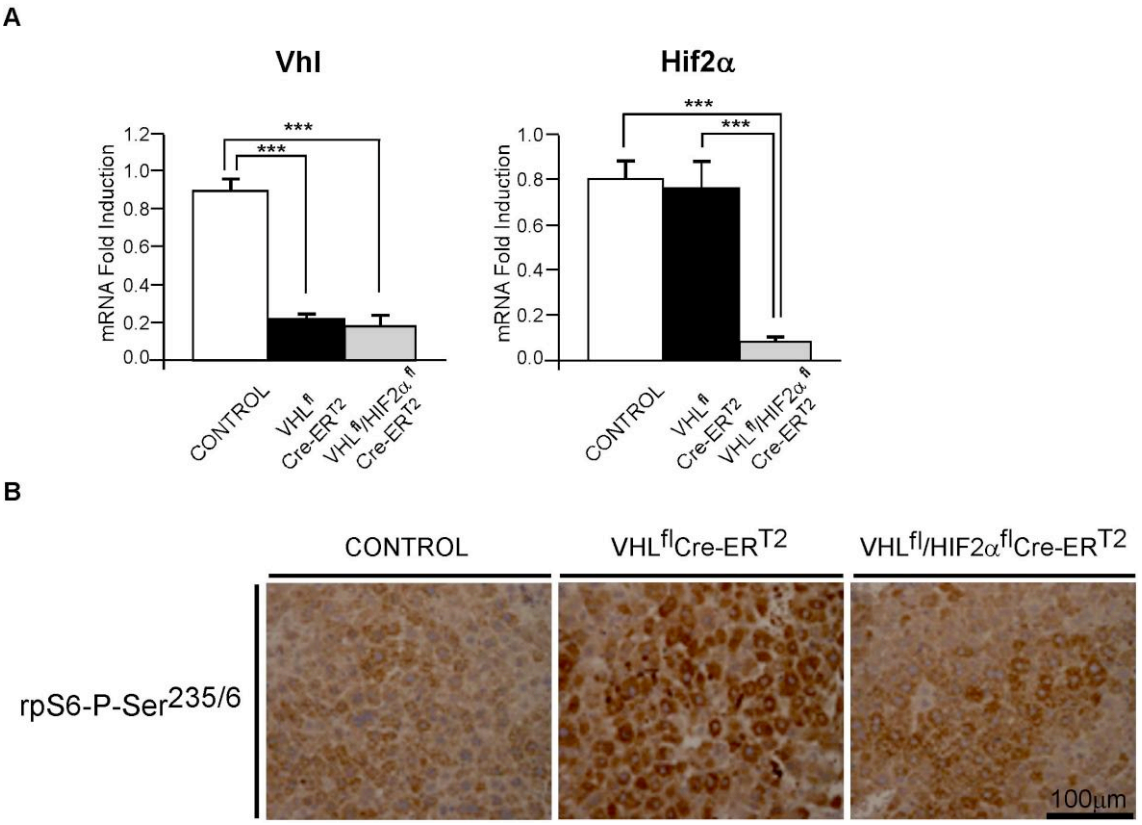

Figure S6. HIF2α-Dependent mTORC1 Activation in the Liver upon *Vhl* Gene Inactivation, Related to Figure 7

(A) *Vhl* and *HIF2α* expression in the livers of Vhl^{fl}-UBC-Cre-ER^{T2} (n = 7), Vhl^{fl}HIF2α^{fl}-UBC-Cre-ER^{T2} (n = 6) and corresponding control mice (n = 7), normalized to that of *Hprt*. The mean is shown; error bars represent SEM (***p<0.001). (B) Phospho-rpS6-Ser$^{235/236}$ immunostaining of liver tissue (hepatocytes) from Vhl^{fl}-UBC-Cre-ER^{T2}, Vhl^{fl}HIF2α^{fl}-UBC-Cre-ER^{T2} and corresponding control mice.

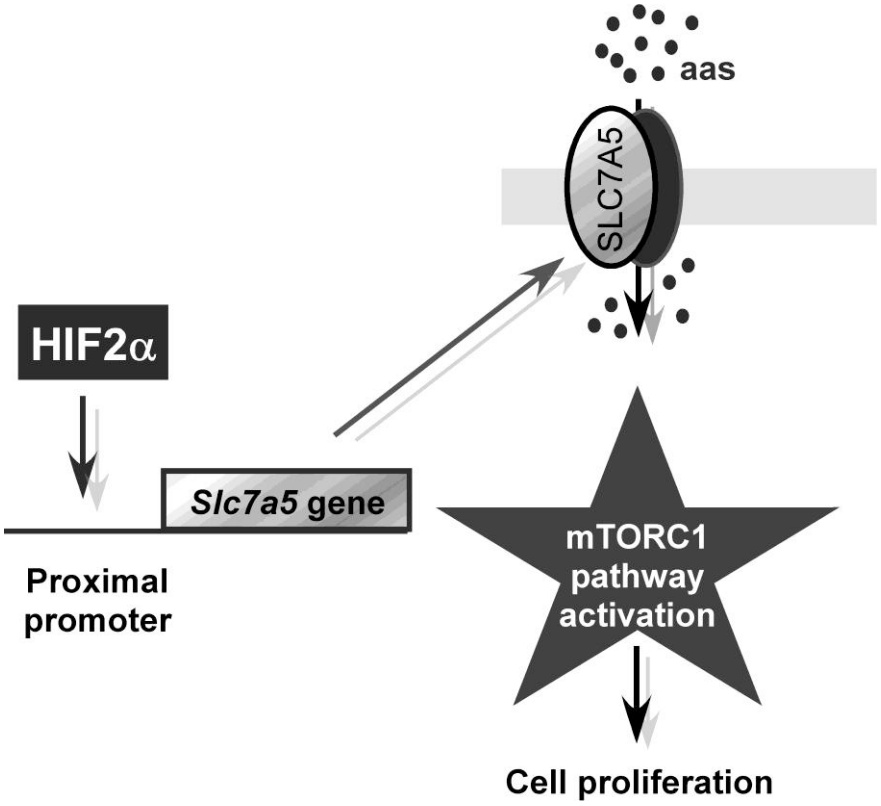

Figure S7. mTORC1 Activation by the HIF2α-SLC7A5 Pathway

The HIF2α oxygen pathway induces the expression of the amino acid carrier SLC7A5, which facilitates the amino acid-dependent mTORC1 activity and the subsequent cell autonomous proliferation advantage.

Supplemental Experimental Procedures

DNA constructs. To generate stable transfectants in WT8 cells we used a retroviral vector encoding HIF2α P405A;P531A (HIF2α $(P\text{-}A)^2$), which is a stable HIF2α form lacking critical proline residues that is not recognized by VHL and that is therefore constitutively active in normoxic conditions regardless of the oxygen tension (Kondo et al., 2003). As an additional control, we used a retroviral vector encoding HIF2α $(P\text{-}A)^2$bHLH*, which is a version of the stable HIF2α $(P\text{-}A)^2$ protein that contains a five amino acid substitution within the HIF2α basic helix–loop–helix (bHLH) domain, resulting in the loss of its transcriptional activity (Kondo et al., 2003; Kondo et al., 2002). Moreover we used a retroviral vector encoding the constitutively active form HIF1α P402A;P564A (HIF1α $(P\text{-}A)^2$) lacking critical proline residues (Yan et al., 2007).

Viral infection. For retroviral infection, HEK293T cells were transfected with 4 µg of each retroviral vector and 4 µg of pCL-Ampho Retrovirus Packaging Vector (Imgenex) using Lipofectamine 2000 (Invitrogen), according to the manufacturer´s instructions. Cell culture supernatants were harvested 48 hours after transfection, filtered through a 0.22 µm filter, diluted (1:2) with fresh medium containing 6 µg/ml polybrene (final concentration) and added to WT8 and 786-O cells. This step was repeated during the next 2 days. For lentiviral infection, 786-O cells were cultured for 24 hours with commercial lentiviral particles, according to the manufacturer´s instructions.

Western blot and antibodies. Cells were lysed in Laemmli buffer. Pulverized mouse livers were homogenized in lysis buffer (50mM Tris HCl, pH 7.4, 1%Triton X-100, 0.2%SDS, 1mM EDTA) supplemented with an EDTA-free protease inhibitor and a phosphatase inhibitor (both from Roche) and protein extracts were then quantified. Western blots were performed using 8-12% SDS-polyacrylamide gels and the membranes were probed with antibodies raised against phospho-4EBP1(Thr37/46); phospho-4EBP1(Ser65); 4EBP1; rpS6 (Ser235/236); rpS6; phospho-p70-S6K (Thr389) and p70-S6K (all purchased from Cell Signalling); HIF2α (Abcam, ab199); human HIF1α (BD Transduction

laboratories, 610959); mouse HIF1α (Cayman, 10006421); SLC7A5 (Abcam, ab85226); tubulin (T6199, Sigma) or actin (I-19, Santa Cruz, sc-1616). Immunolabelling was detected by enhanced chemiluminiscence (SuperSignal West Femto Maximum Sensitivity Substrate, Thermo Scientific) and visualized with a digital luminescent image analyzer (Image Quant LAS400 mini).

siRNA-mediated gene silencing. The siRNA experiments were carried out using Lipofectamine 2000 (Invitrogen) with SMARTpool siSLC7A5, siRAGA and siRAGB siRNAs, non-targeting pool of control siRNAs (siSCR) from Dharmacon, MISSION HIF2α siRNA (SASI_Hs_00019152) or MISSION siRNA Universal Negative Control #1 from Sigma, at a final concentration of 100 nM.

RNA extraction and qRT-PCR. Total RNA from cells was isolated using Ultraspec. Mouse livers were homogenized in Trizol (Invitrogen) with two freeze/thaw cycles. Total RNA was isolated using the RNeasy RNA extraction kit (Qiagen). RNA (1 μg) was then reverse-transcribed using Improm-II reverse transcriptase (Promega) and polymerase chain reaction (PCR) amplifications were performed using a Power SYBR Green PCR Master Mix kit (Applied Biosystems). The following primer sets were used: OCT4 (forward, 5′-GCTTAGCTTCAAGAACATGTGTA-3′; reverse, 5′-CTCTCACTCGGTTCTCGAT-3′); human SLC7A5 (forward, 5′-GGAACATTGTGCTGGCATTATACA-3′; reverse, 5′-CCTCTGTGACGAAATTCAAGTAATTC-3′); bNIP3 (forward, 5′-GTCTGGACGGAGTAGC-3′; reverse, 5′-GGCCGACTTGACCAAT-3′); mouse SLC7A5 (forward, 5′-GTGGAAGAACAAGCCCAAGTG-3′; reverse, 5′-GGCAGAGCACCGTCACAGA-3′); VHL (forward, 5′-TCAGCCCTACCCGATCTTACC-3′; reverse, 5′-ATCCCTGAAGAGCCAAAGATGA-3′); HIF2α (forward, 5′-CCTGGCCATCAGCTTCCTT -3′; reverse, 5′-GGTCGGCCTCAGCTTCAG -3′); PGK-1 (forward, 5′-GGTGCTCAACAACATGG-3′; reverse, 5′-CAATCTGCTTAGCCCGA-3′); hypoxanthine-guanine phosphoribosyltransferase-1, human HPRT1 (forward, 5′-ATTGTAATGACCAGTCAACAGGG-3′; reverse, 5′-GCATTGTTTTGCCAGTGTCAA-3′); mouse HPRT1 (forward, 5′-

GTTAAGCAGTACAGCCCCAAA-3′; reverse, 5′-AGGGCATATCCAACAAC AAACTT-3′). The data were analyzed using StepOne Software version 2.0 (Applied Biosystems). All values were normalized to *Hprt* gene expression levels.

Chromatin Immunoprecipitation (ChIP) Assays. Cells were processed as described previously (Pescador et al., 2005). For immunoprecipitations, whole rabbit serum (IgG control) and a polyclonal anti-HIF2α antiserum (Novus Biologicals, NB100-132) or anti-HA (Abcam, ab9110) were used. RT-PCR quantification was performed to evaluate HIF2α binding activity to *Slc7a5* proximal promoter or *Slc7a5* intron using the following primers: proximal promoter (forward, 5′-TCGGTTCTTCCCTCGTC-3′; reverse, 5′-GGAACCTAGGCTCCTGT-3′); Intron 1 (forward, 5′-TTTACGTTCCTGGACCATCC-3′; reverse, 5′-CAAGAGGCTGGGAGTATTGC-3′). RT-PCR quantification for evaluation of HIF1α binding activity to *Pdk1*regulatory sequences was performed using the following primers previously described (Kim et al., 2006; Papandreou et al., 2006): *Pdk1* region#1 positive control (forward, 5′- CGCGTTTGGATTCCGTG-3′; reverse, 5′-CCAGTTATAATCTGCCTTCCC TATTATC-3′); *Pdk1* region#2 negative control (forward, 5′- AAAGGACATTCTACAACGATTCTGC-3′; reverse, 5′-CAATTGTCTGGTTACTGAAAGTCTCC-3′).

Xenograft tumor generation. A total of 18 immunosuppressed SCID mice (Charles River) were subcutaneously injected with 786-O cells expressing either scrambled shRNA (786-O-shScramble control cells) or SLC7A5 shRNA (786-O-shSLC7A5). During the exponential growth phase, 786-O cells were trypsinized and resuspended in RPMI media without serum. Mice were injected in each dorsal flank with 4.4 x 10^6 cells in 0.2 ml of media. The left flank carried control cells and the right flank the shSLC7A5 silenced cells. Starting from 15 days after injection, tumor size was measured weekly with digital calipers, in two perpendicular diameters. Tumor volume was calculated by using the formula [D*d*d]/2, where ‘D’ is the larger tumor diameter and ‘d’ the shorter diameter. Animals were sacrificed humanely according with the bioethics approval of this particular experiment (CBA PA 77_2011-v2).

Clinical material and protein expression analysis. All cases were reviewed and diagnosed according to the criteria of the World Health Organization classification. Samples were processed as previously described (Gimenez-Bachs et al., 2012). Briefly, tissues were disaggregated by using the Polytron dispersing System PT-2100 (Kinematica AG, Lucerne, Switzerland) in lysis buffer (100mM HEPES, pH 7.5, 50mM NaCl, 0,1% Triton X-100, 5mM EDTA, 0,125M EGTA). Protease and phosphatase inhibitors (0.2 mg/ml Leupeptin, 2 mg/ml, Aprotinin, 1mM PMSF and 0.1mM Na_3VO_4) were added prior to lysis. Indicated amounts of protein were loaded onto 6-12% SDS-PAGE, transferred to PVDF filters and blotted against different proteins using specific antibodies. Total protein was quantified and 100μg of extract from neoplastic tissue and adjacent healthy renal tissue were evaluated by Western blotting using antibodies against SLC7A5 (Cell signaling, 5347), CAIX (Abcam, ab15086) or Erk2 (c-14, Santa Cruz, SC-154). Western blotting against extracellular signal-regulated kinase-2 (ERK2) was performed as loading control.

Immunohistochemistry. Lung and liver tissue was paraffin-embedded after an overnight fixation in 4% paraformaldehyde. Microwave-induced antigen retrieval (15' at 240W) was performed in 0.01M sodium citrate (pH 6). Endogenous peroxidase and biotin were blocked using 0.3% H_2O_2 in methanol and an avidin/biotin blocking kit (Vector Laboratories), respectively. Sections were stained overnight with antibodies against SLC7A5 (1:400, SAB2500586, Sigma-Aldrich), and phospho-S6 ribosomal protein (1:300, #2211, Cell Signaling Technology). Antibody binding was visualized using a LSAB + Peroxidase kit with 3,3'-diaminobenzidine as the chromogen, according to the manufacturer's recommendations (Dako). Afterwards, sections were dehydrated and mounted with Eukitt mounting medium (Sigma-Aldrich).

Supplemental References

Gimenez-Bachs, J.M., Salinas-Sanchez, A.S., Serrano-Oviedo, L., Nam-Cha, S.H., Rubio-Del Campo, A., and Sanchez-Prieto, R. (2012). Carbonic anhydrase IX as a specific biomarker for clear cell renal cell carcinoma: comparative study of Western blot and immunohistochemistry and implications for diagnosis. Scandinavian journal of urology and nephrology, [Epub ahead of print].

Kim, J.W., Tchernyshyov, I., Semenza, G.L., and Dang, C.V. (2006). HIF-1-mediated expression of pyruvate dehydrogenase kinase: a metabolic switch required for cellular adaptation to hypoxia. Cell metabolism 3, 177-185.

Papandreou, I., Cairns, R.A., Fontana, L., Lim, A.L., and Denko, N.C. (2006). HIF-1 mediates adaptation to hypoxia by actively downregulating mitochondrial oxygen consumption. Cell metabolism *3*, 187-197.

Pescador, N., Cuevas, Y., Naranjo, S., Alcaide, M., Villar, D., Landazuri, M.O., and Del Peso, L. (2005). Identification of a functional hypoxia-responsive element that regulates the expression of the egl nine homologue 3 (egln3/phd3) gene. The Biochemical journal 390, 189-197.

Yan, Q., Bartz, S., Mao, M., Li, L., and Kaelin, W.G., Jr. (2007). The hypoxia-inducible factor 2alpha N-terminal and C-terminal transactivation domains cooperate to promote renal tumorigenesis in vivo. Molecular and cellular biology 27, 2092-2102.